



*Background image:* A high-resolution image generated by the Mars Orbiter Laser Altimeter (MOLA), an instrument on board NASA's Mars Global Surveyor spacecraft, showing the topography of Mars. Low-altitude areas are shown in blue, highlands in yellow to red. The deep-blue region in the south is the giant Hellas impact basin, which is nearly 9 km deep and 2100 km across. The pale-blue area in the centre of the image is the Isidis Planitia basin, which contains the proposed landing site for ESA's Mars Express/Beagle 2 mission.

*Thumbnail images:* (from left to right) Ultraviolet image of Venus taken from the Pioneer Venus orbiter, the main belt asteroid Gaspra (image taken by the Galileo spacecraft while en route to Jupiter), close-up of the surface of Jupiter's moon Io showing a volcanic region, close-up of the planet Mercury showing impact craters on its surface.

This publication forms part of an Open University course S283 *Planetary Science and the Search for Life*. The complete list of texts which make up this course can be found on the back cover. Details of this and other Open University courses can be obtained from the Course Information and Advice Centre, PO Box 724, The Open University, Milton Keynes MK7 6ZS, United Kingdom: tel. +44 (0)1908 653231, e-mail [ces-gen@open.ac.uk](mailto:ces-gen@open.ac.uk). Alternatively, you may visit the Open University website at <http://www.open.ac.uk> where you can learn more about the wide range of courses and packs offered at all levels by the Open University.

To purchase a selection of Open University course materials visit the webshop at [www.ouw.co.uk](http://www.ouw.co.uk), or contact Open University Worldwide, Michael Young Building, Walton Hall, Milton Keynes MK7 6AA, United Kingdom for a brochure. Tel. +44 (0)1908 858785; fax +44 (0)1908 858787; email [ouwenq@open.ac.uk](mailto:ouwenq@open.ac.uk)

The Open University  
Walton Hall, Milton Keynes  
MK7 6AA

First published 2003

Copyright © 2003 The Open University

All rights reserved. No part of this publication may be reproduced, stored in a retrieval system, transmitted or utilized in any form or by any means, electronic, mechanical, photocopying, recording or otherwise, without written permission from the publisher or a licence from the Copyright Licensing Agency Ltd. Details of such licences (for reprographic reproduction) may be obtained from the Copyright Licensing Agency Ltd of 90 Tottenham Court Road, London W1P 0LP.

Edited, designed and typeset by The Open University.

Printed and bound in the United Kingdom by Bath Press, Bath.

ISBN 0 7492 5674 5

1.1

# **PLANETARY SCIENCE AND THE SEARCH FOR LIFE COURSE TEAM**

## **Course Team Chair Academic Editors Authors**

Iain Gilmour  
Iain Gilmour, Neil McBride, Mark A. Sephton  
Philip A. Bland  
Andrew Conway  
Iain Gilmour  
Barrie W. Jones  
Neil McBride  
Tony McDonnell  
Elaine A. Moore  
David A. Rothery  
Mark A. Sephton  
Mike Widdowson  
Ian Wright  
John Zarnecki

## **Course Manager**

Jennie Neve

## **Course Secretary**

Valerie Cliff

## **Editors**

Peter Twomey  
Pamela Wardell

## **Software Designers**

Will Rawes  
Fiona Thomson

## **Multimedia Producer**

Kate Bradshaw

## **Web Developer**

Hong Yu

## **Graphic Designers**

Debbie Crouch, Jenny Nockles

## **Graphic Artist**

Sara Hack

## **Indexer**

Jane Henley

## **Picture Researcher**

Lydia Eaton

## **Book Assessors**

Prof. F.W. Taylor, Atmospheric,  
Oceanic and Planetary Physics,  
Department of Physics, University of Oxford.  
Dr Alan Penny, Rutherford Appleton Laboratory.

## **Course Assessor**

Prof. David W. Hughes, Department of Physics  
and Astronomy, The University, Sheffield.

The book made use of material originally produced for the S281 *Astronomy and Planetary Science* Course Team by Elaine Moore (Chapter 6), and, Ian Wright and Colin Pillinger (Chapter 9).



# CONTENTS

## CHAPTER 6 THE GIANT PLANETS 201

Elaine Moore

6.1	Introduction	201
6.2	The structures of the giant planets	202
6.3	Jupiter and Saturn	209
6.4	Uranus and Neptune	233
6.5	Summary of Chapter 6	242

## CHAPTER 7 MINOR BODIES OF THE SOLAR SYSTEM 245

Neil McBride and Tony McDonnell

7.1	Introduction	245
7.2	Orbits and Kepler's laws	245
7.3	Asteroids	251
7.4	The Kuiper Belt	262
7.5	Comets	268
7.6	Interplanetary dust	275
7.7	Summary of Chapter 7	280

## CHAPTER 8 THE ORIGIN OF THE SOLAR SYSTEM 281

Ian Wright

8.1	Introduction	281
8.2	Physical formation processes	283
8.3	Summary of Chapter 8	313

## CHAPTER 9 METEORITES: A RECORD OF FORMATION 315

Ian Wright

9.1	Introduction	315
9.2	The forensic record	323
9.3	Summary of Chapter 9	346

## ANSWERS AND COMMENTS A1

## APPENDICES A15

## ACKNOWLEDGEMENTS A25

## INDEX A27



## CHAPTER 6

# THE GIANT PLANETS

### 6.1 Introduction

The previous chapter dealt with objects with definite surfaces – the terrestrial planets. We turn now to objects for which there is no discernible surface and where the greater part of the object (possibly all) is fluid (i.e. gas or liquid). These are the **giant planets**: Jupiter, Saturn, Uranus and Neptune (Figure 6.1).

We start by considering the overall structure of these planets. Much of the detailed evidence has come from instruments on board spacecraft, and it is hoped that even more information will be gathered by future missions. However, Earth-based instruments are by no means obsolete in this field and observations by space telescopes (in orbit around the Earth) have provided much valuable data. Ground-based observations were necessary as a starting point for data collection by the spacecraft. One advantage of Earth-based and space-telescope observations is that they can be used to study changes in a planet's appearance over a long time (in the case of Jupiter, hundreds of years), whereas fly-by and lander spacecraft observe for only a limited time.

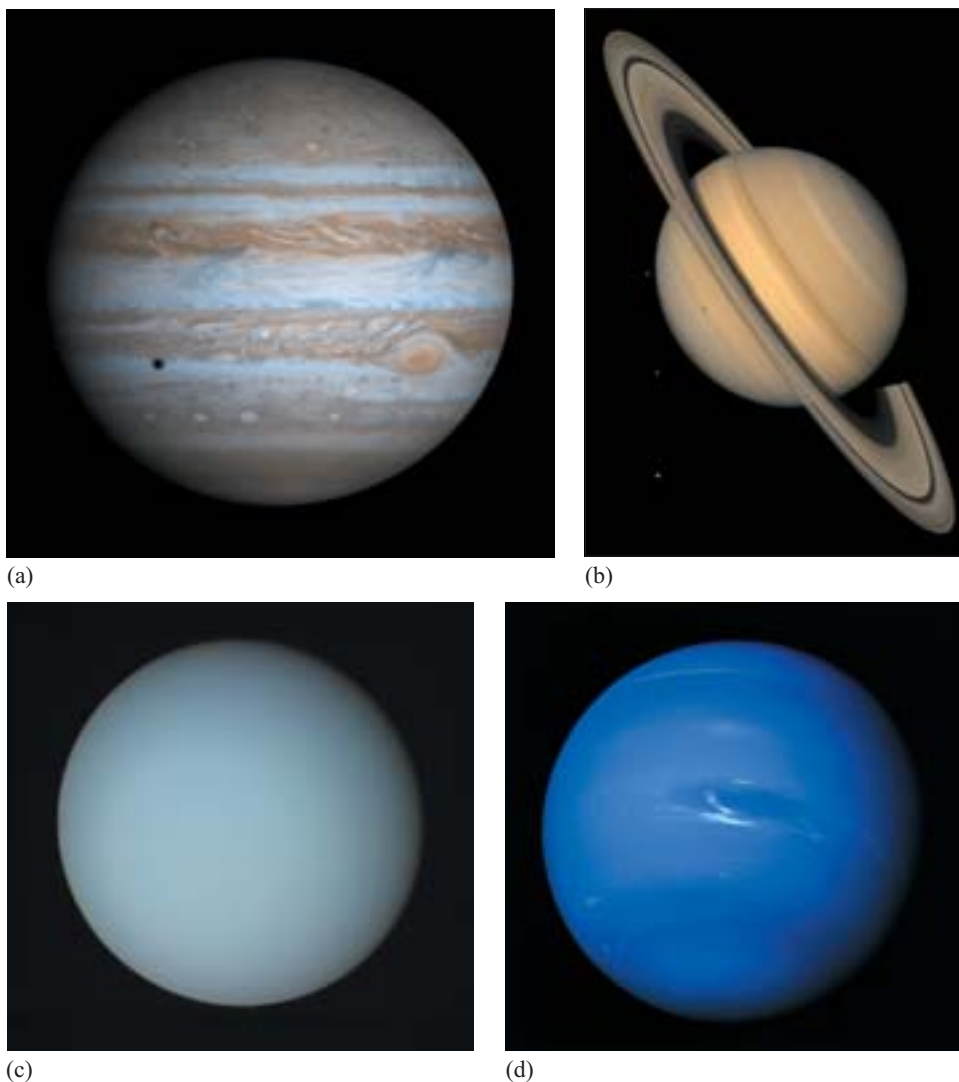


**Figure 6.1**  
(a) Jupiter (mean radius 69 910 km),  
(b) Saturn (mean radius 58 230 km),  
(c) Uranus (mean radius 25 360 km)  
and  
(d) Neptune (mean radius 24 620 km).

We have a fairly accurate picture of the composition and structure of the outer layers or atmospheres of these planets, because we can detect and positively identify molecules in them. Our knowledge of the interiors, however, is less certain and is based on indirect measurements and modelling. As none of the four planets has an accessible surface (if they have any surfaces at all), we do not know where the base of the atmosphere is. The radii of the planets are therefore often defined as the distance from the centre of the planet to the 1 bar pressure level (1 bar being approximately the pressure of the Earth's atmosphere at sea-level). This level corresponds roughly to the base of the directly observable layers of the planets. In general when we refer to the atmosphere of a giant planet, we shall mean the layers of the planet from the 1 bar pressure level outwards. In some cases, for example the results of the Galileo probe measurements (see Box 6.1), we shall include layers slightly deeper than this.

In 1997 the Cassini spacecraft planned jointly by NASA, ESA (the European Space Agency) and ASI (the Italian space agency) was launched. This is due to reach Saturn in July 2004 and study the planet, its rings, magnetosphere and its satellites. As Cassini passed Jupiter in December 2000, observations of Jupiter were made by Galileo and Cassini simultaneously.

You will start this chapter by studying the evidence that is available for the nature of the interiors of these planets and how the data can be interpreted. You will then move on to study the atmospheres.

For an atmosphere, we can determine not only its composition and structure but also how it moves. Are the processes determining this motion the same as those on the terrestrial planets, or does the far greater depth of fluid on the giant planets mean that different processes occur? Can the way gas is transported around the atmosphere tell us anything of what goes on in the interior of the planet? We shall be looking at the observed wind motions and seeing if we can draw any conclusions from them.

Finally you will be studying the magnetic fields of these planets and how these interact with, for example, the solar wind and satellites of the giant planets.

Because of the difficulties in collecting data from these bodies, you will often find that there is no one clear-cut explanation and that several plausible models will fit the data that we have. Consequently, there are some sections in which you will not be asked to learn an accepted explanation but to consider whether a particular model is ruled out by the information available. This is particularly true of Uranus and Neptune. Do not worry, therefore, if you leave this chapter feeling you are not quite sure, for example, what the internal structure of Uranus is. Nobody is sure!

## 6.2 The structures of the giant planets

### 6.2.1 Models of the structure

You saw in Chapter 2 that we are not even sure about the composition of the interior of the Earth. We have less observational data on the giant planets and so our knowledge of their interiors is much less certain. From the data we have and laboratory experiments on how the density of materials varies with temperature and pressure, possible models can be put forward. The current models of the planets predict a layer structure. Basically, Jupiter and Saturn would have a rocky core, a layer of icy materials surrounding this and a thick outer gaseous (hydrogen and helium) envelope, and Uranus and Neptune would have an inner icy-rocky core with



## BOX 6.1 VOYAGER AND GALILEO

These space missions have provided a huge amount of data on the giant planets; you will find that many of the images in this chapter were obtained from them. Such missions require years of planning – scientific, technical and political. Because of the distance of the giant planets from Earth, such spacecraft are launched years before they can provide the data they are planned to measure. The NASA Voyager missions comprised two spacecraft, Voyager 1 and Voyager 2, which between them studied all four giant planets and many of their satellites and are now heading out of the Solar System. The Voyager project was conceived in the 1960s when it was realized that in the late 1970s, the four giant planets would be in such positions that a single spacecraft could encounter all of them, an opportunity that would not occur again for 175 years. The original aims of obtaining data on the four giant planets was magnificently achieved by 1989, indeed for Uranus and Neptune the Voyager-2 data remain the most comprehensive set we have. The decision was then made to continue collecting data in order to learn about the boundary of the Solar System. In 10 to 20 years from the time of writing (2002) the spacecraft are expected to leave the heliosphere — the region under the influence of the Sun’s magnetic field — and head for interstellar space. We give below a timetable of launch dates and main encounters.

- **1972** First project director starts work.
- **1977** August 20, Voyager 2 launch.
- **1977** September 5, Voyager 1 launch.
- **1979** March 5, Voyager 1 closest approach to Jupiter.
- **1979** July 9, Voyager 2 closest approach to Jupiter.
- **1980** November 12, Voyager 1 closest approach to Saturn.
- **1981** August 26, Voyager 2 closest approach to Saturn.
- **1986** January 24, Voyager 2 closest approach to Uranus.
- **1989** August 25, Voyager 2 closest approach to Neptune.
- **1998** February 17, Voyager 1 outdistances Pioneer 10 to become the furthest human-made object in space.
- **2020** Predicted last date at which data can be received from the Voyagers.

The NASA Galileo mission was designed to study Jupiter and its satellites in greater detail. On its way to Jupiter, Galileo flew past Venus and the Earth using these planets to change its direction and send it towards Jupiter with sufficient speed. As the spacecraft approached Jupiter, it separated into two – the Galileo probe and the Galileo orbiter. The probe descended into the atmosphere of Jupiter giving the first direct measurements of the composition and wind speed of the atmosphere. The orbiter studied Jupiter remotely and went on to obtain data on Jupiter’s magnetosphere and satellites. One of the final manoeuvres, made in 2002, was to put the spacecraft on an orbit which will result in Galileo entering the atmosphere of Jupiter, where the spacecraft will be destroyed.

- **1989** October 18, Galileo spacecraft launch.
- **1990** February 10, observations on Venus.
- **1990** December 8, fly-by of Earth.
- **1991** October 29, encounter with asteroid Gaspra.
- **1992** December 8, observations of Earth.
- **1993** August 28, encounter with asteroid Ida.
- **1994** July, observations of collision of comet Shoemaker–Levy with Jupiter.
- **1995** December 7, Galileo probe enters atmosphere of Jupiter. Galileo orbiter starts tour of Jovian system. (Note that ‘Jovian’ is the adjective for Jupiter.)
- **1997–1999** Fly-by observations of Europa.
- **1999** Fly-by observations of Callisto and Io.
- **2000** January, fly-by of Europa.
- **2000** February–May, fly-by of Io.
- **2000** May–September, fly-by of Ganymede.
- **2000** October–December, observations of Jupiter.
- **2001** October, fly-by of Io.
- **2002** January, final fly-by of Io.
- **2002** November 5, fly-by of the inner satellite Amalthea.
- **2003** September 21, end of Galileo mission – spacecraft collides with Jupiter.

an outer gaseous envelope. Current modelling does not however, assume that icy and rocky materials are completely differentiated from each other or from the gaseous component. The innermost layers are generally thought to consist of icy and rocky material. Some models distinguish two regions within this layer of differing density. At the centre of the planets, the temperatures and pressures are, according to the models, extremely high: 8000 K to 16 000 K and  $13 \times 10^6$  bar to  $50 \times 10^6$  bar. Although high, these figures are not unrealistic given that the corresponding figures for the Earth are 4300 K and  $3.3 \times 10^6$  bar. The giant planets contain far more rocky material than any terrestrial planet but the icy–rocky layers occupy only a small fraction of their total volumes. Outside these layers the composition is predominantly hydrogen and helium, although rocky and particularly icy materials are still present. For much of the volume, the temperatures and pressures are still high but gradually decrease. Atmospheric temperatures are low.

Remember that the ‘atmosphere’ is above the 1 bar level and the ‘interior’ is below the 1 bar level.

The layer structure with rocky materials concentrated towards the centre supports the view that differentiation has occurred subsequent to the formation of the planets. The evidence is not sufficiently detailed to say whether the rocky materials themselves have differentiated as in the Earth to give a central core of iron. That such differentiation has occurred is probable but the models used to try to reproduce the observational data use only an average composition for the rocky materials, based on a mixture of materials such as iron, iron sulfide, and silicates, that on the available evidence, are present in the interiors of terrestrial planets.

Figure 6.2 shows sketches of the interiors of Jupiter, Saturn, Uranus and Neptune. These represent one interpretation of the data currently available. Estimated temperatures and pressures at the boundaries of the layers are given. The nature of the layer labelled ‘metallic hydrogen’ will be explained when we consider Jupiter and Saturn in more detail. Not all these boundaries are as sharp as they appear in Figure 6.2. The outermost layers are gaseous and the innermost are liquid but in descending through the interior, a point would be reached where the conditions are such that the material is in a fluid phase where gas and liquid are indistinguishable. It is therefore probable that these planets not only have no sharp solid–gas (i.e. solid-to-gas) boundary, but have no sharp liquid–gas (i.e. liquid-to-gas) boundary either. In both of these respects, the giant planets differ from the terrestrial planets.

- From the temperatures marked on Figure 6.2, does the presence of icy materials imply that the layer is cold?
- No. All the temperatures shown are extremely high except for the tops of the outermost layers, i.e. the bases of the atmospheres.

The term ‘icy material’ simply denotes volatile compounds such as water, ammonia and methane and does not imply that the material is cold.

Note that the regions are shown by volume and that this does not represent the mass ratios of the different regions. The *cumulative* masses of the layers are labelled on Figure 6.2. For example, the inner core of Jupiter contains 3 to 3.5 Earth ( $M_{\oplus}$ ) masses of material (i.e. about one-hundredth of the mass of Jupiter) but it occupies only one-thousandth of Jupiter’s volume. Then the inner core of Jupiter *and* the next layer out together contain 5 Earth masses of material.

Before we go on to look at the interiors in more detail, let's consider the evidence on which such models are based.

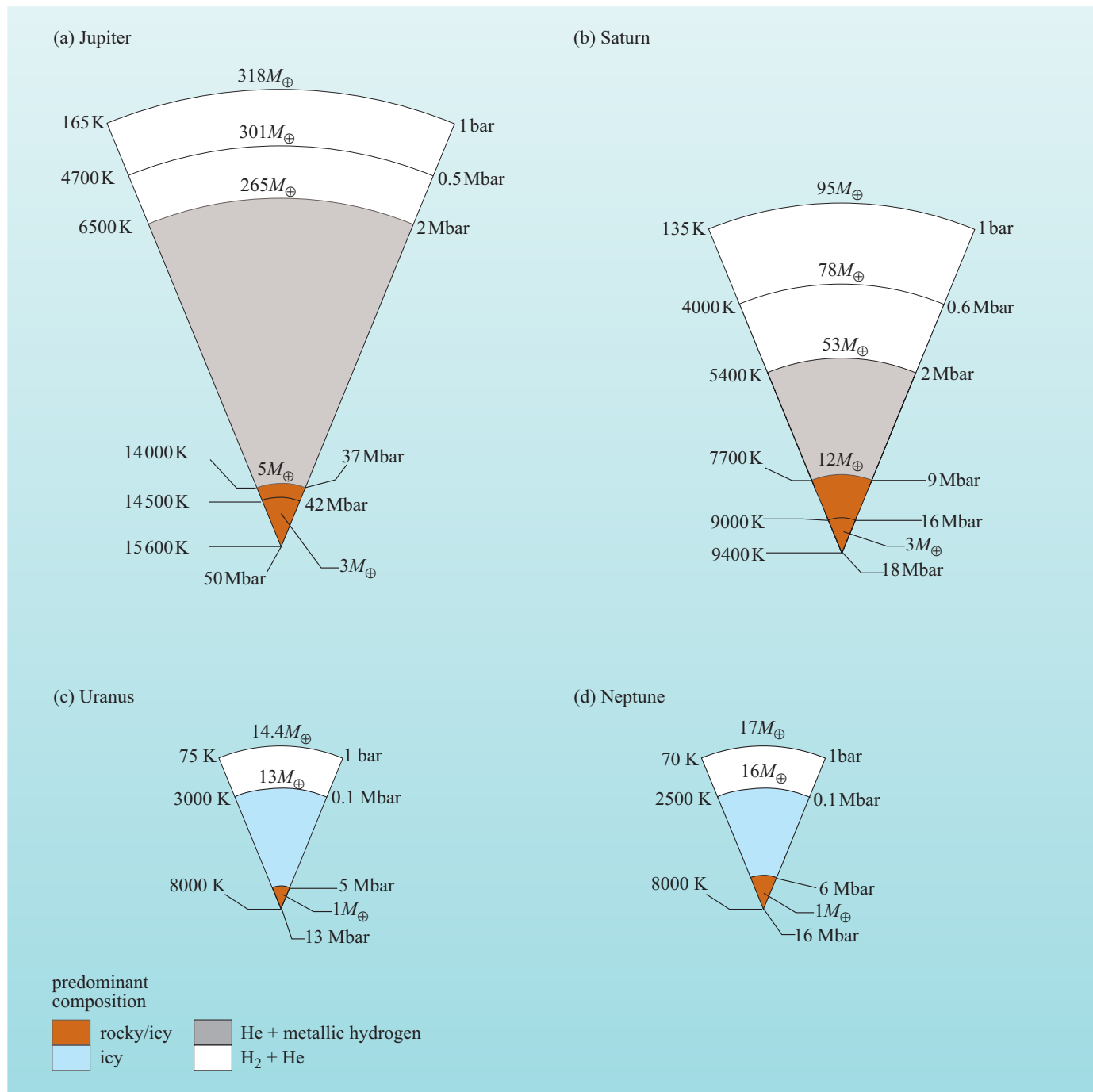


**Figure 6.2** Cross-sections through (a) Jupiter, (b) Saturn, (c) Uranus and (d) Neptune, showing the various layers that are thought to exist in the interiors of these planets. Note that in each case, the 1 bar level is considered to be the *inner* boundary of the atmosphere. Although the outer two layers on Jupiter and Saturn are both labelled ' $H_2 + He$ ', there is a distinction between them as we will see shortly. There is also a distinction between the innermost rocky/icy layers. The cumulative masses contained within a layer are shown also (note  $M_{\oplus}$  means Earth-mass).

## 6.2.2 Obtaining evidence

The first and incontrovertible piece of evidence is the average density of each planet as a whole. The giant planets are not quite spherical, being somewhat flattened at the poles. However, the volume can be calculated if the polar and equatorial radii are measured (as given in Appendix A, Table A1). From this we obtain the mean radius which is the value the planet's radius would have if it were spherical.

- Saturn has a mean radius of 58 230 km. Assuming Saturn is a sphere, what is its volume?
- The volume of a sphere is  $\frac{4}{3}\pi R^3$ , where  $R$  is the radius. Thus the volume of Saturn,  $V_{\text{Sat}}$  is:

$$\begin{aligned} V_{\text{Sat}} &= \frac{4}{3}\pi R_{\text{Sat}}^3 \\ &= \frac{4}{3}\pi \times (58\,230\text{ km})^3 \\ &= 8.3 \times 10^{14}\text{ km}^3 \\ &= 8.3 \times 10^{23}\text{ m}^3 \end{aligned}$$

The other quantity needed to calculate the density is the planetary mass. The masses of all four giant planets have been obtained by studying the paths of their satellites and of spacecraft flying past. These smaller bodies are affected by the gravitational attraction between them and the planet, which of course depends on the planetary mass.

### QUESTION 6.1

The orbital period  $P$  of a satellite of Saturn, Enceladus, is 1.370 days and its average distance  $a$  from Saturn is 238 000 km. Assuming that the mass of Saturn  $M_{\text{Sat}}$  is much greater than that of Enceladus and that the satellite's orbit is roughly circular, the mass of Saturn can be estimated using the formula:

$$M_{\text{Sat}} = 4\pi^2 \frac{a^3}{GP^2}$$

where  $G = 6.67 \times 10^{-11}\text{ N m}^2\text{ kg}^{-2}$  is the gravitational constant. Calculate the mean density of Saturn.

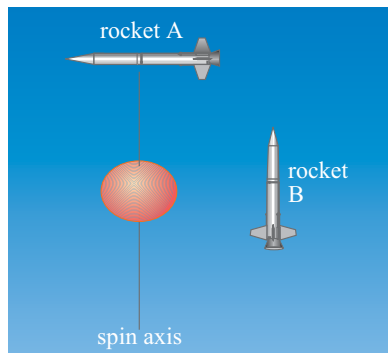


**Figure 6.3** The gravitational pull on spacecraft A differs from that on spacecraft B although they are equidistant from the planet's centre.

The generally accepted densities obtained from the volumes and masses are given in Appendix A, Table A1. The value obtained for Saturn in Question 6.1 agrees very well with the value in this table.

The passage of spacecraft and satellites tells us more than just the mass of the planet. Because the planets are not spherical, it turns out that from the gravitational field we can also learn something of the distribution of density within the planet. For example, as the giant planets are not spherical but are squashed along the polar axis the gravitational pull on a body at the pole differs from that on one at the equator. Furthermore, two objects that are the same distance from the centre of the gas giant planet, feel a slightly different gravitational pull depending on whether they are over the pole or over the equator (Figure 6.3).

How the gravitational pull differs depends not only on the degree of flattening but also on how material is distributed in the planet. More sophisticated analysis of how the gravitational field varies with latitude and longitude is possible and leads to the conclusion that there are denser and lighter materials, and that the denser materials lie near the centre, as in Figure 6.2.

Incidentally, this method is also the best way of measuring the internal variation of density for Venus for which there is no seismic data (Chapter 2) and Mars for which there is very little such data. The measurements we obtain do not give us a definitive model for the nature of the interior, but any model proposed must be able to reproduce the observed results. Models with different proportions of rocky/icy materials, hydrogen and helium in the different layers can be tested to see which fits the gravitational evidence most closely.

Another source of information on the interiors of the planets is measurements of the magnetic fields. Like the Earth, the four giant planets have a magnetic field that behaves as though it originated in a magnetic dipole.

- What properties does the Earth's core need to have to explain its magnetic dipole field?
- It has to be liquid, electrically conducting, and in motion.

Jupiter's magnetic field has been known and studied for many years, but Voyager 2 produced the first comprehensive measurements of the magnetic fields of Uranus and Neptune. The existence of the magnetic fields means that somewhere in the interior of each planet lies an electrically conducting liquid.

- What is the electrically conducting liquid inside the Earth and where is it located?
- It is the outer core, which is liquid iron with about 4% nickel and some lighter elements.

Extensive mapping of the magnetic fields has allowed the region in which the magnetic field originates to be determined and this does not support a liquid-iron core as the main source of the magnetic field for the four giant planets. Figure 6.4 shows the main features of the magnetic fields. The bar magnets representing a dipole will approximately reproduce the observed fields.

For our purposes, the main conclusion from such measurements is that there must be an electrically conducting liquid layer in the metallic-hydrogen regions of Jupiter and Saturn, or in the icy-materials region of Uranus and Neptune.

More evidence on the nature of the interiors comes from the heat given out by the planets. The effective temperatures of the planets are very low: 120 K (Jupiter), 89 K (Saturn), 53 K (Uranus) and 54 K (Neptune). They are, however, except for Uranus, higher than would be expected based on their distance from the Sun, if the Sun were their only source of energy. The additional energy needed to produce the observed temperature is known as the **heat excess**. Jupiter, Saturn and Neptune must therefore have an internal source of energy, the origin of which will be discussed when we consider the individual planets. We shall also put forward one explanation for the apparent lack of an internal energy source in Uranus.

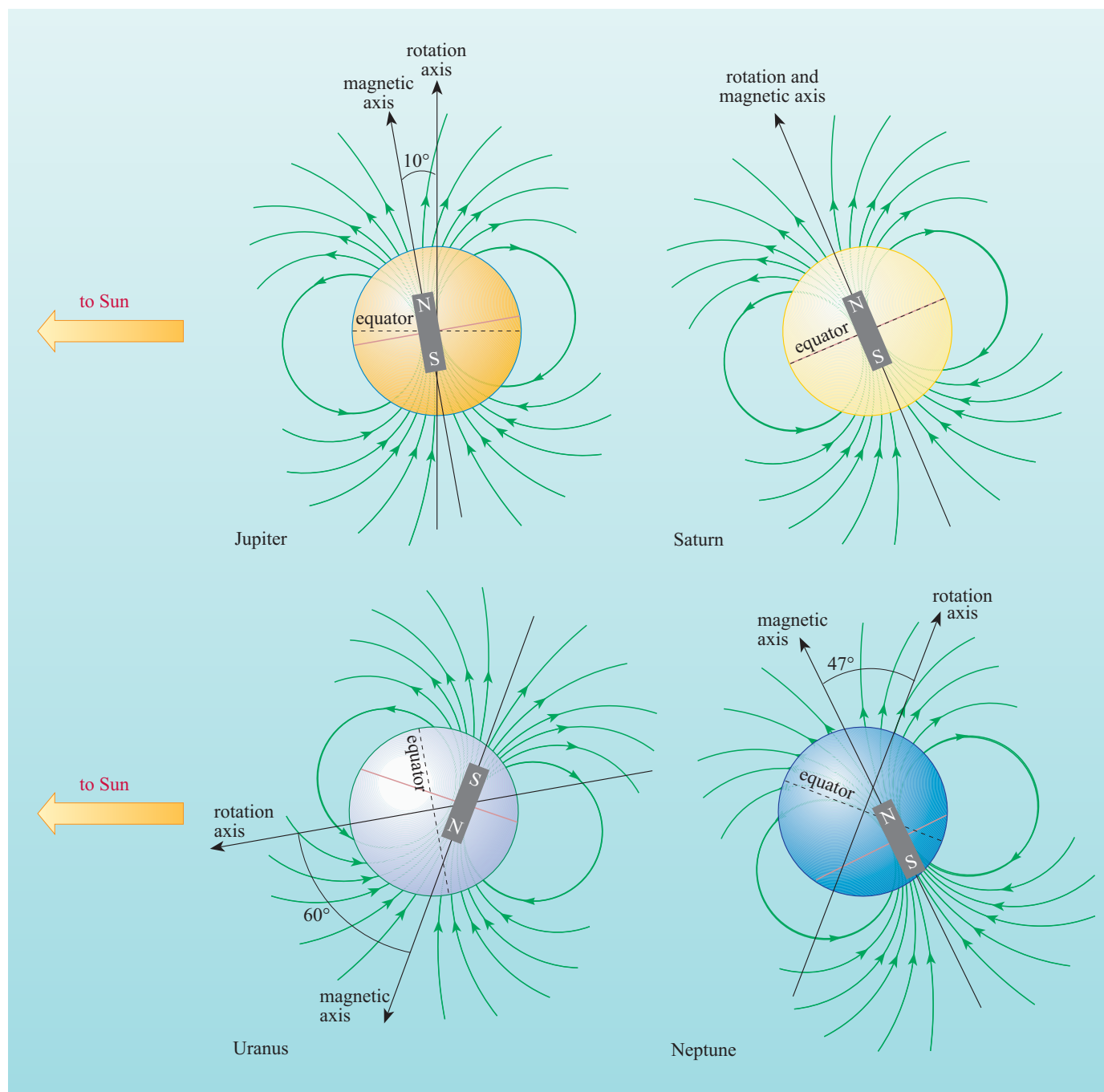


**Figure 6.4** Magnetic dipoles of Jupiter, Saturn, Uranus and Neptune. The bar magnets indicate the position of the centre of the dipole and its polarity. The length is arbitrary. The lines represent observed magnetic field lines. The direction to the Sun as shown, is at one point in the orbit. However the directions of the rotation and magnetic axes are fixed with respect to the stars, not the Sun.

The amount of energy radiated by the planet can be used as a constraint in estimating the temperature of the interior. In the case of Jupiter, the core temperature was estimated by a recent model (1999) based on data from the Galileo orbiter to be between 15 600 K (Figure 6.2) and 16 000 K. Other models have suggested temperatures in excess of 20 000 K.

Finally, in the absence of evidence to the contrary, it is assumed that heavy elements are present in roughly solar ratios and that the planets are more likely to contain substances made from more abundant elements than less abundant ones. On these grounds, for example, ammonia ( $\text{NH}_3$ ) is a more likely major constituent of icy materials than hydrogen fluoride ( $\text{HF}$ ) because the solar abundance of nitrogen is greater than that of fluorine.

### QUESTION 6.2

Outline the reasons why the element mercury ( $\text{Hg}$ ) is not a suitable candidate for the material responsible for producing the magnetic dipole fields in the four giant planets. (The relative abundance by number of  $\text{Hg}$  is 12 on a scale that sets the abundance of  $\text{H}$  at  $10^{12}$ . On this scale the relative abundances of some common elements are  $\text{Si } 3.5 \times 10^7$ ,  $\text{N } 1.1 \times 10^8$ ,  $\text{Fe } 3.2 \times 10^7$ . Note that the density of  $\text{Hg}$  is about  $1.36 \times 10^4 \text{ kg m}^{-3}$ .)

## 6.3 Jupiter and Saturn

### 6.3.1 Interiors

The densities of the giant planets are very low compared to the terrestrial planets; indeed that of Saturn is lower than the density of water at everyday temperatures on the surface of the Earth. However, the mass of material in these planets is so large that the interior must be at a very high pressure; in the case of Jupiter, the pressure increases from 1 bar at the edge of the atmosphere to 50 million times this at the centre of the planet. With such high pressures, the only way to account for the low overall density is that the composition of these planets is mainly of the light elements, hydrogen and helium, in some form.

- Saturn is less massive than Jupiter. Saturn is also less dense than Jupiter. Does it follow that the two planets differ in composition?
- Not necessarily. The greater mass of Jupiter means that the material will be subject to greater self-compression (Chapter 2) and therefore will be more dense. From density measurements it is probable that Jupiter and Saturn have similar chemical compositions.

### QUESTION 6.3

By considering the effect of self-compression only, an approximate value of the pressure at the centre of a planet,  $P_c$  is given by

$$P_c \approx \frac{2\pi G}{3} \rho_m^2 R^2$$

where  $G$  is the gravitational constant ( $6.67 \times 10^{-11} \text{ N m}^2 \text{ kg}^{-2}$ ),  $\rho_m$  is the mean density of the planet and  $R$  is the radius of the planet. Calculate the pressure at the centre of (a) Earth, (b) Saturn and (c) Jupiter using this formula.

Take relevant values from Table A1 in Appendix A.



A further inference from density measurements is that Jupiter and Saturn each contain about 5 to 10 Earth masses of icy and rocky material. Measurements of the gravitational fields of these planets are consistent with most of this being in the central core. Models of the planets that fit these measurements, and agree with our current knowledge of how the density of materials varies with temperature and pressure, show a core of dense material. In the absence of further information, we can reasonably assume that this core is composed of common rocky and icy planetary materials, such as silicates, iron, iron compounds, water, ammonia and methane. The materials are probably further differentiated within the core to give metallic iron at the centre but current modelling methods use an average rocky material whose composition is based on solar abundances and the composition of typical rocky bodies. Observational data is not sufficiently precise to distinguish details of the core structure. The outer and inner core layers are similar but the outer layer has a higher proportion of helium.

Surrounding each core is a very thick layer taking up the greater part of the planet and labelled helium and metallic hydrogen in Figure 6.5. The helium is believed to be present as a fluid, similar to that used on Earth in very low temperature studies and in superconducting magnets, but at much greater temperatures and pressures.

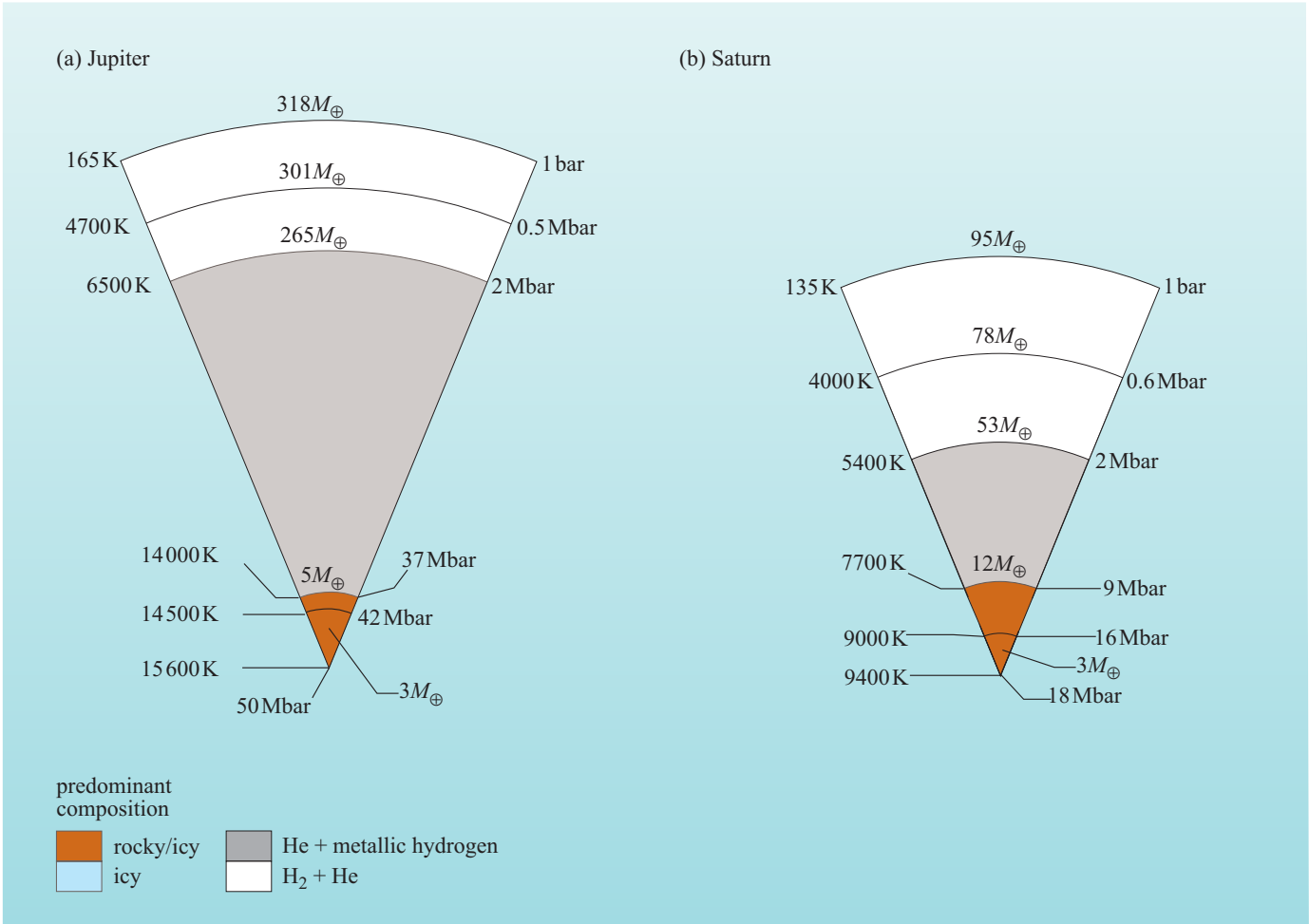


Figure 6.5 Cross-sections through (a) Jupiter and (b) Saturn.



The hydrogen is generally accepted to occur in a most unusual form – **metallic hydrogen**. On Earth, hydrogen is a colourless gas that is very difficult to liquefy and is certainly not metallic. To see how hydrogen can occur in a form described as metallic, read Box 6.2.

## BOX 6.2 METALLIC BONDING

A simple picture of a metal such as aluminium, familiar to us on Earth, is of an orderly set of positively charged ions surrounded by electrons, which are shared. Imagine some aluminium ions arranged as in Figure 6.6.

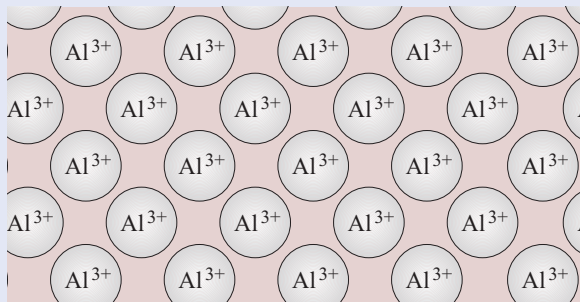


**Figure 6.6** Aluminium ions ( $\text{Al}^{3+}$ ) arranged as though in a crystal of aluminium. The electrons ‘lost’ from the atoms wander freely through the solid.

Now, the most common ion formed by aluminium is  $\text{Al}^{3+}$ , in which the aluminium atom has lost three electrons. Suppose the lost electrons are allowed to wander freely about the crystal. You may recall that two atoms can form a chemical bond by sharing electrons. In our picture of aluminium, the freely wandering electrons are shared by all the ions in the crystal, and thus serve to bond together all the ions. This sharing of electrons by a whole crystal constitutes **metallic bonding**. The electrons are responsible for many of the characteristic metallic properties of elements such as aluminium. In particular, they can move through the solid and, because they are electrons, they carry negative electrical charge with them. A moving electrical charge is an electric current, and so metallic bonding leads to electrical conductivity.

- Aluminium is a solid at everyday temperatures and pressures, but there is one common liquid metal found at the Earth’s surface. What is it?
- Mercury (Hg). You may have a mercury thermometer or barometer at home.

In liquid mercury, the situation is similar to that shown in Figure 6.6 except that because mercury (Hg) is a liquid, the ions are not so ordered (Figure 6.7).

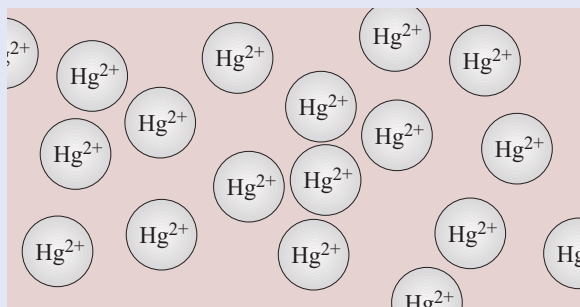


**Figure 6.7** Mercury ions ( $\text{Hg}^{2+}$ ) arranged as though in liquid mercury. The ‘lost’ electrons are free to travel through the liquid, but the arrangement of the ions is less regular than in solid aluminium.

At the very high pressures in the interior of Jupiter and Saturn the hydrogen nuclei are squashed together so that, instead of just two hydrogen nuclei sharing electrons to form  $H_2$  (which is the normal form of the element hydrogen on Earth), large numbers of hydrogen nuclei share their electrons, and metallic bonding results as in liquid mercury. Metallic hydrogen is liquid at the temperatures and pressures inside these two planets.

Detailed measurements of Jupiter and Saturn show that the magnetic source is outside the core in the layer labelled ‘metallic hydrogen’ in Figure 6.5. The region where the magnetism originates is a spherical shell in this layer, and the magnetic dipole field produced by such a shell is centred in the planetary core. This provides an explanation for the magnetic field. The electrically conducting fluid is liquid metallic hydrogen. The heat of the interior will cause the liquid to be in motion through convection currents.

As we move further out from the core, temperatures and pressures are reached where hydrogen is more stable as  $H_2$  molecules than as a metal. This is the case for the outer two layers. Recent (2000) experiments on hydrogen under extremely high pressure suggest that this transition is gradual and thus the boundary between metallic and molecular hydrogen in Jupiter is not sharp. As we rise through the outer layer, the hydrogen changes imperceptibly from liquid to gas. Although these layers are predominantly hydrogen and helium, they do contain some icy materials and a very small amount of rocky materials. The researchers who proposed this model distinguished the two  $H_2 + He$  layers (Figure 6.5) by the different fractions of rocky materials contained in these layers.

For Jupiter, the model that we have described accounts for the measurements of gravity, magnetic field and internal energy including the heat excess. Jupiter is large enough for the internal energy to be residual accretional heat (Chapter 2) which will have led to extremely high temperatures as Jupiter formed, and heat due to past differentiation of rocky and icy materials. Energy from these sources will have been comparatively slowly lost to space due to the low surface area of Jupiter relative to its volume.

- What is the ratio of surface area to volume for a sphere of radius  $r$ ?
- The surface area is  $4\pi r^2$ . The volume of a sphere is  $\frac{4}{3}\pi r^3$ . Therefore the required ratio is

$$\frac{\text{surface area}}{\text{volume}} = \frac{4\pi r^2}{\frac{4}{3}\pi r^3} = \frac{3}{r}$$

So the surface-to-volume ratio gets smaller as  $r$  gets larger.

For Saturn, we have to introduce a further refinement to account for the heat excess. We might expect that Saturn should have had a lower initial temperature than Jupiter, and with a larger surface-to-volume ratio also, would have lost energy more rapidly and so cooled down long ago. However, a heat excess remains.

- What is the main heat source for the interior of the Earth?
- Radiogenic heating.

The bulk of Saturn, however, is hydrogen (metallic *and* molecular) and helium, and the low density precludes sufficient abundances of radioactive isotopes for this to be a major form of heating.

#### QUESTION 6.4

Jupiter generates a heat flux of about 7 watts per square metre of surface at the 1 bar level. The decay of  $^{40}\text{K}$  and other radiogenic isotopes produces  $4.8 \times 10^{-12} \text{ W kg}^{-1}$  of heat in the Earth today. If Jupiter has a core of which  $4M_{\oplus}$  (i.e. 4 Earth-masses) is rocky materials, what would be the rate of radiogenic heat generation in the core of Jupiter, assuming that the core is of similar composition to the Earth? Compare this with the observed heat flux.

The heat excess in Saturn may come from the separation of hydrogen and helium in the metallic hydrogen layer. In Jupiter, this layer is hotter and well stirred by convection. At higher temperatures, helium is soluble in hydrogen. As the temperature falls however, helium becomes less soluble and the two liquids tend to separate out. If the layers are well-stirred, however, an emulsion is formed in which small droplets of helium are dispersed throughout the hydrogen. This situation is rather like olive oil and water. If you stir the two liquids vigorously you can get them mixed (as for example in salad dressing). If the stirring becomes less vigorous, larger droplets of one liquid form in the other and gradually sink to the bottom to form a separate layer. Convection stirs the layers in Jupiter so that the hydrogen and helium are still mixed, but the liquid helium in Saturn's metallic hydrogen layer is forming larger droplets which, because they are denser than the hydrogen, fall towards the centre of the planet and will eventually form a separate layer.

- How does this separation cause the interior of Saturn to heat up?
- This is an example of heat from differentiation. The helium droplets release gravitational energy as they fall, and this energy is converted into heat.

#### QUESTION 6.5

Measurements of the gravitational field of Saturn indicate that the hydrogen/helium ratio in the molecular hydrogen layer is roughly solar and that helium is not depleted. Does this fit in with the attribution of the heat excess of Saturn to differentiation of helium from metallic hydrogen?

## 6.3.2 Atmospheres — structure and composition

### Studying the atmosphere

The atmosphere of these planets is, as we said in the introduction, formally defined as the layer outside the 1 bar level. This coincides roughly with the layer above the outermost cloud layer and hence the layer we can view. Some of the studies we are going to discuss include measurements at slightly deeper levels but all are concerned only with a very small fraction of the radius of the planets.

The atmospheres of the giant planets were studied at radio, infrared (IR), visible and ultraviolet (UV) wavelengths by instruments on the Voyager probes. More detailed measurements of Jupiter were obtained by the Galileo Orbiter. The impact of the comet Shoemaker–Levy 9 with Jupiter’s atmosphere (1994) resulted in ejection of material from Jupiter which was studied by Earth-based instruments. Initially it was thought that the water detected in this way was from Jupiter but it proved difficult to establish how much material came from Jupiter and how much from the comet. The Galileo probe used a mass spectrometer and other instruments to sample the atmosphere from the 0.5 bar level to the 21 bar level.

As the Galileo probe sampled the atmosphere directly, you might consider the results from this probe to be definitive. However, the probe only entered Jupiter’s atmosphere at one point and there is no guarantee that the atmospheric composition at this point is the same as the average composition. Indeed it has been suggested that the probe entered the atmosphere at a site which was particularly dry, i.e. lacking in water. Earth-based and space telescopes have also provided valuable information. All these sources of evidence have to be considered when putting together a picture of the nature of the atmosphere.

Because of the low temperatures of the atmospheres, most elements are present as molecules rather than atoms, and most of the molecules are identified from their vibrational spectra.

- Vibrational spectroscopy was discussed in Chapter 5. What wavelength of radiation is usually associated with vibrational spectra?
- Infrared (IR).

It has been possible to detect molecules with relatively low abundances, such as ethyne (acetylene),  $C_2H_2$ , and phosphine,  $PH_3$ , through their absorption of IR radiation. These molecules act approximately as black-body emitters from layers at pressures of about 1 bar, and because the atmospheric temperatures are so low, the peak of the black-body radiation curve lies in the IR (see Box 5.5).

- What do you suppose is the source of the IR radiation absorbed?
- The planets themselves.

The more abundant ammonia and methane were first detected through their absorption of visible sunlight reflected by the planetary atmosphere and received by telescopes on Earth. Methane and ammonia are colourless gases, and their electronic spectra lie in the UV. How then can we observe them by their absorption of visible light?

In vibrational spectra in the laboratory, the lines are usually produced by each molecule going from the lowest vibrational energy level to the next highest. It is possible for the molecules to go from the lowest level to higher levels, as in Figure 6.8, but this happens less often.

If there is a very large number of molecules in the path of the radiation, as is the case for planetary atmospheres, then there are enough molecules jumping several vibrational energy levels for the corresponding spectral lines to be observed. The absorption of red light by methane in the atmosphere of Uranus due to jumps of this sort is responsible for the blue–green tinge of the planet.

So far, we have not discussed the detection of the most abundant chemical species in the atmospheres, hydrogen (as  $\text{H}_2$ ) and helium.

- Can you spot a difficulty in detecting these elements through their vibrational spectra?
- Helium occurs as atoms, and so has no bonds to vibrate and no vibrational spectrum. Molecular hydrogen has vibrational energy levels but, as you saw in Chapter 5, homonuclear diatomic molecules, such as  $\text{H}_2$ , do not have a strong vibrational spectrum.

Because hydrogen is so abundant, it is actually possible to detect weak lines originating from higher energy vibrational levels. These were first observed telescopically in the 1960s. Hydrogen can also be detected in the UV through its electronic spectrum. The detection of helium is a major problem. Its spectrum is in a part of the UV not normally covered by common instruments, and in which it is difficult to work; helium was not detected on Jupiter until the Pioneer 10 encounter in 1973. The Galileo probe mass spectrometer measured abundances of noble gases including helium. Helium abundance has also been measured indirectly by Voyager and Galileo. These methods depend on assuming that the major component of the atmosphere not accounted for, must be helium atoms.

One method used by Voyager was to look at the shape of the lines in the vibrational spectrum of, say, methane ( $\text{CH}_4$ ). One factor affecting the width of the lines is the pressure of the atmosphere. If we have direct measurements of the abundance of the major constituents of the atmosphere other than helium, then we can calculate the effect these would have on the line shape. Assuming the rest of the atmosphere is helium, we can then calculate what pressure of helium is necessary to give the observed line shape.

- Why do we assume the rest of the atmosphere is helium rather than some other atom or molecule with no suitable spectrum?
- In the absence of evidence to the contrary, we assume roughly solar abundances, and helium is the second most abundant element in the Sun.

The second method involved sending radio waves through the atmospheres from a spacecraft and detecting them on Earth. Just as a ray of light travelling from air to water bends as it enters the water, so the radio waves are bent (or refracted) by the planetary atmosphere (Figure 6.9).

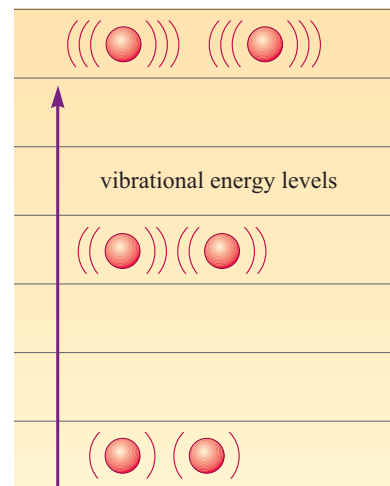
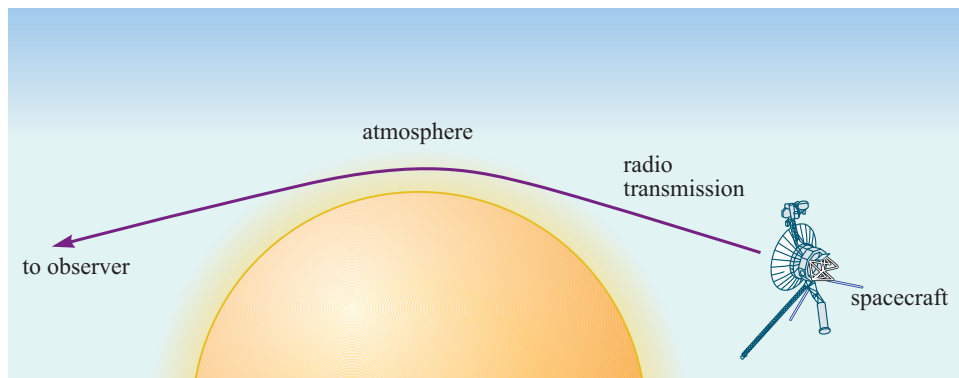


**Figure 6.8** A molecular vibrational transition to a high vibrational energy level.

**Figure 6.9** The path of the radio waves through a planetary atmosphere. The depth of atmosphere penetrated by the radio waves is exaggerated to show the deflection.



The amount by which the beam is deflected depends on the refractive index of the atmosphere which in turn depends on the average molecular mass of the gas mixture. Again, we assume that the undetected component is helium, and calculate how much helium is needed to give the average molecular mass measured. The identification of the missing constituent as helium was strengthened by the close agreement of the abundance of helium calculated by the two different methods.

The Galileo probe obtained an estimate of helium abundance from the refractive index of the atmosphere, again assuming this was a mixture of hydrogen and helium, as well as direct determination via mass spectrometry.

The first two indirect methods can also be used to estimate the temperature as both the line width and the deflection depend on temperature as well as pressure or average molecular mass. The deflection of radio waves was used by Voyager. The Galileo probe measured density and pressure. The temperature could then be obtained from these measurements using an established equation relating pressure, density and temperature. For example, let us see how the temperature can be estimated using a simple *ideal gas* model.

The ratio of the number of hydrogen molecules,  $H_2$ , to helium atoms,  $He$ , in the atmosphere of Jupiter is 0.864 : 0.136. The relative molecular mass of  $H_2$  is 2 and of  $He$  is 4 and these gases make up most of the atmosphere so that we can calculate the average molecular mass ignoring other contributions.

Since 0.864 and 0.136 add up to 1, the average molecular mass is

$$(2 \times 0.864) + (4 \times 0.136) = 2.272$$

The mass of a hydrogen atom is  $1.67 \times 10^{-27}$  kg. So the average mass of a molecule in the atmosphere of Jupiter is  $2.272 \times (1.67 \times 10^{-27})$  kg =  $3.79 \times 10^{-27}$  kg.

For ideal gases, the pressure, temperature and volume of *one mole* are related by

$$P = \frac{(1.38 \times 10^{-23}) \rho T}{m} \quad (6.1)$$

where  $P$  is the pressure in pascals,  $1.38 \times 10^{-23}$  is a constant which has the units  $J K^{-1}$ ,  $\rho$  is the density in  $kg m^{-3}$ ,  $T$  is the temperature in kelvin and  $m$  is the average mass of one gas molecule in kilograms. 1 bar corresponds to  $10^5$  Pascal. The density of Jupiter's atmosphere at the 1 bar level was measured as  $160 kg m^{-3}$ . We can thus calculate the temperature at this level using Equation 6.1.

Rearranging Equation 6.1, the temperature is given by:

$$\begin{aligned}
 T &= \frac{Pm}{(1.38 \times 10^{-23})\rho} \\
 &= \frac{10^5 \times (2.272 \times 1.67 \times 10^{-27})}{(1.38 \times 10^{-23}) \times 160} \\
 &= 440 \text{ K}
 \end{aligned}$$

Thus this ideal-gas method obtains a temperature of 440 K. In fact, Jupiter's atmosphere is not an ideal gas and in practice a more sophisticated equation is needed, and the temperature obtained is lower.

#### QUESTION 6.6

Outline reasons why it might be difficult to detect neon, Ne, in the atmospheres of the giant planets by remote methods.

#### QUESTION 6.7

At the 0.42 bar level on Jupiter, the number density (i.e. the number of molecules per unit volume) is  $2.4 \times 10^{25} \text{ m}^{-3}$ . Use this information to estimate the temperature at this level. (Note that the number density is equivalent to  $\rho/m$ .)

### Atmospheric composition

The chemical compositions of the atmospheres of Jupiter and Saturn are given in Table 6.1. The *abundance* of each molecule is given as the fraction of the total number of molecules.

**Table 6.1** Chemical composition of the atmospheres of Jupiter and Saturn.

Atom or molecule	Abundance <sup>a</sup>	
	Jupiter	Saturn
H <sub>2</sub>	0.864	0.80 to 0.85
He	0.136	0.15 to 0.20
CH <sub>4</sub> (methane)	$1.81 \times 10^{-3}$	$4.4 \times 10^{-3}$
NH <sub>3</sub> (ammonia)	$1.7 \times 10^{-10}$ to $8.6 \times 10^{-6}$	$6 \times 10^{-4}$
H <sub>2</sub> O	$(1 \text{ to } 30) \times 10^{-6}$	$(2 \text{ to } 20) \times 10^{-9}$
H <sub>2</sub> S	$<1 \times 10^{-7}$	$<2 \times 10^{-7}$
C <sub>2</sub> H <sub>6</sub> (ethane)	$(2.6 \text{ to } 8.6) \times 10^{-8}$	$2 \times 10^{-7}$
C <sub>2</sub> H <sub>2</sub> (ethyne)	$<2 \times 10^{-6}$	$1.1 \times 10^{-7}$
C <sub>2</sub> H <sub>4</sub> (ethene)	$6 \times 10^{-9}$	—
PH <sub>3</sub> (phosphine)	$1 \times 10^{-7}$	$2 \times 10^{-7}$
CO (carbon monoxide)	$1 \times 10^{-9}$	$1 \times 10^{-9}$
GeH <sub>4</sub> (germane)	$7 \times 10^{-10}$	$4 \times 10^{-10}$

<sup>a</sup> A dash indicates that the atom or molecule has not been detected. The number of significant figures given reflects the uncertainty, so that a number quoted as 2 implies that the quantity lies between 1 and 3, whereas 2.0 implies that it lies between 1.9 and 2.1.



There are several things to note that are relevant to theories of planetary evolution and to our models of the interiors of Jupiter and Saturn.

The most obvious point is that both atmospheres are predominantly hydrogen and helium, with a roughly solar ratio of hydrogen to helium. The predicted proportion of helium, assuming solar abundances, is 0.15. Another important point to note is the types of molecule found. In the atmospheres of the terrestrial planets, carbon, as you saw in Chapter 5, is found mainly as carbon dioxide,  $\text{CO}_2$ . The carbon is joined to oxygen and is said to be in an oxidized form.

- In the molecules listed in Table 6.1, what is carbon joined to?
- Mostly hydrogen (e.g.  $\text{CH}_4$ ,  $\text{C}_2\text{H}_6$ ,  $\text{C}_2\text{H}_2$ ). There is also a small amount of  $\text{CO}$ , in which the carbon is joined to oxygen but to only one atom of oxygen not two as in  $\text{CO}_2$ .

Carbon in these molecules is in a reduced form.

- Are the other elements detected present in reduced forms?
- Yes. Nitrogen is present as  $\text{NH}_3$ , phosphorus as  $\text{PH}_3$ , and germanium as  $\text{GeH}_4$ .

As we said in Chapter 5, the atmospheres of the four giant planets are reducing atmospheres. Iron oxide, for example, left in such an atmosphere would eventually be reduced to iron, with the oxygen combining with hydrogen to form water. This is in contrast to Earth's atmosphere where, as you know, iron is oxidized to an oxide – rust!

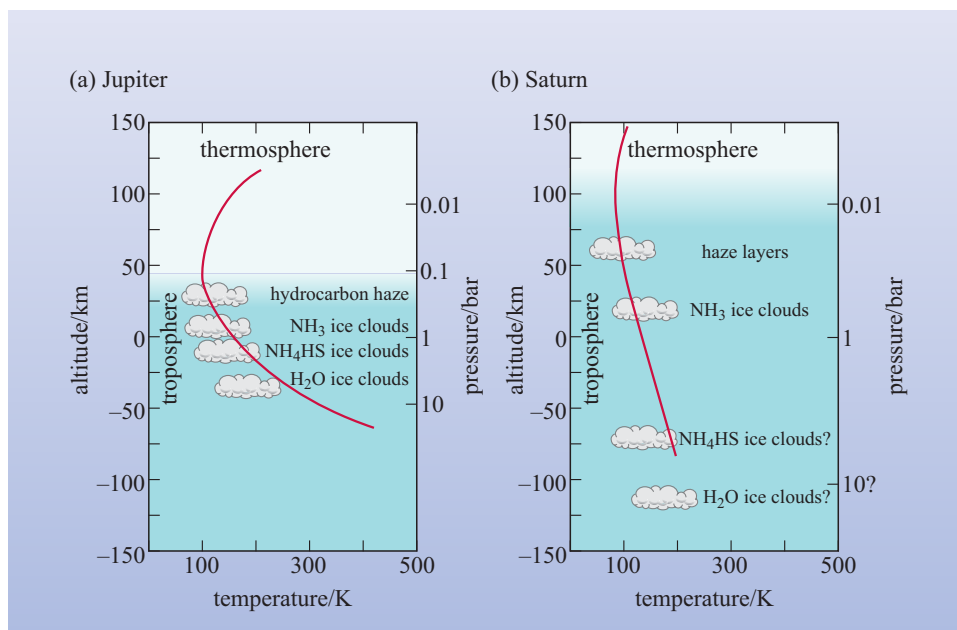
### Atmospheric profiles

Figure 6.10 shows how the temperature and pressure vary with depth in the atmosphere and the layers just below this, for Jupiter and Saturn. The curves shown are averages for the whole planet, as there are some variations in temperature from pole to equator at any one pressure.

Both curves show a fall in temperature with increasing altitude at the lower depths and an increase in temperature with altitude in the outer atmosphere. The atmospheres can thus be divided into a troposphere (dark area in Figure 6.10) and, above this, a thermosphere (pale area). In the troposphere the decrease in temperature with altitude corresponds approximately to the adiabatic lapse rate ( $1.963 \text{ K km}^{-1}$  and  $0.714 \text{ K km}^{-1}$  for Jupiter and Saturn respectively) and convection is present. The topmost layer of cloud has been identified as ammonia, and particles have been detected at the level labelled  $\text{NH}_4 \text{HS}$ , but the nature of the lower cloud layers marked in Figure 6.10 has not been definitely confirmed and is based on models of the atmosphere.

The usual way to model the lower cloud layers is as follows. It is assumed that the elements are present in their relative solar abundances. The temperatures and pressures are known so we now need to decide in what form the elements will be present – atoms or molecules, gas, liquid or solid. The atmospheres are very well mixed and have been present for a very long time, and so they would be expected to have reached chemical equilibrium in the layers beneath the clouds. **Chemical equilibrium** is explained in Box 6.3.



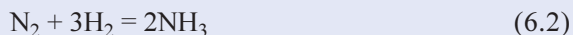


**Figure 6.10** Vertical profiles of the atmospheres of Jupiter and Saturn. Zero altitude is taken to be where the pressure is 1 bar; the profiles extend below this in those cases where measurements are available. In each case, the troposphere is dark and the thermosphere is pale.

### BOX 6.3 CHEMICAL EQUILIBRIUM

If we take a box containing a mixture of chemicals, say nitrogen, hydrogen and ammonia and leave it for a very long time, ensuring that the temperature and pressure remain constant and that no chemicals or radiation leave or enter the box, then the chemicals will reach equilibrium. At equilibrium, chemical reactions will be taking place but the total rate of production of each compound equals the total rate of its destruction so that the amounts of the various compounds present will stay the same. For any chemical reaction occurring, the relative amounts of the compounds involved that are present at equilibrium, are given by the **equilibrium constant**,  $K$ , for that reaction. The value of  $K$  varies with the temperature, but does not depend on the total amount of chemicals present.

Let us take as an example of chemical equilibrium; the reaction between nitrogen,  $N_2$ , and hydrogen,  $H_2$ , to form ammonia,  $NH_3$ :



We can put into our box any amount of nitrogen, hydrogen and/or ammonia. It does not matter whether

we start with a mixture of nitrogen and hydrogen, or with ammonia, or with a mixture of hydrogen and ammonia, so long as both elements are present in sufficient amounts. After a very long time, we will have nitrogen, hydrogen and ammonia present in equilibrium amounts. If we measured the concentrations of the three compounds at equilibrium we could obtain the equilibrium constant,  $K$ . For the reaction in Equation 6.2, the equilibrium constant is given by

$$K = \frac{[NH_3]^2}{[N_2] \times [H_2]^3} \quad (6.3)$$

where the square brackets  $[ ]$  denote concentrations and the exponents reflect the numbers in the chemical equation, e.g.  $3H_2$  in Equation 6.2 translates to  $[H_2]^3$  in Equation 6.3. The value of  $K$  is such that if the concentration of hydrogen is very much higher than that of nitrogen, as it is on Jupiter, then most of the nitrogen will be converted to ammonia. Thus we expect to find  $NH_3$  rather than  $N_2$  in Jupiter's atmosphere.

In a planetary atmosphere, there is not just one chemical reaction to consider but a very large number, and any one compound may be involved in more than one equilibrium reaction. Even in the simple case of a mixture of two elements, we have to think about all the compounds that might be formed.

For example, in the atmospheres of Jupiter and Saturn, several molecules containing just carbon and hydrogen are observed. We have to include equilibrium constants for the reaction between carbon, C, and hydrogen, H<sub>2</sub>, to form methane, CH<sub>4</sub>, ethane, C<sub>2</sub>H<sub>6</sub>, ethene, C<sub>2</sub>H<sub>4</sub>, and ethyne, C<sub>2</sub>H<sub>2</sub>. Given the equilibrium constants we can calculate the relative amounts of hydrogen, methane, ethane, ethene and ethyne. But in addition we have to consider the equilibria between carbon, hydrogen and other elements such as nitrogen and oxygen to form compounds such as carbon monoxide, CO, ammonia, NH<sub>3</sub>, and water, H<sub>2</sub>O. All these equilibria are linked so that a large number of equations have to be solved to obtain the abundances. Luckily this is just the sort of problem that computers are good at. From our knowledge of how chemicals react, we can choose, for any planetary atmosphere, a set of reactions involving the most likely molecules formed from the most abundant elements.

The calculations start where the temperature is relatively high (one very comprehensive study started at 2000 K). The equilibrium constants of all the reactions thought to be likely and the relative abundances of the elements, for example solar abundances, are fed into the computer and the relative abundances of the various possible molecules calculated. In the chosen region for starting the calculation, the temperature, as we have said, is high but the pressure is not very high so that all the icy materials will be gaseous.

We then imagine a parcel of this hot atmosphere rising into the cooler layers. As the temperature falls, the equilibrium constants change and so there is a slight reshuffling amongst the different molecules. A more dramatic change occurs when molecules condense out. Table 6.2 compares the predicted abundances of various molecules in the gas at the 300 K and 150 K levels in Jupiter’s atmosphere. The observed abundances are also given for comparison.

**Table 6.2** Predicted and observed abundances for selected molecules in Jupiter’s atmosphere.

Molecule	Predicted at 150 K (1 bar level)	Observed at 1 bar level	Predicted at 300 K (4 bar level)	Observed at 4 bar level	Observed below the 4 bar level
H <sub>2</sub>	0.89	0.864	0.89	0.864	0.864
He	0.11	0.136	0.11	0.136	0.136
CH <sub>4</sub>	6 × 10 <sup>-4</sup>	1.8 × 10 <sup>-3</sup>	6 × 10 <sup>-4</sup>	1.8 × 10 <sup>-3</sup>	1.8 × 10 <sup>-3</sup>
NH <sub>3</sub>	1.2 × 10 <sup>-5</sup>	(2 to 9) × 10 <sup>-6</sup>	1.5 × 10 <sup>-4</sup>	3 × 10 <sup>-4</sup>	7 × 10 <sup>-4</sup>
H <sub>2</sub> O	8.8 × 10 <sup>-13</sup>	<1 × 10 <sup>-6</sup>	10 <sup>-3</sup>	<1 × 10 <sup>-6</sup>	5 × 10 <sup>-5</sup> (at 12 bar) 5 × 10 <sup>-4</sup> (at 19 bar)
GeH <sub>4</sub>	~ 0	7 × 10 <sup>-10</sup>	≪ 6.3 × 10 <sup>-9</sup>	7 × 10 <sup>-10</sup>	
H <sub>2</sub> S	8.8 × 10 <sup>-13</sup>	<1 × 10 <sup>-7</sup>	2.9 × 10 <sup>-5</sup>	<1 × 10 <sup>-7</sup>	7 × 10 <sup>-6</sup> (at 8.7 bar) 7 × 10 <sup>-5</sup> (at ≈ 16 bar)

Ethane (C<sub>2</sub>H<sub>6</sub>) and ethyne (C<sub>2</sub>H<sub>2</sub>) are observed in the upper atmosphere (further out than the 1 bar level) but are not *predicted* to be present in observable quantities by this equilibrium model. The presence of these compounds can be explained by looking at the chemical reactions in the atmosphere triggered by the absorption of light.

The interaction of sunlight with methane leads to a series of reactions in which steady state abundances of ethane and ethyne are maintained. This is a similar situation to the one which maintains ozone in the Earth's stratosphere.

- Which molecules are predicted to have a very marked drop in abundance on going from 300 K to 150 K?
- $\text{H}_2\text{O}$  and  $\text{H}_2\text{S}$ .
- Why do you suppose that these molecules are particularly affected?
- These are molecules believed to form clouds at layers between 300 K and 150 K (Figure 6.10: the  $\text{H}_2\text{S}$  is incorporated into the  $\text{NH}_4\text{HS}$  cloud).

The  $\text{NH}_3$  abundance also drops, but not as dramatically because the  $\text{NH}_3$  clouds lie at or near the 150 K level.

The water and ammonium hydrogen sulfide ( $\text{NH}_4\text{HS}$ ) layers in Figure 6.10 are predicted from this type of calculation. Consider, for example, the  $\text{NH}_4\text{HS}$  layer. Ammonium hydrogen sulfide, when pure, is a white solid formed by the reaction of ammonia with hydrogen sulfide:



Equation 6.4, like all chemical reactions, has an equilibrium constant  $K$ , given by:

$$K = \frac{[\text{NH}_4\text{HS}]}{[\text{NH}_3][\text{H}_2\text{S}]} \quad (6.5)$$

and this tells us how much hydrogen sulfide must be present if the ammonia is to react and form appreciable amounts of ammonium hydrogen sulfide. The Voyager instruments failed to detect  $\text{H}_2\text{S}$ . The Galileo probe detected  $\text{H}_2\text{S}$  at lower altitudes (a relative abundance of  $6 \times 10^{-6}$  at a pressure of 8.7 bar and  $6.6 \times 10^{-5}$  at deeper levels where the pressure was 16 bar or greater). This could mean that the  $\text{H}_2\text{S}$  condenses out at a lower level than predicted, either as  $\text{NH}_4\text{HS}$  or another compound.

The Galileo probe was not able to positively identify the ammonium hydrogen sulfide and water cloud layers shown in Figure 6.10 although it made measurements down to the 21 bar level which lies below where they were predicted to be formed. The nephelometer – an instrument designed to detect the presence of particles (liquid drops or small crystals) in the atmosphere – found a tenuous cloud at the 0.5 bar level, another at 1.34 bar, a less tenuous but still thin cloud at 1.6 bar and an even more tenuous structure between the 2.5 bar and 3.6 bar levels. The most substantial of these at 1.6 bar could be the  $\text{NH}_4\text{HS}$  cloud but the chemical composition of the particles could not be determined. The density of all the measured clouds was much less than predicted by the model assuming solar relative abundances of the elements, but gave some agreement with a model in which the abundances of ammonia and particularly hydrogen sulfide were very much less than solar. It is possible, however, that the Galileo probe descended through a ‘gap’ in the clouds and that the results were atypical of the planet as a whole. Indeed, the Galileo Orbiter results indicated that lower cloud layers were patchy.



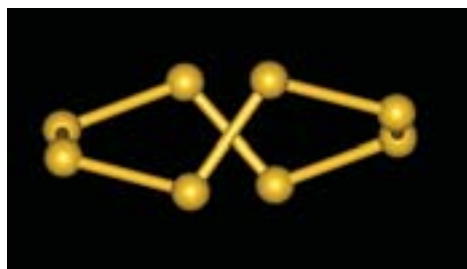
**Figure 6.11** Jupiter's clouds showing true colour.

One possible reason for the low observed abundance of  $\text{H}_2\text{S}$  lies in the colour of Jupiter's clouds (Figure 6.11). Ammonia, ammonium hydrogen sulfide and water ice are all colourless. Hydrogen sulfide can undergo chemical reactions that lead to the formation of compounds in which several sulfur atoms are joined together. Some examples of such compounds are given with their colours in Figure 6.12.

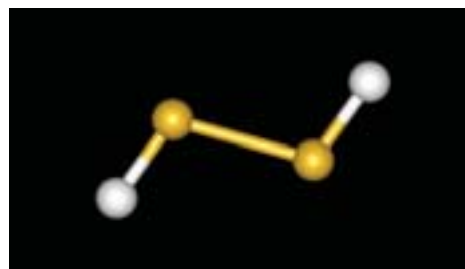
If these substances are formed it would explain both the colour of the clouds and the lack of  $\text{H}_2\text{S}$ . There are, however, other possible candidates for the origin of the colour, including phosphorus compounds and carbon compounds, and the spectral evidence is inconclusive.

#### QUESTION 6.8

Methane is a relatively abundant molecule in the atmospheres of Jupiter and Saturn. However, no methane cloud layers are predicted there. What might be the reason for this?



(a)



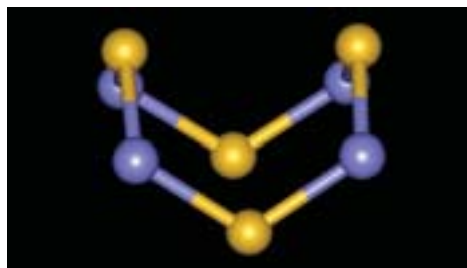
(b)



(c)



(d)



(e)

**Figure 6.12** Structures of some molecules containing sulfur chains, which are coloured. Molecules such as these may be responsible for the colour of the clouds on Jupiter. (a)  $\text{S}_8$ , (b)  $\text{H}_2\text{S}_2$ , (c)  $\text{S}_4^{2+}$ , (d)  $\text{S}_4\text{N}_3^+$ , and (e)  $\text{S}_4\text{N}_4$ . Molecules (a–d) give a yellow colour, whereas molecule (e) gives an orange colour.

### 6.3.3 Winds and storms

When we look at the giant planets through a telescope, what we see is the outermost layer of clouds, but these clouds are not stationary features. They are circulating around the planets, sometimes with speeds in excess of those found for hurricanes on Earth, and the speed changes with latitude. Wind speeds have been measured directly by the Galileo probe and by tracking clouds using images from Voyager, the Galileo Orbiter and the Hubble Space Telescope. Before we look at the results, however, you need to be clear what we mean by a wind speed on these planets.

If we wanted to measure the **wind speed** on Earth by tracking clouds, we could stand on the surface and measure the speed at which the clouds passed us. The giant planets probably do not have surfaces, and certainly no surface has been detected. So think for a moment about the speed at which clouds in our atmosphere are observed to travel by someone standing on the Earth and the speed observed by someone in a passing spacecraft.

- Would the speed of the cloud observed by the person on Earth be the same as that observed from a passing spacecraft?
- No. Standing on the surface we would be rotating with the surface so that we would measure the speed of the cloud relative to the surface. The spacecraft measurement would be with respect to a point outside the Earth and so would include the Earth's motion relative to the spacecraft due to its rotation as well as that of the cloud with respect to the surface.

From cloud images of Jupiter we obtain the speed relative to the spacecraft or telescope. So how are we going to allow for the rotation of the planet?

An ingenious method has been employed to measure the rotation of the planetary interior. Around the planets are charged particles, electrons and ions – the ionosphere which you will study further in Section 6.3.4. These particles are accelerated by the magnetic field of the planet and, as a consequence, emit radiation. Because the axis of the magnetic field is inclined to the rotation axis, the electrons and ions experience a magnetic field that varies with the planet's rotation. This leads to bursts of radiation whose interval gives the rotation period and thus the expected speed of rotation at the 'surface' (1 bar level). The period of rotation of all four giant planets has been measured in this way by monitoring bursts of radio-frequency radiation. Figure 6.13 shows the intensity of radio-frequency (481 kHz) emission from Uranus as a function of time for five consecutive rotations of the planet. Note that particular types of feature, for example the period of minimum intensity labelled 'bite-out', occur at the same time in each rotation. The rotation period was obtained by noting how often such a feature occurred.

As we do not have more direct measurements of the rotation periods, the values obtained using this method are used to determine wind speed.

The measured wind velocities from equator to pole are shown in Figure 6.14 for Jupiter and Saturn. The term **wind velocity** is used when we want to indicate the direction of motion as well as its magnitude (speed). Here we distinguish winds in the same direction as the rotation of the planet (positive velocity) from those in the opposite direction (negative velocity).

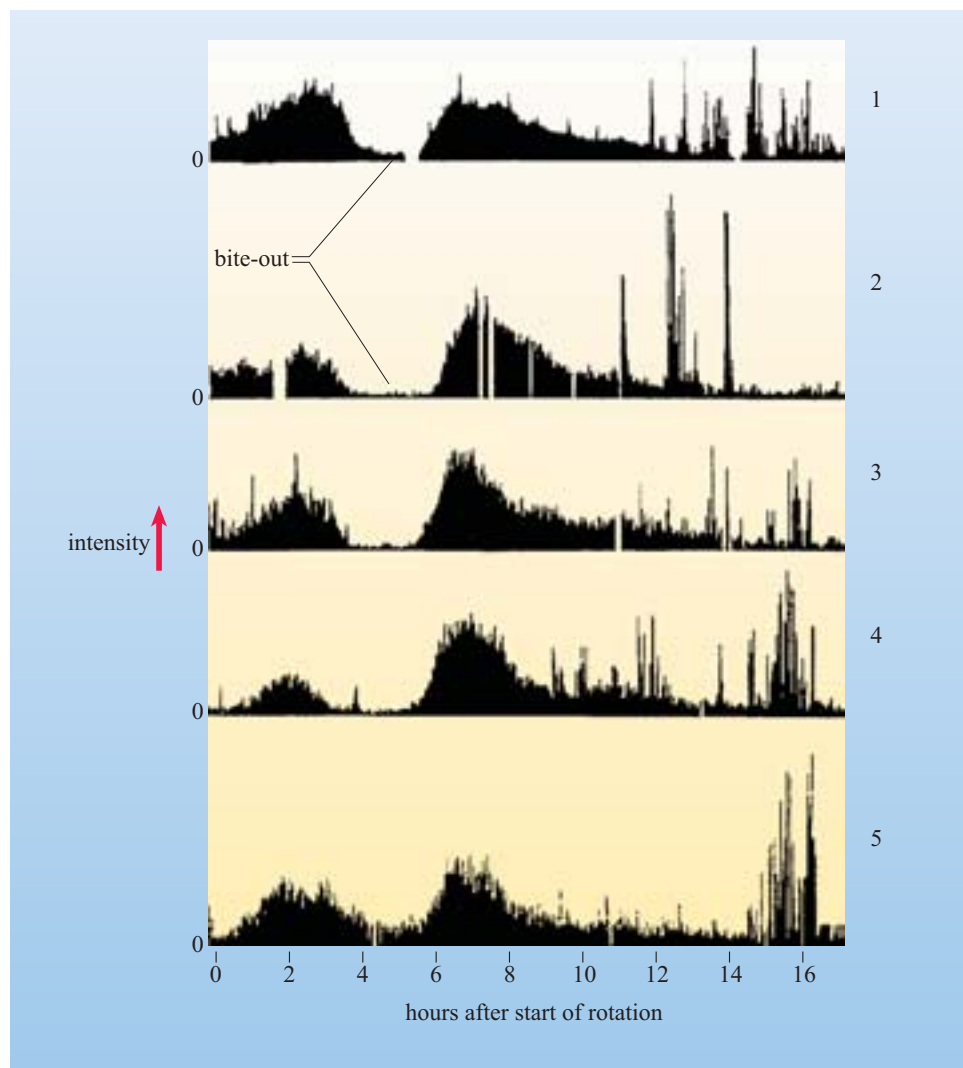


**Figure 6.13** The 481 kHz frequency emission from Uranus shown for five consecutive rotations. It is seen that the rotation period is approximately 17 hours.

The wind velocities shown were obtained by tracking cloud images. The direct measurements from the Galileo probe gave somewhat higher wind speeds for Jupiter ( $160 \text{ m s}^{-1}$  to  $220 \text{ m s}^{-1}$ ). Further analysis of Voyager images indicated that cloud features large enough to be studied from Earth interact with the prevailing wind and move more slowly than the jet stream constraining them, so that the Galileo speeds are probably more accurate. Galileo, however, only measured wind speeds at one latitude and so the data in Figure 6.14 remain the best for studying the variation of velocity with latitude.

### Jupiter

The visible layer of Jupiter shows a pattern of alternate dark and light bands parallel to the equator, called **belts** and **zones**, respectively (Figure 6.15).

It has been shown that in the dark belts the atmosphere is sinking and in the light zones it is rising. These observations lead to a picture of a series of convection cells (Figure 6.16). Convection cells, as you may recall from Chapter 5, are a feature of atmospheric motion on the terrestrial planets.

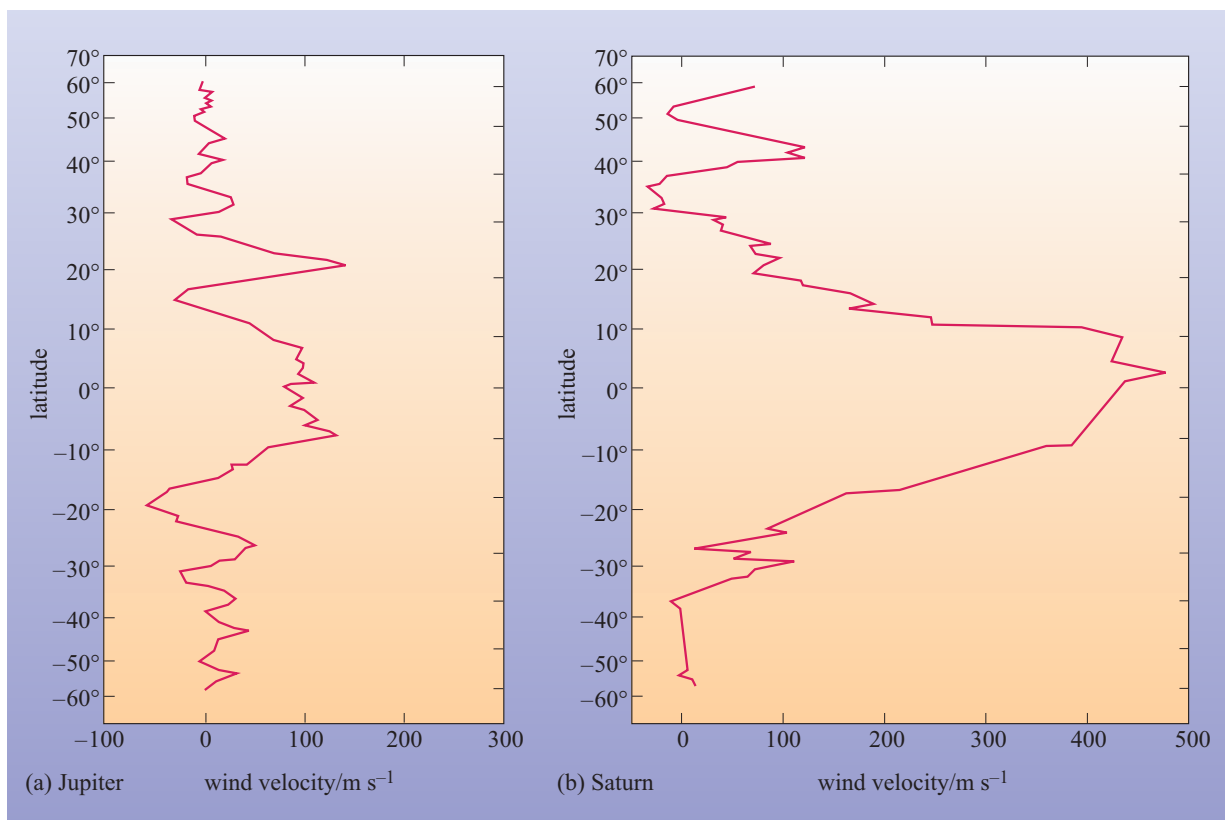


**Figure 6.14** Measured east–west wind velocities at different latitudes for (a) Jupiter and (b) Saturn.



**Figure 6.15** Close-up of Jupiter showing belts and zones.

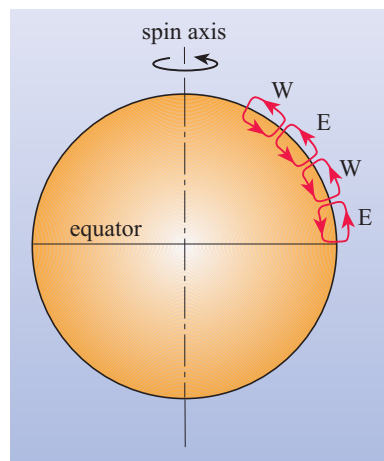


**Figure 6.16** Schematic convection cells for Jupiter. Note that the high rotation speed of Jupiter leads to a succession of small cells. E means that there is flow to the east, and W means flow to the west.



As the atmosphere rises it expands and cools; ammonia condenses out and forms white clouds, which give the zones their light appearance. The atmosphere cools radiatively and begins to sink. The atmosphere at the top of the belts therefore contains less ammonia and as it sinks it gets hotter so that the remaining ammonia does not condense out and we can see the coloured material underneath. It has been suggested that the lack of water in the region studied by the Galileo probe was a consequence of this region being one of sinking atmosphere from which water as well as ammonia had condensed out as it was rising. Subsequent remote measurements suggest that the surrounding regions contained 100 times as much water as the region through which the probe travelled.

What is driving these convection cells and why are there so many?

- On Earth, convection cells are formed when air is heated at the Earth's surface. What sources of heating are available on Jupiter?
- There is no solid surface as far as we know and certainly none in the layers where sunlight penetrates, but the cloud layers absorb solar radiation (and emit IR). The internal energy of the planet will contribute. (There is also some heat given out when gases condense to form clouds.)

For the atmospheres of the giant planets, the internal energy is the most significant source of heating. Convection would be the most efficient way of transporting this heat from the interior to the outer atmosphere. The vertical temperature profile of the troposphere shows that the rate of cooling across this region is close to the adiabatic lapse rate, so we can be fairly sure that convection cells occur here. It is possible that the cells extend deep into the interior, but we have no measurements of motion below the troposphere or of how far into the interior the troposphere extends. However the wind speeds measured by Galileo remained fairly constant with altitude and this is consistent with deep-seated convection cells powered by the internal energy of the planet.

The Coriolis effect (Section 5.6) plays a major role on the giant planets. Its role on Earth arises from the rapid rotation of the planet. Despite its greater size, Jupiter rotates more rapidly than Earth. The following question asks you to calculate the speed at which a windless atmosphere on Jupiter is moving with respect to an external non-rotating observer.

#### QUESTION 6.9

Jupiter has a radius (at the 1 bar level) of 71 490 km at the equator. Its period of rotation is 0.412 days. At what speed (with respect to a non-rotating observer in space) would a windless atmosphere at the equator be moving?

The equivalent figure for Earth is  $465 \text{ m s}^{-1}$ . The Coriolis effect is thus much greater for Jupiter than for the Earth. Whether it is sufficient to cause the banding is unknown.

One possible model considers Jupiter as a rapidly spinning, fluid sphere. Convection in the interior of such a sphere leads to a series of coaxial cylinders rotating at different speeds about the rotation axis. Each cylinder reaches the surface at a different latitude and forms a zone, as shown in Figure 6.17.

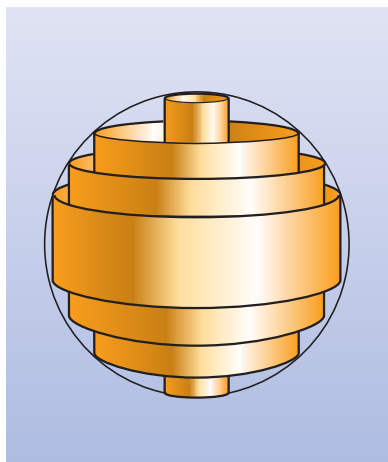


**Figure 6.17** Coaxial cylinders in a fluid sphere, which may represent the zones on Jupiter.



The observation of coherent winds as rotating circles near the north pole of Jupiter has thrown doubts on this model as an explanation for the wind patterns at high latitudes. The rotation of a cylinder that would have to go through the core of the planet could not be maintained. It is still possible, however, that winds near the equator and at mid-latitudes arise from such coaxial cylinders.

The beautiful close-up images from Voyager (Figure 6.15) enable us to see that there are also regions of turbulent motion, particularly at boundaries of zones and belts.

The most famous region of turbulent motion is the Great Red Spot.

### The Great Red Spot

The **Great Red Spot**, Figure 6.18, is a prominent feature of the Jovian atmosphere. It covers a vast area, being some 14 000 km from north to south and 26 000 km from east to west. (In either direction, it spans a distance much greater than the diameter of any terrestrial planet.) Because of its size and the contrast in colour between itself and the surrounding atmosphere, it can be observed by ground-based telescopes of only moderate power. The first record of the Great Red Spot dates from 1830, but the earliest sighting of a large spot on Jupiter is thought to be by the Italian–French astronomer Jean Cassini (1625–1712), Figure 6.19, in 1665.

Thus the Great Red Spot has been present for at least 170 years and possibly for more than 300 years. This would not be surprising if it were a surface feature, such as the mountains of Earth or Mars, but close-up time-lapse pictures show clearly that it is a region of circulating atmosphere, i.e. a giant storm. It is rotating anticlockwise about its centre and completes one rotation every six days. Its rotational energy is so great that it survives encounters with smaller storms.



**Figure 6.18** The Great Red Spot on Jupiter. The image shows a region about 40 000 km across.



**Figure 6.19** Jean-Dominique Cassini was born in Italy in 1625. In his youth, he was intrigued by astrology. Later he discarded astrology as a folly but continued to study astronomical objects, accepting a position to set up the Paris Observatory.

Close to the Great Red Spot are three white vortices (see Figure 6.18). Between the visits of Voyager and the Galileo Orbiter these drifted eastwards relative to the spot and closer together. The Great Red Spot itself has moved westwards. The features surrounding the Great Red Spot appear to be in continual change. Figure 6.20 shows the way the Great Red Spot and its surroundings have changed from 1992 to 1999.

Both Voyager and Galileo detected convective thunderstorms near the Great Red Spot. Those viewed by Voyager occurred roughly once every ten days and lasted a few days each. Voyager could not determine the altitude of the storms, but the Galileo Orbiter could. Figure 6.21 shows a thunderstorm imaged by the Galileo spacecraft on 26 June 1996. The white cloud in the centre is 1000 km across and 25 km higher than the surrounding clouds. Its base extends 50 km below the surrounding clouds, placing it at the level of the predicted water cloud.

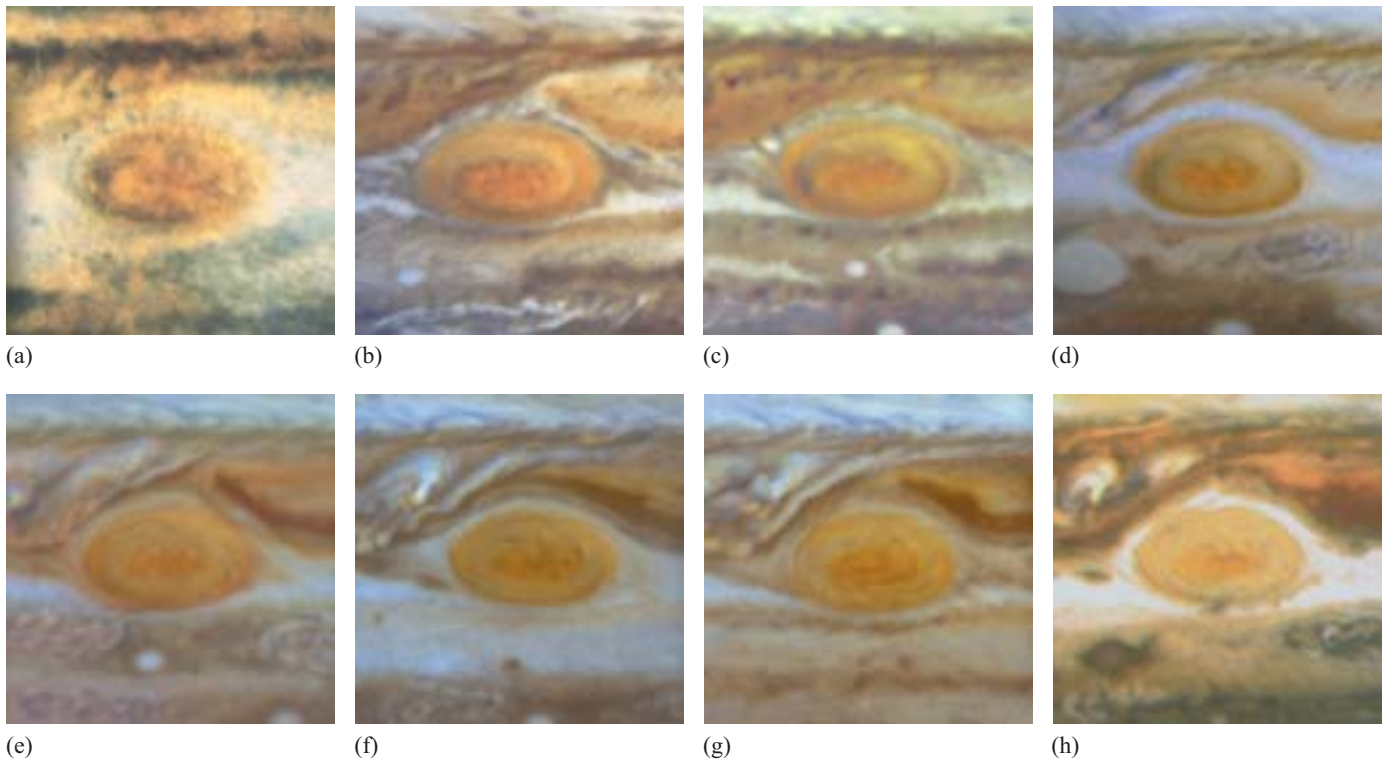


**Figure 6.20** The Great Red Spot imaged by the Hubble Space Telescope over the period 1992–1999.

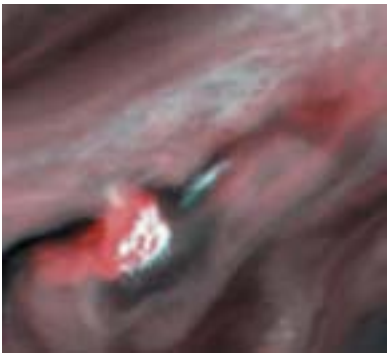


**Figure 6.21** Thunderstorm on Jupiter imaged by the Galileo Orbiter.

Computer modelling has shown that large, stable eddies can be produced regardless of the process maintaining the winds. Thus the presence of the Great Red Spot does not allow us to decide between competing models of Jupiter's atmosphere. More detailed analysis of how the Great Red Spot interacts with the surrounding atmosphere may enable us to narrow down the possible models.

There remain many unsolved problems. For example, why is there only one Great Red Spot, rather than one in each hemisphere? The colour of the spot is also puzzling. The temperature of the Spot as measured by IR techniques is the same as that of the surrounding white ovals, which are also storms. Yet on Jupiter as a whole, the coloured layers are deeper and at a higher temperature than the white clouds. Is the colour due to the same material as in the coloured cloud layers? If so, why does it occur at a different depth in the Great Red Spot?

We shall have to leave these questions unanswered and turn now to Saturn.

## Saturn

The wind pattern on Saturn is in some ways similar to Jupiter. Saturn's atmosphere is banded, and contains streams moving at different velocities. Figure 6.22 is a close-up of Saturn's atmosphere showing flow patterns similar to those on Jupiter.

The pattern is notably different from that on Jupiter, however. A major difference is the stream of very high-speed wind near the equator. As you can see in Figure 6.14, the wind speed reaches  $500 \text{ m s}^{-1}$  (which is about two-thirds of the speed of sound in that region of the atmosphere of Saturn). The highest wind speeds on Jupiter are about  $220 \text{ m s}^{-1}$ . None of the models put forward to explain the banding in the atmospheres of Jupiter and Saturn can account for this.

The other main difference is that, unlike on Jupiter, the changes in wind velocity on Saturn are not closely allied to zone boundaries. The contrast between belts and zones is much more muted. A true-colour image shows a fuzzy, orangey planet with only very faint markings (Figure 6.1b). If we enhance the contrast, the banded structure becomes apparent as in Figure 6.23.

The different colour stripes do not correlate particularly well with different wind velocities.

Eddies appear on Saturn, as for example in Figure 6.22. The largest found was 6000 km long, considerably smaller than the Great Red Spot.

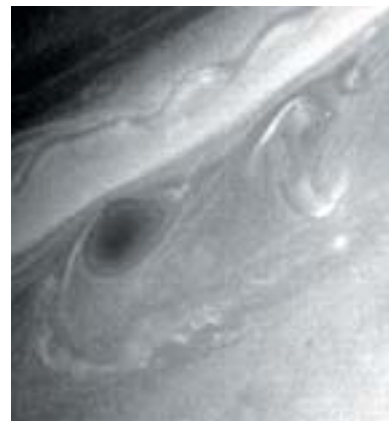


**Figure 6.22** Close-up of Saturn's atmosphere imaged by Voyager 2.

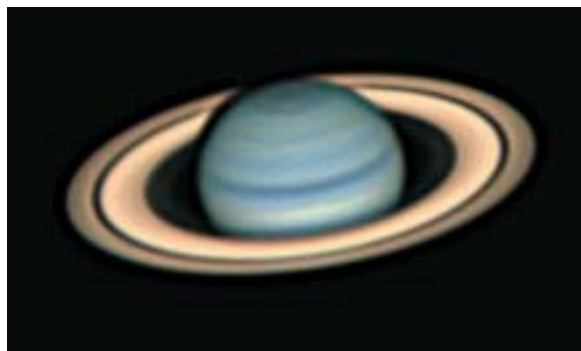


**Figure 6.23** Image of Saturn from the Very Large Telescope of the European Southern Observatory showing banded structure.



(a)



(b)



(c)

**Figure 6.24** The Great White Spot on Saturn. These images (a–c) from the European Southern Observatory show the rapid expansion of the Great White Spot during October 1990.



**Figure 6.25** Hubble Space Telescope image of Saturn showing a storm as a white arrowhead shaped feature near the equator.

In 1990, a **Great White Spot** appeared on Saturn and over the course of about a month spread to encircle the whole planet (Figure 6.24a–c). A similar feature had been observed earlier at roughly 30-year intervals (1933, 1960) but was not present when either Voyager spacecraft flew by (December 1980 and August 1981). (The 1933 sighting, incidentally, was first reported by an amateur astronomer, the Scottish comedian Will Hay.) The Great White Spot forms at the north boundary of the equatorial band, thus reinforcing the theory that such features form when two streams of different velocity meet. The atmosphere is rising in this region, and the white colour is due to ammonia crystallizing out. In 1994, a similar, but smaller, feature was recorded by the Hubble Space Telescope (Figure 6.25). There is as yet no accepted explanation for these storms.

#### QUESTION 6.10

Some of the wind velocities in Figure 6.14 are shown as negative and yet the entire atmosphere is rotating in the same direction. Explain this.

### 6.3.4 Magnetospheres

#### Jupiter

The strength of the magnetic dipole of Jupiter is about 20 000 times that of the Earth. Additionally as Jupiter is further from the Sun, the strength of the interplanetary magnetic field is less and the density of charged particles from the solar wind is lower. These two factors result in Jupiter having the largest magnetosphere in the Solar System; when the solar wind is weak the magnetopause can be 100 Jovian radii from the centre of Jupiter and the magnetotail can extend beyond the orbit of Saturn. Electrons escaping from Jupiter's magnetosphere have even been detected at the Earth. Figure 6.26 shows the main features of the Jovian magnetosphere.

Broadly, the magnetosphere resembles a greatly magnified version of the Earth's magnetosphere, but is even less like a sphere, more closely resembling a disc. As for the Earth, the magnetosphere contains ionized matter (plasma) and there are toroidal belts resembling the Van Allen belts. The Galilean satellites – Io, Europa, Ganymede and Callisto – lie within the plasma belts and are continually bombarded by charged particles.

The Galilean satellites of Jupiter are so called because they were first observed by Galileo in 1610 with the telescope he invented.

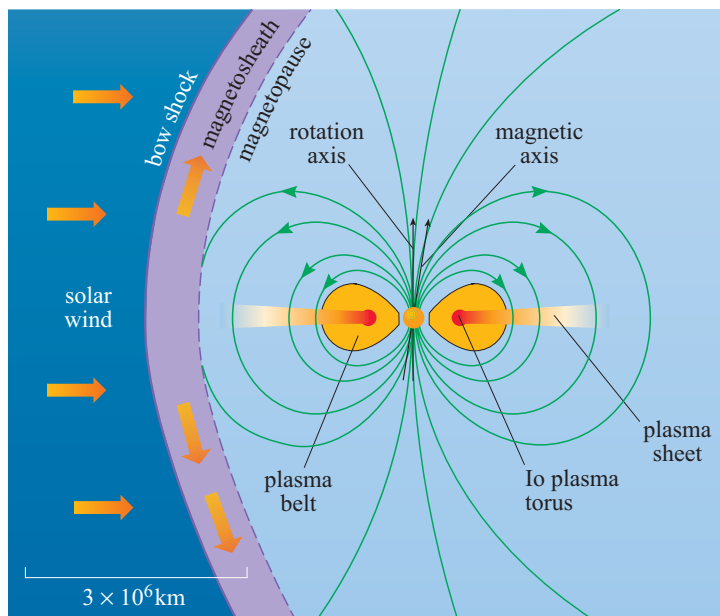


**Figure 6.26** Magnetosphere of Jupiter.

A unique feature of the Jovian system is the Io plasma torus. On the approach to Jupiter, the Voyager spacecraft detected UV emission from sulfur and oxygen ions in a torus around Jupiter which enveloped the orbit of Io. As the spacecraft flew through the plasma torus it was able to identify the ions as  $O^+$ ,  $O^{2+}$ ,  $S^+$ ,  $S^{2+}$ ,  $S^{3+}$  and an ion which could be  $SO_2^+$  or  $S_2^+$ .

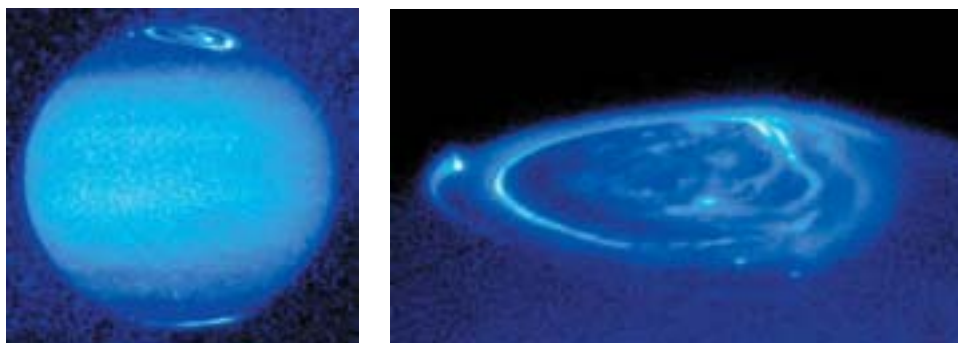
- The plasma science instrument which identified the ions did so on the basis of mass-to-charge ratio. Why could it not distinguish between  $SO_2^+$  and  $S_2^+$ ?
- These ions have the same charge and both have the same relative molecular mass of 64.

Io has a thin atmosphere composed mainly of  $SO_2$  and other molecules deriving from its volcanic activity (Chapter 3). Charged particles from the plasma heat the atmosphere, and energetic atoms and molecules are thrown out to form a neutral cloud around Io. Further interaction of this cloud with magnetospheric plasma produces the ring of plasma which stretches around Io's orbit (i.e. the plasma torus). Io is in fact a substantial source of the plasma in Jupiter's magnetosphere. As the atoms are ionized, the electron and the newly-formed ion are separated, the ions being picked up by Jupiter's magnetic field and led to the ionosphere of Jupiter. This produces an electrical current of several million amps.

- When high-energy particles enter the Earth's atmosphere, they cause atoms to be excited. What phenomenon does this give rise to?
- Aurorae. The excited atoms emit radiation when returning to the ground state. In the case of Earth, oxygen atoms and nitrogen molecules emit red, green and violet light (Chapter 5 Section 5.7).



**Figure 6.27** Auroral oval around the north pole of Jupiter imaged by the Hubble Space Telescope (left) and a close-up view (right).



The Galileo spacecraft captured images of aurorae in Jupiter's atmosphere (Figure 6.27).

- What is the most abundant molecule or atom in the atmosphere of Jupiter?
- Hydrogen,  $H_2$ .

Auroral emissions in the visible spectrum on Jupiter are mainly due to H and  $H_2$ , not O and N, and so will not be similar in colour to those seen on Earth.

Plasma particles can also excite atoms in the neutral cloud around Io. Red, green and violet light emitted by these excited atoms was imaged by the Galileo spacecraft (Figure 6.28).

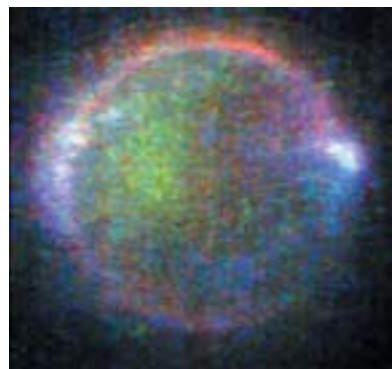


**Figure 6.28** Io's aurora imaged by Galileo spacecraft. The blue light is thought to be due to volcanic plumes.

- Which atoms might emit the red and green light in this image?
- Red and green were emitted by O atoms in the Earth's atmosphere and O atoms from the dissociation of  $SO_2$  will be present in the neutral cloud. So O atoms are probably the source.

The first evidence for Jupiter's magnetosphere came from observations of non-thermal (Chapter 5, Box 5.1) radio-frequency radiation in 1955. It was soon realized that this radio emission was due to energetic charged particles moving in a strong magnetic field and thus that Jupiter must have a significant magnetic field. Highly energetic electrons spiralling around the magnetic field lines give rise to radio emission which is beamed out from the region of the magnetic pole. Since the magnetic axis and rotation axis do not coincide, the variation of this emission can be used to determine the rotation speed of the planet as we noted in Section 6.3.3. Radio emission with a wavelength of order 10 m is modulated by Io.

### Saturn

The magnetosphere of Saturn is similar to that of Jupiter but smaller in extent and without the perturbations caused by Io. Auroral ovals have been observed in the UV region by the Hubble Space Telescope (Figure 6.29).

Unlike those on Earth, Jupiter and Io, aurorae on Saturn have not been observed in visible light.

Whether the major satellite Titan has a role in populating the plasma of the magnetosphere is debatable as its orbit means that it is sometimes outside the magnetosphere.



**Figure 6.29** Auroral ovals around both poles of Saturn imaged by the Hubble Space Telescope in the UV.

#### QUESTION 6.11

Describe the interaction that produces the bow shock of the magnetosphere for Jupiter.

## 6.4 Uranus and Neptune

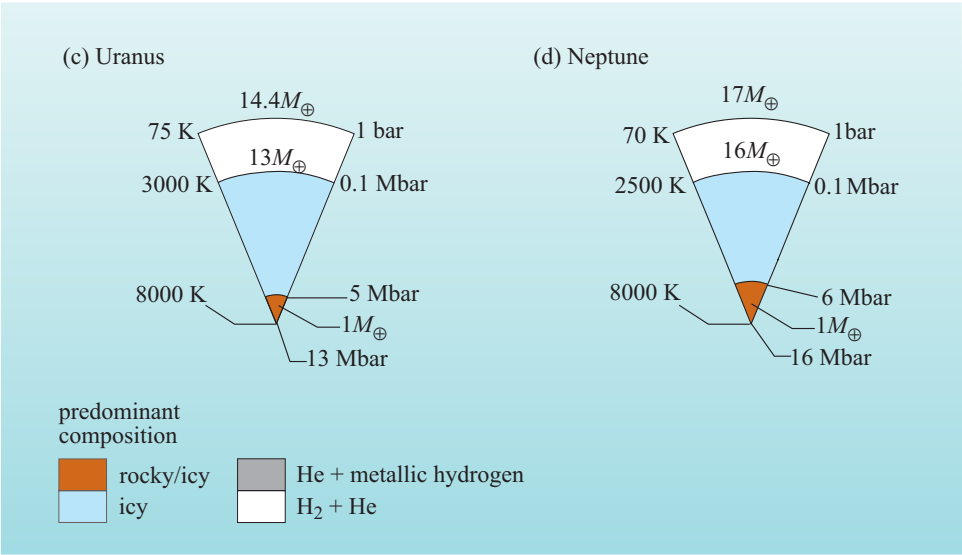
### 6.4.1 Composition and interior

These two planets are believed to be very similar to each other but different from Jupiter and Saturn. Uranus and Neptune are considerably smaller than Saturn so that their higher densities tell us that they have a higher ratio of heavier elements to hydrogen and helium.

- If Uranus and Neptune had a similar elemental composition to Jupiter and Saturn, how would you expect their densities to compare?
- The densities of Uranus and Neptune would be much lower because the smaller masses of these planets would result in less self-compression.

Theories of planetary formation suggest that Uranus and Neptune began life with rock/ice kernels, but there is no direct evidence for differentiated rocky cores today. Measurements on the gravitational field are consistent with the density increasing towards the centre, but this could be due to the increasing self-compression of icy materials. It is however difficult to use the density to distinguish between icy materials and mixtures of rocky materials, hydrogen and helium. Most models indicate that complete separation of icy and rocky materials has not occurred. However our knowledge of other bodies in the Solar System would suggest that there is a core of mainly rocky materials. The boundary between the icy layer and the hydrogen–helium layer is probably not sharp, and the model illustrated in Figure 6.30 assumes icy materials are found in the outer layers.

**Figure 6.30** Cross-sections through (a) Uranus and (b) Neptune.



The magnetic fields of Uranus and Neptune originate in a magnetic dipole source that is some way from the centre of the planet and whose axis is considerably tipped with respect to the rotation axis (Figure 6.4). When it was found that the magnetic axis of Uranus was at 60° to its rotation axis, it was suggested that Voyager may have caught the planet as its magnetic field was changing its polarity. A change of magnetic field polarity is not unknown in planetary science: the magnetic field of the Earth is known to have changed polarity many times.

When Neptune’s magnetic field was also found to be tilted, this time at 47° to the rotation axis, then it was felt there must be some other explanation as the coincidence of two planets simultaneously undergoing a change of polarity was too unlikely. Some calculations indicate that, if the electrically conducting shell is thin ( $0.1R_U$  or  $0.2R_N$ ) then the magnetic axis has to be tilted.

The position of the magnetic dipole source (roughly one-third of the way out from the centre for Uranus and just over half-way out for Neptune) puts it well outside any rocky core that may be there, in a layer believed to be mostly liquid icy materials.

A mixture dominated by water, ammonia and methane does not look a very promising candidate for an electrically conducting layer. However, experiments on water under high pressure and extrapolation to the temperatures and pressures found in Uranus and Neptune suggest that there will be much greater ionization of water in these layers than in the more familiar surroundings of the Earth’s surface. In addition, ammonia dissolved in water forms  $\text{NH}_4^+$  (ammonium) ions. The most popular view, therefore, is that the currents giving rise to the magnetic fields of Uranus and Neptune are carried by the ions  $\text{NH}_4^+$ ,  $\text{H}_3\text{O}^+$ , and  $\text{OH}^-$ .

The final line of evidence that is available is the internal heat of the planets. Uranus and Neptune have almost identical effective temperatures, despite Neptune’s greater distance from the Sun. These temperature measurements lead to the conclusion that Neptune emits more heat than it absorbs (as do Jupiter and Saturn) but that Uranus does not. The lack of a heat excess for Uranus is a problem. The two planets are in other respects very similar and so would be expected to have similar internal energy sources and indeed the presence of the magnetic field suggests a hot interior. It has been proposed that Uranus does have an internal energy source but that energy from

$R_U$  = radius of Uranus,  
 $R_N$  = radius of Neptune.



the interior is only transferred slowly to the upper atmosphere from where it can be radiated to space. The slow rate of transport may be a consequence of the unusual inclination of Uranus' rotation axis (Figure 6.4). The source of the internal energy could be heat of differentiation from the continuing differentiation of rocky and icy materials but the evidence on the current extent of differentiation is, as you have seen, sparse.

**QUESTION 6.12**

Laboratory work on a mixture of icy materials at very high pressures (around  $2 \times 10^6$  bar = 2 Mbar) has led to a suggestion that Uranus and Neptune do not have rocky cores at all but are composed entirely of icy materials plus hydrogen and helium. Does such a suggestion conflict with the observational evidence?

### 6.4.2 Atmospheres

#### Composition

The chemical compositions of the atmospheres of Uranus and Neptune are given in Table 6.3. The *abundance* of each molecule is given as the fraction of the total number of molecules.

**Table 6.3** Chemical composition of the atmospheres of Uranus and Neptune.

Atom or molecule	Abundance <sup>a</sup>	
	Uranus	Neptune
H <sub>2</sub>	$0.83 \pm 0.025$	$0.80 \pm 0.025$
He	$0.15 \pm 0.025$	$0.18 \pm 0.025$
CH <sub>4</sub> (methane)	$0.02 \pm 0.015$	$0.02 \pm 0.015$
NH <sub>3</sub> (ammonia)	—	—
H <sub>2</sub> O	—	—
C <sub>2</sub> H <sub>6</sub> (ethane)	—	$3 \times 10^{-5}$
C <sub>2</sub> H <sub>2</sub> (ethyne)	$3 \times 10^{-8}$ to $2 \times 10^{-7}$	$3 \times 10^{-7}$

<sup>a</sup> A dash indicates that the atom or molecule has not been detected.

As with Jupiter and Saturn, the atmospheres are predominantly hydrogen, as H<sub>2</sub>, and helium. The methane abundances above the cloud layers are  $3 \times 10^{-5}$  for Neptune and  $<10^{-7}$  for Uranus. The abundances quoted in Table 6.3 relate to depths below the visible cloud layers.

- What does this suggest about the composition of the outer cloud layers on these planets?
- The outermost cloud layers on Uranus and Neptune are composed of methane.

The temperatures on Jupiter and Saturn are too high for methane to condense at the atmospheric pressures of these planets, but at the lower atmospheric temperatures on Uranus and Neptune, methane will condense. Ammonia and water, the other major icy materials, have not been detected.

- Does this necessarily mean that Uranus and Neptune are depleted in ammonia and water?
- No. It is likely that these materials have condensed out at lower depths than those investigated.

### QUESTION 6.13

No oxygen-containing molecules have been detected in the atmosphere of Uranus, but this does not mean that there is no oxygen in Uranus. Why not?

### Atmospheric profile

The atmospheric profiles of Uranus and Neptune are given in Figure 6.31.

As for Jupiter and Saturn, the observed atmosphere can be divided into two regions – a troposphere and a thermosphere. The decrease of temperature with altitude in the atmosphere of Neptune is about that of the adiabatic lapse rate,  $0.853 \text{ K km}^{-1}$ . On Uranus, however, the rate of cooling is less than the adiabatic lapse rate,  $0.676 \text{ K km}^{-1}$ .

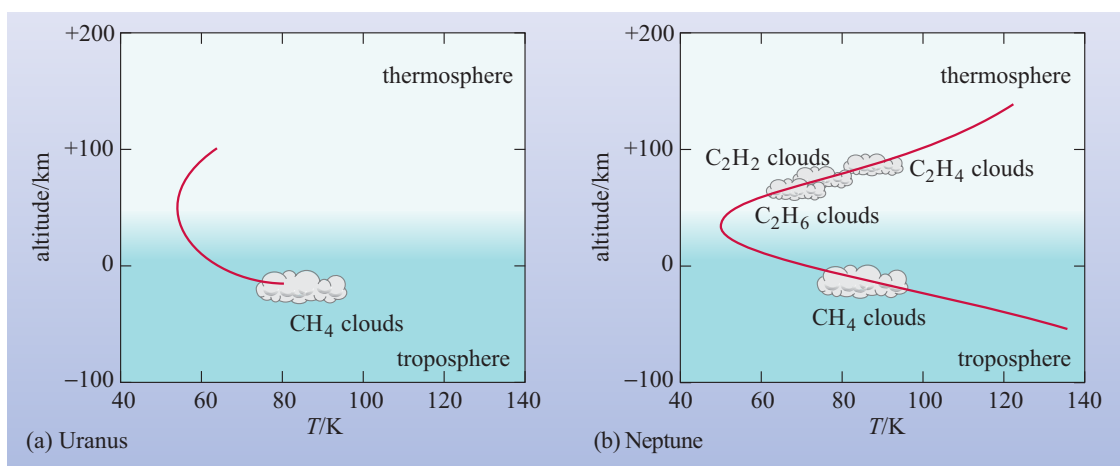


**Figure 6.31** Atmospheric profiles of Uranus and Neptune. The C<sub>2</sub>H<sub>2</sub>, C<sub>2</sub>H<sub>4</sub> and C<sub>2</sub>H<sub>6</sub> clouds are tenuous and form a ‘hydrocarbon haze’.

- If the rate of cooling is less than the adiabatic lapse rate, what does this imply about heat transfer in the troposphere of Uranus?
- Energy is not transferred through convection.

This will reduce the efficiency of heat transfer from the interior of Uranus to the outer atmosphere and this may be the cause of the low effective temperature that we noted above. Models of Uranus suggest that convection does occur in deeper layers.

In Figure 6.31 only the methane clouds and a hydrocarbon haze that lies above these clouds, have been positively identified. Models suggest that there may be a lower hydrogen sulfide (H<sub>2</sub>S) cloud.

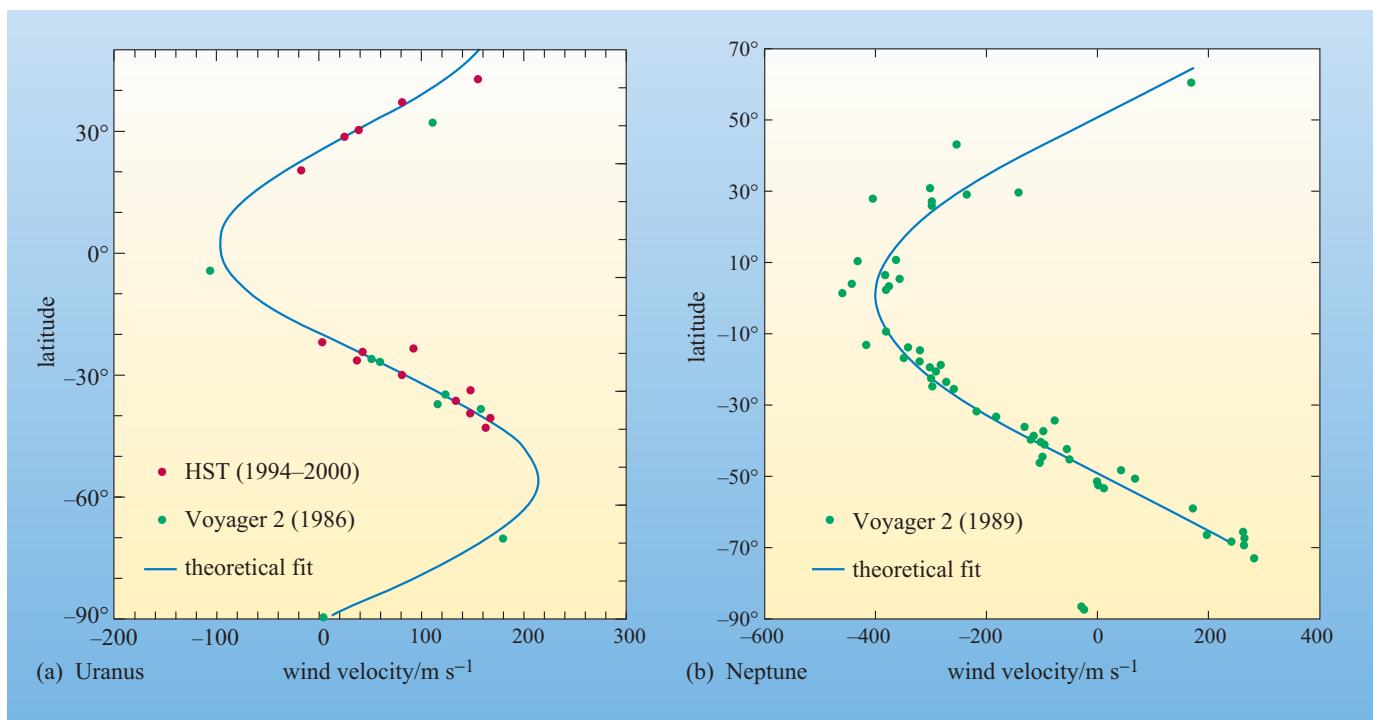


**Figure 6.32** Measured wind velocities for (a) Uranus and (b) Neptune. The curves indicate an idealized picture based on the available data.

### Winds and storms

Figure 6.32 shows wind velocities on Uranus and Neptune. As you can see from this figure, the data are much less complete and less certain than for Jupiter and Saturn (Figure 6.14).

Data on atmospheric motion on Uranus are sparse owing to the lack of discernible features (as for Venus, there is total coverage of clouds with uniform hue) so we consider Neptune first.

- Why is it important to be able to distinguish features such as spots in the cloud layers?
- In remote studies, the velocities of the cloud layers are measured by tracking features across the planet as it rotates. If the cloud layers appear uniform then we cannot track features.

Neptune, like Jupiter and Saturn, has a banded structure, in this case patterned in blue and white (Figure 6.33). Wind velocities were obtained by tracking the white clouds seen in this figure.

Unfortunately, many of the features at the time of the single Voyager fly-by (Voyager 2, August 1989) were relatively short-lived, and wind velocities obtained from small-scale, short-lived features and the longer-lived, large-scale features do not always coincide. This may be due to the small-scale features moving relative to the wind. There is sufficient information to draw some conclusions, however.

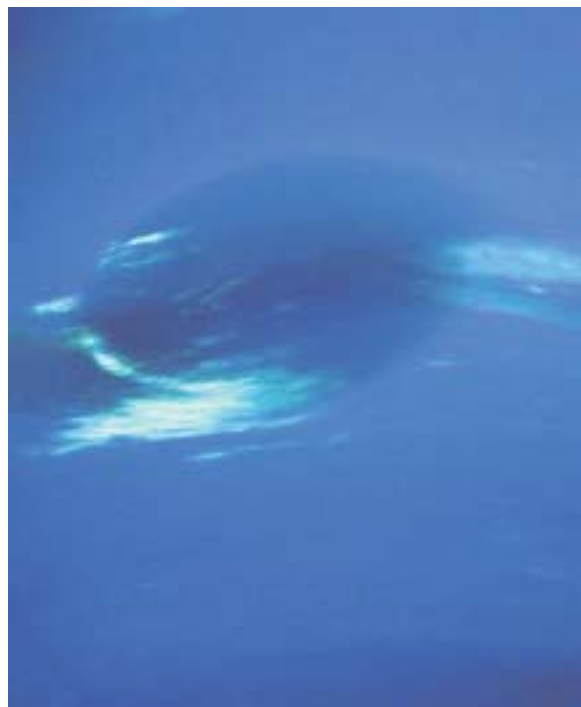
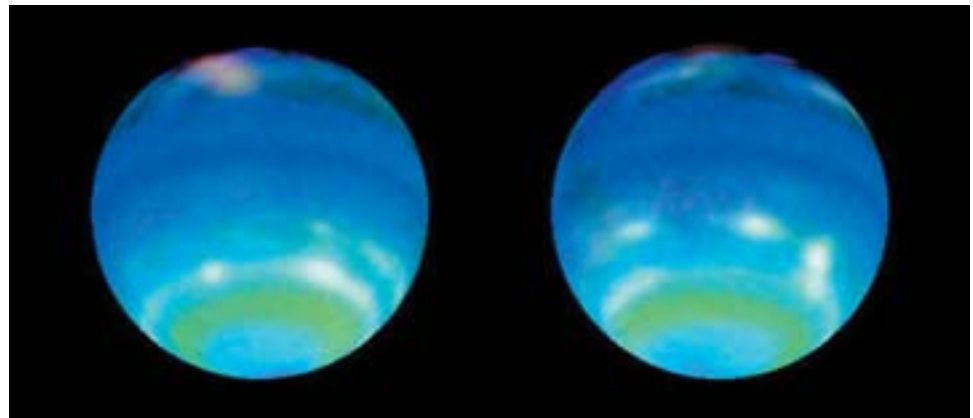


**Figure 6.33** Neptune showing bands and white cloud features.

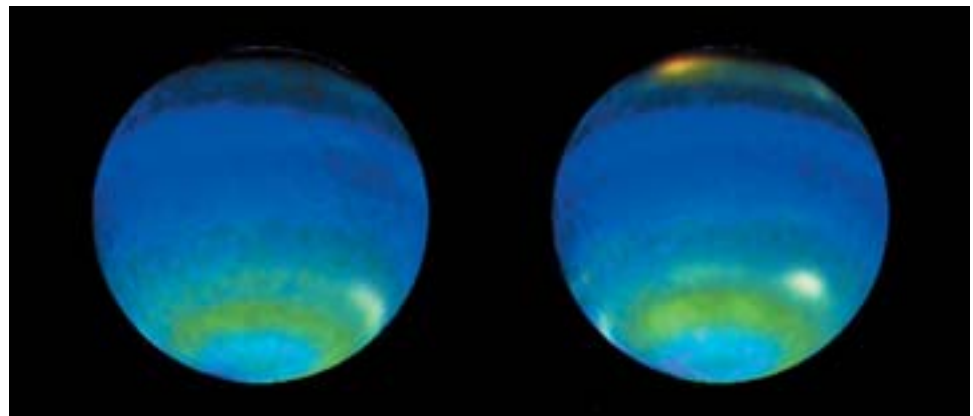
- Look carefully at the wind-velocity scales in Figures 6.14 and 6.32, and state one obvious difference between the winds on Neptune and those on Jupiter and Saturn.
- The wind velocities on Neptune, except near the poles, are negative. That is, the atmosphere is rotating more slowly than the interior.

On Jupiter and Saturn there are both positive and negative wind velocities, but the majority are positive. The equatorial wind velocity on Neptune, as well as being negative, is also very high, at least  $-300 \text{ m s}^{-1}$ . Time-lapse images obtained from the Hubble Space Telescope and the NASA Infrared Telescope Facility in Hawaii have been examined and indicate an equatorial wind velocity of  $-400 \text{ m s}^{-1}$ . It seems then that Neptune has an equatorial stream like Saturn, but in the opposite direction.

Voyager 2 observed a large dark spot, possibly a giant storm, when it passed Neptune. By 1996, Hubble Space Telescope observations showed that this had vanished and a new, smaller spot had emerged. These spots showed little visible evidence of jet streams confining them above and below, as happens with the Great Red Spot of Jupiter. Continued observations by space and ground-based telescopes have shown that large, short-lived storms are a feature of the atmosphere. Figure 6.34 for example, compares storm features in the atmosphere as imaged by the Hubble Space Telescope in 1996 and 1998.



(a)



(b)

**Figure 6.34** Views of Neptune in (a) 1996 and (b) 1998 showing how the white features associated with storms changed in this period.

A distinguishing feature of Uranus when compared to Jupiter, Saturn and Neptune, is the orientation of its rotation axis.

- Find the tilt of the rotation axis of Uranus from Appendix A, Table A1 (axial inclination).
- The planet is effectively tipped over by  $97.9^\circ$ , so that for large fractions of the Uranian year, a pole receives more solar radiation than the equator. Figure 6.35 shows the inclination to the Sun at the time of the Voyager 2 observations (January 1986).

The rotation axis of Uranus is always at the same angle to the ecliptic plane but, like the Earth and all other planets in the Solar System, the hemisphere facing the Sun varies as the planet orbits. With the rotation axis almost in the ecliptic plane, Uranus at some times in its orbit has a pole facing the Sun and at other times the equator faces the Sun. When Voyager 2 passed, the south pole was facing the Sun but after one-quarter of an orbit, the equator would be facing the Sun. When a pole is facing the Sun, rotation about the rotation axis does not move the other pole into the sunlight, but when the equator is facing the Sun all the planet receives some solar radiation. Averaged over the 84-year orbital period, Uranus receives more solar energy at the poles than at the equator. This could lead to a convection cell originating at the pole and producing negative wind velocities at mid-latitudes through the action of the Coriolis effect.

- What other features of Uranus might cause the pattern of atmospheric circulation to differ from that on the other three giant planets?
- Uranus has a negligible heat excess. The internal heat source may be a significant factor in atmospheric circulation.

At the time of the Voyager 2 fly-by, Uranus appeared to be enveloped in a blue–green fog in which virtually no features are discernible, as in Figure 6.1c. In false colour (Figure 6.36) it is possible to make out a banded structure similar to those on the other three giant planets. Note that the banding runs parallel to the equator as on the other giant planets, despite the unusual tilt of the rotation axis. Such methods made it possible to find a few features, such as small spots, which were used to obtain wind speeds, but only for latitudes greater than  $20^\circ$  and only in the southern hemisphere. More recent images from the Hubble Space Telescope (Figure 6.37) have identified about 20 clouds.

These clouds have been tracked using the Hubble Space Telescope and the Keck 10 m telescope in Hawaii and wind velocities were obtained for the northern hemisphere as well as the latitudes studied by Voyager 2. Figure 6.32 showed the wind velocities obtained from all three sources. The measured velocities are almost all positive. Extrapolation as indicated in Figure 6.32 suggests negative velocities within  $20^\circ$  of the equator. As with the other giant planets, wind speeds can be very high, up to  $200 \text{ m s}^{-1}$ . The orange feature seen on the white band in Figure 6.37, for example, is moving at  $140 \text{ m s}^{-1}$  relative to the planet.

**Figure 6.37** Enhanced colour image of Uranus in 1998 from Hubble Space Telescope.

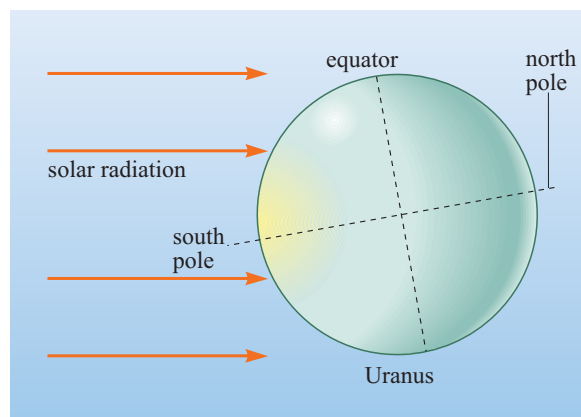


**Figure 6.35** The tilt of Uranus, showing how one pole receives more solar radiation than the equator at certain times during the planet's year. Uranus was at this point in its orbit when Voyager 2 passed by.

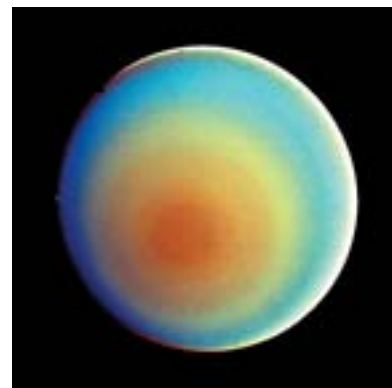


**Figure 6.36** Uranus in false colour showing banded structure, imaged by Voyager 2.



### 6.4.3 Magnetospheres

As well as discovering the unusual tilting and position of the magnetic dipoles of Uranus and Neptune, Voyager 2 also mapped their magnetospheres. These have the same main features as those of Earth, Jupiter and Saturn:

- a bow shock where the solar wind and the interplanetary magnetic field (IMF) are resisted by the planetary magnetic field,
- a magnetopause,
- a plasma sheet,
- radiation belts forming a torus around the magnetic equator,
- an extended magnetotail.

The magnetic fields of the planets are aligned by the magnetic dipole (Figure 6.4) but the planets are rotating rapidly about their rotation axes. Since the angle between the rotation and magnetic axes is large, the planetary magnetic field is constantly changing with respect to the IMF and the field lines in the magnetotail are wound into a corkscrew. Figure 6.38 shows the magnetospheres as they were at the Voyager approach. Note the positions of the magnetic poles and the radiation belts relative to the solar wind.

Aurorae have been detected for Neptune but do not form neat ovals round the poles.

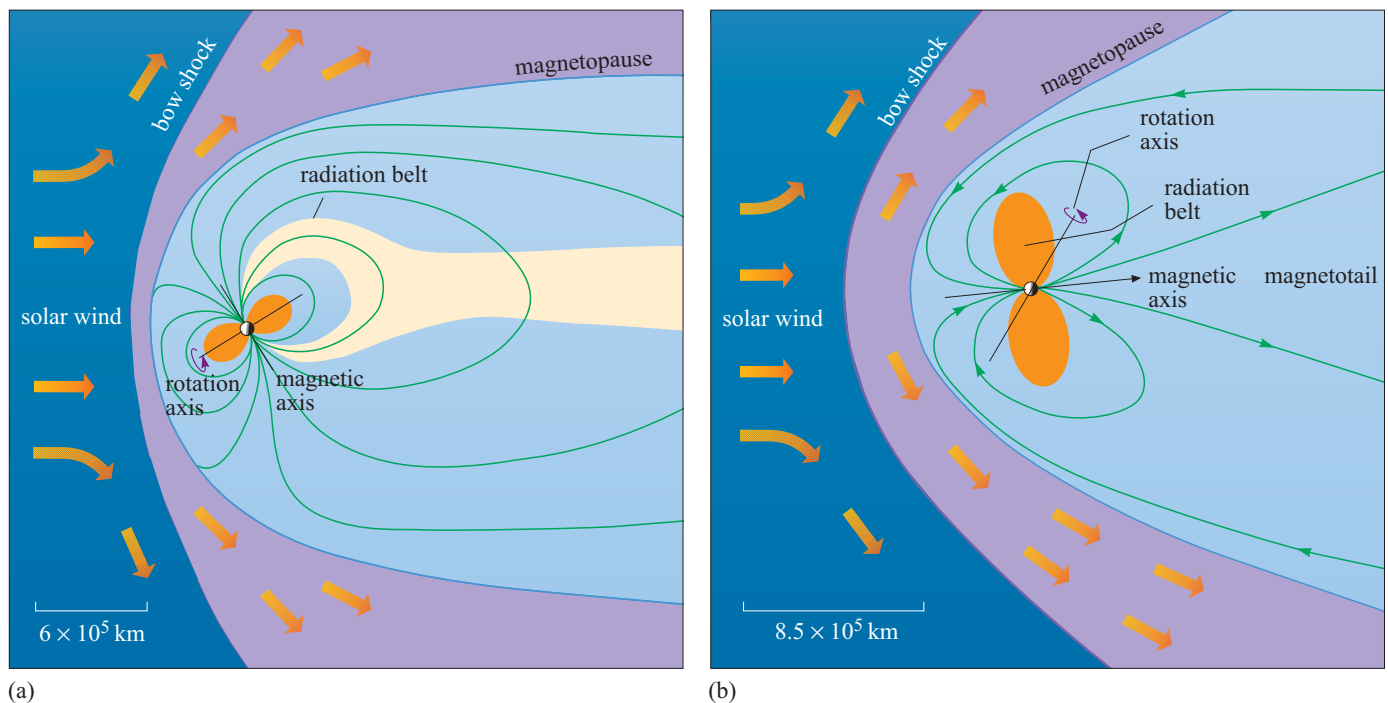


**Figure 6.38** Magnetospheres of (a) Uranus and (b) Neptune at the time of Voyager 2's approach.

**QUESTION 6.14**

Until the Voyager encounter, there was no direct evidence for the magnetic field of Uranus. If the planet did not have a magnetic field, what would its magnetosphere be like?

**QUESTION 6.15**

The average density of Jupiter is very similar to that of Rhea, the icy satellite of Saturn. Rhea is thought to be composed of one-half rocky and one-half icy materials. How is the same average density compatible with very different chemical compositions of the two bodies?

**QUESTION 6.16**

Nitrogen molecules in the atmosphere of Titan were detected by the UV spectrometer on Voyager 1. Why would it be difficult to detect the nitrogen molecules using ground-based instruments on Earth?

**QUESTION 6.17**

List some observations on heat sources and heat transport on Jupiter that must be taken into account when developing theories to explain the pattern of winds.

**QUESTION 6.18**

The Earth is protected from harmful energetic particles by its magnetosphere. Is the same true for Jupiter?

**QUESTION 6.19**

Before the Voyager 2 mission reached Uranus and Neptune, it was suggested that Uranus had a hot, molten, rocky core, which gave rise to a magnetic field, but that the core in Neptune was solid and so Neptune would have no magnetic field. How far does this model fit the current observational data? (Consider magnetic field measurements and other measurements.)

**QUESTION 6.20**

Given the composition of the atmospheres of Uranus and Neptune, which atoms might give rise to auroral emissions on these planets?

---



## 6.5 Summary of Chapter 6

- Data on the interiors of the giant planets can be obtained from measurements of density, gravitational field, magnetic field, emitted heat and atmospheric composition.
- Jupiter and Saturn probably do not have a definite liquid or solid surface. Current models of Jupiter and Saturn distinguish five layers. The two innermost layers constitute a core of rocky and icy materials. This core is surrounded by layers that are mostly hydrogen and helium, which account for most of the planets' mass. The layer adjacent to the core in Jupiter and Saturn is predicted to contain hydrogen in a metallic state. The deep interiors of both Jupiter and Saturn are very hot (over 15 000 K in the case of Jupiter).
- Uranus and Neptune may not have a definite liquid or solid surface. They may have rocky cores but current models suggest that rocky and icy materials are not completely differentiated. Surrounding the core is a mantle of mainly icy materials and around this is a layer of mainly hydrogen and helium. Overall, these two planets are less dominated by hydrogen and helium than Jupiter and Saturn and the layers are probably less differentiated in composition.
- Jupiter, Saturn and Neptune emit more energy than they receive from the Sun (heat excess). The heat excess of Jupiter is thought to be due to the continuing escape of original accretional heat and heat of differentiation. Saturn's heat excess is thought to have an additional contribution from helium droplets separating out from metallic hydrogen and sinking. Neptune and Uranus are both thought to have internal energy arising from continuing heat of differentiation. The cause of the heat excess for Neptune is still debatable. The cause of the lack of heat excess for Uranus may be associated with its unusual spin-axis inclination.
- The magnetic fields of Jupiter and Saturn are believed to originate in the shell of liquid metallic hydrogen. The magnetic fields of Uranus and Neptune are thought to originate in a shell of liquid icy material containing the ions  $\text{H}_3\text{O}^+$ ,  $\text{OH}^-$  and  $\text{NH}_4^+$ .
- The atmospheres of the giant planets have hydrogen,  $\text{H}_2$ , and helium as their major components. Other molecules detected are reduced forms of the heavier elements, for example  $\text{CH}_4$  and  $\text{NH}_3$ .
- Most of the molecules in the atmospheres are detected by IR or UV spectroscopy. The Galileo probe used mass spectrometry to obtain the relative abundances of molecules in the region of atmosphere it entered.
- The outermost cloud layer can be identified as ammonia on Jupiter and Saturn. Clouds of methane have been observed in the atmospheres of Neptune and Uranus.
- Models assuming chemical equilibrium can predict the composition of the lower cloud layers, but these compositions have not been positively identified by observation. The Galileo probe detected a very tenuous cloud which could be part of the ammonium sulfide cloud layer.
- The variation of temperature with depth on the giant planets divides the atmospheres into two regions. In the lower part (the troposphere) the temperature decreases the further out from the centre we go. The decrease is close to the adiabatic lapse rate, except for Uranus where the rate of decrease is slower. In the upper layers of the atmosphere (the thermosphere) the temperature increases with distance from the centre.

- Wind velocities on the giant planets are measured, remotely, by tracking the movement of cloud features. These measurements will give a velocity that includes the rotation speed of the planetary interior and so this has to be subtracted. The rotation speed of the interior can be measured from radio bursts.
- On Jupiter and Saturn, there is evidence for a series of deep convection cells giving rise to the observed pattern of wind velocities. On Jupiter, major changes in wind velocity correlate with the boundaries between different coloured bands. There is no such correlation on Saturn.
- Jupiter and Saturn have positive wind velocities at the equator. Equatorial wind velocities can be very high; up to  $500 \text{ m s}^{-1}$  on Saturn. The Galileo probe measured wind velocities on Jupiter directly. These were higher than the values obtained by Voyager but were only for one latitude. Neptune has a large negative equatorial wind velocity, and extrapolation suggests that Uranus has a negative equatorial wind velocity too.
- Jupiter, Saturn, Uranus and Neptune all have large magnetospheres produced when the solar wind and IMF interact with the planetary magnetic fields. The main features of the magnetospheres are similar to those of the Earth's magnetosphere. Io contributes to Jupiter's magnetosphere. The large angles between the magnetic and rotation axes of Uranus and Neptune cause the magnetic field lines to vary substantially with time.



## CHAPTER 7

# MINOR BODIES OF THE SOLAR SYSTEM

### 7.1 Introduction

In this chapter, you will be taking a closer look at the minor bodies of the Solar System. Although most asteroids and comets may seem relatively tiny compared to the planets, they have an important role to play in shaping the appearance of planetary surfaces. You considered this when looking at impact cratering processes in Chapter 4. Furthermore, the study of fragments of asteroids that land on the Earth as meteorites, can give us crucial information on the elemental abundances of the material that formed the solar nebula from which the planets were made. This was discussed in Chapter 2, and will be considered again in Chapter 9. Similarly, the study of comets, both remotely using telescopes, and via the dust particles that they release, gives us information about the processes involved in the formation of the Solar System. For these reasons, the minor bodies of the Solar System can be of major importance.

Before we look at the minor bodies themselves, we need to consider the orbits of bodies in the Solar System in more detail than we have up until now. This is important because, due to the gravitational influence of the planets, the orbits of minor bodies can change significantly, and rapidly enough, to transport the minor body from one region of the Solar System to another – for example, from the asteroid belt to the Earth. Understanding orbits is also the key to understanding the motion of the planets, their satellites, tidal heating process, and even the structure of the ring systems around the giant planets.

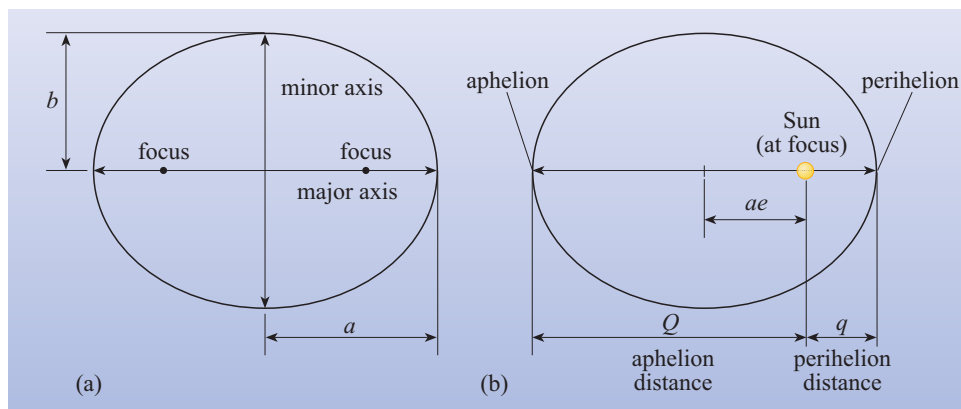
### 7.2 Orbits and Kepler's laws

The German astronomer Johannes Kepler (1571–1630) worked at a time when it was generally believed that the orbits of celestial bodies were based on circles. Complex schemes using many circles were devised to try and explain the apparent path of the planets across the heavens. However, in trying to reconcile actual observations of the movements of Mars with his notions of how he thought the Solar System should be constructed, Kepler realized that the apparent motion of Mars could be described simply by an ellipse. From this starting point, Kepler went on to formulate three laws of planetary motion, which remain fundamental to understanding the functioning of the Solar System. They apply not only to the movements of the planets around the Sun, but to all bodies orbiting under the influence of gravity. Kepler was working at a time when the absolute distances of the planets from the Sun and from the Earth were unknown, so he worked entirely in relative terms – astronomical units (you met these in Chapter 1). **Kepler's first law** states that:

Planets move in elliptical orbits, with the Sun at one focus.

An **ellipse** is shown in Figure 7.1a. The 'length' and 'width' of the ellipse are defined by the major axis and the minor axis respectively. We usually refer however to the **semimajor axis**  $a$  and the **semiminor axis**  $b$  (Figure 7.1a) which are simply

**Figure 7.1** (a) An ellipse defined by its major axis and its minor axis. (b) An elliptical planetary orbit. The Sun is located at one of the foci.



half the lengths of the major and minor axes. Two *foci* lie along the major axis (*foci* is the plural of *focus*). The positions of the foci depend on the degree of flattening (or elongation) of the ellipse. The flatter the ellipse, the further the two foci are apart. The distance of a focus from the centre is given by  $ae$  where  $e$  is called the **eccentricity** of the ellipse. The eccentricity  $e$  is a dimensionless number (i.e. it has no units) whose value can lie between 0 and 1. For a circle  $e = 0$ , whereas for an extremely flattened (or elongated) ellipse the value of  $e$  approaches 1.

Figure 7.1b shows the ellipse again, now representing the orbit of a planetary body around the Sun. We see that the Sun is located not at the centre, but at a focus (Kepler's first law). The point on the orbit that is closest to the Sun, is known as the **perihelion**, and the point that is furthest from the Sun is the **aphelion**. The semimajor axis represents the orbiting body's mean distance from the Sun. Given an orbit defined by a semimajor axis  $a$  and eccentricity  $e$ , it is useful to be able to calculate the distances from the Sun of the perihelion and aphelion points, that is the **perihelion distance**  $q$ , and the **aphelion distance**  $Q$ , respectively. These quantities are related to  $a$  and  $e$  by the following expressions:

$$q = a(1 - e) \quad (7.1)$$

$$Q = a(1 + e) \quad (7.2)$$

As  $e$  has no units associated with it, these equations will work regardless of what units  $q$ ,  $Q$  and  $a$  are in (as long as they are all in the *same* units as each other). If the value of the perihelion distance is held constant, and the eccentricity is increased, then the semimajor axis (and thus the aphelion distance) must also increase. This is shown in Figure 7.2 where a circle and several ellipses with the same perihelion distance are plotted.

#### QUESTION 7.1

Pluto has a semimajor axis of 39.48 AU and an eccentricity of 0.249. What are Pluto's perihelion and aphelion distances?

#### QUESTION 7.2

Neptune has a semimajor axis of 30.07 AU and an eccentricity of 0.009. What are Neptune's perihelion and aphelion distances?

**QUESTION 7.3**

In general, we consider Pluto to be the outermost planet in the Solar System. Considering your answers for Questions 7.1 and 7.2, is this always the case?

**Kepler's second law** is less obvious than his first. It states that:

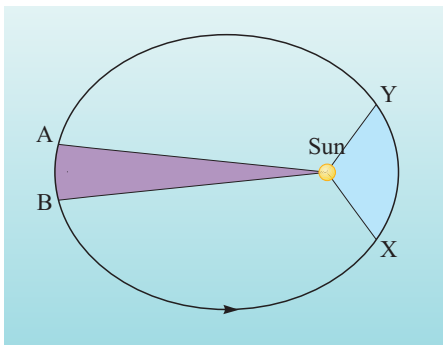
A line connecting the Sun to a planet would sweep out equal areas of space in equal times.

Figure 7.3 shows an orbital ellipse with two such equal areas highlighted. Study this figure, and think about what implications the second law has for the speed of a planet along different parts of its orbit.

- Referring to Figure 7.3, how does the speed of a planet between A and B compare with its speed between X and Y?
- If the shaded areas in Figure 7.3 are swept out in the same time, the planet must move more slowly from A to B than from X to Y.

As a planet on an elliptical orbit approaches the Sun, it speeds up. As it recedes, it slows down. The speed at any particular position depends on the distance of the planet from the Sun at that time. Similarly, bodies with larger semimajor axes move more slowly. Furthermore, a planet with a large semimajor axis has further to travel to complete one orbit. It might be expected then, that the time to complete one orbit (i.e. the **orbital period**) would be related to the semimajor axis. This relationship has been formulated as **Kepler's third law**, which states that:

The square of a planet's orbital period is proportional to the cube of its semimajor axis.



**Figure 7.3** Kepler's second law states that a planet sweeps out equal areas in equal times. Two equal areas are shown. The planet's speed along its orbit is not uniform, but varies with its distance from the Sun.

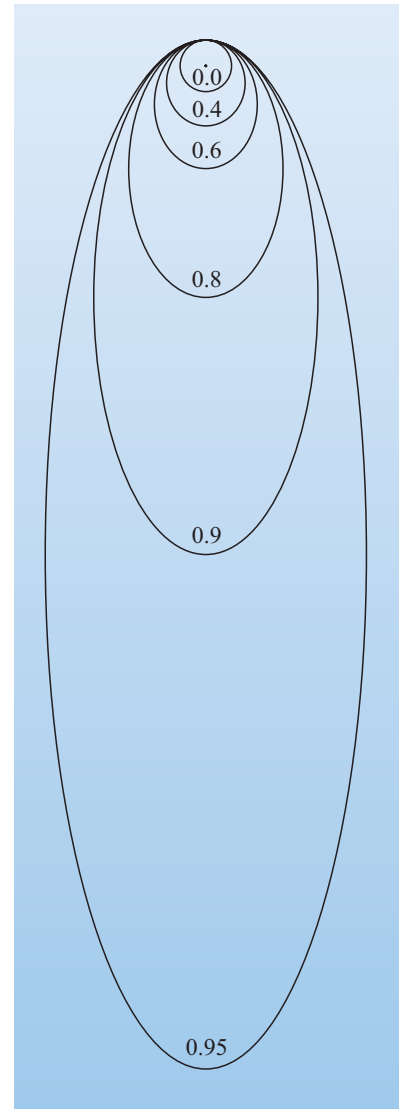


**Figure 7.2** Elliptical orbits with different eccentricities (the eccentricity value is shown). If the perihelion distance is kept constant, the semimajor axis increases as the eccentricity increases.

If we were stating Kepler’s third law mathematically, we would write

$$P^2 = ka^3 \tag{7.3}$$

where  $P$  is the orbital period and  $a$  is the semimajor axis. The constant of proportionality,  $k$ , depends on the mass of the body that is being orbited. Thus  $k$  will be the same for all planets orbiting the Sun, but will have a different value for a satellite orbiting a planet. (Indeed you used a more explicit form of this equation, given in Question 6.1 in Chapter 6, to calculate the mass of Saturn from the orbital period of its satellite Enceladus.) When considering a planet orbiting the Sun however, the numerical value of  $k$ , can be simplified by carefully choosing the units for  $P$  and  $a$ . It is most convenient to work in years, and astronomical units. As an example, consider the Earth, for which  $P = 1$  year (yr), and  $a = 1$  AU. Thus  $k$ , which is simply  $P^2/a^3$ , equals  $(1 \text{ yr})^2/(1 \text{ AU})^3 = 1 \text{ yr}^2 \text{ AU}^{-3}$ . So in doing a calculation,  $k$  can be essentially ignored as its numerical value is 1.

QUESTION 7.4

Mercury has a semimajor axis of 0.39 AU. What is Mercury’s orbital period?

Kepler’s laws apply to the motion of a small body around a large body. The small body can thus be described as being in a **Keplerian orbit**. If however other massive bodies gravitationally influence the motion (such as Jupiter influencing the orbit of Mars) then subtle modifications (called *perturbations*) to the orbit are continuously made. However, at any one moment, the Keplerian orbit is an excellent approximation to the actual motion of the body.

So far, we have defined an orbit by just two parameters, the semimajor axis,  $a$ , and the eccentricity,  $e$ . However, we also need to be able to describe the orientation of the orbit with respect to the rest of the Solar System. You will remember from Chapter 1 that the Earth and the other planets orbit the Sun in approximately the same plane. We referred to this as the **ecliptic plane**. In fact, the ecliptic plane is *defined* by the plane of the Earth’s orbit. Thus the Earth orbits *exactly* in the ecliptic plane, and the other planets orbit approximately in the ecliptic plane. However, other planetary bodies, for example asteroids or comets, might have orbits that are not confined to the ecliptic plane. This is described by a quantity called the orbital **inclination**,  $i$ . This is the angle between the plane of an orbit and the ecliptic plane, and is shown in Figure 7.4. The inclination angle is defined to be between the values  $0^\circ$  and  $180^\circ$ . Orbits that have a general motion around the Sun in an anticlockwise direction, as viewed from above the Sun’s north pole, are called **prograde**, whereas orbits that have a general motion around the Sun in a clockwise direction, are called **retrograde** (Figure 7.5).

Prograde orbits have values of inclination between  $0^\circ$  and  $90^\circ$ .  
 Retrograde orbits have values of inclination between  $90^\circ$  and  $180^\circ$ .

If you have studied some astronomy, you might recognize that the ecliptic plane is defined by the apparent motion of the Sun across the sky throughout the year.



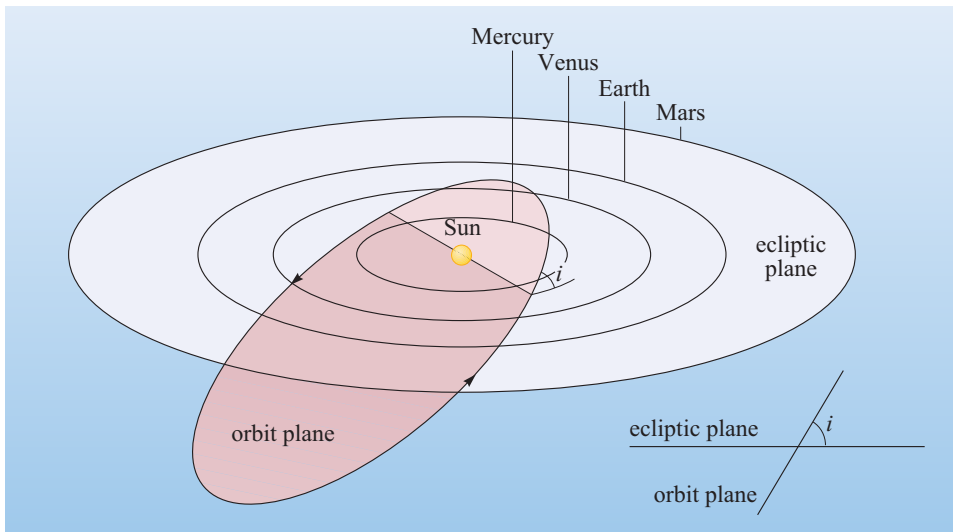


**Figure 7.4** An orbit need not be confined to the ecliptic plane but may be inclined at an angle called the orbital inclination,  $i$ .

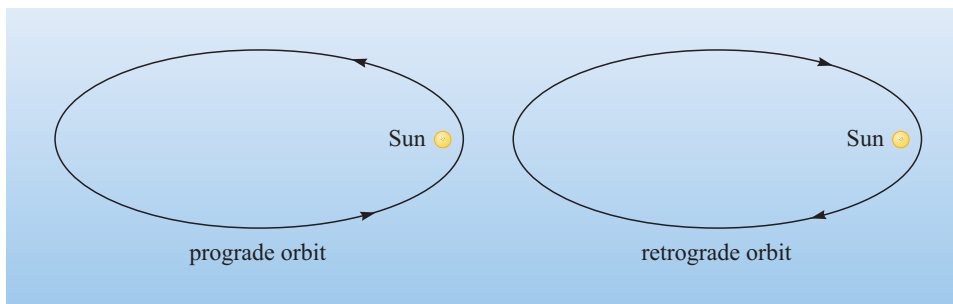


**Figure 7.5** Prograde and retrograde orbits, as would be viewed from above the north pole of the Sun. The arrows indicate the direction of motion of a planetary body on these orbits.

- If two bodies in space collide, what type of orbit does each of the bodies need to have (prograde or retrograde) to obtain the maximum impact speed?
- Just like vehicles on a road, the maximum relative impact speed occurs when there is a head-on collision. This can only be the case when one body has a prograde orbit, and the other has a retrograde orbit.

### 7.2.1 Tidal heating

Now we have looked at orbits more closely than before, we can consider in more detail, how the mechanism of tidal heating operates. You will remember from Chapters 2 and 3 that tidal heating played a crucial role in some instances. In particular, Jupiter's satellite Io is the most volcanically active body in the Solar System, and the major heat source that drives this comes from tidal heating. You considered previously a satellite orbiting a planet. For example, we can think of the Moon orbiting the Earth. The mutual gravitational pull acts to distort both the Moon, and the rotating Earth, creating tidal bulges that try to align themselves towards and away from the neighbouring body. On Earth, this gives rise to the ocean tides, and even manages to distort the shape of the Earth by around 1 m as it rotates. This continuous kneading of Earth gives rise to frictional heating (i.e. tidal heating).

However we saw previously that virtually all of the satellites of the planets have *synchronous rotation*, i.e. their rotation period equals their orbital period, such that the same face points to the planet at all times. In this case, the satellite is essentially not rotating with respect to the planet. Thus the tidal bulge produced by the gravitational pull of the planet does not move, and so does not produce a frictional heating effect in the satellite. Indeed, the satellites of the planets have reached their current state of synchronous rotation because the action of tidally-induced frictional heating, slows the rotation of the satellite down, due to rotational energy being converted to heat. The slowing continues until the satellite reaches synchronous rotation. At this point, we might expect tidal heating to stop. However it is clear that bodies like Io are undergoing significant tidal heating *now*. Why is this?

The answer lies in the effect of orbital eccentricity, and Kepler's laws. The example in Figure 7.6, shows a synchronously rotating satellite at ten places on its elliptical orbit, separated at equal time intervals (and because of Kepler's second law, equal areas are swept out in these equal time intervals). The red radial lines drawn from the planet to the satellite represent the direction of the gravitational force, and thus the line along which the tidal bulge of a satellite will act. The blue arrows show the direction of a face of the satellite. When the satellite is at its closest point to the planet, the face points along the gravitational force direction. We know that the planet will then rotate  $360^\circ$  in each complete orbit, and so during each of the ten equal time intervals, it will rotate just  $36^\circ$  (i.e. each successive blue arrow is rotated by  $36^\circ$ ). However, you can see that, as a result, for most of the orbit the face does not then precisely point along the line of gravitational force. In fact only at two points in the orbit does it do this. As the satellite orbits, the face moves 'forward' of the red line, and then moves 'behind' the red line. If you were watching the satellite while standing on the planet, you would see the face turn slightly one way for half the orbit, and then turn back the other way for the second half. This is called **libration**. As the satellite *librates*, the gravitational bulge is 'dragged' back and forth, causing frictional heating.

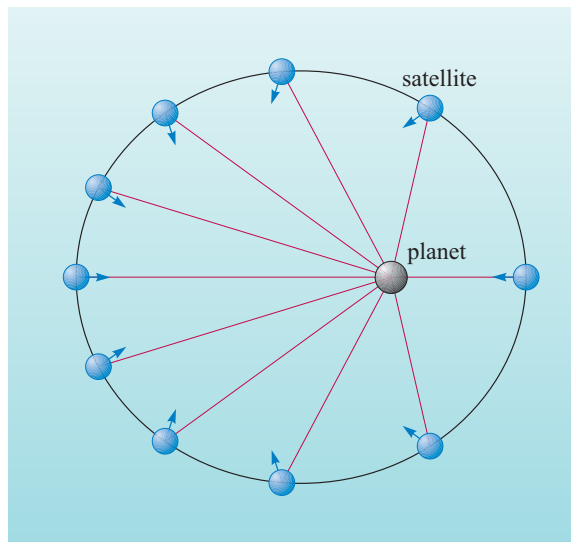


**Figure 7.6** The figure represents a synchronously rotating satellite at ten places on its elliptical orbit, separated at equal time intervals. The planet rotates  $360^\circ$  in each complete orbit, and so during each of the ten equal time intervals, it rotates  $36^\circ$  (i.e. each successive blue arrow is rotated by  $36^\circ$ ).

Thus bodies that are in synchronous rotation can undergo significant tidal heating *only* if they are in orbits that have eccentricities that are not zero. This is the case for many of the satellites of the giant planets, and this mechanism gives rise to the tidal heating within satellites such as Io.

### QUESTION 7.5

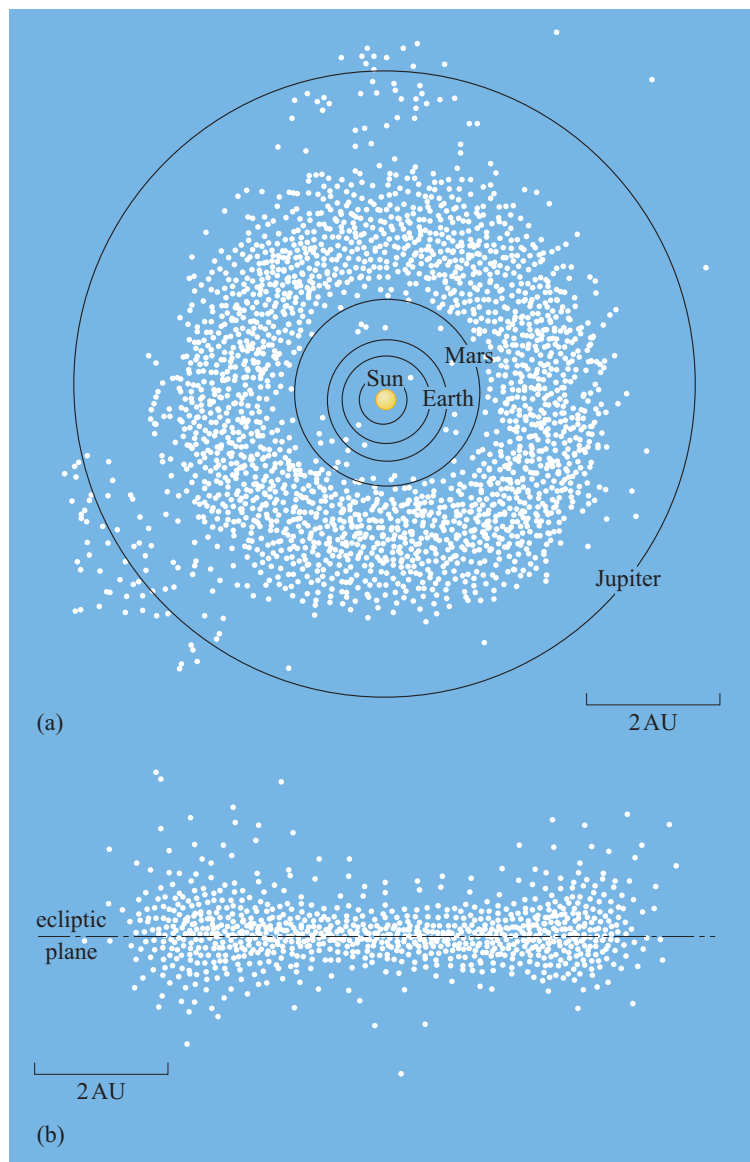
In the following cases, decide whether the satellite might undergo tidal heating.

- (a) A newly formed satellite that is in a circular orbit, and has a rotation period that is much less than its orbital period.
- (b) An ancient satellite that has acquired synchronous rotation, and has a circular orbit.
- (c) An ancient satellite that has acquired synchronous rotation, and has a significant orbital eccentricity.

## 7.3 Asteroids

Asteroids are by far the most abundant named objects in the Solar System. Over one hundred thousand asteroids have been detected, with over thirty thousand having well determined orbits, most of these occupying the **asteroid belt** between about 2 and 4 AU from the Sun (between the orbits of Mars and Jupiter, Figure 7.7). The total mass of all the bodies in the current asteroid belt is only about one-thousandth of an Earth mass, although originally, a few Earth masses of material would have been available in the solar nebula in the region. In the 19th and early 20th centuries, astronomers thought that the asteroid belt represented fragments of a single planet which had somehow disintegrated catastrophically. However the asteroids are now thought to represent fragments of *many* small planetary bodies that never managed to accrete into one single body. This is due to the strong gravitational influence of the newly formed Jupiter ‘stirring up’ the asteroid population, causing collisions which would repeatedly break up the bodies and so impede the formation of one single large object.

**Figure 7.7** (a) A representation of the asteroid belt. It is seen that the asteroid belt is actually a diffuse cloud, or swarm of orbiting bodies. (b) A cross-section through the belt, shown on the same scale. Each individual asteroid shown moves in an orbit inclined to the ecliptic plane, so that sometimes it is above it, and sometimes below. You can imagine that collisions between asteroids will be quite common.



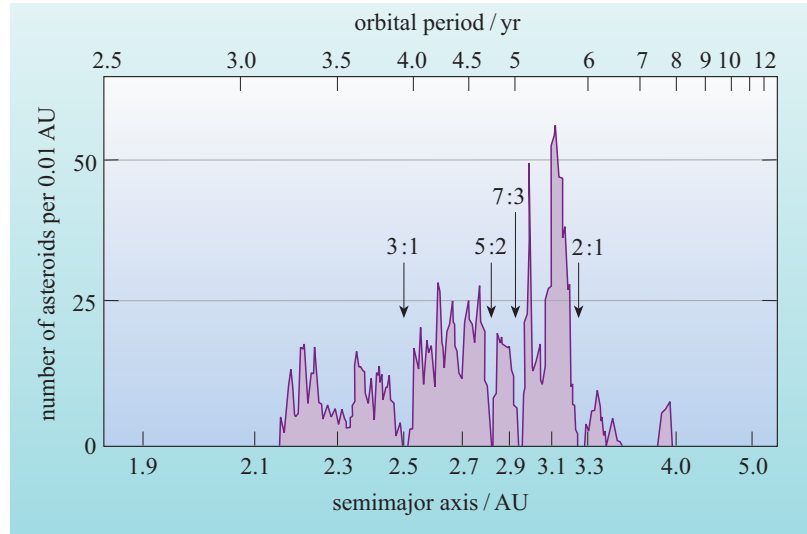


**Figure 7.8** Variations in the abundance of asteroids within the asteroid belt, showing the Kirkwood Gaps at values of semimajor axis which correspond to orbital resonances with Jupiter.

Jupiter continues to exert a strong influence on the asteroid belt. When we plot the number of asteroids with a given semimajor axis interval against semimajor axis, a striking pattern emerges, as shown in Figure 7.8. There are spaces, or gaps, where there are very few asteroids with a particular value of semimajor axis. These gaps, known as **Kirkwood Gaps** after their discoverer, are not random. They occur when the orbital period associated with a given value of semimajor axis, is a simple fraction of the orbital period of Jupiter. This is known as **orbital resonance**. For example, if an asteroid had an orbital period half that of Jupiter, then it would be said to be in a 2 : 1 resonance (we say, ‘two-to-one resonance’), i.e. it makes two orbits around the Sun for every one Jupiter makes. Sometimes you can confuse yourself depending on whether you think in terms of the asteroid’s period being half that of Jupiter, or Jupiter’s period being double that of the asteroid. It is of course the same thing, but it can cause people to be confused as to whether to write 2 : 1 or 1 : 2. One way to avoid confusion is to consider the number of times the bodies make complete orbits of the Sun. Then use an often followed convention where, the number on the left side signifies the number of orbits that the body *closer to the Sun* would make in a given period of time, and the number on the right signifies the number of orbits the body *further from the Sun* would make in the same time. Thus the number on the left will be larger than the number on the right.

We can readily calculate the value of the semimajor axis associated with an object in the 2 : 1 resonance using Kepler’s third law. We know that Jupiter has a semimajor axis of 5.20 AU (from Appendix A, Table A1) and thus an orbital period of 11.86 years (using  $P^2 = ka^3$  from Section 7.2). So an object in the 2 : 1 resonance has an orbital period one-half of this, i.e. 5.93 years, which corresponds to a semimajor axis of 3.28 AU.

**QUESTION 7.6**

At what semimajor axis value, would you expect to find a gap in the asteroid belt semimajor axis distribution corresponding to a 3 : 1 resonance with Jupiter?

The effect on a small body that is orbiting the Sun, and is also in orbital resonance with a large body, can have two outcomes. For the small body in the resonance, there will be times when it is being accelerated forward in its orbit by the gravitational pull of the larger body, and other times when it is being decelerated. The cumulative effect of these forces is to distort the orbit of the smaller object, until it no longer has a resonant period, and its former orbit remains unoccupied. This is the process at work to produce the Kirkwood Gaps, where many of the resonances are cleared of objects. However, another possible outcome of some resonances, is that the small object gets locked into its orbit, and the gravitational influence of the larger body essentially holds the smaller object in its orbit for long periods of time. These *stable resonances* can be very important, and we will return to this point in Section 7.4.

**QUESTION 7.7**

If you travelled to the distance from the Sun equal to the semimajor axis associated with a Kirkwood Gap, might you find any asteroids there? (*Hint*: think about the effect of orbital eccentricity.)

The changing of a body's orbital elements (or orbital parameters) is called **orbital evolution** and is the key to understanding the distribution of various minor bodies throughout the Solar System today. Orbital evolution means that over time (this could mean thousands or millions of years) a minor body could change its orbit significantly within the Solar System. A good example where orbital evolution is critical, is in the *Near Earth Asteroid* population.

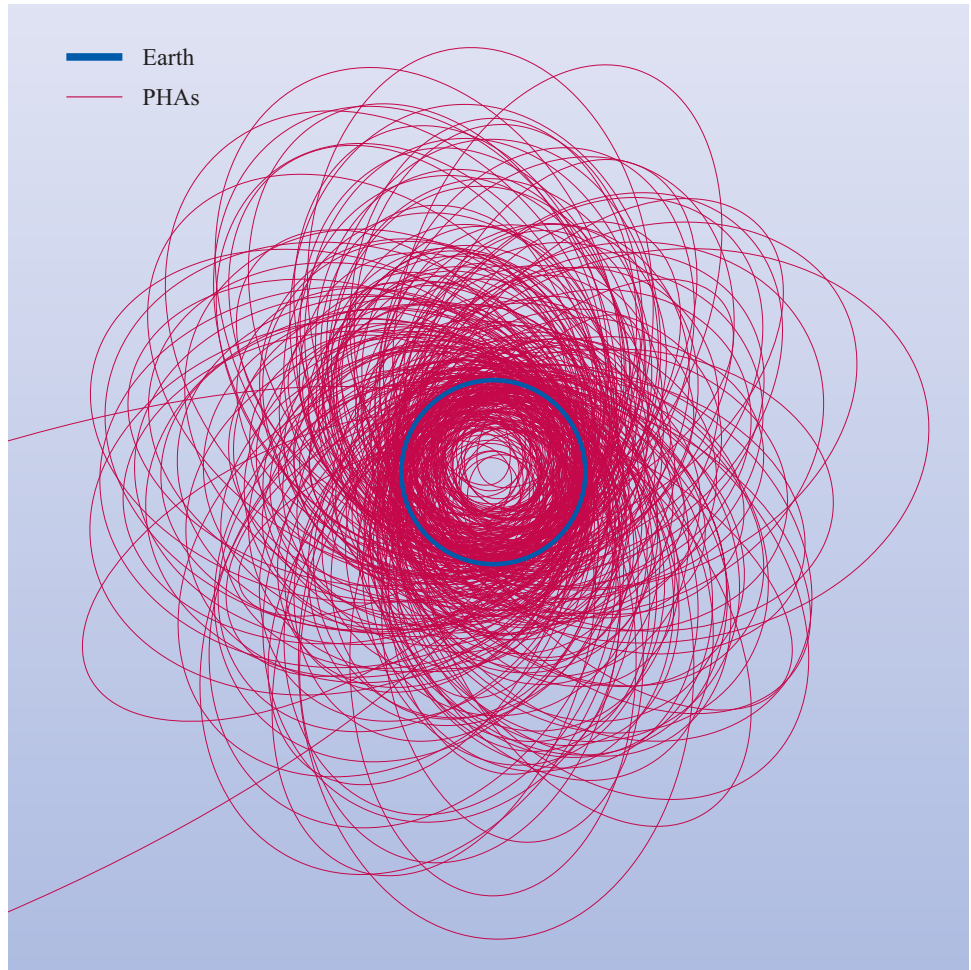
**Near Earth Asteroids** (NEAs), are bodies that have orbits which come near (or indeed cross) the orbit of the Earth. You might have already noticed a few of these objects in Figure 7.7. There are almost 2000 NEAs currently known. Some objects in the NEA group can come very close to the Earth, and could collide with the Earth at some time in the future. This subset, of which around 400 are currently known, are called **Potentially Hazardous Asteroids** (PHAs). Figure 7.9 shows the orbits of known PHAs in relation to Earth's orbit. Looking at the PHA orbits, it is perhaps not surprising that the Earth occasionally suffers an asteroid impact!

It is thought that some members of the Near Earth Asteroid population might in fact be more related to comets, and so you may see reference to Near Earth Objects (NEOs) instead of Near Earth Asteroids (NEAs).

■ Today, well over 4 billion years after the origin of the Solar System, there are still numerous asteroids that could collide with the Earth. The lifetimes of these asteroids must be short relative to the age of the Solar System, because they are rapidly removed by collisions with the terrestrial planets. What does this imply?

□ The supply of Earth-crossing asteroids must somehow be replenished.

**Figure 7.9** The orbits of known Potentially Hazardous Asteroids (PHAs). The orbit of Earth is also shown.



The very fact that we see NEAs today, means that the NEA population is being continually replenished, and this happens because of the orbital evolution of objects in the inner asteroid belt. The long-term gravitational effects of Jupiter (and even Mars) give rise to a slow ‘conveyor belt’, which delivers bodies to the inner Solar System (although you should also appreciate that it can be a two-way process – bodies that are already in the inner Solar System can evolve outwards again). Some of the objects that make it into the inner Solar System might eventually hit one of the terrestrial planets.

### 7.3.1 Asteroid sizes

The largest main belt asteroid, discovered in 1801, is (1) Ceres (pronounced ‘series’) which has a diameter of 913 km. The next biggest is (2) Pallas, with a diameter of 523 km. (Note that the asteroids are numbered, and so the full name is, e.g. (1) Ceres, although often, you will see only the name being used.) As we go smaller and smaller, the asteroids become more numerous. So while there is only 1 asteroid larger than, say, 600 km (i.e. Ceres), there are 7 larger than 300 km, 81 larger than 150 km, and so on. Note that for each reduction in size the number rises steeply. This behaviour is described by a size distribution. This concept will sound familiar to you after considering impact crater size–frequency distributions in Chapter 4 (Box 4.1). It is exactly the same concept, except we are now thinking in terms of asteroid diameter rather than crater diameter.



Figure 7.10 shows the cumulative size distribution of known asteroids in the asteroid belt. We see that there are many more small asteroids than large ones. The data ‘flattens out’ at small sizes (10 km or smaller) but this partly due to *observational selection*; we simply have not yet discovered all the small asteroids. The gradient of the dashed line in Figure 7.10 is significant when considering where most of the material in the asteroid belt is concentrated. In other words, we could ask, is most of the material (i.e. the mass) to be found in the few largest asteroids, or is most of it distributed amongst the numerous small bodies? It turns out that, if all the data followed the same slope as the dashed line shown in Figure 7.10, the total mass of objects contained in each logarithmic diameter step, would be approximately the same. For example, the total mass of all asteroids with diameters between 1 and 10 km, would be the same as those with diameters between 10 and 100 km. If however the slope of the data was shallower than the dashed line (i.e. more towards the horizontal), this would indicate that the largest bodies accounted for most of the mass contained in the asteroid belt. Conversely, if the data were steeper than the dashed line, most of the mass would be contained in the smaller bodies. The data in Figure 7.10 lies close to the dashed line in the middle region of the plot, but if we were to take all the data together, a best fit straight line would be somewhat shallower than the dashed line. Thus most of the mass in the asteroid belt is concentrated in the few largest asteroids.

As many of the impact craters seen on planetary bodies are caused by the impact of asteroids, it follows that the impact crater size distribution must broadly reflect the asteroid size distribution in some way. So if we expect a large asteroid to make a large crater, and a small asteroid to make a smaller crater, then because there are far more small asteroids, we would expect to see far more small impact craters on planetary surfaces. Indeed, this is what you found in Chapter 4, with the crater size–frequency distribution.

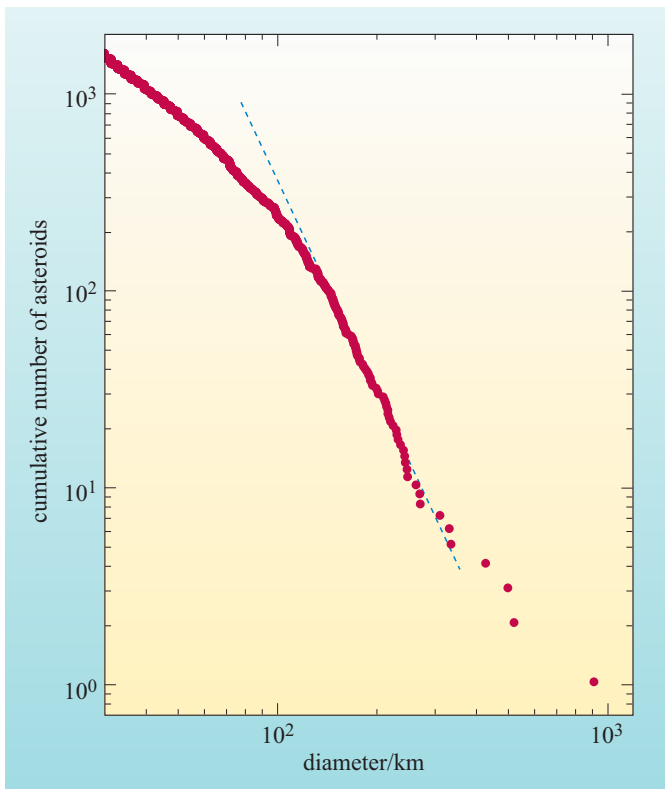


**Figure 7.10** The cumulative size distribution of the known bodies in the asteroid belt, plotted logarithmically. The graph tells us the number of asteroids that have diameters greater than a given value.



7.3.2 Asteroid types

Not all asteroids are the same. The composition will depend on how and where an asteroid was formed, and what thermal, physical and chemical processing has happened to it since. Different types of asteroid are sorted into **taxonomic classes**, and the basis for deciding what class a body belongs to, comes from observational astronomy.

One useful parameter that we would like to know, is how reflective the asteroid’s surface is. In other words we would like to determine the *albedo* (a concept you came across in Chapter 5), and more precisely how the albedo changes at different wavelengths of light. However, much of the time, we cannot easily determine absolute values of the albedo, as we do not have an accurate knowledge of how big the asteroid actually is. In other words, you cannot always tell if you are observing a reflective small object, or a less reflective but larger object. What we can do however is to determine the *relative* efficiency with which the asteroid reflects sunlight, as a function of the wavelength of the light. This is called a **reflectance spectrum**. For example, a body that simply reflected all the sunlight equally, would have a *neutral* reflectance spectrum, whereas a body that reflected light more efficiently at longer wavelengths, would have a more *red* appearance. It is the precise nature (particularly the slope) of the reflectance spectrum that identifies the taxonomic class. Figure 7.11 shows typical reflectance spectra associated with three taxonomic classes. Because we do not know the absolute reflectance values, we plot the different asteroids simply over the top of each other, forcing the relative reflectance value to be 1.0 at the wavelength of about 0.55  $\mu\text{m}$ , i.e. a representative value for visible light. For example, a relative reflectance value of 2.0 at 1.0  $\mu\text{m}$  means that the body reflects light with double the efficiency at 1  $\mu\text{m}$  as it does at visible wavelengths (where the relative reflectance value is 1.0). This would be true for an object with an albedo of, for example 0.04 at visible wavelengths and 0.08 at 1  $\mu\text{m}$ . It would be equally true for an object with an albedo of 0.3 at visible wavelengths and 0.6 at 1  $\mu\text{m}$ .

**Table 7.1** The typical albedo values of selected taxonomic classes of asteroids.

Taxonomic Class	Albedo
E	0.25 to 0.60
S	0.10 to 0.22
C	0.03 to 0.07
M	0.10 to 0.18
P	0.02 to 0.06
D	0.02 to 0.05

The taxonomic classes themselves are due to compositional differences. There are many classes, and sub-divisions, but we need only mention a few here. C-type asteroids (carbonaceous types) are rather dark (i.e. non-reflective – see the typical albedo values for the different taxonomic classes in Table 7.1). They have neutral reflectance spectra, and contain carbon-rich rocky material. S-type asteroids are generally a stony (or stony–metallic mix) and are more reflective and somewhat more red. E-types are often highly reflective and appear to be predominantly composed of the mineral enstatite (magnesium silicate  $\text{MgSiO}_3$ ).

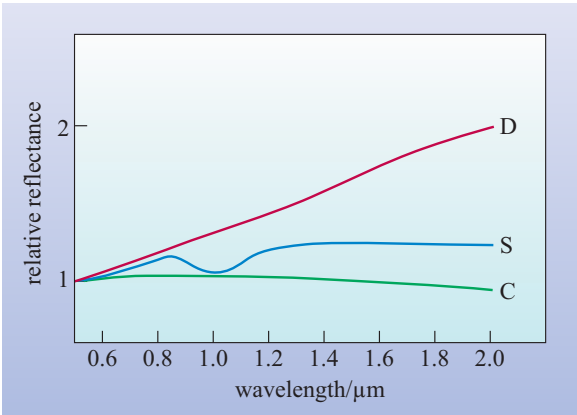


**Figure 7.11** The reflectance spectra of a few taxonomic types of asteroids. If a body reflected all wavelengths equally (i.e. neutral) the spectra would have a value of 1.0 throughout; C-types approximate this behaviour. D-types however reflect longer wavelengths better, and so would appear red. S-types have a distinctive ‘S-shape’ feature in their spectra.

D-types (dark type) are extremely dark and red. M-types (metallic type) are thought to be made of mostly iron and nickel, with P-types (pseudo-M type) also thought to have a major metallic component in the composition. It is thought that C and D-types are probably quite primitive (least processed) bodies, whereas E-types, S-types and M-types are likely to be fragments from a larger body, which underwent differentiation (as discussed in Chapter 2) so producing a metallic core, and a rocky mantle. Such fragments might collide with Earth and be collected as meteorites. Figure 7.12 shows that different classes of asteroid generally occupy different regions in the asteroid belt. This is a consequence of the fact that the region of formation (distance from the Sun) affected the composition of the asteroid.

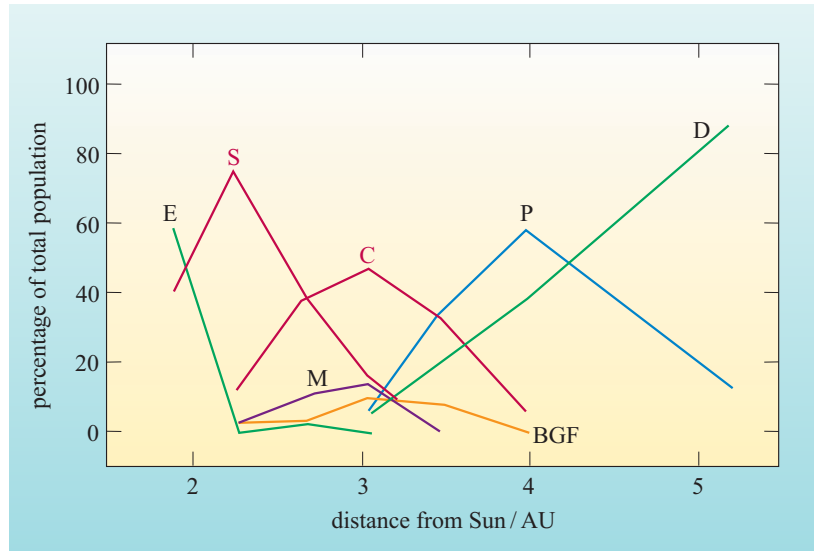


**Figure 7.12** Distribution of some of the major classes of asteroid within the asteroid belt as a function of distance from the Sun. B, G and F-types are sub-classes of C-types.

### 7.3.3 Asteroids up close

Until relatively recently, what we knew about asteroids was based on ground-based observations. But now a handful of spacecraft missions have come very close to asteroids allowing us to learn about these minor bodies in much greater detail than before. Table 7.2 details some close fly-bys of asteroids by spacecraft. The Galileo spacecraft, while en route to Jupiter, flew by (951) Gaspra (Figure 7.13), obtaining the first ever high-resolution image of an asteroid. A rather irregularly shaped body peppered with impact craters was seen. Galileo's second, much larger, asteroid target, (243) Ida, showed a similar scenario (Figure 7.14) with many impact craters and irregular features.

**Table 7.2** Parameters of the asteroids that have had spacecraft fly-bys. The sizes indicated refer to the major and minor axes of the body. Porosity describes the relative volume of voids within the object (so a completely solid body has a porosity of 0%). Remember that  $a$  is the semimajor axis of the orbit and  $e$  is the eccentricity of the orbit.

Asteroid	Spacecraft	Encounter date	Asteroid size/km	Taxonomic class	Density / $\text{kgm}^{-3}$	Porosity	$a$ /AU	$e$
(951) Gaspra	Galileo	29 Oct 1991	$19 \times 12$	S-type	$2500 \pm 1000?$	30%?	2.21	0.17
(243) Ida	Galileo	28 Aug 1993	$58 \times 23$	S-type	$2600 \pm 500$	30%	2.86	0.05
(253) Mathilde	NEAR	27 Jun 1997	$59 \times 47$	C-type	$1300 \pm 200$	80%	2.65	0.27
(433) Eros	NEAR	14 Feb 2000 <sup>a</sup>	$33 \times 13$	S-type	$2700 \pm 30$	25%	1.46	0.22
(9969) Braille	Deep Space 1	29 July 1999	$2.2 \times 1$	?	?	?	2.34	0.43
(5535) Annefrank	Stardust	2 Nov 2002	$8 \times 4$	?	?	?	2.21	0.06

<sup>a</sup>NEAR went into orbit around Eros on this date. It remained there for a year and then landed on the surface of Eros on 12 February 2001.



**Figure 7.13** (above)  
Image of main belt S-type asteroid (951) Gaspra ( $19\text{ km} \times 12\text{ km}$ ) taken by the Galileo spacecraft.



**Figure 7.14** (above) Image of main belt S-type asteroid (243) Ida ( $58\text{ km} \times 23\text{ km}$ ), taken by the Galileo spacecraft. The rather jagged shadow line is a consequence of the asteroid being illuminated only from one direction (from the Sun). This causes a great contrast between the sunlit areas and the shadow areas, which look as black as the background space.

#### QUESTION 7.8

Look at Figure 7.14, the image of the  $58\text{ km} \times 23\text{ km}$  asteroid, (243) Ida. Remembering the types of crater that you met in Chapter 4, how would you describe the craters on Ida?

Surprisingly, Ida was also found to have a much smaller satellite asteroid (named Dactyl) orbiting around it (Figure 7.15). Binary asteroids that orbit each other now appear to be more common than was previously thought, with several examples being discovered recently by ground-based telescopic studies.

Gaspra and Ida are S-type asteroids, but a C-type asteroid, (253) Mathilde (Figure 7.16), was encountered by the NEAR (or NEAR Shoemaker) spacecraft, on its way to its main target (433) Eros (an S-type Near Earth Asteroid). On reaching Eros (Figure 7.17), NEAR went into orbit about the asteroid (a major technical achievement) and spent a full year taking scientific data.



**Figure 7.15** Image of Ida's satellite asteroid, Dactyl ( $1.6\text{ km} \times 1.2\text{ km}$ ) taken by the Galileo spacecraft.



**Figure 7.16**  
Image of main belt C-type asteroid (253) Mathilde ( $59\text{ km} \times 47\text{ km}$ ), taken by the NEAR spacecraft.



**Figure 7.17** Image of near Earth S-type asteroid (433) Eros ( $33 \text{ km} \times 13 \text{ km}$ ) taken by the NEAR spacecraft.

The asteroid (9969) Braille was encountered by the technology-proving spacecraft, Deep Space 1. Indeed the flyby was the closest yet undertaken, being just 15 km from the asteroid. However imaging of the asteroid was not very successful. Asteroid (5535) Annefrank however, was encountered by the Stardust mission in November 2002, returning the image shown in Figure 7.18.

A close fly-by of a spacecraft is not the only way that detailed information on the shape of an asteroid can be determined. By using some of the world's most powerful radio transmitters in conjunction with some of the world's largest radio telescope dishes (for example the huge Arecibo radio telescope in Puerto Rico), radar techniques can be used to image the asteroid. This technique involves sending radio wave pulses towards an asteroid, and then receiving a reflection, or echo, back on Earth. By complex processing of the returned signals, an image representation of the asteroid can be constructed. Such an image, of the asteroid (4179) Toutatis, is shown in Figure 7.19. Repeated observations of an asteroid as it rotates, allows a full 'shape model' to be derived, an example of which is shown in Figure 7.20.

We have seen that the asteroids imaged so far, are non-spherical. A good description of them might be 'potato-shaped'. This is not unexpected. Observations from the ground often show the brightness of asteroids increasing and then decreasing regularly. This behaviour is illustrated in Figure 7.21, which is an example of an asteroid's **lightcurve**. As the light we see from the asteroid is simply reflected light from the Sun, the amount of light we receive is related to its albedo, and the cross-sectional area of the region of the asteroid that is illuminated. So if a 'potato-shaped' body is spinning, then you will see a changing cross-sectional area, and hence a changing brightness. You can convince yourself of this by simply looking at an irregularly shape body (e.g. a potato) and turning it while considering how the cross-sectional area changes. The *period* of the lightcurve tells us how long the asteroid takes to spin, and the *amplitude* of the lightcurve (the difference between the maximum and minimum brightness) depends on how elongated the body is. Thus the lightcurve tells us the spin rate, and the ratio of the longest side to the shortest side.

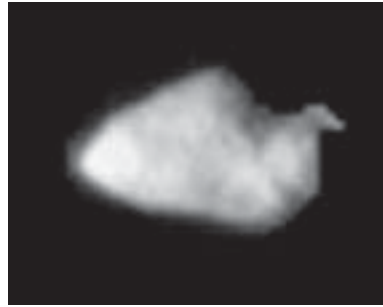


**Figure 7.18** Image of the main belt asteroid (5535) Annefrank ( $8 \text{ km} \times 4 \text{ km}$ ) obtained by the Stardust spacecraft.



**Figure 7.19** The radar image of Near Earth Asteroid (4179) Toutatis ( $5 \text{ km} \times 2 \text{ km}$ ). Toutatis is extremely elongated.

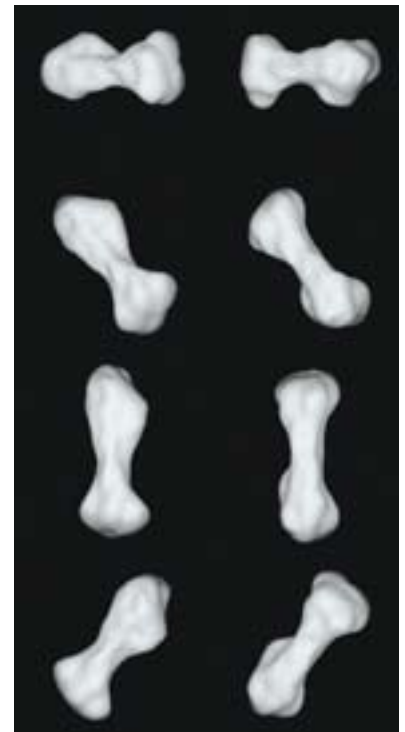


**Figure 7.20** The 'shape model' of main belt asteroid (216) Kleopatra ( $220 \text{ km} \times 95 \text{ km}$ ) derived from radar observations. Kleopatra bears a remarkable resemblance to the kind of bone favoured by dogs!

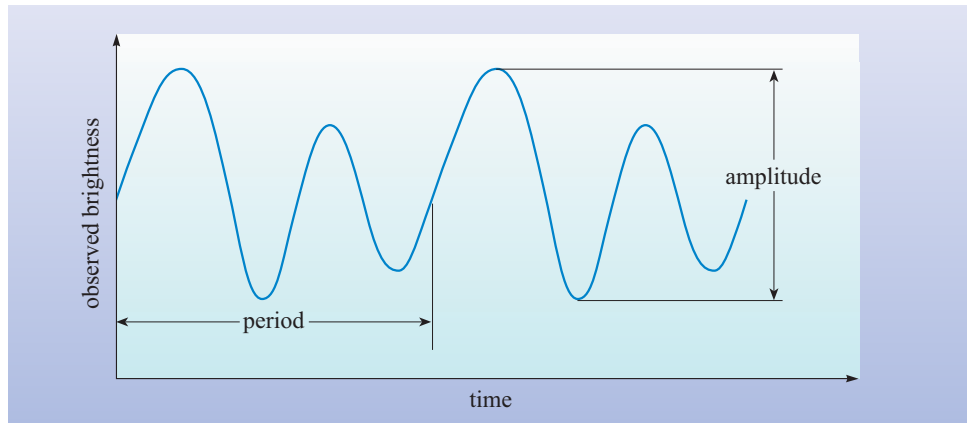


**Figure 7.21** A schematic of an asteroid lightcurve, showing the amplitude (difference between the maximum and minimum brightness) and the period (time taken for one full axial revolution of the body). Note that a lightcurve produced by the irregular shape of an object is double peaked (rather than a sine wave), and that a spherical object would give an amplitude of zero (i.e. we would say it had a ‘constant lightcurve’).

Some asteroids have lightcurves that display very little variation, indicating that the asteroid is spherical (or near spherical). Some of the largest asteroids are thought to have undergone differentiation in a similar way to the terrestrial planets (as you met in Chapter 2). During this process the body maintains a spherical shape due to compression under its own gravity. However, subsequently, when the asteroids had cooled so that they were solid throughout, impacts could fragment and break parts off the parent asteroid, creating much more irregular shapes. This said, most asteroids that are larger than a few hundred kilometres in diameter, tend to be approximately spherical due to gravitational compression.

The motion of binary asteroids with respect to each other, or indeed the motion of a spacecraft around an asteroid, can be used to derive masses for the asteroids, and thus (if the asteroid size is known) indicate the density of the asteroid. S-type asteroids Ida and Eros were found to have densities of around  $2600 \text{ kg m}^{-3}$  and  $2700 \text{ kg m}^{-3}$  respectively. Remembering that S-types are predominantly rocky, one might have anticipated a density somewhat higher than this. For example, typical stony meteorites (which are thought to come from fragmented S-type asteroids) have densities of around  $3400 \text{ kg m}^{-3}$ . The lower densities of Ida and Eros suggest that the bodies might be slightly *porous*, i.e., the asteroids are not solid rock, but have a structure with voids in it (similar to what you would find for a pile of rocks). Even more surprising, the density of the C-type Mathilde was found to be around  $1300 \text{ kg m}^{-3}$  which appears very low indeed. Additionally, ground-based observations of another C-type asteroid, Eugenia, have indicated a similar density of  $1200 \text{ kg m}^{-3}$ . In fact these results suggest that C-type asteroids might be up to 80% porous. Even recent observations of some M-type binary asteroids have indicated a much lower density than might have been expected, again suggesting high porosity. These results show that some (perhaps most) asteroids are probably not solid lumps of rock and metal, but are more like a **rubble pile** of fragments of all sizes, bound together by their own gravity.

After the NEAR spacecraft had been orbiting Eros for a year, the decision was made to manoeuvre NEAR such that it landed on the surface of Eros (even though it was not designed to do this!). This allowed some images to be obtained during the descent,



of unprecedented resolution. Figure 7.22 shows three images taken just before ‘touch down’. Boulders and pebbles are clearly seen, with many of the boulders being partly buried by regolith (i.e. fine particle ‘soil’). To the lower left of Figure 7.22c, there are fewer boulders and a smoother dusty area. These type of regions have been nicknamed *ponds* and are thought to be areas where fine regolith has gathered, covering larger boulders beneath the surface. Figure 7.23 also shows views of the surface of Eros. ‘Ponds’ are also seen in Figures 7.23a and c, with a more ‘rugged’ appearance (i.e. more boulders, and less regolith covering) being seen in Figure 7.23d.

The NEAR data shows that impacts that produce boulders and other smaller particles, play a large part in determining the nature of the asteroid surface. Asteroids can no longer be thought of as lumps of bare rock, but are often collections of smaller fragments, or at least can suffer significant *fracture* due to impacts. Future spacecraft missions will further investigate the nature of asteroids. For example, the Japanese MUSES-C mission has been designed to go to a Near Earth Asteroid, and attempt to bring some small samples of the surface back to Earth, allowing detailed chemical composition analyses to be done in the laboratory.

#### QUESTION 7.9

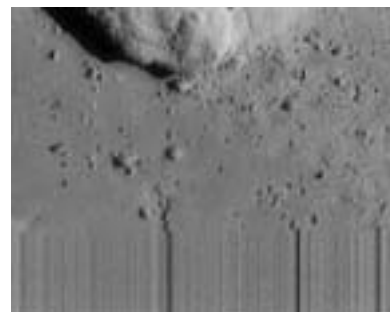
Imagine an asteroid of diameter 1 km, of unknown taxonomic class, is about to hit the Moon. Will it make any difference to the impact crater produced, whether the asteroid was S-type, or C-type?



(a)



(b)



(c)

**Figure 7.22** The last images from the descent sequence of NEAR. Part (a) shows a region 54 m across taken at a range of 1150 m, (b) shows a region 12 m across taken at a range of 250 m, and (c) shows a region 6 m across taken at a range of 120 m; this is the final image obtained before the loss of signal (the lines at the bottom of the image indicate when signal was lost). The spacecraft probably landed about 7 m to the left of the edge of image (c).



(a)

(b)



(c)

(d)

**Figure 7.23** Four images of the surface of Eros, where regolith appears to have collected in depressions on the surface. A ‘pond’ is particularly evident in the lower left region of Figure (a). Figures (a) and (b) show regions about 550 m across. Figures (c) and (d) show regions about 230 m across.

## 7.4 The Kuiper Belt

In Chapter 1 we considered the layout of the Solar System, and saw that a large population of planetesimals lies beyond Neptune – the **Kuiper Belt**. These objects were first discovered in 1992 – but not by chance. A small group of astronomers had been specifically searching for these objects for a number of years. Before considering the properties of Kuiper Belt objects in detail, let us take a step back and consider why astronomers suspected the existence of the Kuiper Belt.

Consider the layout of the outer Solar System. The gas giant Jupiter contains about 318 Earth masses of material. Saturn contains 95 Earth masses, and then Uranus and Neptune contain about 14 and 17 Earth masses respectively. As we go further from the Sun, the amount of material that accreted into the gas giants appears to decrease. However, Uranus and Neptune still contain a huge amount of material from the solar nebula. But what happens beyond Neptune? Do we expect the significant mass contained in the planetary bodies to just stop at Neptune? We do of course have Pluto, but Pluto accounts for just 0.002 Earth masses. So perhaps we might expect a lot of material from the solar nebula to be contained in bodies beyond Neptune.

It is this sort of reasoning that led astronomers to hypothesize that the Solar System most likely continues beyond Neptune and Pluto, if not with major planets (gas giants) then in a multitude of smaller bodies. And so the existence of the Kuiper Belt (named after the astronomer Gerard Kuiper who did some work on this concept in the 1950s) was suspected for many years. But technology took a long time to catch up. Bodies like Pluto (and smaller) so far from the Sun, appear extremely faint, and they move very slowly with respect to the fixed star background. Even with large telescopes they are difficult to identify. A hint of things to come, was seen in 1977 when an unusual asteroid, named (2060) Chiron (pronounced ‘kye-ron’), was discovered in an orbit far beyond the asteroid belt. Chiron was observed to have a semimajor axis of 13.6 AU and an eccentricity of 0.38 indicating a perihelion distance of 8.4 AU and an aphelion distance of 18.8 AU. This meant Chiron occupied the space between Jupiter and Uranus, crossing the orbit of Saturn. Another object on an even more surprising orbit, (5145) Pholus, was also discovered ( $a = 20.3$  AU,  $e = 0.57$ ) and this object crossed the orbits of Saturn, Uranus and Neptune (Figure 7.24). This new class of objects was called **Centaurs**, for which a loose definition would be objects with orbits that cross those of the giant planets. But objects in these sorts of orbits must be quite short lived, as they would suffer strong gravitational perturbations, or even close approaches and impacts with the giant planets. So if we see them today, it means they must be being replenished (a bit like the case of Near Earth Asteroids). But from where do they come? The most likely answer is that Centaurs are actually objects that started in the Kuiper Belt and have undergone orbital evolution, slowly making their way into the inner Solar System.

You can see that the expectation that the Solar System did not just abruptly stop at Neptune and Pluto, and the observations of Centaurs, meant that astronomers felt reasonably sure that other bodies must occupy space beyond Neptune. It was also becoming apparent that a belt of comet-like bodies beyond Neptune could be the source of short-period comets (this will be discussed further in the next section). It was astronomers Dave Jewitt and Jane Luu, who found the first object, designated 1992 QB<sub>1</sub>, while using a relatively newly introduced CCD camera, so confirming the existence of the Kuiper Belt (see Figure 7.25).

Somewhat before Gerard Kuiper published his ideas, a British astronomer, Kenneth Edgeworth, published some short communications outlining the same ideas, but this only really came to light after the term ‘Kuiper Belt’ was generally accepted. However, you may see references to the ‘Edgeworth–Kuiper Belt’.

You can appreciate how difficult it is to observe Kuiper Belt objects when you realize that a typical Kuiper Belt object is 100 000 000 times fainter than a typical star in a constellation we see with the naked eye.



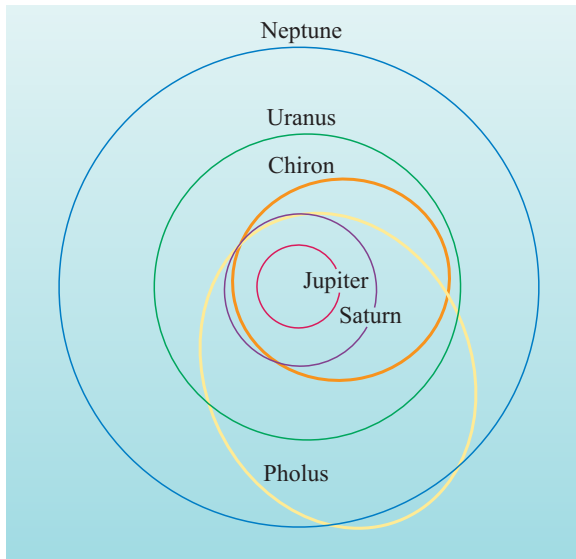


**Figure 7.24** The orbits of Centaur objects (2060) Chiron and (5145) Pholus. For comparison, the orbits of the giant planets are also shown.

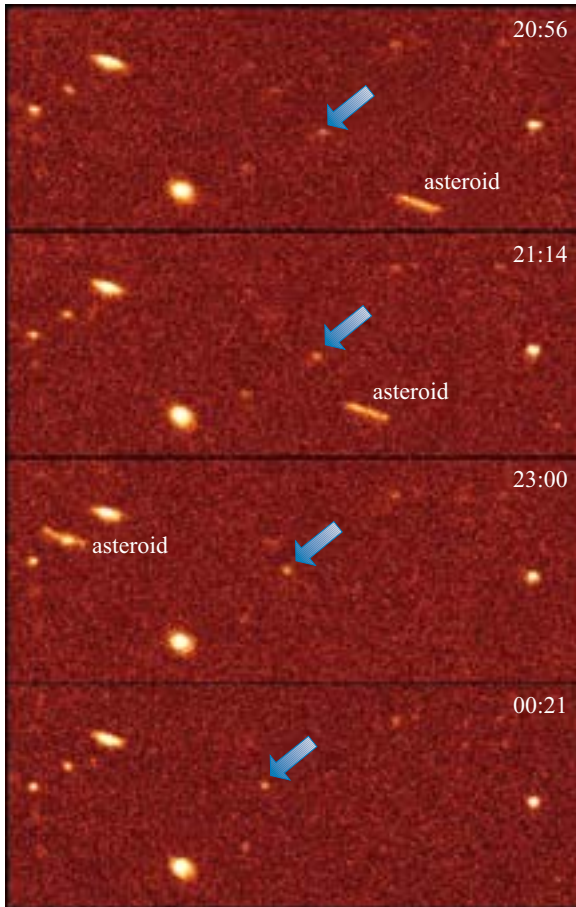


**Figure 7.25** The discovery CCD images of Kuiper Belt object 1992 QB<sub>1</sub>. The four frames are taken over almost 4 hours, and in this time the object has moved (mostly due to the Earth's motion rather than the Kuiper Belt object's motion) so proving that it is not a star. Further observations confirmed the orbit, and that the object was orbiting the Sun at a distance of 44 AU (semimajor axis).

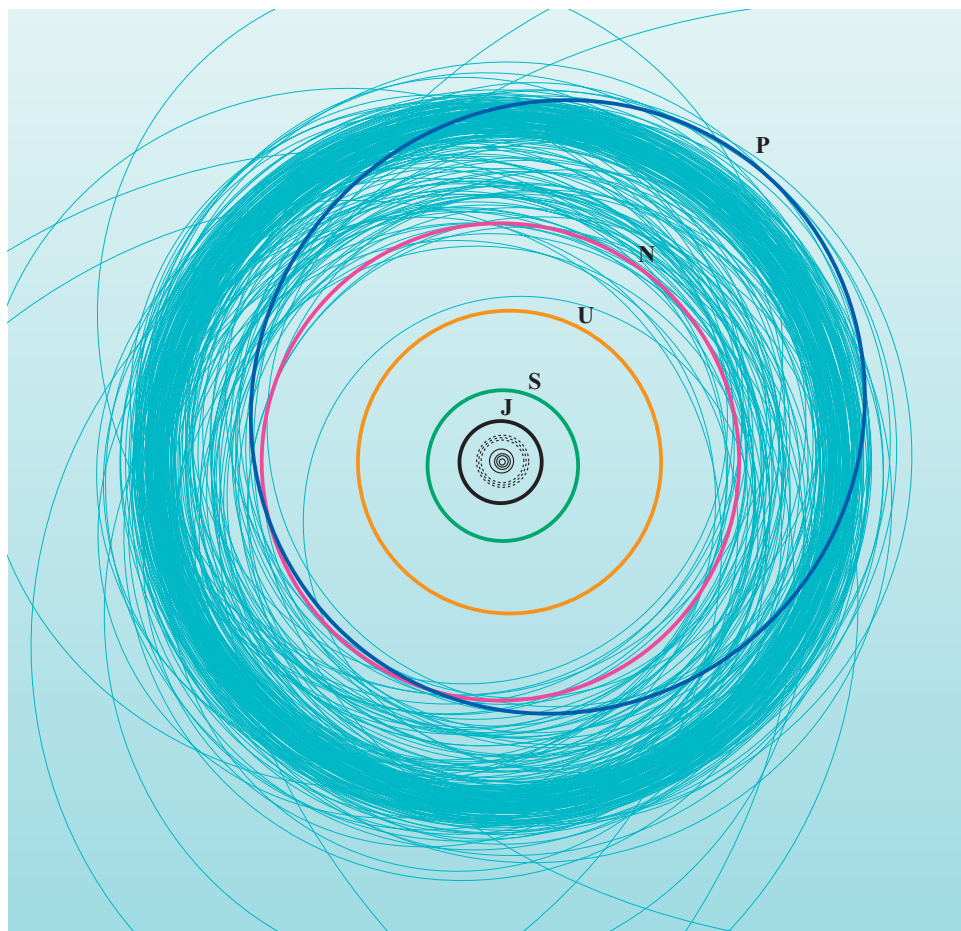


**Figure 7.26** The orbits of the known Kuiper Belt objects. The labels J, S, U, N and P denote the orbits of Jupiter, Saturn, Uranus, Neptune and Pluto, respectively.

Two more Kuiper Belt objects were discovered in 1993, and four more in 1994; since then the discovery rate has grown greatly as more astronomers have made the effort to look for these bodies. Several hundred objects have now been identified (the orbits are shown in Figure 7.26), many of which have quite well determined orbits. It is now clear that, based on their orbits, there are 3 distinct classes of Kuiper Belt objects. This is shown by plotting the orbital eccentricity against the semimajor axis, as has been done in Figure 7.27. Firstly, there are many objects that have a semimajor axis of (or close to) 39.4 AU. The significance of this becomes clear, when we note that the semimajor axis of Neptune is 30.0 AU, and so if we compare orbital periods (using Kepler's third law) we find that this type of object is in a 3 : 2 orbital resonance with Neptune. Thus Neptune orbits 3 times around the Sun for every 2 orbits of these particular Kuiper Belt objects.

Orbital resonances were discussed in Section 7.3, and it was noted that some resonances can result in objects being quickly removed from a particular semimajor axis (like the Kirkwood Gaps) and some can be locked in to a resonance for a long time. The 3 : 2 resonance with Neptune is the latter type (i.e. an example of a *stable resonance*), and so objects stay in these orbits for a long time.

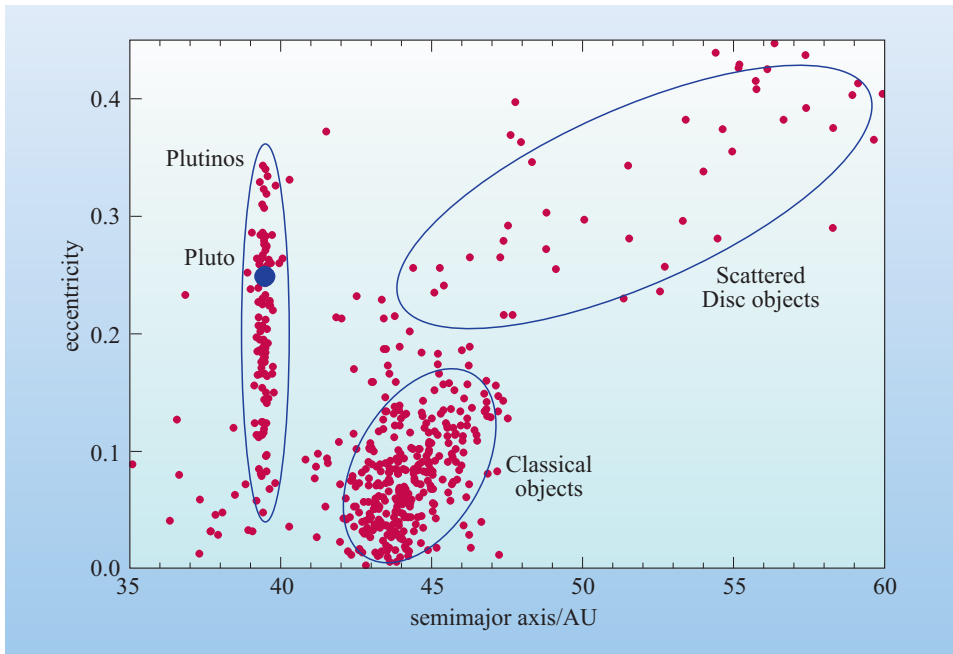


**Figure 7.27** The distribution of eccentricity versus semimajor axis for the known Kuiper Belt objects. The dynamical groups (Plutinos, Classical objects and Scattered Disc objects) are shown. Note the position of Pluto.

Referring to Figure 7.27 you will notice that Pluto sits right in the middle of all the 3 : 2 resonance Kuiper Belt objects. This is no coincidence. Pluto is indistinguishable from the other 3 : 2 resonance Kuiper Belt objects in terms of its orbit. This leads us to ask the question, is Pluto really worthy of the designation ‘planet’? In fact, Pluto is just another member of the Kuiper Belt. Its fame as the ninth planet has only arisen because it is larger than other objects so far discovered, and thus considerably brighter and easier to detect. Because of this, Pluto was first identified in 1930, i.e. 62 years before the *next* Kuiper Belt object was found (1992 QB<sub>1</sub>). Today we have identified Kuiper Belt objects with diameters over 1000 km (compared with Pluto’s diameter of 2370 km) and we may even find larger bodies over the next few decades.

Some astronomers and planetary scientists have called for Pluto to be officially demoted from the status of a planet, and to join the ranks of bona fide Kuiper Belt objects. The arguments for doing so are not easily ignored, and certainly it fits into a tidier concept of the Solar System, where we have the small rocky terrestrial planets near the Sun, and large gas giants in the outer Solar System. However, we have lived with the idea of a nine-planet Solar System for over 70 years, and old habits die hard. Furthermore, it might seem somewhat disrespectful of the many years of effort that astronomer Clyde Tombaugh expended before discovering Pluto in 1930 (although he also felt that Pluto was not quite the ‘Planet X’ that he had been looking for, and he spent a further 10 years looking for a more massive planet). And so, it has generally been agreed that Pluto will retain its status as the ninth planet.

Returning to the consideration of the 3 orbital classes of Kuiper Belt object, we have seen that there are the Pluto-like 3 : 2 resonance objects. This group is often called the *Plutinos* (i.e. ‘mini-Plutos’). The next group, are objects that have somewhat larger semimajor axes (generally greater than 42 AU) and small eccentricities. These objects are known as the *Classical* objects, and as the first object discovered, 1992 QB<sub>1</sub>, was one of this class, members of this group are

sometimes referred to as ‘*Cubewanos*’ (i.e ‘QB<sub>1</sub>-os’). Finally there is a group of objects with large eccentricities. These are known as *Scattered Disc* objects, and their large eccentricities mean that their aphelia (plural of aphelion) can be at large distances (up to 100 AU or more). Some Scattered Disc objects have perihelia (plural of perihelion) that come within the orbit of Uranus, and so begin to look rather like Centaurs, and so the distinction between Centaurs and Scattered Disc Kuiper Belt objects is rather vague.

#### QUESTION 7.10

Of the three dynamical classes in the Kuiper Belt (Plutinos, Classical and Scattered Disc), which group of objects are most likely to have close approaches with (or impact) the giant planets?

The total mass of the Kuiper Belt is probably in the region of about 0.1 Earth masses. This can be compared to the asteroid belt which is thought to contain currently only about 0.001 Earth masses of material.

### 7.4.1 Observational properties of Kuiper Belt objects

Because these objects are so faint, it is hard to deduce a great amount of information from observations. However we can at least obtain a broad picture of the physical nature of the bodies. We can obtain reflectance spectra, as for asteroids, and thus learn something of the surfaces of the bodies. The first outer Solar System bodies to be investigated in this way were the Centaurs, Chiron and Pholus. They could not have been more different. Chiron had a neutral spectrum (not unlike a C-type asteroid) whereas Pholus had the steepest (that is, reddest) spectrum of any Solar System object ever observed. Figure 7.28 shows the reflectance spectra, in comparison with those of the main asteroid types that you met previously.

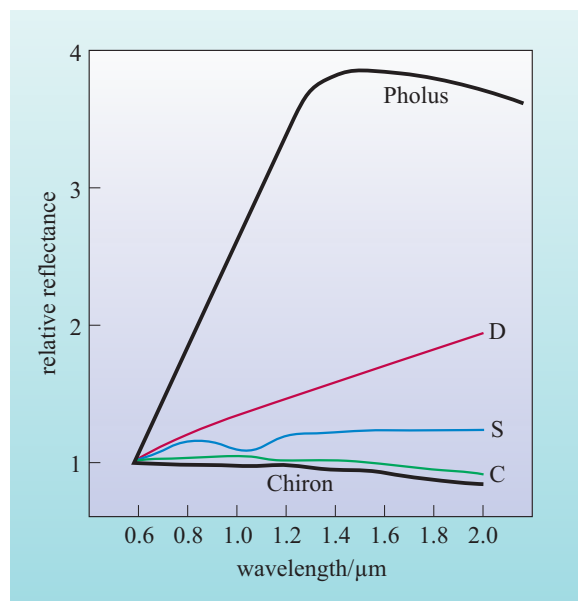


**Figure 7.28** The reflectance spectra of the Centaurs Chiron and Pholus, with some asteroid types shown for comparison. Pholus shows the reddest spectrum of any Solar System body.

Observations of Kuiper Belt objects (and indeed other Centaurs), show that their spectra have great diversity, with slopes essentially lying anywhere between those of Chiron and Pholus (i.e. Chiron and Pholus by chance happen to represent the most extreme examples of spectra). This behaviour probably suggests that Centaurs and Kuiper Belt objects are indeed the same types of body — the Centaurs being objects from the Kuiper Belt slowly moving inwards due to orbital evolution. But how can we get such diversity within the Kuiper Belt group? Surely if all the objects formed together from much the same material, they should look the same?



**Figure 7.29** An artist's impression of the proposed New Horizons mission. A spacecraft would take about 10 years to reach Pluto, and then could continue, hopefully performing a fly-by of a Kuiper Belt object.

The answer might lie in the way the surfaces of these bodies age, and are subsequently altered by impacts. It is thought that the surface material in Kuiper Belt objects will chemically change over time due to the exposure to the Sun's radiation and also galactic cosmic rays. The material might slowly form complex organic molecules at the surface which turns the appearance very dark and red (e.g. giving a Pholus-type reflectance spectrum). This dark layer might only extend to less than a metre from the surface. With more time, the surface might become more neutral again due to the organic molecules eventually breaking down. In addition, impacts to the surface will excavate 'fresh' sub-surface material which could coat the surface. And so the object returns to its initial neutral colour. If this scenario is correct, then the diversity in reflectance spectra shows that the objects are at various stages of the ageing and impact re-surfacing process – a cycle that may occur many times during the lifetime of an object. On the other hand, it is also possible that the colour diversity is unrelated to impacts, but a consequence of differing original composition. Or perhaps some other as yet undetermined factors are involved.

What is clear, is that *some* impacts *must* occur in the Kuiper Belt, and this would probably give rise to fragmentation of the objects (rather like in the asteroid main belt). Recent lightcurve observations of object 2000 WR<sub>106</sub> (named Varuna) suggest a reasonably elongated object (i.e. another ubiquitous 'potato-shaped' object!) with a rotation period of about 6 hours. Consideration of the expected material strengths of the object has led to a conclusion that Varuna is most likely a fragmented rubble pile which is distorted into an elongated shape due to its relatively rapid rotation. Furthermore, recent observations have identified binary objects, somewhat like the Pluto–Charon system (or some asteroid binaries).

Our understanding of the nature and evolution of Kuiper Belt objects is far from complete. Although ground-based observations will continue to give us information about the objects, a spacecraft mission to a Kuiper Belt object would clearly be highly desirable. NASA's proposed New Horizons mission (Figure 7.29) may offer such an opportunity. While the main aim of a mission like this would be to perform a close fly-by of Pluto, the spacecraft would continue into the Kuiper Belt and perhaps perform a fly-by of a Kuiper Belt object. We will have to wait to see what surprises a future mission of this type might bring us.



## 7.5 Comets

Our discussion of Kuiper Belt objects leads us naturally to comets, because as you will see, the two types of object may have much in common.

Comets have been observed for as long as the stars and the planets. However, their unexpected appearance in the sky, and the fact that they are generally only observable for a relatively short duration (weeks or months) set them apart from other heavenly bodies. An apparition of a comet was once generally thought to be a portent of terrible events to come. It is certainly easy for us to understand how spectacular a comet might have appeared to ancient civilizations, when we see images such as the ones shown in Figure 7.30. The bright *head* of the comet, called the **coma**, leads into a wispy *tail* which can extend significantly across the sky (for example several times the angular width of the Moon). So what exactly gives rise to this spectacular object in the sky?

As we said in Chapter 1, the comet itself is a relatively small body, rich in ices and small solid particles (i.e. dust). As the ices are heated when the comet comes near to the Sun, the ices turn directly to gas (i.e. the ices *sublimate*) and escape from the surface into space, carrying the solid dust particles with them. This process is seen in action, in Figure 7.31. Figure 7.31a shows one of the most famous comets, Halley's Comet, as seen from Earth in 1986. Figure 7.31b shows the cometary body itself, usually referred to as the **cometary nucleus**, as imaged by a spacecraft that passed within 600 km of the body. The image shows *jets* of gas and dust leaving the nucleus, which initially might typically be a few km or a few tens of km across, to form the tenuous coma and tail structure which can be hundreds of thousands (or even millions) of km in size. Another example of a cometary nucleus is seen in Figure 7.32.

If then, comets are ejecting significant amounts of gas and dust, then it is clear that the cometary emission process causes the comet to loose mass (i.e. decay). For example, Halley's Comet (which is quite an active comet) loses over  $10^{11}$  kg of mass during each perihelion passage, which would be equivalent to about a metre

**Figure 7.30** Examples of comets as observed from Earth. (a) Comet Hale–Bopp seen in 1997 and (b) Comet Hyakutake in 1996, were both naked-eye comets, i.e. one could see them in the sky without the aid of a telescope. These images however were taken using a telescope. Note that in (a), the tail appears in two parts. The bluish part is called the *ion tail*, and is seen due to the gaseous ions from the comet emitting light, while travelling directly away from the Sun under the influence of the solar wind. The other part is called the *dust tail*, and is due to light reflected and scattered from small dust particles that were ejected from the comet and are now also orbiting the Sun.



(a)



(b)

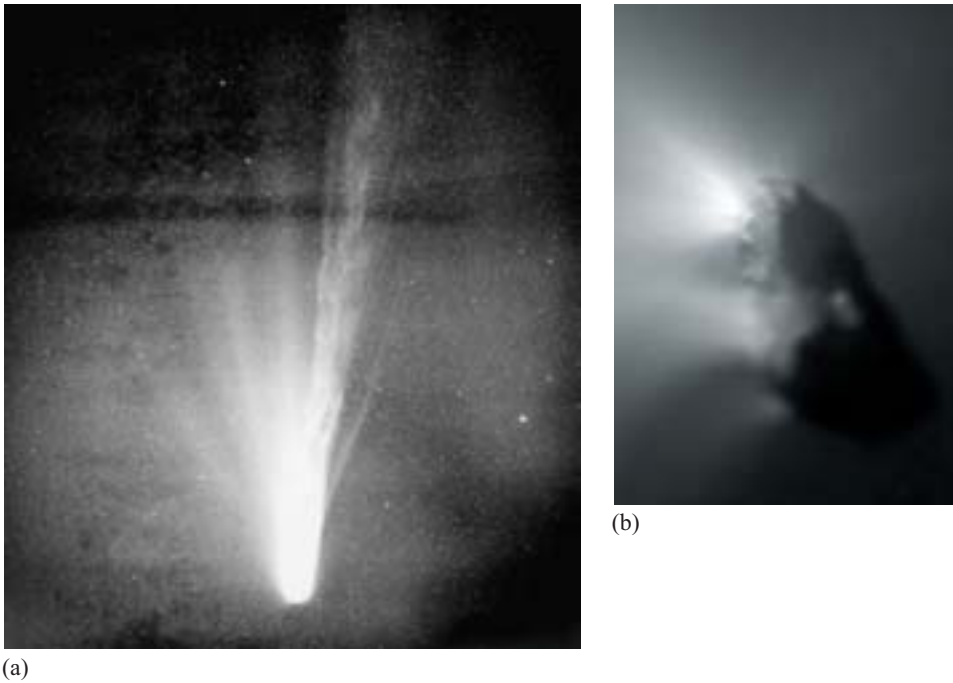


**Figure 7.31** Halley's Comet. (a) The image shows what was observed from Earth in 1986, whereas, (b) shows the nucleus ( $15 \text{ km} \times 7 \text{ km}$ ), imaged by the European Space Agency's Giotto spacecraft in 1986.

of material from the surface. After a few thousand more perihelion passages, the comet will have decayed away completely. Indeed comets may decay far faster than this, as they are occasionally seen to split and fragment. The ejection of nucleus fragments (metres or tens of metres across) is probably quite commonplace, and almost every cometary nucleus *may* undergo some sort of splitting event at least once during its lifetime. These effects mean that once a comet enters the inner Solar System, its lifetime is relatively short compared to the age of the Solar System – a comet might only last a few thousand or tens of thousands of years in the inner Solar System.

The ices in a comet are mainly water ice ( $\text{H}_2\text{O}$ ). However other ices are present also, such as frozen ammonia ( $\text{NH}_3$ ), carbon dioxide ( $\text{CO}_2$ ), carbon monoxide ( $\text{CO}$ ) and others. The ices are mixed with the dust particles, which are rocky particulates (mainly silicate minerals) forming what is often referred to as 'dirty snow'. This is probably a good description, since the ices are certainly not as compact and homogeneous as an ice cube from a freezer. We would expect a more fluffy and randomized structure, analogous to snow with fine dust mixed with it. The nucleus is expected to be a very porous, low density body (perhaps analogous to an icy version of a C-type asteroid). Indeed the bulk density of a cometary nucleus might be as low as one-tenth that of compact ice. As ices at the surface sublime, some dust is left behind on the surface, so building a dark, unreflective layer. This layer could shield the icy layers beneath from sunlight, and so a cometary nucleus will not be releasing gas from its entire surface. Regions on the surface (so called 'active regions') with exposed ices may account for most of (e.g. 90% or more) the gas and dust output of the nucleus (indeed the nucleus of Halley's Comet shown in Figure 7.31b appears to be significantly outgassing from only around 10% of its surface). Cracks and fissures in the surface may give rise to 'jets' or active spots. A visualization of what we might expect for the structure of a nucleus, is shown in Figure 7.33.



**Figure 7.32** Comet Borelly ( $8 \text{ km} \times 3 \text{ km}$ ). The image was obtained in 2001, by NASA's Deep Space 1 spacecraft. It shows a nucleus similar to that seen for Halley's Comet.





**Figure 7.33** The expected structure of a cometary nucleus. The ‘dirty snowball’ of the nucleus is almost certainly very porous and low density, with a structure probably more akin to a rubble pile rather than a homogeneous body.

#### QUESTION 7.11

If a ‘typical’ comet nucleus were to split apart while in the inner Solar System (i.e. when it is undergoing significant heating from the Sun), why might we expect to see an outburst of cometary activity associated with the event.

While we now understand something of a comet’s outgassing behaviour due to the ‘snowy’ ices present, we have not discussed *why* comets are predominantly icy. In fact, they are icy due to their formation process. Comets are planetesimal bodies, formed by accretion from the material in the solar nebula. They are the leftovers from the planetary formation process.

- Remembering the division between the inner Solar System ‘rocky’ terrestrial bodies, and the outer Solar System icy satellites, where in the Solar System might comets have originally formed?
- Comets must have formed in the outer Solar System (i.e., in the regions associated with the giant planets) to have maintained their icy content. Thus comets must be the *outer* Solar System leftovers from the planetary formation process.

Indeed, icy planetesimals will have formed in the region associated with the giant planets (and further out, i.e. in the Kuiper Belt), where the temperatures in the solar nebula allowed ices to exist. While the huge majority of these cometary planetesimals will have accreted into planetary embryos and eventually formed the giant planets, some will have survived unscathed. However the survivors in the Jupiter to Neptune region will have undergone rapid orbital evolution due to the large gravitational influences of the newly forming giant planets. This process would have effectively scattered the comets. Some would have been thrown into the inner Solar System where many will have collided with the newly formed terrestrial planets. Some will have been thrown out of the Solar System altogether,

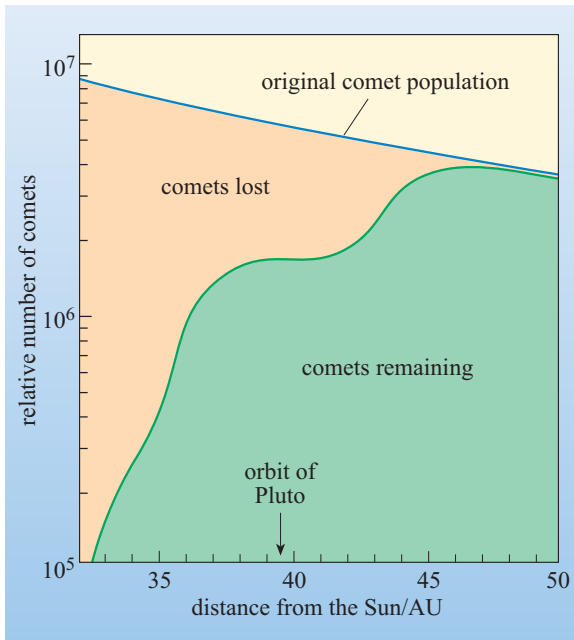


**Figure 7.34** The relative number of cometary bodies in the outer Solar System.

leaving a huge number orbiting the Sun at great distances, so forming a huge cloud of comets around the Solar System. This cloud is the Oort cloud, which you met in Chapter 1. So while the Oort cloud was produced from comets formed in the giant-planets region of the Solar System, the comets that had formed near, and beyond Neptune, were far less gravitationally influenced by the giant planets (particularly Jupiter), and were not expelled like the Oort cloud comets. Some of these cometary bodies still exist today in the region beyond Neptune, i.e. they make up the Kuiper Belt.

Figure 7.34 indicates the relative number of comets that are thought to have originally existed in the outer Solar System (beyond Neptune), and what are thought to remain today, as a function of the distance from the Sun. The ‘missing comets’ have either been ejected or accreted by the giant planets. Beyond the orbit of Pluto the population is thought to be more representative of the original population, albeit with many of the 1 to 10 km size comets accreting to form the 100 to 1000 km sized bodies, which we referred to in the previous section as Kuiper Belt objects.

It is tempting then to consider that Kuiper Belt objects (or indeed Pluto) must be just like very big comets. However, with large bodies (a few hundred kilometres or more in diameter) gravitational compression would play a significant role, increasing the density to nearer that of compact ice. Furthermore, radioactive elements within the large body will have supplied a heat source significant enough to fuel some chemical alteration, or melting of the inner material. In the end then, the larger bodies will be considerably more geologically processed than a small cometary nucleus. However, they will still retain much of the original cometary (icy) material.

If then, objects in the Kuiper Belt are somewhat cometary in nature, might we expect them to behave like comets and produce gaseous emission? The answer is yes, *but* we must consider carefully the distance of the body from the Sun. As the main component of the cometary ices is water ice, then a comet will produce its major outgassing when it is close enough to the Sun in order to heat the surface to

a temperature sufficient to sublimate water ice. This happens at a distance of less than 3 AU from the Sun (and indeed most of the gas production from a comet occurs when it is closest to the Sun, at perihelion). It would seem then that a Kuiper Belt object, or indeed a Centaur, is not close enough to the Sun to produce water-driven sublimation. However, the other components in the cometary ices (e.g.  $\text{NH}_3$ ,  $\text{CO}_2$ ,  $\text{CO}$ ) are more volatile than water ice, and sublimate at much lower temperatures. Hence some cometary outgassing could occur at much greater distances from the Sun than we might first expect. The first evidence of this came from the first Centaur object we considered, Chiron. When discovered in 1977, it was designated an asteroid. However, some years later, some images of Chiron showed that it appeared to have a faint ‘cometary coma’ associated with it, even when at a distance of 15 AU from the Sun. Whether Kuiper Belt objects, at 30 AU and more, can undergo routine cometary outgassing is not yet known. However, it is likely that some cometary outbursts might occur, related to impacts. If an impact of a much smaller body onto the Kuiper Belt object excavated some subsurface ices, then some of those ices would presumably be sublimated (due to the input of energy from the impact) producing some transient tenuous atmosphere. This scenario might well account for some of the diversity in colours (and reflectance spectra) seen in the Kuiper Belt object population. If a transient atmosphere recondensed on the surface, it might produce a thin *frost*. Although the frost layer would be thin, it could be enough to change the appearance (i.e. reflectance) of the body. Hence some of the diversity we see in the Kuiper Belt object population *might* be due to sporadic impact events.

It is the fact that cometary material represents relatively unaltered accreted material from the solar nebula that makes comets so scientifically interesting. Because they formed in the colder regions of the Solar System, they have not lost their volatile components (i.e. the ices), and as most of the comets are relatively small, they will not have been greatly affected by gravitational compression. Comets do indeed offer an excellent opportunity to sample pristine relatively unprocessed material reflecting the composition of the solar nebula. Space missions that will land on comets and sample the cometary material directly (for example the European Space Agency’s Rosetta mission) will return valuable data on the precise composition of the cometary material, and thus give us an insight about the solar nebula. These data will also complement the studies of meteorites (which you will be looking at in detail in Chapter 9).

### 7.5.1 Comet orbits

In terms of the orbits, there are two distinct groups of comets. The first group are the **long-period comets**. These comets come from the Oort cloud and thus can have semimajor axes of hundreds or even thousands of AU. As the Oort cloud surrounds the Solar System in a spherical distribution, the comets can enter the Solar System from any direction, and so the orbital inclinations can take any value. Thus we see as many retrograde long-period comets as prograde ones. Furthermore, the large values of semimajor axis mean that the comets have very long orbital periods (hence the name) and so it is unlikely that we will have observed a long-period comet before, at its previous perihelion passage. Thus long-period comets appear unannounced – we cannot predict when and from what direction they will come.

The second group of comets have orbits which are confined to the planetary system, i.e. we might consider this group as having semimajor axes less than that of Neptune (which corresponds to an orbital period of less than 200 years). These **short-period comets** generally have orbits with relatively low inclinations (i.e. they are mostly prograde orbits), although they can often have quite large eccentricities (for example, a value of  $e = 0.6$  might be typical). Most of the short-period comets are thought to come not from the Oort cloud but from the Kuiper Belt. Some bodies in the Kuiper Belt will slowly evolve inwards, to Centaur orbits (as discussed in Section 7.3), from where they might evolve into short-period comet orbits under the influence of Jupiter (mainly) and Saturn. Thus orbital evolution provides a mechanism for replenishment of the short-period comet population. It is evident that some mechanism of replenishment *must* exist, because short-period comets will be destroyed, either by collision with the planets or by sublimating themselves to nothing, over relatively short timescales (relative to the age of the Solar System). Figure 7.35 shows inclination as a function of orbital period, for the known comets with periods less than 100 years. The majority of these comets have prograde orbits, reflecting the fact that the objects in the Kuiper Belt also have prograde orbits. The few comets that are retrograde, are likely to have been long-period comets that were gravitationally captured into short-period orbits by a close approach to Jupiter.

You may find that comets with periods between 20 years and 200 years are sometimes referred to as *intermediate-period* comets.

The exact future position of a comet in its orbit at a given time (and indeed the comet's orbit itself) is often very hard to predict accurately. As comets undergo outgassing as they approach their perihelion, the emission of gas and dust applies a small force to the nucleus (like a small rocket). These are referred to as *non-gravitational forces*, and are enough to alter the comet's orbit very slightly. Because we cannot know exactly the orientation of the cometary emission on the surface, we cannot easily predict whether the non-gravitational forces might act to slightly speed the comet up in its orbit or slow it down. Thus there is an inherent uncertainty in predicting *precisely* the behaviour of an active comet's orbit in the future. This may affect our prediction of the exact time of the next perihelion passage, to the level of days or even weeks.

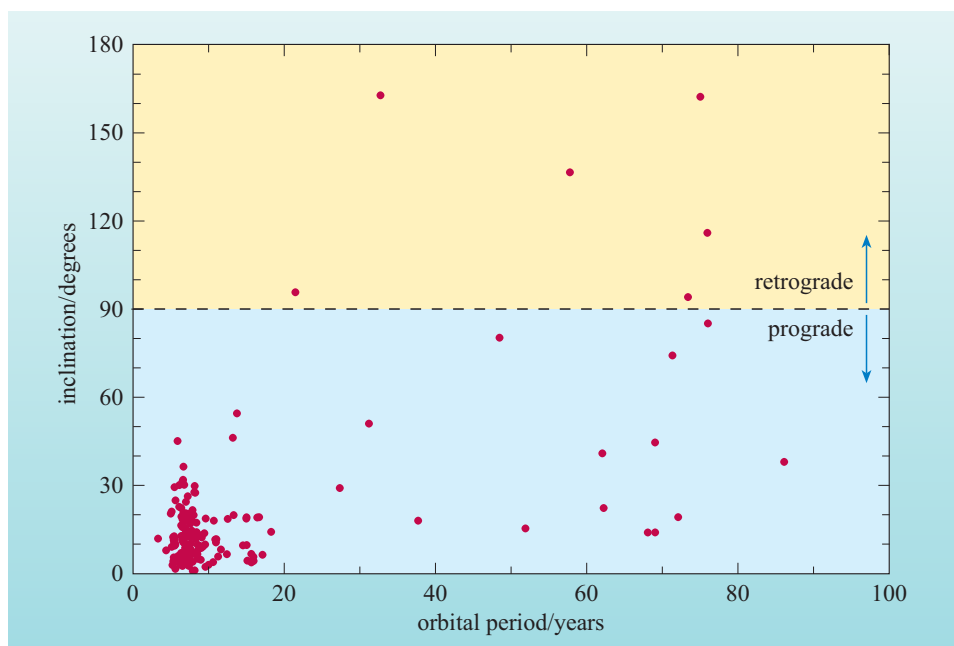


**Figure 7.35** The distribution of inclination for short-period comets. Most have prograde orbits, i.e. inclination less than  $90^\circ$ .

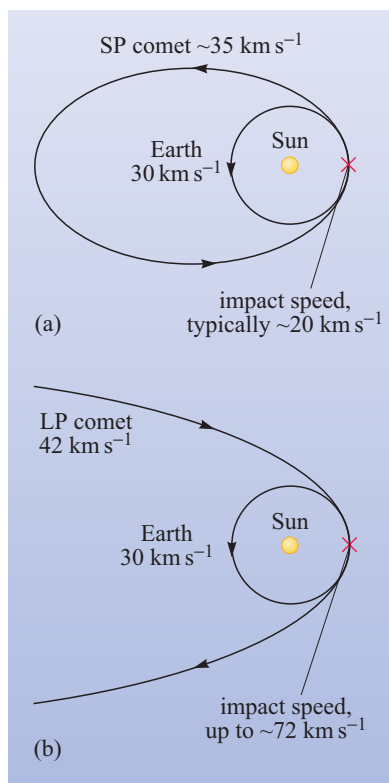


**Figure 7.36** Impact scenarios between two different comet orbits and the Earth. (a) A low-inclination short-period comet orbit produces a relatively low impact speed, whereas (b) this possible long-period comet orbit produces a much higher impact speed.

As was discussed in Section 7.1, the potential impact speed of a minor body colliding with a planet crucially depends on its orbit. Thus, the possible impact scenarios involving long and short-period comets can, on average, be somewhat different. As the majority of short-period comets have prograde orbits (like the planets), then impact speeds are somewhat limited. Figure 7.36a shows what might be regarded as a typical impact scenario between Earth and a low-inclination short-period comet. Earth orbits the Sun at around  $30 \text{ km s}^{-1}$ . If the impact is near the comet's perihelion, then the comet will be travelling somewhat faster than this, perhaps  $35$  to  $40 \text{ km s}^{-1}$  depending on the exact orbit. The collision is akin to cars travelling the same way on a road, coming together side by side, i.e. the impact speed is considerably less than the speeds of the individual cars. In this case the comet impact speed might be in the region of  $15$  to  $20 \text{ km s}^{-1}$ . However, if we consider an impact of a long-period comet, the comet orbit could well be retrograde (remember half the orbits are) and so a possible impact scenario can occur as shown in Figure 7.36b. The long-period comet can be travelling up to  $42 \text{ km s}^{-1}$  if its perihelion is near Earth's orbit, and thus a head-on collision with Earth (travelling at  $30 \text{ km s}^{-1}$ ) can occur resulting in an impact velocity of up to  $72 \text{ km s}^{-1}$ .

One comet impact, which was well observed by scientists on Earth, happened in 1994. A comet, named Shoemaker–Levy 9, had been captured by the gravitational pull of Jupiter after a very close approach to the planet in 1992. As the comet effectively orbited Jupiter, it underwent tidal stresses. The tidal stresses were sufficient to split up the cometary nucleus into many fragments (the fact that this could happen gives an indication of the relatively low material strength of the cometary material). The fragments then collided with Jupiter in 1994. Figure 7.37a shows the Shoemaker–Levy 9 fragments before the impact, and the Figure 7.37b shows the ‘scars’ in Jupiter’s atmosphere after several of the fragment impacts. We should hope that impacts like these do not happen in the near future on Earth!

#### QUESTION 7.12

It is clear that the inner Solar System is visited by comets from the outer Solar System (i.e. the Kuiper Belt or the Oort Cloud), and so these comets could impact the Earth and other terrestrial planets. Why might the presence of Jupiter result in the number of comets impacting the Earth being lower than otherwise might be expected?



(a)

**Figure 7.37** The impact of comet Shoemaker–Levy 9 with Jupiter. (a) The comet, imaged by the Hubble Space Telescope, is seen to have split into fragments which spread out along the comet's orbit. (b) The ‘scars’ in Jupiter’s atmosphere left after the impact of several of the comet fragments.



(b)



## 7.6 Interplanetary dust

You will now be familiar with the term ‘dust’ that we use to describe small particles of solid material. The term **interplanetary dust** literally means dust that is found between the planets. The Solar System is actually a rather dusty place, and in this section we’ll look at some of the sources of the dust, and how it is distributed.

We have seen in the previous section, that as a consequence of cometary emission, the dust particles locked within the cometary nucleus can be ejected into space. The dust particles thus become free of the parent body, and become members of what is often called the **interplanetary dust cloud** (a term describing the collection of dust particles in the inner Solar System).

Comets are undoubtedly one of the most important sources of interplanetary dust, but cometary emission is not the only source of dust. Impacts on the surfaces of minor bodies and other planetary bodies (or indeed complete fragmentation of bodies due to impacts), will eject small fragments and dust particles into space. At this point, it might be useful to define the size regime that we are discussing when using terms such as ‘dust’ or ‘fragments’. Although the division is vague, we usually describe particles that are less than about 1 mm in diameter as ‘dust’. Larger particles are often called **meteoroids**, although objects metres, or tens of metres across might be better described as (for example) ‘asteroidal fragments’ (or indeed small asteroids).

- If impact events are a source of dust, where in the inner Solar System might we expect impacts to occur relatively frequently, so producing a relatively large amount of dust?
- We would expect most impacts to occur in a region that has a high concentration of minor bodies, e.g. the asteroid belt.

The asteroid belt is indeed a major source of interplanetary dust, possibly as important as the production of dust from comets. However other sources of dust also contribute. All impact events will generate dust. For example, impacts on the satellites of a giant planet will produce dust particles that may predominantly stay within the giant planet’s system (think of the rings of Saturn, which consist of solid fragments that themselves must be generating impact related dust). Impacts on the Moon must eject lunar dust particles, some of which might subsequently collide with the Earth. The volcanoes on Io eject solid material into the Jupiter system. Indeed, experiments designed to be sensitive to dust impacts have detected these tiny (about  $0.01\ \mu\text{m}$  across) volcanic dust particles streaming away from Jupiter, highly influenced by Jupiter’s magnetic field. In Section 7.4, we considered impacts within the Kuiper Belt possibly ejecting subsurface icy material. It follows that dust particles, meteoroids and even larger fragments must occupy the Kuiper Belt.

The composition and structure of the dust particles depend on the source of the dust. For example, impact fragments from the surface of a rocky asteroid will be solid ‘chunks’ of the asteroidal material, i.e. rock. Cometary dust however has a more complicated structure. The dust in comets originally came from agglomerations of the tiny silicate dust particles present in the solar nebula. Larger particles can be a collection of smaller dust particles stuck together, often with ices in the voids. Figure 7.38 shows an interplanetary dust particle thought to come from a comet. The structure is very porous, the tiny (submicron) particles acting as the ‘building blocks’ of the larger particle are clearly seen.

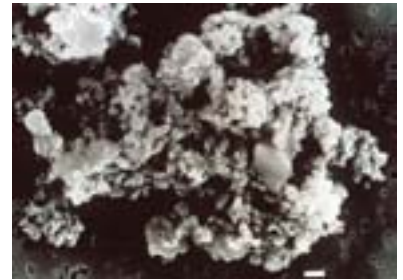


**Figure 7.38** An interplanetary dust particle, thought to be from a comet. This sample was collected in the stratosphere by a high-altitude aircraft, and is shown in this electron microscope image. The dust particle is very porous. When in the comet, the voids probably would have had ices in them, but these will have sublimated when heated by the Sun.

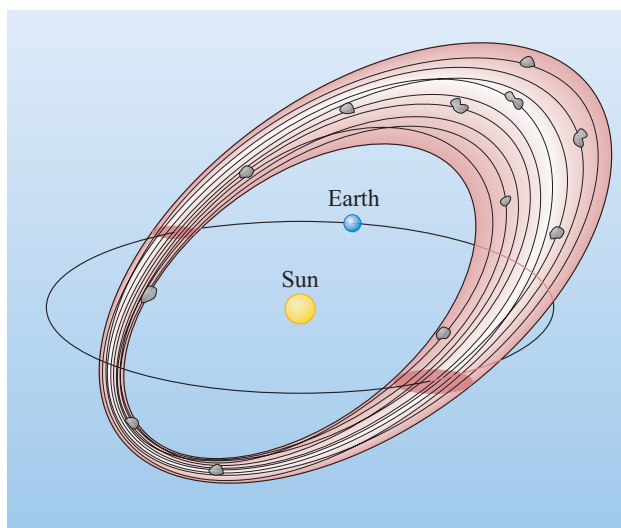


**Figure 7.39** A meteoroid stream produced by the ejection of dust particles from a comet. The orbits of the dust particles are reasonably similar to the parent comet, producing a tube of dust in space, which is thickest at the aphelion region.

As was stated above, the main sources of dust in the inner Solar System are comets and the asteroid belt. Let us consider the emission of cometary dust in more detail. When dust particles leave the surface of the comet, they are then on their own. They orbit the Sun on their own orbital paths, (i.e. on Keplerian orbits) and have little or no interaction with other dust particles and the parent nucleus (the gravitational influence of the nucleus being very small). However, the orbits that the dust particles take are, perhaps not surprisingly, very similar to the parent comet's orbit. This means that around the comet's orbit, there is a multitude of dust particles whose orbits form a sort of tube. This tube of dust particles is called a **meteoroid stream**, and one such stream is represented in Figure 7.39. The slight differences in the orbits of the various dust particles (i.e. differences in the semimajor axes) mean that the dust particles have a range of orbital periods. Thus quite quickly (a matter of a few tens of orbits) the dust particles become uniformly distributed around the meteoroid stream.

All active comets will produce meteoroid streams. However in most cases, observing the stream directly can be virtually impossible. The exception is when the orbit of the Earth happens to pass *through* a meteoroid stream. Once a year the Earth passes through the stream, as the stream passes through the ecliptic plane. In fact, for a few streams, the Earth could pass through the stream twice per year, 6 months apart (this is the scenario shown in Figure 7.39). When the Earth passes through a stream, the meteoroids in the stream will collide with the upper atmosphere of the Earth. As a particle hits the atmosphere, friction between the meteoroid and air heats both air and the meteoroid (which usually completely vaporizes due to the heating). As the meteoroid passes into the atmosphere (at an altitude of around 100 km) the atoms of the air close to the path of the meteoroid are excited (heated) and emit light, producing a short lived 'streak' of light. This streak of light is called a **meteor**, or a 'shooting star', and when many meteors are observed associated with the same meteoroid stream, the display is called a **meteor shower**. The typical size of a meteoroid that gives rise to a meteor visible with the naked eye, is about the size of a grain of sand. There are at least 50 meteor showers throughout the year that have been identified, although only a few produce sufficient meteors to be particularly noteworthy. Table 7.3 lists the major showers seen in the Northern Hemisphere, and the likely hourly rate of meteors that an observer would see (observing in ideal conditions). Significant activity can occur for a number of days around the date of maximum rate. Also listed are the parent bodies associated with the shower.



**Table 7.3** Major annual meteor showers. The name of the shower derives from the constellation where the ‘radiant’ lies. The radiant is the position in the sky that the meteors appear from.

Date of maximum rate	Name of shower	Hourly meteor rate	Parent body
Jan 3	Quadrantids (Bootids)	130	Unknown
Aug 12	Perseids	80	Swift–Tuttle
Oct 21	Orionids	25	Halley
Nov 17	Leonids	25 <sup>a</sup>	Tempel–Tuttle
Dec 13	Geminids	90	(3200) Phaethon <sup>b</sup>

<sup>a</sup>This rate is usually what is observed, but every 33 years or so, this shower can display much higher rates (see text).

<sup>b</sup>When discovered, (3200) Phaethon was assumed to be an asteroid as no cometary coma was observed. However it is likely that there has been some activity in the past.

Occasionally, the Earth passes through a particularly well populated part of a meteoroid stream, and the rate of meteors seen in a shower can increase significantly. For several years, between 1997 and 2002, this was the case for the Leonid meteor shower in November, where a peak hourly rate of up to several thousand was seen. An all-sky image of the Leonids shower in 1998 is shown in Figure 7.40. If you have never seen a meteor, then we would highly recommend trying to view one of the showers listed in Table 7.3, on or within a few days of the dates given. However, on any clear night you will see meteors. These meteors are not associated with an identified shower, but are just the random background of dust particles entering the Earth’s atmosphere (often called **sporadic meteors**). On average you will typically see a meteor every 15 minutes or so.

#### QUESTION 7.13

If you observed sporadic meteors throughout the night, you would notice that the rate increases significantly *after* midnight. Why might this be the case?

As you found with comet impacts in Section 7.5.1, meteoroids can collide with Earth at high speeds – depending on the orbits involved, speeds of between around  $11 \text{ km s}^{-1}$  and  $70 \text{ km s}^{-1}$  are possible. Imagine if a particle travelling at these speeds hit a spacecraft orbiting the Earth. The large kinetic energy involved means that even a relatively small meteoroid (for example 1 mm or so in size) could do a considerable amount of damage. Thankfully the risk of a major meteoroid impact is low, although evidence of small impacts is clearly seen on surfaces that have spent time in space and have then been retrieved. Figure 7.41 shows the result of a particle travelling at high speed hitting a solar array.

#### QUESTION 7.14

The kinetic energy of a body of mass  $m$ , travelling at a velocity,  $v$ , is given by  $\frac{1}{2}mv^2$ . Calculate and compare, the impact energies (i.e. the kinetic energies) of a small car travelling at 50 mph, and a meteoroid of mass 1 g travelling at  $20 \text{ km s}^{-1}$ . (Assume the car has a mass 1000 kg, and note that 50 mph is approximately  $20 \text{ m s}^{-1}$ .)

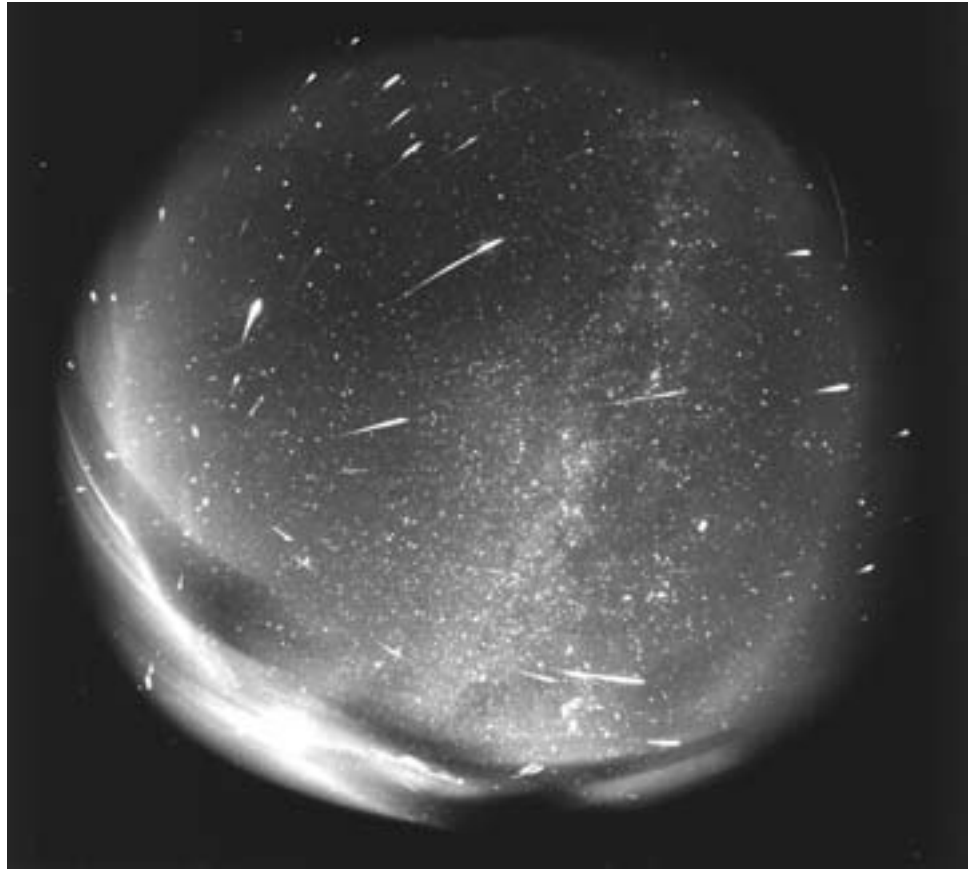


**Figure 7.40** An all-sky image taken during the 1998 Leonid meteor shower, when the peak rate of meteors reached several hundred per hour.

We have discussed various dust sources, such as dust in meteoroid streams, and dust in the asteroid belt, but dust particles are not confined to these well-defined regions. This is because of several mechanisms that can cause the orbits of dust particles to change significantly, so transporting them to different regions of the Solar System. The first of these mechanisms, is the orbital evolution that you have met for asteroids and other minor bodies. Meteoroids undergo exactly the same effects, and so for example, asteroid fragments could be slowly transported from the asteroid belt to Near Earth Asteroid type orbits, in exactly the same way as we described for the Near Earth Asteroid population in Section 7.2.

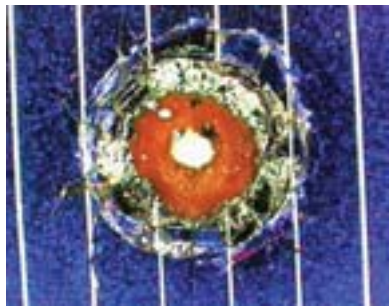


**Figure 7.41** An impact crater found on the solar arrays of an Earth-orbiting satellite. The vertical lines are about 1 mm apart. The crater could have been made by a particle just 100  $\mu\text{m}$  across.

The second important mechanism is that of **radiation pressure**. This effect arises because photons of light have momentum. When you shine light on an object, the photons can transfer their momentum to the object, in a way analogous to throwing heavy balls at an object in order to try and make it move. The force exerted by light in this manner is actually very small, but is most effective for very small objects. This is because the amount of light intercepted by the particle is directly related to its cross-sectional area, whereas the effect on the particle (the acceleration resulting from the radiation force) is inversely proportional to the particle's mass. Thus the radiation pressure has a maximum effect when the ratio of cross-sectional area to particle mass is maximized – and this ratio increases as the particle size decreases. However, the light ceases to effectively interact with particles that are very much smaller than the wavelength of light (typically  $0.5 \mu\text{m}$ ). Thus the effect of radiation pressure is a maximum for particles in the approximate diameter range  $0.1 \mu\text{m}$  to  $1 \mu\text{m}$ . For these small dust particles, the force exerted by solar photons (a force which acts in a direction radially outwards from the Sun) can be larger than the

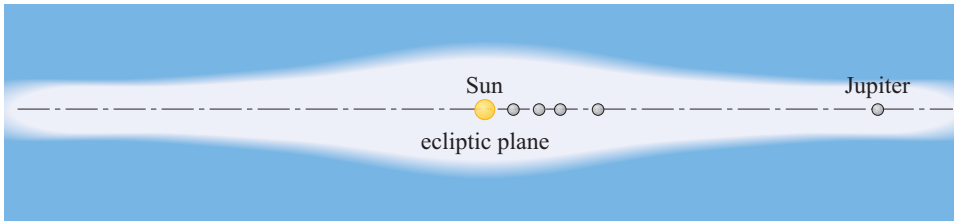


**Figure 7.42** A diagram indicating the interplanetary dust cloud. The concentration of dust increases towards the Sun, as particles slowly spiral in towards the Sun due to the Poynting–Robertson effect.

force of gravity. The result is that these small particles, as soon as they are produced in an impact event, or emitted from a comet, can be pushed out of the Solar System, a bit like being blown away in a wind. (This is why the comet dust tail appears to ‘flow’ away from the Sun, see Figure 7.30a.)

A third important effect for particles larger than about  $1\ \mu\text{m}$  (diameter) is called the **Poynting–Robertson effect**. This is also related to radiation pressure, but has almost opposite results. As photons travelling radially outwards from the Sun hit a dust particle, one might expect the force to also act radially outwards. However, as the dust particle has some transverse motion (i.e. perpendicular to the motion of the photon), the resulting impact of the photon appears to come slightly from the side. This acts to slow down the dust particle slightly in its orbit (like a braking effect) which in turn causes the semimajor axis of the orbit to decrease. Thus over many orbits, the dust particle gradually spirals into the inner Solar System. Many of these particles reach the near-Sun region, where they are vaporized due to the intense heat. The Poynting–Robertson effect thus supplies a mechanism whereby dust in the asteroid belt slowly spirals in towards the orbit of Earth and the other terrestrial planets. In fact many of the meteors that are not associated with specific cometary meteoroid streams (i.e. the sporadic meteors), are caused not by cometary dust, but by small dust particles that originally came from asteroids in the asteroid belt. This mechanism also affects larger objects such as centimetre-sized fragments, although it takes longer for these larger objects to reach the orbit of the Earth. A  $10\ \mu\text{m}$  sized particle would take only about 10 thousand years or so to spiral in from the asteroid belt, whereas a 1 cm object would take over 10 million years.

These radiation pressure and orbital evolution effects ensure that dust particles slowly move away from the region of their source. This results in the Solar System being filled by a dust cloud (i.e. the interplanetary dust complex mentioned above), an impression of which is given in Figure 7.42. This dust cloud is even sometimes visible with the naked eye. About an hour after sunset (or an hour before sunrise) if the sky is clear and you are observing in a good dark environment, you might just be able to see a faint glow extending up from the horizon nearest the Sun. This is referred to as the **zodiacal light** (Figure 7.43), and is due to the dust particles in the interplanetary dust cloud reflecting and scattering sunlight, just like particles in a cometary coma.



**Figure 7.43** A photograph, taken after sunset in 1997, of the zodiacal light (which extends up from the centre horizon) which is due to sunlight being scattered from the dust particles in the interplanetary dust cloud. Also seen in the photograph is comet Hale–Bopp.

## 7.7 Summary of Chapter 7

- The motion of the planets under the influence of the Sun's gravity is described by Kepler's laws. (i) Planets move in elliptical orbits, with the Sun at one focus, (ii) A line connecting the Sun to a planet would sweep out equal areas in equal times, (iii) The square of a planet's orbital period is proportional to the cube of its semimajor axis.
- Kepler's laws also apply to a satellite orbiting a planet (or any body orbiting another large body under the influence of gravity).
- The size and shape of an orbit are described by the parameters, semimajor axis ( $a$ ), eccentricity ( $e$ ). The orientation of the orbit plane with respect to the ecliptic plane is described by the inclination ( $i$ ).
- Asteroids are rocky and metallic minor bodies, most of which reside in the asteroid belt between Mars and Jupiter. Asteroids that have orbits that can come close to Earth are called *Near Earth Asteroids*.
- Asteroid diameters have a *size distribution*, quite similar to the size distributions of impact craters (Chapter 4). Many planetary impact craters were produced by the impact of an asteroid.
- Asteroids are given different taxonomic classes, which are related to their composition and determined by astronomical observations.
- A large belt of objects, called the Kuiper Belt, lies beyond the orbit of Neptune. Kuiper Belt objects are thought to be quite icy in nature. The planet Pluto represents the largest known member of the Kuiper Belt.
- Comets are icy bodies formed in the outer Solar System; leftovers from the planetary accretion process. They thus have very old, relatively unprocessed material within them.
- Comets eject gasses (due to sublimation of the ices) and small rocky dust particles, that give rise to meteoroid streams and interplanetary dust.
- Minor bodies in the Solar System undergo orbital evolution, such that over a long time (thousands and millions of years) the orbits are changed significantly.
- Orbital evolution offers a mechanism by which objects in the Kuiper Belt can slowly evolve into the inner Solar System, so renewing the short-period comet population. Similarly, Near Earth Asteroids come from the asteroid belt by the action of orbital evolution.

## CHAPTER 8

# THE ORIGIN OF THE SOLAR SYSTEM

### 8.1 Introduction

*In the beginning there was a formless void of emptiness known as chaos; from this darkness emerged a black bird known as Nyx (the goddess of night). Eventually the bird laid a golden egg, out of which was born Eros, the god of love. The shell of the egg broke into pieces, one of which rose into the air and became the sky (which Eros called Uranus) and the other became the Earth (called Gaia).*

This is one version of the Greek creation myth. It considers that we started with ‘nothing’ and evolved fairly rapidly towards the environment which we experience today. In fact, this is a feature of nearly all creation myths – the Sun, the Earth, its inhabitants, and by inference, the planetary system around us, all formed soon after a divine event had acted to add purpose to the pre-existing nothingness, or chaos.

The details of the traditional scientific view are somewhat different. The Universe was created about 13 Ga ago, in the *Big Bang* (the exact age is unclear although somewhere between 10 and 20 Ga is the current consensus). Clumps of material then formed into galaxies, and galaxies spawned stars. From that time until the present day, the cycle of stellar birth and death has continued remorselessly. Our own Solar System formed 4.56 Ga ago from materials that had been cycled in and out of stars several times (see Box 8.1).

There have been (and still are) many different theories of how our Solar System formed. A fundamental difference in approach, considers whether the processes that formed the Sun and the planets took place simultaneously in a single integrated event, or whether the planetary system was added to a pre-existing Sun, some time after the Sun’s formation. These two approaches are referred to as *monistic* (single event) and *dualistic* (two separate events). An example of a dualistic theory of Solar System formation, would be the theory that another star passed close to the Sun, causing matter to be pulled from the Sun into a single filament, which then broke up along its length to form individual planets. (Indeed this theory was proposed in 1917.)

#### BOX 8.1 CYCLING OF STELLAR MATERIAL

The fact that Earth and all its constituent components (including life forms) are made largely of materials that have been produced in stars (which, necessarily existed before the Sun) may be somewhat surprising! In brief, except for hydrogen and helium, all the elements are made in stars. Now, we know that the Sun is about 4.56 Ga old, and it is predicted that it will last a further 5 Ga or so. In other words, stars that are about the same size as the Sun last for about 10 Ga. Smaller stars last longer, and larger stars (where most of the heavy elements are made) have shorter lifetimes. However, the relationship between size and lifetime is not linear. A star that has 3 times more mass than the Sun will have a lifetime of 0.5 Ga. One that is 25 times more massive will last for less than 10 Ma. It should thus be apparent, that in the billions of years before our Solar System formed, many generations of stars would have come and gone. The debris from these previous generations of stars is what the Solar System is made of.



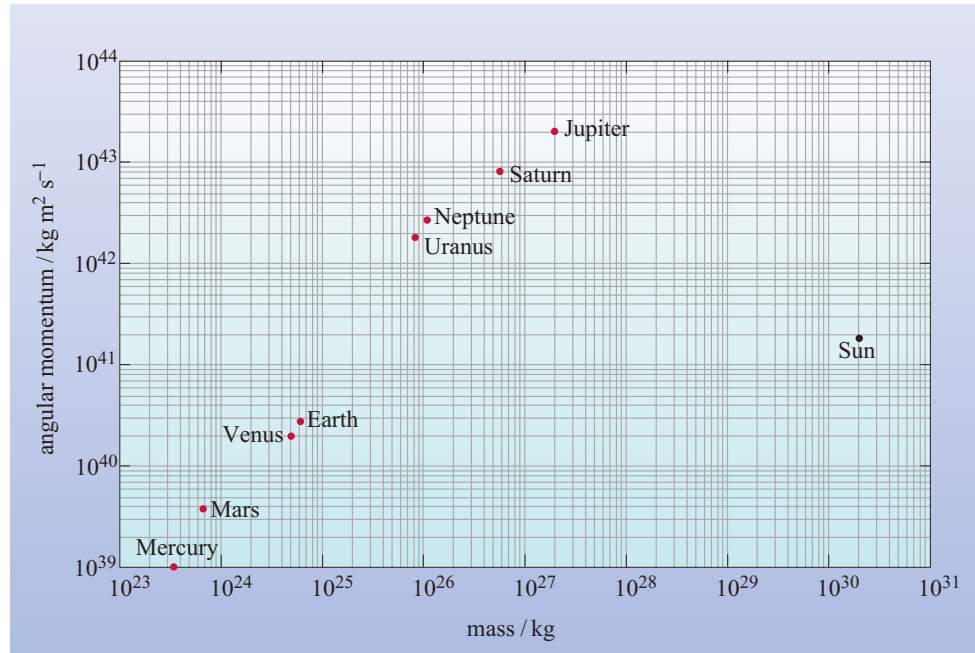


**Figure 8.1** Angular momentum plotted against mass for the Sun (axial rotation) and the planets (orbital motion). The contribution to orbital angular momentum from Pluto and the satellites of the planets, and the contribution from axial rotation of the planets and satellites, are too small to show on this plot. Note that both axes are logarithmic. [Comment: The nearly straight-line relationship for the planets, between angular momentum and mass, is because angular momentum is directly proportional to mass, but (as a consequence of Kepler’s third law, and the dependence of the planet’s orbital velocity on the orbital radius) it depends only weakly on orbital radius (in fact on its square root). If you very carefully draw a line at  $45^\circ$  passing through the data point for Mercury, you will find that the data points for the other planets fall progressively further from this line as orbital radius increases.]

It is fair to say, that currently, a monistic view of Solar System formation is supported by most scientists. It should be understood that the details of the process are still open to interpretation, and are matters of research and great debate. There is no one single ‘this is exactly how it happened’ theory. However, in this chapter we will discuss an overall formation process that best fits the data known today, pointing out where details are uncertain as appropriate.

By the close of the 18th century, the French mathematician Pierre-Simon Laplace had derived the classical monistic model of Solar System formation – an idea that was eventually to be called the **nebula hypothesis**. Laplace, demonstrated that a rotating sphere of gas eventually flattens into a spinning disc. As matter begins to contract towards the centre (matter that will eventually form the **protoSun**), the disc starts to spin faster, due to conservation of angular momentum. (See Box 5.7.) Much of the material in the disc eventually goes on to accrete into the planets (the details of which we will discuss throughout this chapter). This is the overall process you looked at in Chapters 1 and 2.

However, this hypothesis was not always accepted. One of the major problems that brought the nebula theory into question, involved the disparity between the present-day distributions of mass and angular momentum in the Solar System. This is normally referred to as ‘the angular momentum problem’. Put simply, while only about 0.14% of the total mass of the Solar System is contained in the planets, they nonetheless account for more than 99% of the angular momentum of the system as a whole (i.e. within their orbital motions). In contrast, any simple view of the formation of the Solar System from a nebula would have at the centre, a body containing most of the mass and correspondingly most of the angular momentum. Thus we might expect the Sun to be rotating far more rapidly than it actually is. (The Sun currently rotates on its axis once every 25.5 days; this is entirely typical for stars that are in other ways similar to the Sun.)

The example that we have used before to illustrate angular momentum is that of an ice skater performing a spin. With arms outstretched the skater rotates at one speed, but as he brings his arms inwards towards his body (thereby concentrating mass, like an accreting Sun), he rotates more rapidly (i.e. conserving angular momentum). However, this is not what is observed in the Solar System. The magnitude of the deficit is shown in Figure 8.1.

Let us now look at the formation process in more detail, and see how the nebula theory does, in the end, ‘solve’ the angular momentum problem, and does indeed form a good model of the origin of our planetary system.

## 8.2 Physical formation processes

### 8.2.1 The beginnings of a solar system

In this section we shall examine how the Solar System may have formed, about 4.56 Ga ago. You may recall that you encountered this same value in Section 2.4.3 where it was quoted as the age of the Earth. In fact, the age itself is derived from meteorites which, being small bodies that cooled quickly after their formation, effectively document the age of the Solar System, thus

the age of meteorites = the age of the Solar System = the age of the Earth

We shall start our enquiry before the Solar System formed and then follow the story from the time that the dust and gas cloud around the protoSun began forming into planets. Some very general sense of these processes has already been given in Chapters 1 and 2. Here we supply more detail.

In order to understand the details of how a planetary system forms it will be necessary to understand a few astronomical principles, and to be aware of certain telescopic observations of objects beyond the Solar System. After all, the Sun is merely a star, of which there are some  $10^{11}$  in our Galaxy, the Milky Way. Ideas about how stars form come from observations of stellar objects and their precursors – since there are so many stars potentially available for study, it is



inevitable that we will be able to see examples of objects at all stages of evolution, from birth, to quiescent normal life, to terminal decline, and ultimately death.

Stars are born out of clouds of molecular gas and dust (see Figure 8.2) and they come in a complete range of sizes from bodies of mass about  $1/25$  times the mass of the Sun (that is  $0.04M_{\odot}$ ) up to giants of about  $50M_{\odot}$ . However, for our purposes we are only really interested in stars that are about the same size as the Sun (a range of, say,  $1$  to  $3M_{\odot}$ ). The reason for this is that stars which are very small are unlikely to support planetary systems, while stars that are relatively large have short lifetimes and, furthermore, above  $8M_{\odot}$  are destined to become supernovae, i.e. stars that will undergo a violent explosive death. While stars in their own right are interesting things to study, when considering the origin and evolution of our own Solar System it makes sense for us to concentrate on the workings of stars that are of a similar size to the Sun. In this regard you should note that the Sun is quite average in terms of its size and other characteristics, such as chemical composition, luminosity, age, etc.



**Figure 8.2** Spectacular HST image of a star-forming region in the Cone Nebula, which is in the constellation of Monoceros (a distance of 2500 light-years away, i.e.  $2.4 \times 10^{16}$  km). The image shows the upper  $2.4 \times 10^{13}$  km of the nebula.

- Since we will be making a number of references to the masses of astronomical objects, check that you are happy with the notion of relating such things to the mass of the Sun. For instance, what is the mass of the Earth expressed in solar masses?
- The Earth has a mass of  $5.97 \times 10^{24}$  kg, while that of the Sun is  $1.99 \times 10^{30}$  kg. Hence, the Earth mass, relative to that of the Sun is  $(5.97 \times 10^{24}) / (1.99 \times 10^{30}) = 3 \times 10^{-6} M_{\odot}$ .  
By a similar calculation, Jupiter has a mass of about  $0.001 M_{\odot}$ .

As the process of starbirth advances, any gas/dust that remains gravitationally bound to a young stellar object, while not actually falling onto the star itself, ends up as a swirl of material around the star (known as a **circumstellar disc**). It is within discs like this that planets may be formed. Some of the details of this process will be described in the next section. For now, it is appropriate to marvel at some truly remarkable images obtained using the Hubble Space Telescope (HST) which show discs of material around young stars (see Figure 8.3). The features themselves are revealed by infrared (IR) observations detecting thermal radiation from dust grains that have been heated by absorption of shorter wavelength radiation from the star at the centre of each disc.

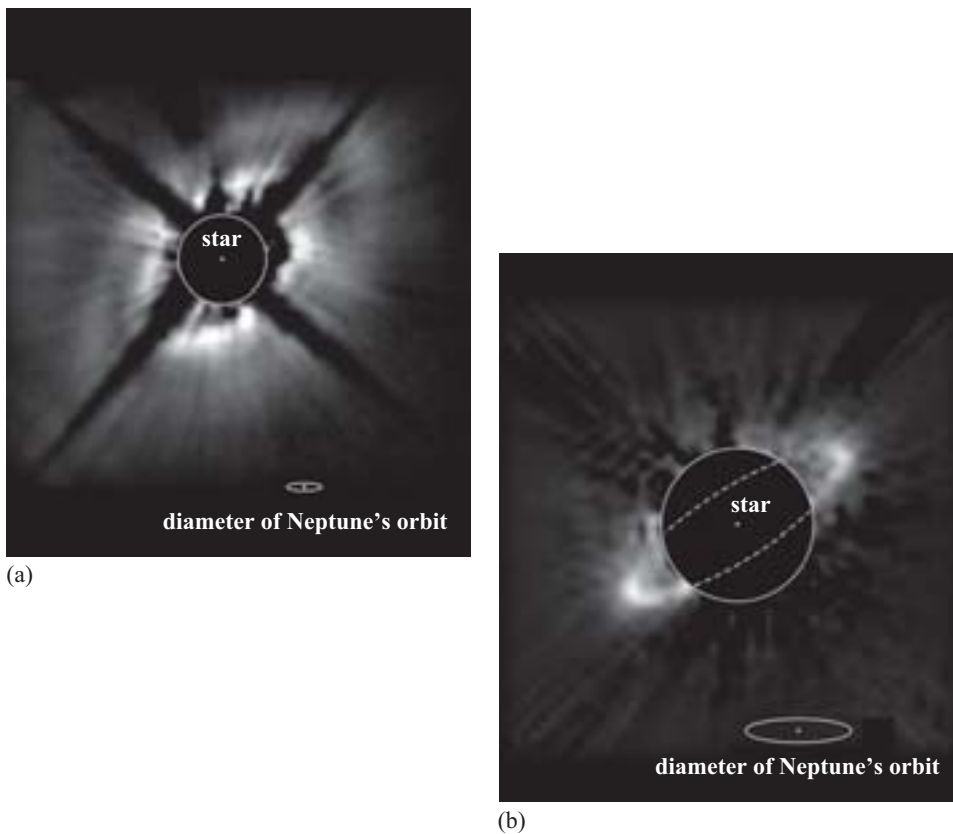
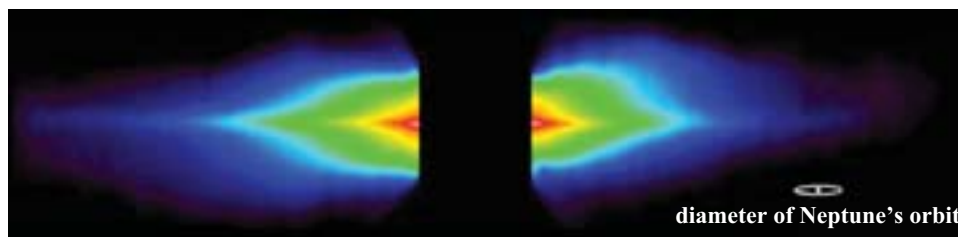


**Figure 8.3** HST images of dusty circumstellar discs around two young stars. (a) HD 141569. (b) HR 4796A. The central dot in each image represents the position of the star; the circles mark the positions of a physical disc positioned so as to restrict the starlight entry to the telescope. The diameter of Neptune's orbit is about  $9 \times 10^9$  km.

**Figure 8.4** HST image of  $\beta$  Pictoris. The diameter of Neptune's orbit is about  $9 \times 10^9$  km.



- Contrast the position of the ring around HR 4796A (Figure 8.3b) with the known dimensions of our own Solar System.
- Neptune orbits at 30 AU, while the Kuiper Belt extends to around (at least) 50 AU. It would appear that HR 4796A is of a similar size to our own Solar System.

The mass of dust in discs around young stars, like those shown in Figure 8.3, ranges from  $0.001M_{\odot}$  to  $0.1M_{\odot}$ , which is in accord with theories of Solar System formation, as will be described shortly. In detail, extremely tenuous discs extend out to hundreds of AU. That observed around the star known as  $\beta$  Pictoris is believed to contain as little as  $10^{-7}M_{\odot}$  of material (Figure 8.4). This particular star is interesting for many reasons, not least because it is the first ever object that was observed to have a dusty disc around it. At an age of about 20 Ma, it is likely that  $\beta$  Pictoris is at a more advanced stage of evolution than the stars considered previously, and it is likely that a planetary system has already formed.

#### QUESTION 8.1

In total extent the  $\beta$  Pictoris circumstellar dust disc is 1500 AU across. Light from the star prevents the disc being seen closer in than about 66 AU, but IR observations indicate that its inner edge lies about 20 AU from the star. How well does the suggested extent of this disc correspond with the distribution of planets and other bodies in our own Solar System?

In addition to observable circumstellar discs there is now a substantial body of evidence for planetary systems around stars obtained from observational methods that target the stars themselves. For instance, an apparent wobble in the position of a particular star is taken to imply the presence of a large planet exerting a gravitational pull as it orbits the star. Alternatively, changes in the apparent brightness of a star can be used to infer the passage of a planet between the star and the observer. So far, the kinds of planets determined by these methods are thought to be Jupiter-sized. But be aware that they are seen to orbit their parent star very rapidly (in some cases a matter of days rather than the 11.86 year orbital period of Jupiter). This necessarily means that these extra-solar planets must be close to their respective stars, which has earned them the name ‘hot jupiters’. At the time of writing about 100 such planets have been discovered, but progress in this area has been rapid and the number is likely to continue to rise. While these are fascinating discoveries and have attracted much interest from astronomers, they are somewhat less relevant to planetary scientists who ultimately would like to find evidence of systems like our own, i.e. with a range of planetary types from Earth-like to gas giants. However, one

extremely important outcome from the discovery of hot jupiters is the realization that in planetary systems as a whole, the orbits of the constituent bodies are subject to change during their lifetimes. This has to be true in the case of the extra-solar planets because there seems to be no logical way to form such large bodies as close to their stars as they appear to be. This finding has alerted people studying the Solar System to the prospect of *planetary migrations* (i.e. changes in orbital distances) affecting our own system.

### 8.2.2 From dust to protostars

You will now examine some of the details of the formation of solar systems, starting with a closer look at the origin of stars. Direct observations of circumstellar discs, achieved with increasing clarity since the early 1980s, support the theory of planetary-system formation proposed originally by Laplace (as was introduced in Chapter 1, Section 1.2). It was suggested by Laplace that the Solar System was formed by the gravitational collapse of a large, initially spherical, rotating mass. According to this theory, the central region grew denser and became the Sun, and the remainder was forced into a disc of gas and dust, called the Solar Nebula, within which the planets formed. This nebula theory has been with us ever since.

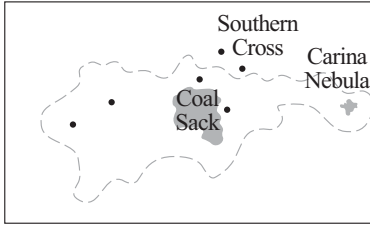
Even though most scientists believe that the Solar System formed from a nebula, there is no general agreement as to how it happened. There are many versions of the nebula theory, but it will not be possible to examine them all here. Instead we will present you in this section with a discussion that fits most of the available evidence, and is at least moderately self-consistent. You should *not* regard it as representing a consensus view in all its details, and we will encourage you to be aware of difficulties and uncertainties when they crop up.

Before we consider what happens to the cloud of gas and dust that forms the Solar Nebula it is appropriate to ask how such an entity arose. To tackle this question we need to consider material beyond the Solar System. When we study the distribution of stars within the Milky Way, we find that it is far from even. You can easily see this in Figure 8.5, which shows a panoramic view of the sky. Apart from the general ‘splash’ of stars across the sky indicating the position of our own Galaxy, the Milky Way, there are, even within the Milky Way, many regions where stars seem to be missing.



**Figure 8.5** Full-sky view of the stars that constitute our own Galaxy – the Milky Way. This image captures almost half of the Milky Way and was taken at a time when the Galactic Centre was overhead (although it cannot be seen in visible light because of the obscuring effects of dust and gas in the plane of the disc).

**Figure 8.6** View of the southern skies showing the Coal Sack region as a dark patch within an otherwise brightly lit region. The Coal Sack itself is a cool dense cloud, located about 500 light-years away; it is situated such that it blocks out the light from the stars beyond it.



5 degrees

An example of a dark region can be seen in Figure 8.6; the so-called Coal Sack region of the Milky Way. However, we now know that this apparent lack of stars is not what it seems. These gaps arise because our view of the stars is obscured in some directions by intervening clouds of gas (consisting mainly of hydrogen) and dust (about 1% of the mass of the gas and consisting mainly of heavy elements and their compounds). These are the **dense clouds**, which are characterized by a low temperature (typically 10 K), a high density (at least by the standards of the interstellar medium, the material between stars, which in our Galaxy consists of 99% gas and 1% dust) and a rich collection of molecules. Such clouds are relatively common. Within the Milky Way there are about 2000 dense clouds in a ring-like structure about half-way between the position of our Solar System and the Galactic Centre (each cloud has an overall diameter greater than about  $10^{15}$  km). Although the typical number density,  $n$ , of gas in the interstellar medium is of the order  $10^6$  particles  $\text{m}^{-3}$ , in the dense clouds  $n$  varies from about  $10^9$  to about  $10^{12}$  particles  $\text{m}^{-3}$ . Since gaseous hydrogen ( $\text{H}_2$ ) is by far the most dominant constituent of these dense clouds, we could also say that  $n$  is equivalent to  $10^9$  to  $10^{12}$  molecules of  $\text{H}_2$  per cubic metre.

The dense clouds are large and contain a significant amount of material. They make up perhaps 45% of the total mass in the interstellar medium.

- Assuming a density of about  $10^9$  particles  $\text{m}^{-3}$ , with each molecule having a mass of  $3.34 \times 10^{-27}$  kg (that is the mass of a hydrogen molecule), what is the overall mass of a typical dense cloud? (Assume a spherical geometry with a radius of  $5 \times 10^{17}$  m.)

- Volume of cloud =  $\frac{4}{3} \pi r^3$   
 $= \frac{4}{3} \pi \times (5 \times 10^{17} \text{ m})^3$   
 $= 5.24 \times 10^{53} \text{ m}^3$



There are  $10^9$  molecules of  $\text{H}_2$  in each cubic metre, i.e.  $1 \text{ m}^3$  contains a mass of  $3.34 \times 10^{-27} \times 10^9 \text{ kg} = 3.34 \times 10^{-12} \text{ kg}$ . So, the overall mass of the cloud would be

$$5.24 \times 10^{53} \times 3.34 \times 10^{-12} \text{ kg} = 1.75 \times 10^{36} \text{ kg}.$$

Since the mass of the Sun is  $1.99 \times 10^{30} \text{ kg}$  we could say that the cloud had a mass of  $8.75 \times 10^5 M_\odot$ , i.e. about a million solar masses (as an order-of-magnitude estimate). You can see that 2000 clouds of this sort would contain about 2 billion  $M_\odot$  of gaseous hydrogen.



**Figure 8.7** Detailed picture of the Orion Nebula – a feature which is visible to the naked eye, although not as portrayed in the figure. The nebula is made mainly of hydrogen gas, which is glowing as a consequence of four young massive stars in the brightest region.



**Figure 8.8** The four young bright stars from the Orion Nebula, known as the Trapezium. The image shows other stars at least some of which are also within the Orion Nebula (the others are foreground stars). The region shown corresponds to the inner, bright part of the image shown in Figure 8.7.

It is the dense clouds where it appears that conditions are particularly favourable for stars to form. Let's look at the evidence that supports the view that dense clouds are the place of starbirth.

Some young star clusters seem to be surrounded by the remnants of the original cloud from which they formed. Figures 8.7 and 8.8 show the Orion Nebula. It is visible to the naked eye as a haze surrounding the star  $\theta$  Orionis in the sword of Orion. Observations with a telescope show this region to be one of the most visually magnificent in the sky. There is plenty of evidence to suggest that star formation took place here very recently (on the astronomical timescale).

All other evidence points to these stars being very young. What interests us here, though, are the vast clouds of glowing gas and obscuring dark clouds of dust and gas. These are almost certainly the remnants of the dense cloud from which the young stars in the nebula formed. Lit up by the intense radiation from these stars, the hydrogen in the cloud is ionized and glows in its characteristic red light.

Another strand of evidence is that some dense clouds are found to contain a large number of compact IR sources. A good example is shown in Figure 8.7, which is a closer view of the Orion Nebula. It is thought to contain some very young stars, unobservable in visible light but detectable in the IR part of the spectrum. It seems that the IR radiation comes not from the young star itself but from the cocoon of dust still surrounding it. Heated to a temperature of a few hundred kelvin by the recently formed star, the warm dust re-radiates in the IR part of the spectrum.

Theoretical models of star formation all point to regions of low temperature and high density as being the most likely sources of starbirth, i.e. the dense clouds. By way of a brief introduction to these models note that each piece of matter attracts every other piece with the force of gravity. When we are dealing with the gas and dust clouds spread through the vast expanses of the interstellar medium, we cannot ignore this force and must consider the gravitational attraction between different sections of these interstellar clouds. Sir James Jeans (1877–1946) was able to show that, under appropriate conditions, a cloud (or part of one) would start to contract under the influence of the gravitational force. He derived a simple formula for calculating the mass and size that a cloud would have to reach, as a function of its temperature and density, before gravitational contraction could start.

We have pointed out that all atoms, molecules and particles in a cloud are attracted to each other by the gravitational force. However, observations show that many clouds appear to be in a state of equilibrium – in other words, they don't seem to be in a state of gravitational contraction. The constituent particles don't all collapse into a very small volume because their continuous motion means that particles undergo random collisions, creating an outward pressure, which counteracts the tendency of the gas to contract. The basis of the approach used by Jeans was to consider the balance between the two forces (pressure and gravity). He proposed that if the force due to gravity was the greater, then gravitational contraction could occur. Using this simple criterion, Jeans was able to show that, for a given set of conditions of temperature and particle number density, there is a minimum value for the mass of a uniform spherical cloud at which the force of gravitational attraction will overcome the force due to the motion of the particles, and contraction will occur. This critical mass is known as the **Jeans mass**. A cloud which possesses the Jeans mass is said to satisfy the *Jeans criterion* for contraction.



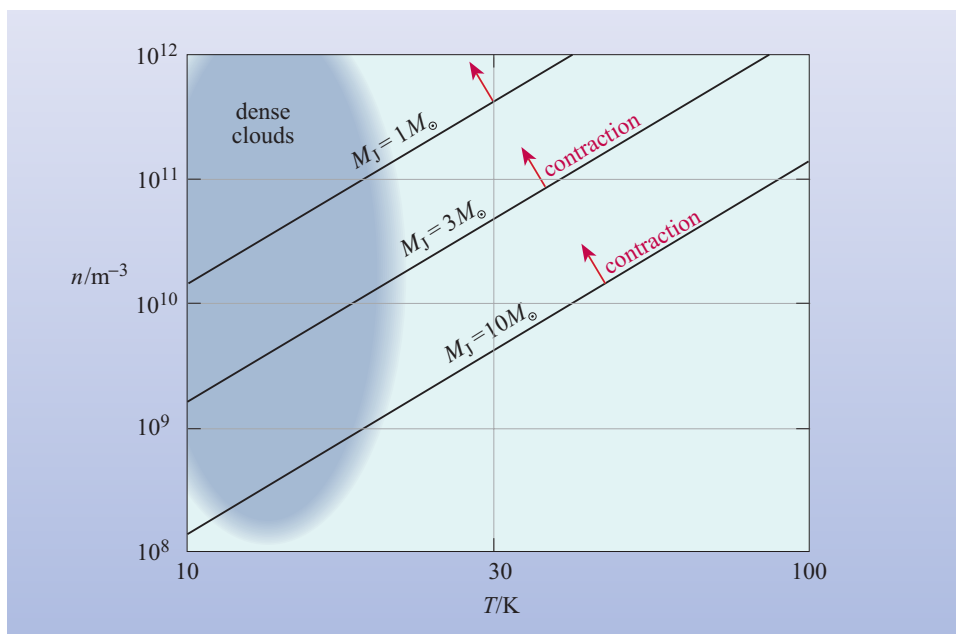


**Figure 8.9** The relationship between particle number density,  $n$ , temperature,  $T$ , and the mass required in a spherical cloud for the gravitational force to cause contraction to occur. This is the Jeans mass,  $M_J$ . It is assumed that the particles are hydrogen molecules such that the molecular mass  $m = 2 \times 1.67 \times 10^{-27}$  kg.

Figure 8.9 shows that dense clouds of only a few solar masses would contract. Many dense clouds are far more massive than this. Moreover, there are yet denser regions within dense clouds (called cores and clumps), with masses between about  $0.3$  and  $10^3 M_\odot$ , that can therefore satisfy the Jeans criterion on their own. Thus, gravitational contraction of dense clouds is to be expected.

The picture that has been painted so far, however, makes simple assumptions.

- What are the factors that could complicate this simplified approach to the gravitational contraction of a dense cloud?
- We wouldn't necessarily expect a typical cloud to be spherical or to have the same temperature and density throughout.

In addition, no account has been taken of rotation or of magnetic fields, which may exert an influence within the cloud thereby affecting the process of gravitational attraction. In detail these effects may be quite negligible at the start of the process, but become more important as cloud collapse proceeds. There may also be other external influences such as the compressive effects of shock waves accompanying the detonation of a nearby supernova.

Despite its over-simplifications, the Jeans approach is a good starting point for more sophisticated, and perhaps more realistic treatments of the early stages of star formation. Exactly how and why the gravitational collapse is triggered in the first place is perhaps more speculative, but there are plenty of ideas, e.g. a shock wave from a nearby supernova, passage of the cloud through one of the Galaxy's spiral arms, two clouds interacting, and so on.

**Figure 8.10** In dense clouds stars form in open clusters of several hundred. This particular example, which has no name (except for its catalogue number, NGC 2264) is about 5 Ma old. The dense cloud, which gave birth to the stars, is still very much in evidence in this visible image.



We know from observations that stars are often found in groups, referred to as clusters (or open clusters). Examples can be seen in Figure 8.10. The stars in each cluster appear to have formed at about the same time. The number of stars in an individual cluster can range from 10 to 1000 (with the volume of space they occupy varying accordingly).

How is the presence of clusters consistent with the picture of gravitational contraction that we've painted so far? The answer is believed to lie in the phenomenon of *cloud fragmentation*. As an individual cloud contracts, it is thought that it starts to break up into fragments, each having the potential to continue collapsing separately from the others. It is quite possible for a breakaway fragment to satisfy the Jeans criterion in its own right and if so, it will continue to undergo gravitational contraction. In this way you can see, at least qualitatively, how a cloud initially with a mass of hundreds or even thousands of solar masses can ultimately produce a large number of small fragments, each collapsing on its own, to yield a cluster.

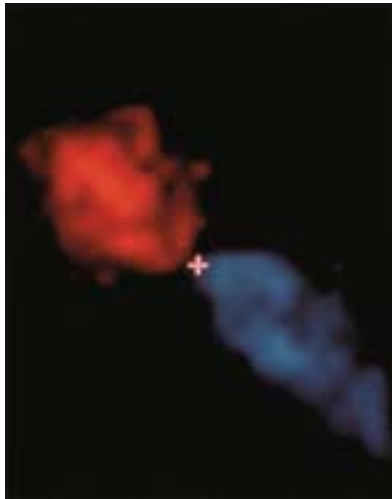


**Figure 8.11** Image taken by a radio astronomy technique of the object known as IRS5 (about 520 light-years away). The outflows from a young star (marked with a cross) are clearly visible as two oppositely directed lobes – the one coloured blue is flowing towards us and the one coloured red is flowing away. These lobes together constitute bipolar outflow.

We have now reached the stage where our dense cloud is contracting, probably in the form of many fragments. Let's now concentrate on the development of a typical fragment. As this contracts, the gravitational energy of the particles is converted, via mutual collisions, into thermal kinetic energy, and the temperature rises. Unfortunately, the process is taking place behind a shield of gas and dust, which effectively screens the fragment from view. For this reason we are forced to fall back on theoretical calculations and computer models of this phase. These seem to show that, after only a few thousand years of gravitational contraction, the edge of the cloud has heated up to between 2000 K and 3000 K. At this stage, the chain of events has started that will lead the fragment, almost inevitably, to become a normal type of star. For this reason, we are now justified in calling the fragment a **protostar**. Virtually all fragments that ultimately become ordinary stars take less than about  $10^8$  years to pass through the protostar phase – rather short on the astronomical timescale.

Knowledge of the protostar phase of stellar evolution has been enhanced by observations made by radio astronomers (a technique which allows us to look through the obscuring gas and dust). It transpires that a large number of protostars show evidence of a phenomenon called bipolar outflow – that is, gas flowing at high velocities (in what is known as a *stellar wind*), typically  $50 \text{ km s}^{-1}$ , in two streams moving in opposite directions. An example is shown in Figure 8.11.

Bipolar outflows are thought to last for only a relatively short time (perhaps  $10^4$  years), but during this period they eject a significant amount of mass and therefore require a lot of energy to sustain them. The outflows accompany the formation of a circumstellar disc or torus, shown schematically in Figure 8.12. Another class of object that is thought to be relevant to the early stages of evolution is **T Tauri** stars, which are young (typically 1 Ma old) and in the process of losing mass through stellar winds (at speeds of up to 100 to  $200 \text{ km s}^{-1}$ ). These objects can lose as much as  $0.5M_{\odot}$  in the form of a stellar wind during the T Tauri stage. Some T Tauri stars also show evidence of thin discs of circumstellar material, which demonstrates a qualitative relationship with stars having bipolar outflow sources (although in T Tauri stars the outflow is in all directions).

Objects that have bipolar outflows, or are designated as T Tauri stars, are protostars in their final stages of birth, i.e. they are just about to start the process of nuclear fusion reactions. They are generally in the mass range of about 0.2 to  $2.0M_{\odot}$ . As a protostar evolves it begins to show a continuous rise in temperature as the protostar contracts. The critical point comes when the temperature and pressure in the centre of the protostar becomes sufficient for nuclear fusion to be triggered in the core. The energy released raises the core temperature (and pressure) sufficiently to halt contraction, and marks the conversion of the protostar into a proper star.

### 8.2.3 The Solar Nebula

Before we start to consider the details of processes occurring within the Solar Nebula, a word of caution is in order. In the following sections we will deal with topics such as condensation, coagulation, planetesimal formation, planetary embryos and planet growth (as were considered in Chapter 2). While in the most general sense, these processes are part of a time sequence which moves in one direction (from the collapse of the gas–dust cloud towards the formation of planets) it is important to realize that they do not take place one after another. There was not an epoch of condensation, followed by one of coagulation, and so on. The Solar Nebula was a very complicated environment and, indeed, one that we do not yet fully understand. It is likely that small clumps of rocky materials (the building blocks of planets) were forming from dust in certain parts of the nebula, while at the same time there were solid materials condensing from the gas phase in other parts. Furthermore, materials were being moved around by phenomena such as stellar winds and the general turbulent motions of particles in the dust cloud itself. Impacts would have acted to transform clumps back into dust (and gas), and in some regions, dust produced within the Solar Nebula was mixing with the unaltered pre-solar dust which had coalesced in the first place. This pre-solar dust would have had any number of origins – as condensates from other stars, materials formed and processed in the interstellar medium, supernova debris, and so on. That such materials were present is not idle speculation – we have examples of pre-solar grains preserved in meteorites, which represent the fossilized remains of Solar Nebula processes (see Chapter 9).

Meteorites help us to constrain the timescales of events which took place during Solar System formation. In fact, the ages of bodies like the Earth and the Sun are based on data acquired from meteorites. The age that we assign to the Solar System is 4.56 Ga.

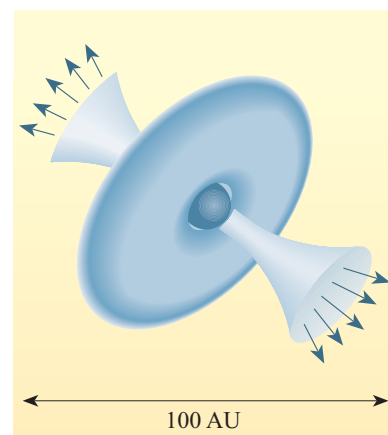


**Figure 8.12** Schematic representation of bipolar outflow showing a central protostar, a circumstellar disc or torus and a strong stellar wind. The torus confines the wind to flow predominantly in two opposing directions.

The concept of the origin of the Solar System as a single event is not without its critics. However, an age for the Solar System is clearly a useful notion and one which we use extensively herein.

In astrophysical terms, four key stages are recognized during the formation of the Solar System:

- 1 Dense cloud collapse (an interval of between 0.1 Ma and 0.5 Ma).
- 2 Disc dissipation, where material falling onto the accretion disc is transported inwards onto the protoSun (an interval of 0.05 Ma).
- 3 Terminal accumulation of the Sun, during which time the protoSun becomes a T Tauri star and planetary accretion begins (an interval of between 1 and 2 Ma).
- 4 Gas dissipation, where planetary accretion in the inner Solar System ends and residual nebula gas is largely removed by T Tauri winds (an interval of between 3 and 30 Ma).

Out as far as Uranus and Neptune the process of accretion may actually have continued for another 500 to 1000 Ma as the planets continued to sweep up the remnants of nebula gas not completely dissipated during the T Tauri stage.

With this potted history of the Solar Nebula in mind let us now get back to the collapsing dust and gas cloud of the type observed around HP 4796A (Figure 8.3b). To understand the dynamics of this environment you may need to refresh your memory regarding the conservation of angular momentum (see Box 5.7).

- If this cloud were originally rotating a little, what would happen to the rate of rotation as the cloud became smaller and denser during collapse?
- The cloud would have to spin faster, in order to conserve angular momentum.

Conservation of angular momentum also explains the directions of rotation of the Sun, and the orbits of most planetary bodies in the Solar System. A remarkable aspect of the arrangement of the Solar System is that the orbits of all the planets, and most asteroids, lie close to the same plane (the ecliptic plane), and that the planetary orbital motion and the Sun's axial rotation are in the same direction (prograde).

The general sense of prograde motion close to a common plane would be a natural consequence of formation from a contracting, rotating cloud. The inward gravitational force on matter contracting within the plane of the cloud's rotation would be opposed by the centrifugal force due to rotation and by gas pressure, but the gravitational force on matter contracting from above either pole of the cloud would be opposed only by pressure, which would not become great enough to halt the polewards contraction until the nebula had become dense. Thus collapse would be easier near the poles, and the cloud would be flattened into a rotating disc, as shown in Figure 8.13.

The conversion of gravitational energy to thermal kinetic energy during contraction leads to the possibility of heating. As the nebula became progressively denser in its centre, where the protoSun was forming, it would have become more opaque. This would inhibit heat loss by radiation, and cause a substantial temperature rise. The pressure of this hot gas would eventually stop the gravitational contraction of the protoSun and of the innermost part of the disc. Gravitational contraction of the outer part of the disc would continue to be opposed mainly by the disc's rotation.

Centrifugal force is an apparent force that pulls an orbiting body away from the centre of its orbit.



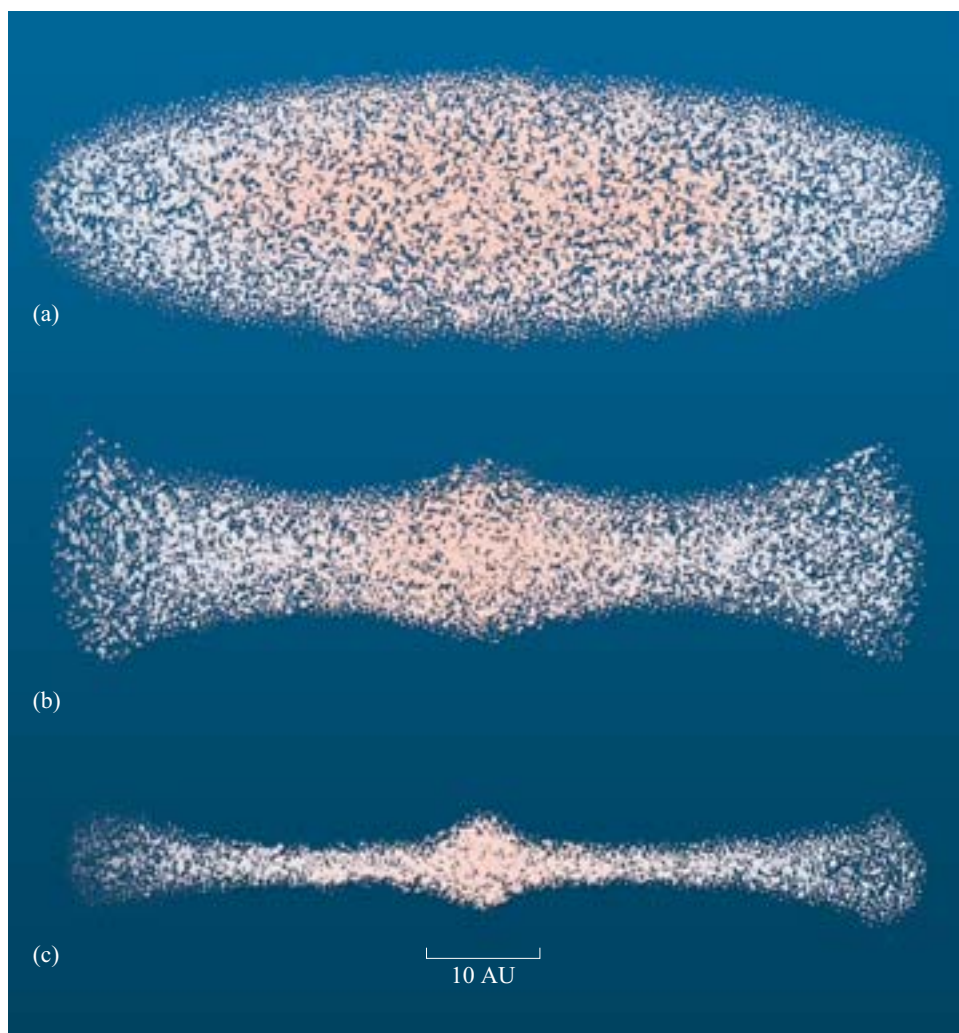


**Figure 8.13** A cross-section through the Solar Nebula, at three stages in its contraction, as rotation forces it into a disc shape. The time difference between (a) and (c) was probably of the order  $10^5$  years.

So far we have not considered in any detail the relative masses of the protoSun and the surrounding nebula. Here we touch on one of the more controversial aspects of Solar System formation. There are two major variants of the nebula theory. One is the low-mass or **minimum solar nebula model**, which assumes that the mass of the nebula around the protoSun was equivalent to the present total mass of the planets, with the addition of just enough hydrogen, helium and icy material to make the overall composition the same as the Sun today. This requires a total nebula mass of about  $0.01M_{\odot}$ . On the other hand, the **massive solar nebula model** has the mass of the nebula around the protoSun to be of order  $1.0M_{\odot}$ . Note that in both solar nebula models the mass of the protoSun itself is considered to be about  $1M_{\odot}$  (in fact, perhaps a little bit more to allow for losses during the T Tauri phase).

Just in case you have calculated the masses of the present day planets (plus asteroids and comets) and realized a figure of  $<0.0015M_{\odot}$ , we will briefly explain the discrepancy with the value of  $0.01M_{\odot}$  used in the minimum model. To have enough matter to produce those Solar System bodies that are *not* composed of hydrogen and helium (i.e. the inner planets) it is necessary to have more than  $0.0015M_{\odot}$  of starting materials (which, as you should recall, are mostly hydrogen and helium). It is apparent that a large proportion of the total hydrogen and helium must be

You will see later in this chapter that hydrogen, helium and ice were prevented from being incorporated into planets with increasing efficacy the closer they were to the Sun.

subsequently lost. The minimum model requires that all the suitable nebula material was converted into planets. In contrast, for the massive solar nebula model to be valid, we have to account for how a large proportion of its mass could have been lost. How this may have happened is tied in with the present distribution of angular momentum within the Solar System.

Recall from Section 8.1. what we called the angular momentum problem. The dynamical problem for models of Solar System formation, is that if the Sun simply represents a contraction of the central part of a rotating nebula we would expect it to be rotating more rapidly than it actually is. Its present 25.5 day rotational period is far too slow, and although the Sun contains over 99.8% of the mass of the Solar System it possesses only a tiny fraction of the Solar System's angular momentum. Most of this resides in the orbital motions of the giant planets, as you saw in Figure 8.1.

For the Sun to have so little angular momentum, the matter that formed the protoSun must have transferred most of its angular momentum to the surrounding disc. This could not have happened if the gas molecules and dust grains in the Solar Nebula were moving independently in orbits dictated by Kepler's laws. They must have interacted, so that the disc as a whole behaved viscously; that is to say, there would have been **viscous drag** between adjacent elements of the disc. There are several factors that could have contributed to this. Probably the most important was **turbulence**, initiated by random motions inherited from the initial contraction.

#### QUESTION 8.2

Consider a disc of gas and dust around the protoSun.

- (a) What would be the relationship between the orbital periods of particles in circular orbits in the inner and outer parts of the disc, if Kepler's third law were applicable, i.e. are the orbital periods the same, or is one much shorter than the other?
- (b) What would tend to happen to the orbital periods in the inner and outer parts of the disc if these were linked by viscous drag, so particles could not orbit entirely independently?

---

Despite this effect, the whole of the disc could not be forced to rotate at a uniform rate unless it were an impossibly strong solid, so even allowing for viscous drag, the outer parts of the nebula would continue to rotate more slowly than the inner parts. However, an important outcome of viscous drag would have been the outward transfer of angular momentum. This occurs because material in the outer part of the disc (having been speeded up) would flow outward, carrying angular momentum with it, but material in the inner part of the disc (having been slowed down) would fall inward onto the protoSun.

Thus, viscous drag within the Solar Nebula can explain the Sun's low angular momentum. The resulting outward flow at the outer edge of the nebula can account for the mass loss that is necessary if we subscribe to a massive solar nebula model. There are two other ways in which the nebula could have lost mass at this stage: loss to space in bipolar outflow (see the previous section), and transfer of mass from the nebula to the protoSun, although neither explains the Sun's low angular momentum. There would have been further losses of both mass and angular momentum later, if the Sun went through a T Tauri phase of violent stellar winds (see the previous section).



It is much easier to explain the Sun's low angular momentum if large quantities of mass were lost from the Solar Nebula. This is a strong argument against the minimum solar nebula model, but we do not have to invoke the full massive solar nebula model in order to account for the present distribution of angular momentum. It seems reasonable to assume that the Solar Nebula began with a mass somewhere between that of the extreme models, say of the order  $0.1M_{\odot}$  (a figure, which you may recall, is at the end of the range of that invoked from observational evidence of circumstellar discs).

### QUESTION 8.3

Why would a rotating Solar Nebula assume the shape of a disc, and what opposes the collapse of this disc?

### QUESTION 8.4

What processes in the Solar Nebula can account for the Sun's low angular momentum, and at what stage in the formation of the Solar System did each of these probably occur?

## 8.2.4 Condensation of materials

Until now, we have considered the composition of the Solar Nebula only in terms of abundances of elements. At temperatures below those of stellar atmospheres, most elements will form chemical compounds, including some well-known minerals. The behaviour of these compounds will have controlled the evolution of the Solar Nebula. Compounds that are important in the evolution of the Solar Nebula include water ( $\text{H}_2\text{O}$ ), methane ( $\text{CH}_4$ ), troilite or iron sulfide ( $\text{FeS}$ ), corundum ( $\text{Al}_2\text{O}_3$ ), and pyroxene ( $\text{CaMgSi}_2\text{O}_6$ ). We are interested to know whether these compounds were present as gases or in the form of tiny solid particles. The answer to this question depends mainly on the temperature within the nebula, which must have been greatest near the centre, and will have to some extent changed over time (especially during the initial stages of its life). Astronomical observations are much better at determining the sizes of grains in circumstellar dust clouds (typically 1 to 30  $\mu\text{m}$  around T Tauri stars), than their compositions, and unfortunately it is not clear whether such grains are dominated by ices, carbon-rich material or silicate minerals. Let us now pursue the story of the Solar Nebula, by considering how solid material might have begun to be gathered together.

The Solar Nebula must have grown hotter as the nebula became too dense for radiation from the protoSun to escape directly to space. This heating would have been augmented by viscous drag, and continued conversion of gravitational energy to thermal kinetic energy. Evidence from meteorites suggests that the temperature never rose above about 400 K at about 4 to 5 AU from the protoSun. However it is likely that the maximum temperature about 1 AU from the protoSun was around 2000 K, near the time of stage (b) in Figure 8.13. This temperature would have been sufficient to break any pre-existing grains (of virtually all feasible compositions) into their constituent atoms. At this stage, most of the elements within 2 to 3 AU of the protoSun would have been in the gaseous state, as dissociated atoms, although there would have been some simple molecules such as  $\text{H}_2$  and CO. Subsequently, as the nebula became more transparent to solar radiation and as the other heat sources ceased to act, it would have begun to cool. This would have allowed new compounds to form, growing as dust grains, by **condensation** (Box 8.2).

## BOX 8.2 TWO TYPES OF CONDENSATION

You probably know condensation as what happens when you breathe out on a cold day, and water vapour condenses to form the tiny droplets that make your breath visible. On cooling, molecules of  $\text{H}_2\text{O}$  in the gaseous state lose energy and come together to form a liquid. This type of condensation is characteristic of molecular substances. However, under low pressure (as in the Solar Nebula) gases of molecular substances condense directly to form solids, with no intervening liquid phase (i.e. this is the reverse of sublimation where a solid goes straight to the gaseous state).

Condensation of ionic substances is a different process and usually occurs at higher temperatures (you have already met ionic substances in Chapter 2). In the Solar Nebula, elements that had existed as free atoms in the nebula gas at high temperature would have joined together as the nebula cooled to form chemical compounds, involving two or more elements. Once a tiny grain has condensed in this way, it is easier for individual free atoms to attach to its surface, rather than to start a new grain.

The nature of the starting material from which the planets in the inner Solar System developed was probably dictated by the highest temperatures reached locally. Further out from the protoSun it becomes more likely that pre-existing grains could have survived; we know from studies of meteorites (Chapter 9) that some of these have survived and can be studied in the laboratory today.

The sequence in which solid particles would have condensed while the Solar Nebula was cooling depends on a complex interplay of the *stability* of compounds

and the *rate* at which they could form from a gas at the prevailing temperature and pressure. A simplified **condensation sequence** was shown in Table 2.4, showing the temperatures at which some notable constituents of the Solar System probably began to condense.

Minerals and other compounds that condense at relatively high temperatures are described as **refractory**, and those that do so at relatively low temperatures are described as **volatile**. The condensation sequence is the reverse of the evaporation sequence, that is to say if the temperature were to increase, the most volatile compounds would evaporate first whereas the more refractory compounds would be the last to do so.

It is generally believed that the planet-forming process began with the cooling of the Solar Nebula after it had reached its peak temperature. We have to imagine progressively more dust-sized grains forming by condensation within the nebula at about stage (c) of Figure 8.13. As these grains formed, they would have settled towards the mid-plane of the nebula, producing a sheet rich in dust and larger particles. This migration of grains towards the mid-plane occurs because of the continuing influence of gravitational forces; once in the mid-plane, particle–particle collisions act to eradicate those trajectories that would otherwise take grains out of the ecliptic. This settling would be possible only after turbulence within the nebula had declined, and it would have become more rapid as the grains grew.

### 8.2.5 Coagulation of grains

Now we have to consider how these grains could continue to grow, especially after much of the nebula material had condensed. Gravitational attraction between individual dust grains is too slight to bring grains together. Instead, chance encounters seem to have been the most important factor. In a collision between two particles, any of three things can happen:

- one or both particles can be fragmented (which is the opposite of what we are looking for),
- they can bounce off each other (which would not help us either), or
- they can stick together (which is what we want).

Fragmentation would be common only if the collisions were more violent than the sort of chance encounters likely in the Solar Nebula. One suggestion as to why colliding grains stuck together instead of bouncing apart is that their surfaces were fluffy, perhaps riddled with cavities caused by evaporation of ice that had previously condensed there. Magnetism and small electric charges may also have helped to hold grains together. Whatever the mechanism, this sticking together of grains that had grown by condensation in the Solar Nebula is generally referred to as **coagulation**.

An alternative term for coagulation is cohesion.

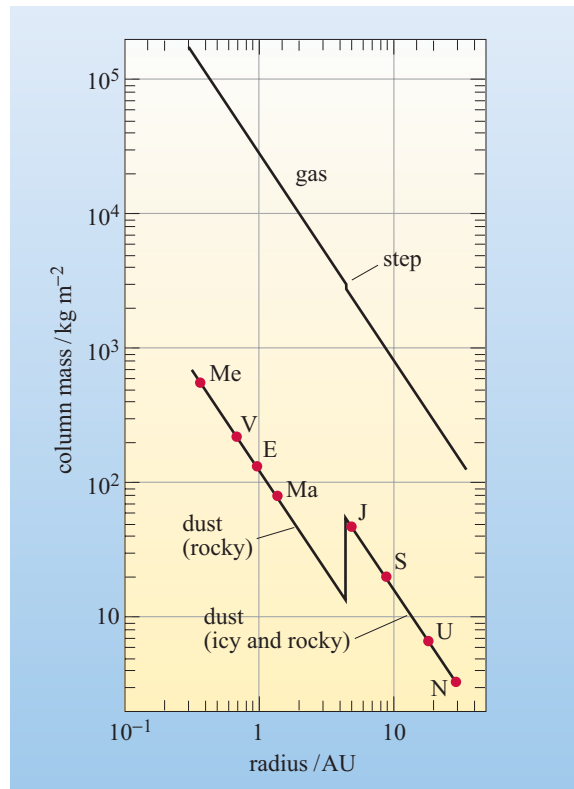
The rate at which coagulation could proceed must have depended on the density of material within the nebula. One model suggests that once settling of dust grains towards the mid-plane had begun, it would have taken only about 2000 years to produce particles up to 10 mm in diameter at 1 AU from the Sun, about 5000 years to produce particles up to 15 mm in diameter at about 5 AU (the Jupiter region) and about 50 000 years to produce particles up to 0.3 mm in diameter at about 30 AU (the Neptune region). You should be aware at this point that we are only here considering the details of initial grain growth. The overall timescales for the formation of planets as a whole depends upon what happens after initial growth (as we consider in the following sections). You will have already seen that, at least in some models, Uranus and Neptune may be formed over extended periods. As far as Jupiter is concerned, we can be sure that this is not the case and that we must be looking at a timescale that is compatible with that of the inner planets. The reason for this is that if Jupiter, as a large body, was not present during the formative stages of accretion of material in the inner Solar System, then the materials which are at the present day represented by the asteroid belt, would have accreted to form a rocky planet (at about 2.8 AU, with a mass of about 4 times that of the Earth). Unlike a number of other aspects of Solar System formation we can be absolutely sure that this did not happen!

So, while there are factors which will inevitably lead to slower rates of accretion in the outer Solar System (i.e. Uranus and Neptune) there must also be some counter-balancing processes which promote accretion in the Jupiter–Saturn region. There are three factors that would contribute to the slower growth of grains further from the protoSun. First, **column mass** decreases outwards, so grains might be expected to condense more slowly in the outer reaches of the nebula (in this context, column mass is the mass per square metre of the Solar Nebula, measured perpendicular to its plane). Second, the lower density would result in less frequent collisions and hence slower coagulation. Third, the nebula was probably fatter in its outer reaches (Figure 8.13b and c), and so the majority of grains forming there would have to fall further to reach the mid-plane, taking longer to complete their journeys. Estimates of the rate of coagulation depend on assumptions made about the densities of both gas and dust present in the Solar Nebula. A reasonable model is shown in Figure 8.14, which shows the variation in column mass against distance from the centre. Note that this model has several orders of magnitude more mass present in the form of gas than as dust, especially in the inner Solar System.

You may also find column mass called column density. The two terms mean the same thing. You met this concept in Chapter 5 when considering atmospheres.

- Given that Figure 8.14 represents the situation after everything able to condense from the nebula has already done so, can you suggest what remains in the gas?
- The gas will be made up of the abundant volatile substances, notably hydrogen (as  $\text{H}_2$  molecules) and atomic helium (He), neither of which would have condensed.

**Figure 8.14** The column mass of gas and dust in the Solar Nebula (at a stage represented by Figure 8.13c) plotted against radius from the protoSun. Obvious abbreviations are used to indicate the positions of the planets that ultimately formed. The reason for the increase in column mass of dust near 5 AU is due to the condensation of water (see text). (Smaller steps associated with the condensation of more volatile compounds such as ammonia have been omitted.)



Considering now the processes that might act in opposition to slower rates of accretion, note from Figure 8.14 that the sharp increase in dust column mass near 5 AU is anticipated because the temperature at this distance would have been low enough for water to condense, in the form of ice. In fact, this ice can be thought of as being quite fluffy in texture, (i.e. more like snow) which will encourage individual grains to stick together. Note that there is a downward step in the column mass of the gas at the same radius. Although this downward step seems a lot smaller than the upward step, when you allow for the logarithmic scale, it exactly compensates for the increase in column mass of dust.

Estimating the rates of processes such as condensation within the Solar Nebula is fraught with difficulties, but the icy nature of most of the major satellites of the outer planets demonstrates that water did indeed condense in considerable quantities near Jupiter and beyond.

- Can you suggest how it is possible for water to have been incorporated in material that condensed at this stage considerably *closer* to the Sun than 5 AU?
- It can be incorporated in hydrated minerals, which condense at higher temperatures than that at which water condenses to ice (see Table 2.4). This is probably the origin of much of the water in the Earth.

‘Relict’ is a term used in meteoritics to describe inherited features, e.g. particles whose formation pre-dates the Solar System.

A possible window back to the time when the processes of coagulation within the nebula had resulted in objects of a few millimetres across, is provided by what may be relicts of these particles in certain meteorites (of which you will learn more in Chapter 9). For now we will just note that these consist of small, irregularly shaped

objects comprised of refractory minerals (known as calcium–aluminium-rich inclusions) and globules of silicate minerals a few millimetres across (known as **chondrules**). Inclusions and chondrules are found embedded in a (predominantly) silicate matrix, in meteorites known as **chondrites**, or chondritic meteorites. The important thing here is that calcium–aluminium-rich inclusions and chondrules *could* represent the types of grains that were available for coagulation. We will consider how these materials and the matrix could have been gathered together, in the next section.

We have now traced the story of the early Solar System from the origin of the Solar Nebula up to the formation of particles a few millimetres in size. The time required for this appears to have been surprisingly brief. Condensation probably took just a few thousand years. We have not considered in any detail whether or not the processes we have discussed are likely to have been going on simultaneously in all parts of the Solar Nebula, but you have seen examples of both time-dependent and space-dependent variations. For example, in the innermost Solar System the temperature was always too high for water to condense as ice. Also, things will have happened more slowly in the outer Solar System because the lower density of the nebula would give grains less frequent opportunities to collide, and thus coagulate. In the next section we will consider how the grains could come together to form the bigger bodies necessary to create the planets.

In less-primitive chondrites, new minerals have replaced the original ones, showing that entities such as chondrules and matrix were heated after they were assembled.

#### QUESTION 8.5

Many chondrules contain small amounts of iron sulfide (FeS) mixed in with the silicate minerals. If we assume that the iron sulfide has not grown within the chondrules subsequently, what constraint (upper limit) does this put on the temperature at which the chondrules formed?

#### QUESTION 8.6

According to the model in Figure 8.14, what are:

- (a) the total proportion of ‘icy and rocky’ dust expressed as a ratio of the total material in the Solar Nebula?
- (b) the ratio between rock-forming and ice-forming material in the nebula?

### 8.2.6 Planetesimals and embryonic planets

Recall that young stars of around  $1M_{\odot}$  experience a T Tauri phase of violent stellar winds, probably when they are about a million years old. This is known from observations of such stars whose light is reaching us today. At face value, therefore, we can conclude that the Sun itself probably went through such a phase (there is also other circumstantial evidence that we will mention in Section 8.2.8). To appreciate the magnitude of the T Tauri phenomenon consider that during such a process it is estimated that freely orbiting bodies in the inner Solar System of up to 10 m in size would have been ‘blown’ out of the Solar System. In the outer Solar System the T Tauri effects were nowhere near as intense because otherwise they would have removed all of the gas, (i.e. there would have been no gas to form the giant planets).

- The density of a typical rock might be around  $3 \times 10^3 \text{ kg m}^{-3}$ . For illustration purposes, what is the mass of a hypothetical cube of rock measuring 10 m on its side?
- Mass = density  $\times$  volume, and volume is  $(10 \text{ m}) \times (10 \text{ m}) \times (10 \text{ m}) = 10^3 \text{ m}^3$ , so  
 $\text{mass} = (3 \times 10^3 \text{ kg m}^{-3}) \times (10^3 \text{ m}^3)$   
 $= 3 \times 10^6 \text{ kg}$  (or 3000 tonnes)

It is clear that any materials destined to form planets in the inner Solar System must have been gathered into masses of greater than this before the onset of the T Tauri phase. Indeed it is widely believed that the next stage in planetary formation after initial coagulation led to the growth of bodies about 0.1 to 10 km across, known as **planetesimals**. One model for how this happened calls for a continuation of coagulation during collisions in the central dust sheet. Another theory is that once this sheet had contracted to a thickness of less than about 100 km it became gravitationally unstable, breaking into a multitude of turbulent knots each of which developed into a planetesimal. Either way, it appears that coagulated grains of all sizes were gathered together to form planetesimals, probably within a few hundred thousand years after condensation began (within the inner Solar System, at least; we have already stressed the point about things taking longer in the outer regions).

- Can you suggest what could become of any dust trapped between larger coagulated grains while a planetesimal was forming?
- This material could become the matrix between chondrules in a chondritic meteorite.

The complex histories indicated by the mineralogy and texture of most meteorites suggest that they are fragments of planetesimals or larger bodies that were broken apart by collision, but the least-altered varieties are the best relicts available of the process of planetesimal formation.

Once a planetesimal has reached about 10 km across, it has become massive enough that its own gravitational attraction is sufficient to perturb the motions of other nearby planetesimals. A larger planetesimal will deflect the trajectories of smaller planetesimals towards it (the phenomenon known as **gravitational focusing**) resulting in more frequent collisions. Provided most of the material in two colliding planetesimals ends up together – the process of **accretion** – instead of fragmenting and dispersing, the bodies that remain will get progressively larger, and the large bodies will become fewer in number.

It is impossible to model exactly how planetesimals would have interacted, because there were far too many of them and there are factors of unknown magnitude, such as the degree of viscous drag due to the remaining gas, that should be taken into account. However one important outcome is clear: because of their greater strength of gravitational focusing, larger planetesimals would have grown more rapidly than smaller ones, while the total mass incorporated in smaller bodies declined. It is probable that a situation of **runaway growth** developed in each neighbourhood, in which the growth of one planetesimal outpaced that of all its rivals, allowing it become a much larger object known as a **planetary embryo**.

It would not be possible for colliding planetesimals to stick together *without* fragmenting, because the collisions would be too violent. After a collision therefore, the new, larger, planetesimal is made of a mixture of accreted fragments from the two planetesimals that collided.



## QUESTION 8.7

Assume the density of the material forming planetesimals was  $3 \times 10^3 \text{ kg m}^{-3}$ . How many 10 km diameter planetesimals would it take to form the Earth, which has a mass of approximately  $6.0 \times 10^{24} \text{ kg}$ ? *Hint:* It is a reasonable approximation to treat these planetesimals as spheres. The volume  $V$  of a sphere of radius  $R$  is given by

$$V = \frac{4}{3} \pi R^3.$$

## 8.2.7 Planetary growth in the inner Solar System

The style and speed of runaway growth is likely to have varied with distance from the Sun, slowing drastically in each vicinity as the supply of smaller bodies available for capture became depleted. Limiting masses calculated for planetary embryos at different distances from the Sun are indicated in Figure 8.15.

We will follow events in the inner Solar System first, before considering what happened further out. In the region where the terrestrial planets are now found (from Mercury to Mars) one planetary embryo probably grew about every 0.02 AU outward from the Sun. One of the many models describing the evolution of a swarm of planetesimals into a planetary embryo in this region is illustrated in Figure 8.16. Please study this figure and its caption; it is probably correct in a *general* sense, though its details are not to be trusted.

If the models illustrated in Figures 8.15 and 8.16 are even roughly correct, runaway growth appears able to have produced substantial planetary embryos before the

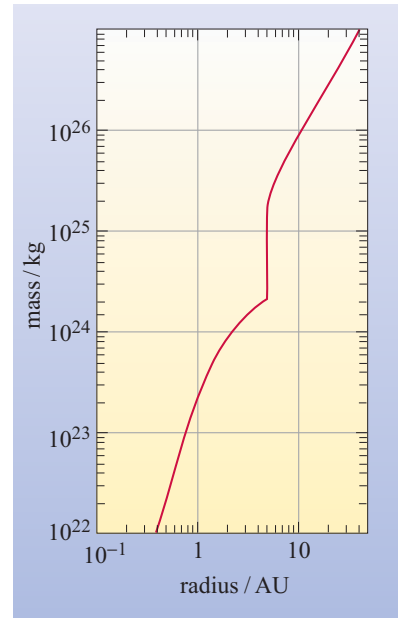


**Figure 8.15** The final masses for the largest planetary embryos produced by runaway growth at different distances from the Sun. The step-up at about 5 AU is because of the condensation of water-ice beyond that distance (see Figure 8.14). Note that the curve does not keep on increasing beyond the edge of the graph. In fact, it reaches a maximum and then declines – otherwise there would be very large planets beyond Neptune.

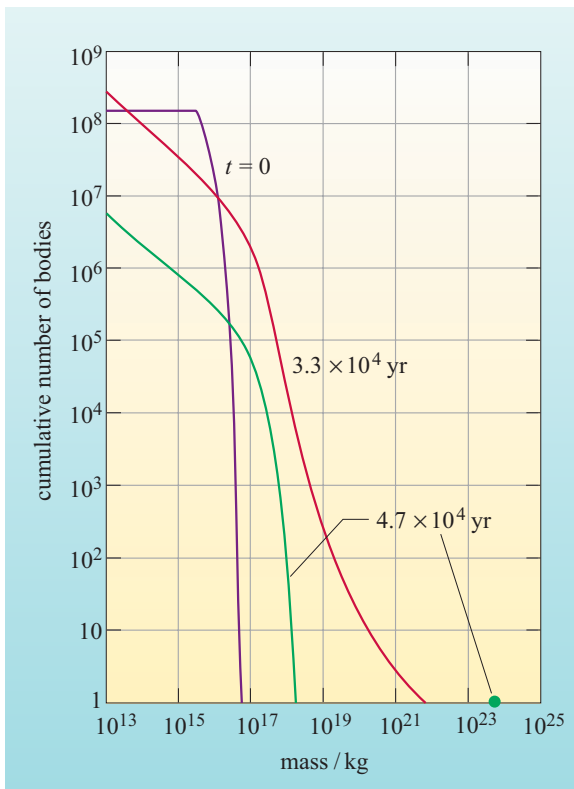
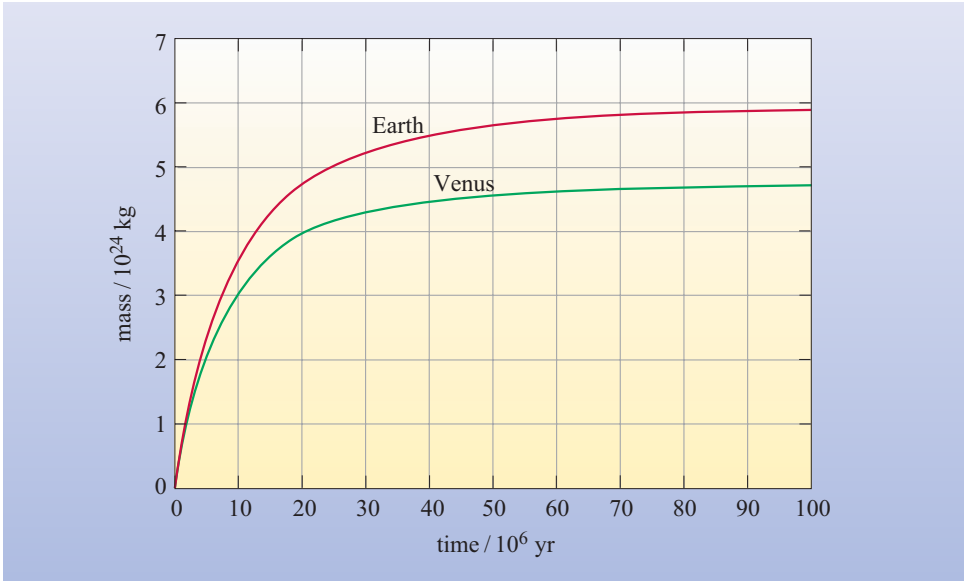


**Figure 8.16** The evolution of a swarm of planetesimals orbiting the Sun between 0.99 and 1.01 AU. The curves show the distribution of planetesimals by mass at three different times, beginning at  $t = 0$  with almost all the planetesimals between about  $10^{16} \text{ kg}$  and  $10^{17} \text{ kg}$  in mass (about 10 km in diameter). At  $33\,000$  years, the largest planetesimal is just under  $10^{22} \text{ kg}$ , and represents the high-mass end of a continuum of planetesimal masses. However, after  $47\,000$  years runaway growth has led to the production of a single planetary embryo of  $10^{23}$  and  $10^{24} \text{ kg}$  in mass. By that stage, no other body in this region of the Solar System has a mass within five orders of magnitude of this. Note that the axes are logarithmic, and that the vertical axis shows the cumulative number of bodies greater than the mass plotted on the horizontal axis.

**Figure 8.17** A model for the timescale for the growth of the Earth and Venus as a result of collision between planetary embryos. Mercury and Mars probably grew at similar rates.



Sun’s T Tauri stage. However the supply of planetesimals within range of each embryo’s gravitational influence, was sufficient only to allow it to reach about one-tenth of the mass of the individual planets that would eventually form.

After this, planetary growth can have proceeded only at a slower pace, as a result of chance collisions between planetary embryos whose orbits crossed. Whenever two embryos collided, the smaller of the two would have been fragmented and mostly accreted onto the larger one. A collision between two embryos of similar mass would probably have broken both into a swarm of debris, most of which would have rapidly come together (accreted) under its own gravitational attraction. Either way, the result would be the same; fewer and fewer remaining embryos that would become more massive after each collision. Calculations for Mercury, Venus, the Earth and Mars suggest that in each case it would take about  $10^7$  years for growth to about one-half of the final planetary mass and about  $10^8$  years for growth to be essentially complete (Figure 8.17). Recall that the curious case of the Moon was examined previously in Section 2.3.

**8.2.8 Formation of the giant planets**

What we will describe in this section is a traditional view of the formation of the giant planets in which the bodies themselves are assumed to have formed at the orbital distances that are observed today. In fact, you will see in the next section that this is probably not the case and that the orbits of the giant planets have migrated from their original formation positions. However, the overriding principles discussed in the present section are likely to be correct. Furthermore, planetary migration is an active and somewhat controversial subject; there are still many people who reject the idea in the case of the Solar System. As such it seems entirely appropriate to continue with a standard model for the formation of the giant planets.

You can see from Figure 8.15 that in the outer Solar System the expected masses of individual planetary embryos in the Jupiter–Neptune region (5 to 30 AU) are at least two orders of magnitude larger than those at 1 AU. However, the large volume

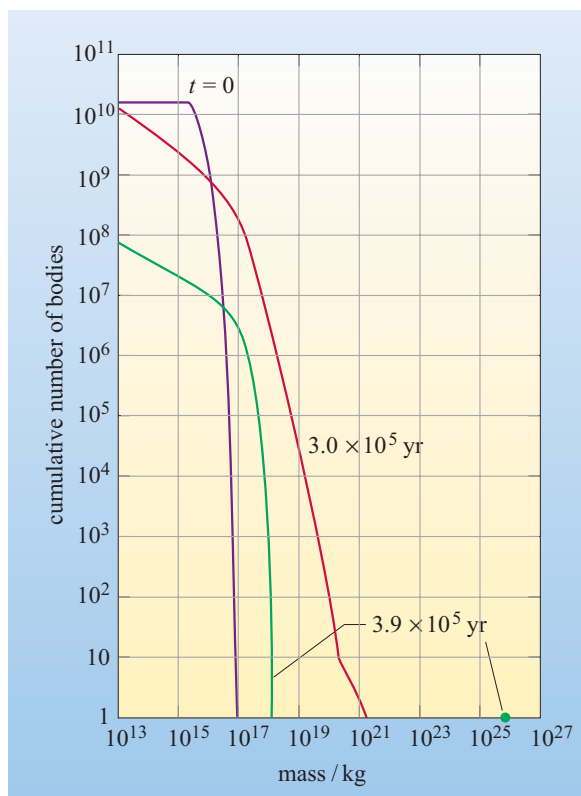


**Figure 8.18** The evolution of a swarm of planetesimals near 5 AU leading to the production of a Jupiter kernel by runaway growth. Compare with Figure 8.16.

of space occupied by the planet-forming material in the outer Solar System makes it more difficult for runaway growth to begin (indeed, some authorities dispute that it could have happened at all), and when it did get underway it would produce fewer but **larger planetary embryos**. Figure 8.18 shows a simulation of how runaway growth might proceed at 5 AU.

According to this, an embryo (probably a mixture of rocky and icy materials) with a mass somewhat less than  $10^{26}$  kg (about  $10M_{\oplus}$ ), is produced after  $3.9 \times 10^5$  years. You may be able to recall from Chapter 5 that Jupiter was estimated to have an icy–rocky core of  $5M_{\oplus}$ . (As is often the case in science, different models and methods produce slightly different interpretations so it is probably wise to consider that the planetary embryo mass was about  $5M_{\oplus}$  to  $10M_{\oplus}$ .) Note that the timescale  $3.9 \times 10^5$  years is about ten times as long as it would take to produce a planetary embryo at 1 AU, according to the comparable simulation shown in Figure 8.16. The hypothetical  $5M_{\oplus}$  to  $10M_{\oplus}$  body would act as a **kernel** that would, with the aid of gravitational focusing, sweep up planetesimals, smaller debris and nebula gas, leading to the formation of the planet Jupiter. As this body grew, it would be able to capture a significant amount of gaseous molecular hydrogen ( $H_2$ ) and atomic helium (He) from the Solar Nebula (a process that would have been enhanced by the large gravitational attraction of the planet). This envelope of gas ultimately became the Jovian atmosphere that we see today.

Runaway growth such as this would take even longer to produce the kernels for Saturn, Uranus and Neptune; probably about 2, 10 and 30 Ma respectively. This increasing timescale with distance from the Sun, is probably the key to understanding the outward trend in composition among the giant planets.

We are using the conventional symbol  $M_{\oplus}$  to indicate the mass of the Earth.

- Look at the data for Jupiter, Saturn, Uranus and Neptune in Table A1, Appendix A. Can you see any trend in their densities as their distance from the Sun increases?
- No, a trend does not appear to exist.

The reason is that the more massive the planet, the stronger its gravity and the more compressed, and therefore denser, will be the material in its interior. If this **self-compression** is taken into account, then the densities of the four giant planets can be explained by each containing roughly similar amounts of rock and ice ( $10M_{\oplus}$  to  $20M_{\oplus}$ ) but diminishing amounts of hydrogen and helium further from the Sun. Jupiter is thought to contain about  $300M_{\oplus}$  of  $H_2$  and He, Saturn about  $70M_{\oplus}$ , and Uranus and Neptune about  $1M_{\oplus}$  each.

- Can you suggest an event that would have prevented the more distant planets from gathering as much gas from the Solar Nebula as Jupiter did?
- If their kernels formed later (as we have suggested) then maybe most of the gas in their neighbourhood had been removed before they grew massive enough to attract much gas gravitationally. The most likely explanation for this removal is the T Tauri wind.

This is the circumstantial evidence that the Sun did pass through a T Tauri phase that we have referred to previously. The T Tauri wind blew away the remaining  $H_2$  and He, so that no more gas could be captured by the giant planets. A related argument is that the Earth should have captured an atmosphere of about  $0.03M_{\oplus}$  from the Solar Nebula. This is  $3 \times 10^5$  times the mass of its present atmosphere, which furthermore has a totally different composition. We can conclude that the Earth's primitive atmosphere (and those of the other terrestrial planets) was probably lost during the T Tauri phase.

#### QUESTION 8.8

The simulations in Figures 8.16 and 8.18 both begin with a population of planetesimals between about  $10^{16}$  and  $10^{17}$  kg in mass, i.e. about 10 km diameter. The flat tops to the curves for  $t = 0$  show that there are no planetesimals less than about  $10^{16}$  kg in mass. In both simulations, at times later than  $t = 0$  the low-mass ends of the curves slope down to the right. What does this tell you about the masses of the smallest bodies present at these later times, and to what process do you attribute this?

#### QUESTION 8.9

What factors are responsible for the giant planets being richer than the terrestrial planets in volatiles such as hydrogen and helium?

### 8.2.9 Planetary migration

In Section 8.2.1 we alluded to planetary migration in respect of extra-solar planets. By planetary migration we mean a change in the orbital radius (i.e. semimajor axis) of a planet with time. If we just take this at face value for the moment, what this

would mean for descriptions of the Solar System is that the orbit of a particular planet, observed today, may not correspond with the orbit of the same body at the time of its formation (this phenomenon is only currently being thought of in respect of the giant planets). If true, there would be no real point in developing a model of planetary formation in which it was implicitly assumed that orbits have remained the same. The gauntlet has now been thrown down, challenging theoreticians who derive models of the formation of the Solar System to contemplate this extra level of complexity.

The issues that have brought this problem to a head can be summarized as:

- The discovery of the Kuiper Belt (see Section 7.4) has shown that the Solar System does not end at Neptune (or Pluto). Between about 20 and 60 AU there are now thought to be 100 000 icy minor planets of 100 to 1000 km diameter mostly orbiting in the plane of the ecliptic.
- The detection of extra-solar planets of Jupiter size orbiting at distances of less than 0.5 AU is problematic because, from theoretical considerations, there would not be enough material in a nebula disc to form large planets so close to a star.
- Recent measurements of volatile elements (e.g. noble gases, carbon, nitrogen and sulfur) in the atmosphere of Jupiter show enrichments which suggest that the planet formed at colder temperatures than previously thought. One way of interpreting this is that Jupiter formed much further away from the Sun (e.g. 30 AU) than its present position (about 5 AU).

Without getting into any of the details of planetary migration you should be aware that in a general sense we could be talking about orbital distances that either decrease or increase, depending upon circumstances. Clearly in the case of ‘hot jupiters’ the orbits are thought to have moved closer to the central star (the original planets having formed at several AU). For the Solar System it has been proposed that the orbits of the giant planets may all have moved further away from the Sun with time. The details of this process are complicated, but in essence the theories are constrained by the presence of Kuiper Belt objects. Theories will undoubtedly become refined as more of these objects are detected. To illustrate the magnitude of the process, the orbital radius of Neptune may have increased by 30%, while those of Uranus, Saturn and Jupiter may have increased by 15, 10 and 2% respectively. The migration itself is presently considered to have taken place over a timescale of less than 0.1 Ga straight after the formation of the Solar System. Because of uncertainties in ideas regarding the length of time required for the formation of the giant planets, it is difficult to state whether migration accompanied the tail-end of planet formation, or took place early in the history of the Solar System.

Planetary migration is a hot topic. Just a few years ago the idea of this having taken place within a Solar System context would have been considered extremely dubious. And yet, should we have been surprised by the phenomenon? It has been known for a long time that the orbits of many planetary satellites have changed since their formation. Taking the example closest to home, the Moon is believed to have formed within 30 000 km of Earth and has subsequently moved out to its present distance of 384 000 km as a consequence of gravitational tidal forces exerted by our planet. A billion years ago the Moon was 100 000 km closer to the Earth; next year it will be 3 cm further away. It is ironic that the object most readily visible in the night sky should be helping to open our minds to the notion of generalized processes taking place in solar systems across the Galaxy.

### 8.2.10 Origin of the asteroids and comets

Jupiter is much the most massive body in the Solar System after the Sun, and its gravitational field is likely to have been an influential factor in the history of the Solar System ever since its formation. The most obvious sign of Jupiter's influence can be seen in the absence of a substantial planet between Mars and Jupiter, even though simulations of runaway growth suggest the appearance there of planetary embryos in excess of  $10^{24}$  kg within  $4 \times 10^5$  years. Today this region is populated only by the asteroids, all less than about  $10^{21}$  kg in mass, and amounting to a total present-day mass of no more than about  $3 \times 10^{21}$  kg (about  $5 \times 10^{-4} M_{\oplus}$ ). The asteroids exist because the gravitational influence of the growing Jupiter kernel perturbed the orbits of planetesimals orbiting near 3 AU, thus increasing their eccentricities. This would have ensured that when these planetesimals collided with each other, the velocity (and hence the kinetic energy) of the impact was so great that fragmentation and dispersal became just as likely as growth by accretion.

As a result, runaway growth never took place, and the orbital perturbations probably led to much of the original material being scattered. By now most of this debris has collided with other bodies, forming the impact craters that characterize old surfaces throughout the Solar System (see Chapter 4). The irregular shapes of the surviving asteroids – which are essentially fragments of the original planetesimals – attest to their violent pasts.

Jupiter is also likely to have played a significant role in the origin of comets. Long-period comets could originally have been icy planetesimals that were flung outwards (or indeed, inwards) as a result of a close encounter with Jupiter or one of the other giant planets. Such encounters would send planetesimals off in very elongated orbits, extending out to form the Oort cloud.

### 8.2.11 Satellite systems

We have described processes that can account for the origin of all bodies in the Solar System except planetary satellites. We will now take a look at the major satellites of the giant planets. With the exception of Neptune's large satellite Triton, these are in orbits close to their planet's equatorial plane, travelling in the same direction as the planet rotates. It is unlikely that these satellites could have formed elsewhere and been captured later by their planets, because in that case their orbits would not be so well-ordered. Instead, the satellites probably condensed from a disc of gas and dust about each primitive planet, rather like the Solar Nebula in miniature. One fundamental difference between the satellite systems of the outer planets and the Solar System as a whole is that, whereas the latter suffers from what we have called 'the angular momentum problem', the planetary satellite systems do not. While the physical mechanics of the satellite systems are readily understood there is still a debate about whether a **protosatellite disc** is more likely to have been shed by a young planet as it contracted, or to have been gathered around it by scavenging of stray planetesimals and other material from the remains of the Solar Nebula.

Whatever the origin of a protosatellite disc, we can imagine it developing into individual satellites in much the same way as the planets had formed. Small particles would have aggregated into larger ones that would, over time, have collided. Eventually the largest bodies would have swept up all the debris in their vicinity to form the surviving satellites. The protosatellite disc would have been rotating in the same direction as the Solar Nebula, and this explains the satellites' consistent orbital directions.



We can learn more about the origin of planetary satellites by examining the four large satellites of Jupiter, known as the **Galilean satellites**, after Galileo who discovered them in 1610 using one of the first telescopes.

#### QUESTION 8.10

- (a) Data on the Galilean satellites (Io, Europa, Ganymede and Callisto) are included in Appendix A, Table A2. Can you see any systematic trend in their densities?
- (b) The density of ice is about  $1.0 \times 10^3 \text{ kg m}^{-3}$ , whereas that of any rock within these bodies is likely to be about  $3.0 \times 10^3 \text{ kg m}^{-3}$ . What does this extra information tell you about the probable compositions of each of these satellites?

Spectroscopic studies of sunlight reflected from the surfaces of Ganymede (Figure 8.19) and Callisto demonstrate that their surfaces at least, are dominated by water-ice. Similar data show that ice is prevalent over the whole of Europa too (Figure 8.20), although Europa's high density demonstrates that its coating of ice can be no more than a few tens of kilometres thick, and its interior is probably mostly rock. Io is an essentially rocky body with no surface ice (Figure 8.21). Its high density shows that its interior contains even denser material, probably in the form of an iron-rich core.

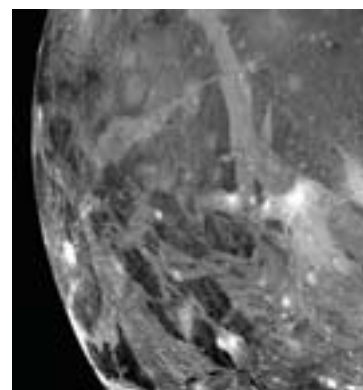


**Figure 8.19** A close-up view of Ganymede. Spectroscopic studies show that the surface is icy, despite the craters and other features that would seem to suggest a rocky surface.

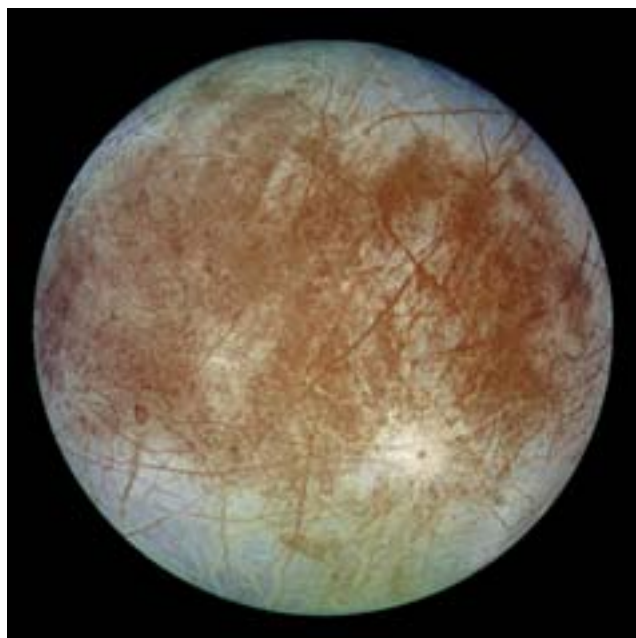


**Figure 8.20** Image of Europa taken by the Galileo spacecraft.

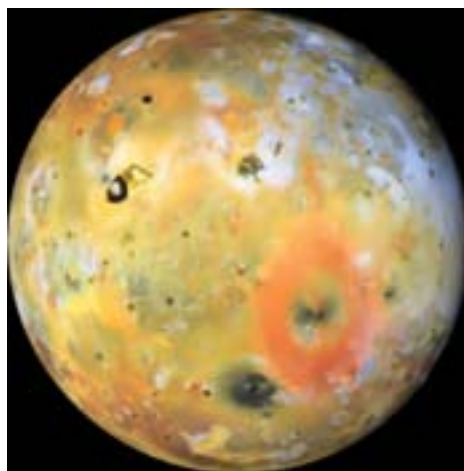


**Figure 8.21** Jupiter's volcanically active moon, Io, as observed by the Galileo spacecraft. Io's surface is covered with volcanic deposits that are thought to contain ordinary silicate rock, along with various sulfur-rich compounds that give the satellite its distinctive colour (see Section 3.4.6). Dark areas are regions of recent or current volcanic activity.

Thus the Galilean satellites resemble the Solar System in miniature. The inner ones are less massive and denser, whereas the outer ones are more massive but less dense.

- Can you suggest a condition within the protosatellite disc around Jupiter that could account for this density trend?
- Perhaps it was too hot in the inner part of this disc for ice to exist, that is above about 180 K, according to Table 2.4.

It is now accepted that heat – generated by the conversion of gravitational energy to thermal kinetic energy as material in the protosatellite disc fell in towards the primitive Jupiter – probably raised the temperature in the inner part of the disc. This either prevented ice from condensing there, or vaporized any ice that had already condensed.

There is no such density trend within the satellite systems of Saturn and Uranus. All their major satellites consist of a rock plus ice mixture, and none are essentially rocky like Io and Europa. However, this cannot be used as evidence that they did not form in a protosatellite disc, because, being less massive, the primitive Saturn and Uranus would have caused less heat to be imparted to infalling material than Jupiter. An additional factor that could be responsible for the lack of consistent density trends is that most of these satellites are much smaller than the Galilean satellites, so the inner ones in particular would have been more vulnerable to fragmentation by impacts involving large comets or other bodies. After fragmentation, but before re-accretion to form the satellites we see today, material from different satellites could become mixed. Although they are smaller, the satellites of Saturn and Uranus are similar in composition to Ganymede and Callisto, except that, having formed further from the Sun and consequently in a lower temperature environment, they were probably able to incorporate methane and ammonia into their ices (see Table 2.4).

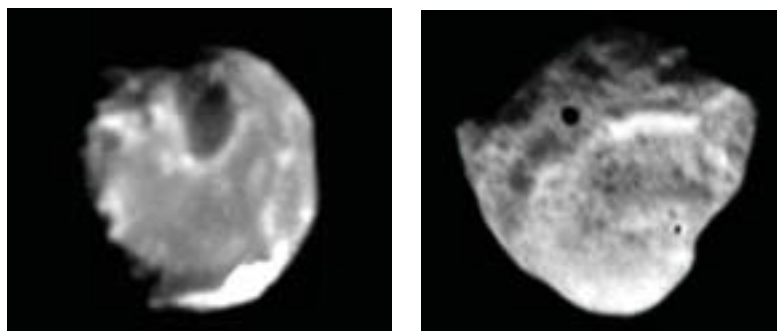
#### QUESTION 8.11

Can you think why inner satellites are more vulnerable to impacts than outer ones, and why smaller ones are more likely to break up as a result of an impact?

Satellites less than about 200 km in radius are mostly irregular bodies (e.g. Figure 8.22), and may be fragments resulting from such collisions. Collisions may also be the origin of the rings of debris that are now known to encircle each of the giant planets (see Figure 8.23). Rings could also result from the break-up of a satellite that strayed so close to its planet that it was pulled apart by tidal forces.

In fact, all bodies less than about 300 km are likely to be irregular because their internal gravitational fields cannot overcome their intrinsic strengths and make them spherical.

**Figure 8.22** Two of the largest irregular-shaped satellites in the Solar System. (a) Amalthea, an inner satellite of Jupiter (radius dimensions  $135 \text{ km} \times 80 \text{ km} \times 75 \text{ km}$ ). (b) Hyperion, an outer satellite of Saturn (radius dimensions  $135 \text{ km} \times 120 \text{ km} \times 75 \text{ km}$ ).



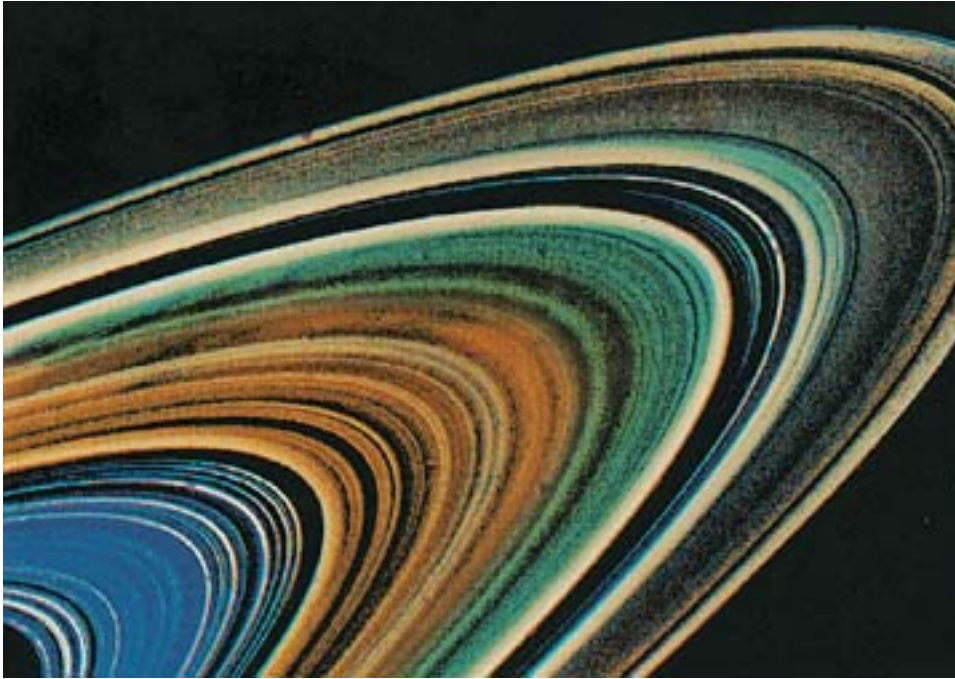


**Figure 8.23** Detailed view of the rings of Saturn as seen by the Voyager 1 spacecraft. The rings consist of icy debris orbiting in the plane of Saturn's equator. The rings are probably the remains of a broken up satellite, and most pieces are only a few centimetres in size.



**Figure 8.24** Phobos, the larger of the two tiny satellites of Mars, both of which are almost certainly captured asteroids.

Other small satellites, notably those in retrograde orbits (i.e. travelling in the opposite direction to their planet's rotation), are more likely to be captured bodies, in which case they probably began life either as asteroids or comet nuclei. The two satellites of Mars, Phobos (Figure 8.24) and Deimos, are almost certainly captured asteroids.

Neptune's only large satellite, Triton (Figure 8.25), has a retrograde orbit, which suggests that it was captured by Neptune after formation, instead of forming in a protosatellite disc. Triton is actually somewhat larger than the planet Pluto, which, so far as we can tell, resembles Triton rather closely in being an ice-rock mixture partly covered by condensed nitrogen. Triton and Pluto may represent stunted planetary embryos, intermediate in size between the Neptune kernel and the more distant bodies in the Kuiper Belt.

#### QUESTION 8.12

State four possible origins of planetary satellites, with examples.

#### QUESTION 8.13

If a planetary system is forming at  $\beta$  Pictoris, what stage (if any) do you think it has reached in the sequence suggested in this chapter for the development of our own Solar System, and why?

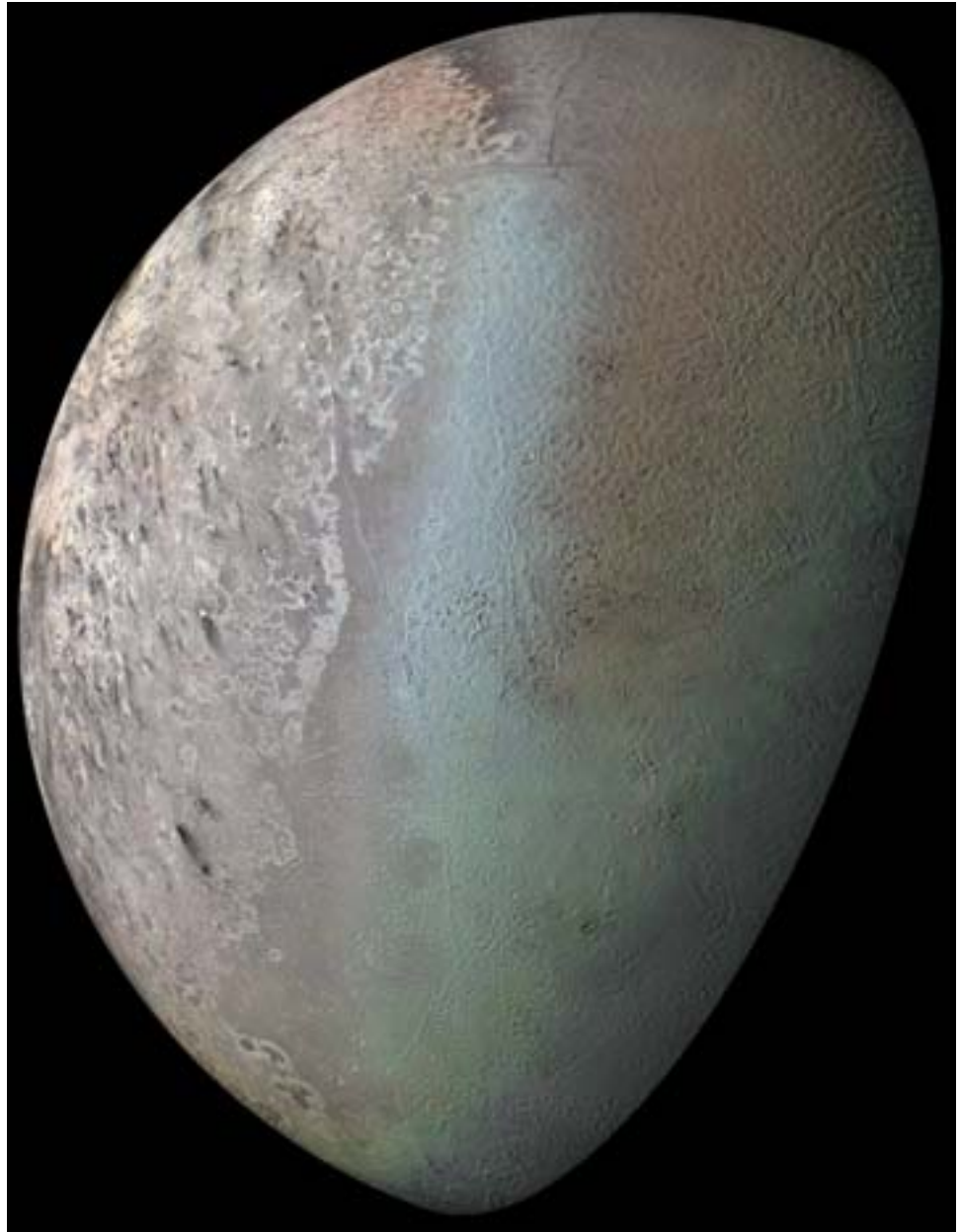


**Figure 8.25** Image of Triton, the largest satellite of Neptune, constructed from a mosaic of the highest resolution images taken by the Voyager 2 spacecraft in 1989.



## 8.3 Summary of Chapter 8

- The currently favoured paradigm for the origin of the Solar System involves the formation of a protoSun surrounded by a disc of material that rotates, flattens and separates to form the planets. This so-called nebula hypothesis is now corroborated by observations of other solar systems in the making.
- Within the rotating disc of the early Solar Nebula, angular momentum was evidently transferred outwards from the protoSun into the nebula.
- Much of the original dust in the Solar Nebula may have been vaporized, especially in the inner Solar System, principally as a result of heat released by loss of gravitational energy within the nebula and within the protoSun. Nebula material would have begun to condense as the temperature dropped, with the refractory substances appearing first and the more volatile substances condensing later, according to the condensation sequence. Within about 5 AU of the Sun the temperature never dropped low enough for ice to condense, although some water will have become trapped within hydrated minerals that condensed.
- Grains of dust that condensed from the Solar Nebula settled towards the central plane of the disc. When they came into contact they tended to do so gently, and stuck together (coagulated) to form larger particles. This sticking together may have been encouraged by fluffy surface textures, magnetism and electric charges.
- Within a few hundred thousand years of the creation of the Solar Nebula, grains in the dust disc that had formed near its central plane became gathered into planetesimals about 0.1 to 10 km in size, either because of gravitationally-driven turbulence or as a result of continued coagulation.
- Once a planetesimal had reached about 10 km in size, its gravitational field would have become sufficient to encourage collisions, by means of gravitational focusing. Eventually, the growth of one body would have outpaced all the others in the vicinity (runaway growth), producing a planetary embryo. At about 1 AU these were probably about one-tenth of the mass of the Earth. The creation of planetary embryos probably took of order  $10^4$  or  $10^5$  years in the inner Solar System, but the timescale goes up by roughly an order of magnitude in turn for each of the giant planets.
- Each terrestrial planet grew by a series of collisions between planetary embryos that took about  $10^8$  years to complete. Runaway growth took longer to get established in the outer Solar System, but the planetary embryos that grew there became sufficiently large that they could act as kernels around which large masses of gas were captured directly from the Solar Nebula.
- The onset of a powerful solar wind as the Sun entered its T Tauri phase swept the remains of the Solar Nebula outwards into space, and this evidently happened early enough to forestall Saturn, Uranus and Neptune from capturing as much gas as the earlier-formed Jupiter was able to. Loss of the primitive atmospheres of the terrestrial planets can be attributed to the T Tauri wind, but the giant planets were able to hold onto most of the gas they had already captured.

- The sub-planetary size of the asteroids can be attributed to gravitational perturbation of the orbits of planetesimals in this region by the young Jupiter, which ensured that mutual collisions were too energetic to lead to runaway growth. Long-period comets are icy bodies that may have been flung outwards after passing close to Jupiter or another giant planet to form the Oort cloud.
- The orbits of the major satellites of Jupiter, Saturn and Uranus suggest that these bodies grew out of a protosatellite disc about each planet, rather like the Solar Nebula in miniature.
- Smaller satellites may be collisional fragments, or captured asteroids and comets.



## CHAPTER 9

# METEORITES: A RECORD OF FORMATION

### 9.1 Introduction

**Meteorites** are pieces of extraterrestrial material (meteoroids) that fall to Earth from the sky having survived the retardation (deceleration) caused by their impact with the atmosphere, and which then survive to be collected as some sort of solid entity. While there are some meteorites that represent small pieces of the Moon or Mars (ejected from their respective surfaces during impact events), the majority are fragments of asteroids. In the present Chapter we concentrate solely on asteroidal meteorites. You should recall from Chapter 7 the nature and basic properties of asteroids, and from Section 8.2.10 the formation of asteroids.

Even today meteorites are the subject of much curiosity, but in the past some samples were revered and worshipped, while others were collected and used for making tools. Because meteorites are now considered collectable items, some individuals are prepared to pay large sums of money for specimens. This has had the effect of (a) pushing up prices, and (b) increasing the number of spurious claims regarding meteorite discoveries. Scientists try to work around these problems by maintaining a network of trustworthy individuals, both professional and private, who provide meteorite samples for all kinds of investigations.

The collection of a meteorite sometimes takes place after it has been observed to travel through the Earth's atmosphere. This is known as a **meteorite fall**. Events like this are rarely witnessed – only about 6 to 8 falls are recorded each year. A relatively recent event, the fall of the Peekskill meteorite in New York, USA, has become a rather celebrated case for two reasons. Not only was the incoming meteorite witnessed by many individuals (Figure 9.1), but the body itself struck a car which has since been displayed around the world (Figure 9.2).

In contrast to observed falls, several hundred meteorite fragments are collected each year without being seen to fall; these are the meteorite **finds**. An example of an impressive meteorite find can be seen in Figure 9.3, which shows the Hoba meteorite (Namibia) being excavated in the 1930s. Note that Hoba is the largest single meteorite ever found, with a mass of about  $5.5 \times 10^4$  kg, and is estimated to have fallen to Earth 80 000 years ago (see Box 9.1). It is still possible to see Hoba in the place it was originally found (Figure 9.4).

The reason we stress the notion of meteorite survival here is that there may be whole classes of potential meteorites which we do not know about because they are completely pulled apart within the atmosphere, or they effectively disappear after contact with the ground. Consider, for instance, a meteoroid composed largely of ice.



**Figure 9.1** The Peekskill fireball.



**Figure 9.2** The Chevrolet Malibu car that was struck by the Peekskill meteorite on display at a minerals exhibition in Munich, Germany.



**Figure 9.3** Excavation of the Hoba meteorite.



**Figure 9.4** The Hoba meteorite as it is displayed today.



**Figure 9.5** Mr. Arthur Pettifor holds a meteorite that struck a tree in his garden in Cambridgeshire, UK, in May 1991. If he had not been outside at the time of its fall, it would, like many thousands of other meteorites, have gone unnoticed.

Meteorites are generally given the name of their collection site, regardless of whether they represent a fall or find – hence Peekskill and Hoba.

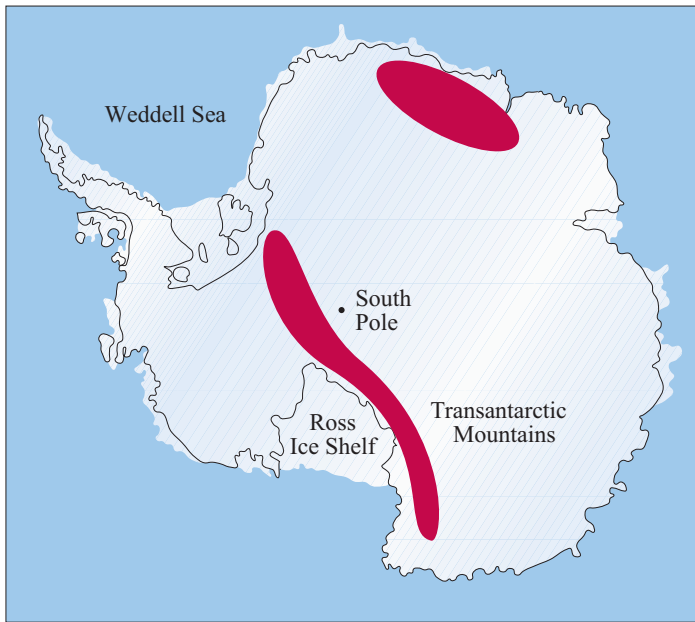
How many meteorites arrive at the Earth annually? It is known from continuous observations of the night sky that 20 000 bodies with masses in excess of 0.1 kg should reach the Earth's surface each year. Even of those that fall on land, it is clear that the vast majority of these meteorites are never recovered.

In principle, meteorites can be found anywhere on dry land (e.g. Figure 9.5), but various factors affect the chances of recovery. For instance, areas of dense vegetation are not good places for finding meteorites. In contrast, meteorites that fall in relatively barren environments, such as hot deserts, have a greater potential for collection. Antarctica is an even better place for finding meteorites, since glacial processes sometimes act to concentrate the samples (see Figure 9.6). Dedicated collection parties frequently visit Antarctica in order to collect materials for scientific research. Figure 9.7 shows some examples of meteorite collection.

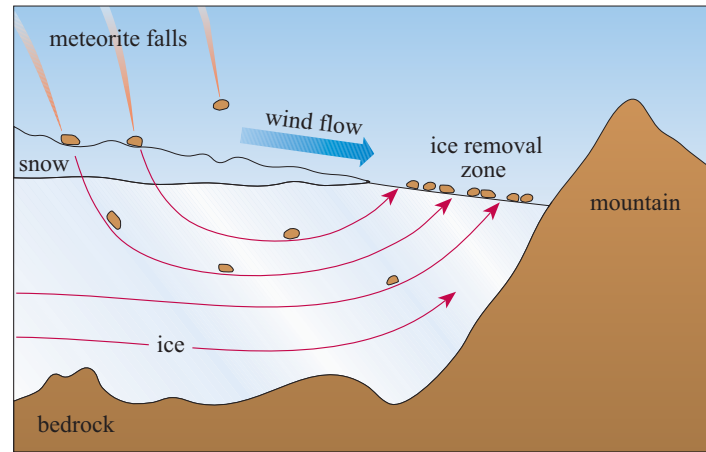
The term meteorite is used to denote a sample of material that has fallen to Earth and has subsequently been collected as a coherent mass. As we saw in Chapter 7, while still in space, the same body is referred to as a **meteoroid**. The term meteoroid refers to fragments of asteroids, or dust/ice particles ejected from comets (to form meteoroid streams, as discussed in Chapter 7). However, as ejected cometary meteoroids are made of relatively 'fluffy' dust and ice, the bodies will not generally be strong enough to survive their journey through the atmosphere (i.e. they will simply burn-up as meteors). Thus, the relatively large meteoroids that subsequently survive atmospheric entry to become meteorites, will almost certainly be asteroidal in nature (i.e. relatively strong rocky/metallic bodies). Direct evidence of this comes from three well-documented cases, where meteoroids (that survived to become

### BOX 9.1 ASSESSING HOW LONG AGO A METEORITE FELL TO EARTH

For observed meteorite falls we can be certain of when the body fell to Earth. For finds, however, this is a more difficult proposition. In the extreme, where meteorite remains are found within geological formations, the date of fall is gauged from the age of the rocks in which they are found. For finds of more recent vintage we use another method. The so-called *terrestrial age* of a meteorite (the period of time that the sample has been resident on Earth) is estimated by measuring the abundances of specific short-lived radionuclides. The nuclides in question are formed when the body is out in space, via the interaction with high-energy particles (cosmic rays – mainly  $H^+$  ions with high kinetic energies – which, themselves, originate beyond the Solar System). In space, an equilibrium is set up between the production of the radionuclides (through cosmic-ray irradiation) and radioactive decay. A recently fallen meteorite shows this equilibrium concentration. Most cosmic rays do not penetrate the Earth's atmosphere, so the short-lived radionuclides in a meteorite start to decay as soon as a sample arrives at the Earth's surface since they are no longer being replenished. Knowing the half-lives of the radionuclides in question, determination of the extent of the decay gives a measure of the terrestrial age of a meteorite.



(a)



(b)

**Figure 9.6** (a) Map of Antarctica showing locations of meteorite finds (red areas). (b) Schematic cross-section through the Antarctic ice sheet showing how ice movement acts to concentrate meteorites from a wide area in which they fall. Where a glacier abuts a mountain range the ice flow (red arrows) is diverted upwards. Strong winds blowing from the South Pole cause the ice to be removed, leaving the meteorite samples exposed.



(a)

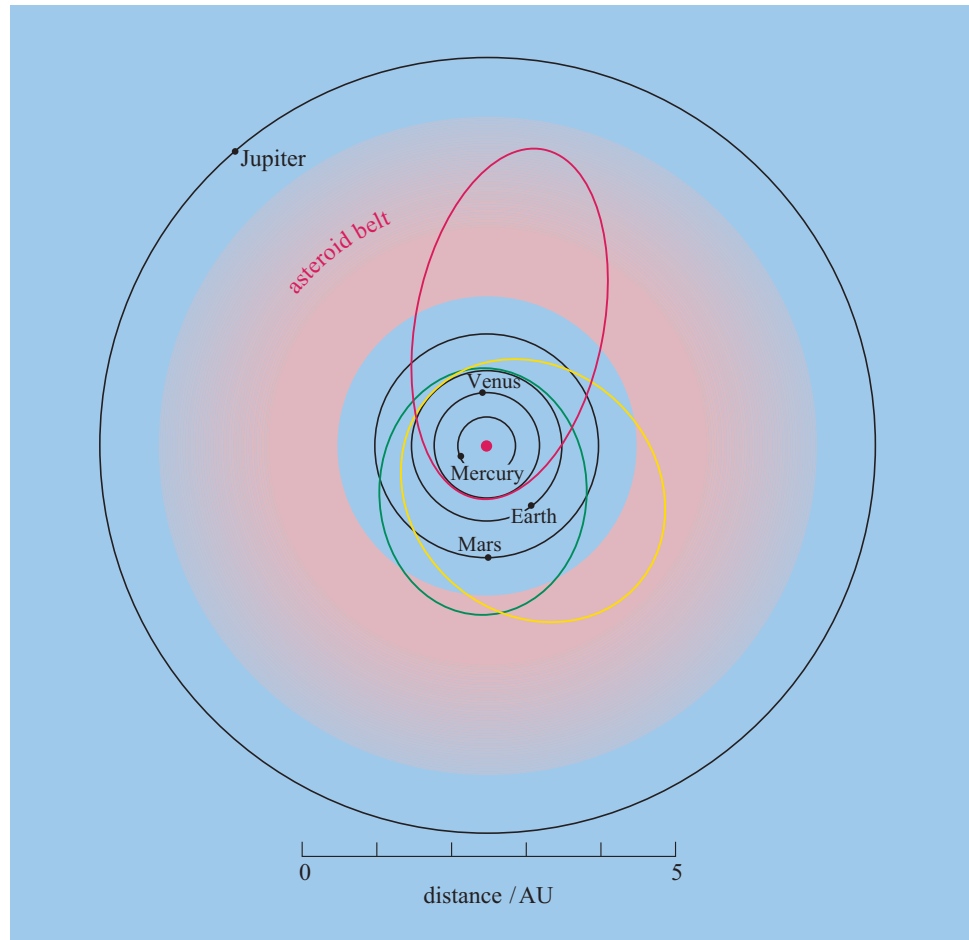


(b)

**Figure 9.7** Meteorites are collected from a variety of environments. (a) The Mbale meteorite fell in Uganda in 1992 as a shower of several hundred fragments, the largest of which had a mass of more than 27 kg. Shown in the picture is one of the smaller fragments, of mass 3 g, which bounced off the leaves of a banana tree and hit a young Ugandan boy on the head. (b) A meteorite being collected in Antarctica. It is being put in an ultra-clean Teflon bag using stainless steel tongs in order to minimize contamination.



**Figure 9.8** The orbits of three meteorites (shown in red, yellow and green) have been determined from data recorded by photographic networks (one in Czechoslovakia in 1959, one in the USA in 1970 and one in Canada in 1977). In these three cases the orbits can be traced back to the asteroid belt. More recently, evidence from video recordings has been used to reconstruct the orbits of two other meteorites (Peekskill and Tagish Lake) and both of these can also be traced back to the asteroid belt.



meteorites) were photographed during their fall, using networks of cameras. From the photographic evidence it has been possible to assess the meteoroids' orbits, which can be traced back to the asteroid belt in each case (Figure 9.8).

For those asteroidal meteoroids that become meteorites, the brief atmospheric passage is quite eventful. People who have witnessed falls can attest to the spectacular visual display and accompanying loud detonations. At an altitude of about 120 km, frictional heating by the atmosphere begins to melt the surface of an incoming meteorite. For a body of  $>10$  mm in diameter, only the outer layers at any instant are heated sufficiently to cause melting and vaporization. This heating of the surface results in the formation of a glassy **fusion crust**, which is a further diagnostic indicator of a meteorite. During the fall, molten material is lost from the surface by a process called **ablation**. For those groups of meteoroids which have ultimately produced meteorites that are well represented in our collections on Earth, perhaps 50% of the total mass is lost this way.

During their fall to Earth the very smallest meteoroids, which are often called **micrometeoroids**, become (not surprisingly) **micrometeorites**. Unlike larger samples, micrometeoroids, which are of roughly micrometre- to millimetre-sized dimensions, become *totally* molten during their fall. Some of these vaporize completely while others survive to form **cosmic spherules**, which can be collected

at the Earth's surface. Ordinarily these spherules go unnoticed. However, they are found in abundance in oceanic sediments (they were first identified in Pacific Ocean clays during the Challenger expeditions of the 19th century). Figure 9.9 shows a picture of cosmic particles extracted from a deep-sea sediment. Curiously, the very smallest micrometeoroids ( $<0.01$  mm in size), which can be cometary in nature, do not melt during their fall to Earth. This is because they are decelerated at sufficiently high altitudes, where the atmosphere is more rarefied, and so avoid melting by frictional heating.

As a meteoroid travels down through the atmosphere it eventually reaches a level at which atmospheric gases surrounding the incoming body become ionized and form a plasma. As the body continues to move, this produces a streak of light known as a meteor (i.e. the process discussed in Chapter 7 for both cometary and asteroidal meteoroids), or, if bright enough, a **fireball**. Typically, meteors appear at an altitude of about 90 to 120 km and become extinguished at about 10 to 30 km (in other words, most of this activity takes place in a layer above the stratosphere). For large meteoroids the fireball can be seen in daylight, as can the accompanying trail of ablated material (which has the appearance of smoke). For smaller bodies, a meteor trail is only visible at night.

As a meteoroid descends to Earth, atmospheric drag causes the body to slow down, and so frictional heating is reduced. Eventually, surface melting ceases. For a meteoroid of  $>0.1$  m diameter, the interior remains relatively cool during atmospheric entry; in fact, immediately following their fall, meteorites that have been broken open have sometimes been observed to form frost on their inside surfaces. Furthermore, the outer layers of a modest-sized meteorite will be cooled in the lower regions of the atmosphere, such that by the time it lands, the outer crust is also usually cool.



**Figure 9.9** Cosmic spherules, collected from the floor of the Pacific Ocean at a depth of about 5 km. Note that ‘ $\mu$ ’ on the scale here stands for ‘micron’, a unit of length equal to  $10^{-6}$  m or 1 micrometre.

### 9.1.2 The meteorite–asteroid connection

Meteorites can be broadly classified as irons, stones or stony–irons, reflecting their parent asteroid composition. As their names might suggest, irons (or **iron meteorites**) are predominantly composed of iron metal while stones (or **stony meteorites**) are composed mostly of silicate minerals. **Stony–iron meteorites** are mixtures of metals and silicates. Figure 9.10 shows a variety of different meteorite types.

In order to learn something of the origins of meteorites it is important to know the relative proportions of irons, stones and stony–irons that arrive at the Earth. For instance, which meteorites are the most common and thus most typically represent the source? Studying the meteorite finds cannot answer this question. This is because a piece of metal weighing several kilograms is obviously unusual and more likely to be collected as a find than a silicate meteorite, which may look like any other piece of rock. In order to properly assess which sorts of meteorites are most common it is necessary to consider only those samples *observed to fall*. Using this criterion, irons constitute about 5% of all meteorites and stony–irons amount to about 1%. Note that if we had considered only the meteorite finds, irons would appear to constitute 40% of all meteorites.

Stony meteorites are thus the samples that fall to Earth most frequently. Of these, more than 90% are **chondrites**, i.e. samples that generally contain **chondrules**.

- What are chondrules?
- Chondrules are globules of silicate minerals, up to a few millimetres in size (see Box 2.3).

**Figure 9.10** Different types of meteorites. (a) A cut and polished surface of an iron meteorite that has been etched with acid.

(b) A carbonaceous chondrite, representing some of the most primitive material in the Solar System. (c) A stony meteorite of basaltic composition, formed by melting processes on its parent asteroid. (d) A stony–iron meteorite, or pallasite, that comes from deep within an asteroid, that is from the boundary of an iron-rich core and silicate-rich mantle.



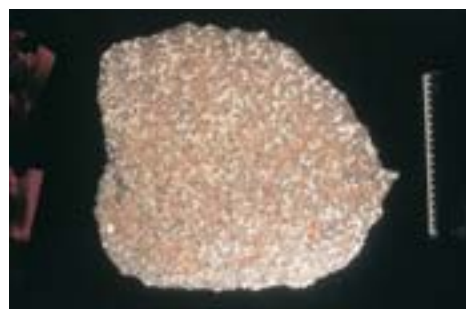
(a)



(b)



(c)



(d)



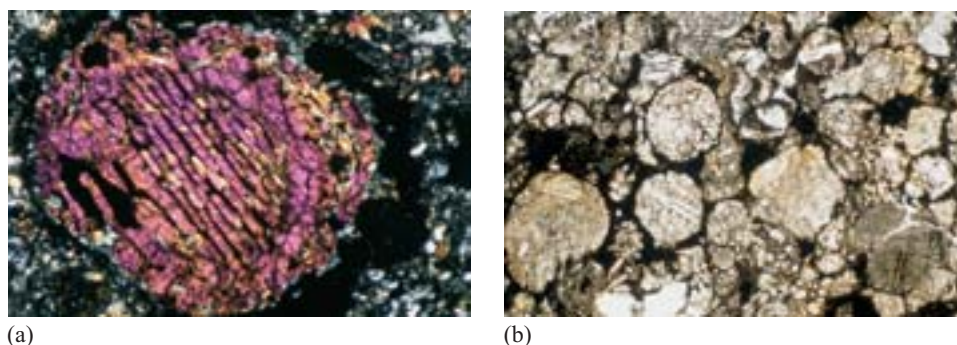


**Figure 9.11** Meteorites under the microscope. (a) A relatively large, mm-sized chondrule from the Cold Bokkveld meteorite (carbonaceous chondrite). Individual crystals are clearly visible within the chondrule. The dark matrix represents a fine-grained silicate dust containing water-bearing minerals and organic compounds. (b) A collection of different types of chondrules, including fragments and one that has been squashed to some extent, from the Sharps meteorite (ordinary chondrite). The scale of both images is the same.

In detail, chondrules are small spherules of silicate materials (olivine, pyroxene and glass, with some minor amounts of iron–nickel metal and iron sulfide) which experienced melting *before* they were incorporated into meteorites. Their generally spherical shapes attest to the formation from molten droplets within low gravitational fields. Laboratory experiments have shown that chondrules would have formed in minutes to hours, implying that they formed in local, transient heating events (and not, for instance, as a result of the entire solar nebula cooling at once). The exact formation mechanisms of chondrules are the subject of much activity and debate. While they are mainly considered to have formed by condensation, or re-melting of dust, in the solar nebula, it is also possible that some of them are formed at the surfaces of planetesimals as the result of impact melting. Some examples of chondrules are shown in Figure 9.11.

Most chondrites belong to a group known as the **ordinary chondrites**. The term ‘ordinary’ is used because they are the most common sort of meteorite. Ordinary chondrites contain varying proportions (5 to 15%) of iron–nickel metal, a factor which, along with the presence of chondrules, makes them distinctive from terrestrial rocks. Another important chondrite group is represented by the **carbonaceous chondrites**; these are carbon-rich meteorites that contain organic compounds such as amino acids. Overall, the carbonaceous chondrites have a *primitive* chemical composition (see Box 2.3). The so-called **achondrites** are stony meteorites that do not contain any chondrules; these have generally been heated to their melting temperatures, and formed by crystallization of magmas on their respective parent bodies. Some achondrites are mechanical mixtures of melted fragments and pieces of chondrites. These meteorites formed at the surface of a parent body where, early in the history of the Solar System, impact processes assembled a variety of materials.

A typical collected stony meteorite has a mass of 1 to 10 kg (diameter 0.1 to 0.2 m), while the mass of an iron is generally in the range 10 to 40 kg. Although meteorites come in all shapes and sizes, there are many more small samples than large ones. Meteorites with masses greater than 100 kg are rather rare (recall that Hoba has a mass of  $5.5 \times 10^4$  kg). The smallest micrometeorites (i.e. micrometre-sized dust) have masses of around  $10^{-15}$  kg. Samples of this nature are constantly falling to Earth. Indeed, a person who spends a few hours outside during the day is likely to be hit by at least one extraterrestrial particle (of this sort of size). This constant rain of material to Earth amounts to at least  $10^7$  kg per year. This sounds a lot, but the *total* annual flux of extraterrestrial material, which includes bodies larger than micrometeorites, is estimated to be about  $10^8$  kg per year. It should be noted that since the mass of the Earth is  $5.98 \times 10^{24}$  kg (that is more than 16 orders of magnitude larger) the yearly input of extraterrestrial material does not cause any obvious changes to the physics or chemistry of our planet as a whole.

**QUESTION 9.1**

Assuming that the flux of extraterrestrial material has remained constant over the last billion years, calculate the mass and volume that this extra matter has added to our planet during this time. If all the extraterrestrial materials were available now as a surface layer spread uniformly across the whole of the planet, how deep would this be? (Assume a density for the incoming material of  $1.5 \times 10^3 \text{ kg m}^{-3}$ .)

What does it feel like to be hit by a small meteorite? Let's consider how fast these objects are travelling. In space they travel at speeds typically of  $20$  to  $40 \text{ km s}^{-1}$  (for comparison, the speed that a rocket needs to escape from the Earth's gravitational field is about  $11.2 \text{ km s}^{-1}$ ; the velocity of a bullet from a gun is of the order of  $1 \text{ km s}^{-1}$ ). Fortunately the Earth's atmosphere acts to retard projectiles with masses of less than a few kilograms (equivalent to a body of  $0.1 \text{ m}$  diameter). These smaller bodies fall to Earth under the influence of gravity opposed by atmospheric drag and have impact speeds of less than  $5 \times 10^{-2} \text{ km s}^{-1}$ . In fact, for sub-millimetre meteorites, the final fall speed is nearer  $10^{-5} \text{ km s}^{-1}$ . The smallest micrometeoroid dust particles (micrometre-sized) are essentially totally decelerated in the atmosphere, and gently 'float' to the ground over a period of days or even months. Much larger objects, on the other hand, arrive at the Earth's surface with a significant fraction of the speed they had in space.

- What physical effects will large meteorites exert on our planet?
- You saw from Chapter 4 that, following the collision of large cosmic debris with various planetary bodies, impact craters are produced which may be many kilometres in diameter.

You have seen how meteorites can be distinguished, on the basis of their principal constituents, as irons, stones etc., and you have learned that meteorites are thought to originate in the asteroid belt. In Chapter 7 you learned about different sorts of asteroids. If we could relate the various meteorite types to asteroid groups we would effectively establish their origin, and be able to study the asteroids in great detail using conventional laboratory-based analytical techniques.

- How are asteroids classified?
- Asteroids can be classified (among others) as C-type and S-type, using observational astronomy (see Chapter 7) which entails measuring the brightness of reflected sunlight at different wavelengths, to obtain reflectance spectra.

Meteorite surfaces can also be analysed using a similar sort of measurement. In this way we find that the C-type asteroids most closely resemble carbonaceous chondrites, while the S-type asteroids represent stony-irons. A further group, the M-type asteroids, look like iron (metallic) meteorites. The agreement between results obtained from the observations of asteroids and analyses of meteorites is strong circumstantial evidence for a relationship between the two. Unfortunately we have not yet found a direct match between the most common group of meteorites, the ordinary chondrites, and any asteroid taxonomic class. This is because the very

surfaces of asteroids (i.e. the parts that are observed) are altered by the phenomenon of ‘space weathering’ which, in the case of the rocky bodies, has resulted in subtle changes that have acted to confound the observational data.

Micrometeoroids do not have a single origin. Some are formed by collisional processes in the asteroid belt, just like their larger counterparts. Others are ablation products formed in the Earth’s atmosphere during the passage of the parent meteoroid. However, the majority of small (sub-mm) micrometeoroids represent fresh debris liberated by comets near perihelion (see Chapter 7).

In addition to asteroids and comets, a few meteoroids have origins on planetary bodies. Several meteorites are known to have come from the Moon. These were ejected when the Moon was itself bombarded by a projectile (asteroid, or comet). How can we be so sure about their lunar origin? One way is to compare the chemistry of these samples directly with materials returned from the Moon (by US and Soviet spacecraft during 1969–76). A further group of meteorites (currently represented by more than 20 specimens) has been recognized as unusual for over a century – these samples are now thought to have originated on Mars.

#### QUESTION 9.2

A meteorite has been found which is composed of a mixture of iron and silicates. Within the silicate portion there are fragments of materials recognizable as chondrites and achondrites. The meteorite has obviously been subjected to intense shock. Consider how it might have formed.

#### QUESTION 9.3

20 000 meteoroids of mass  $>0.1$  kg arrive at the Earth’s surface each year. On average, what is the frequency with which materials of this size would be encountered in a town with a radius of 5 km?

## 9.2 The forensic record

### 9.2.1 Cosmic sediments

The meteorite known as Allende (pronounced eye-endy) fell in 1969. Like many other meteorites, Allende fragmented during descent through the atmosphere, resulting in a shower of stones. More than 2000 kg of material was subsequently gathered over an area of about 300 km<sup>2</sup>, in the vicinity of Pueblito de Allende in Mexico. Murchison, a shower of 500 kg, also fell in 1969, in Victoria, Australia. Meteorites like Allende and Murchison are carbonaceous chondrites and have been studied intensively. You will see in this section how some of the components of these meteorites appear to document changes in formation conditions within the solar nebula. You will also learn that some of their organic compounds pre-date the formation of the Solar System; by studying these materials it is possible to gain an insight into interstellar chemistry.

You may recall from Chapter 2 that, when all but the most volatile elements are considered, the CI carbonaceous chondrites have chemical compositions similar to the Sun.

- Why are Earth rocks not solar in composition?
- Rocks at the Earth's surface are unrepresentative of the Earth as a whole because of geological processes which have acted to segregate elements on a planetary scale (a simple example is the concentration of iron and nickel in the Earth's core).

The carbonaceous chondrites enable us to undertake laboratory studies of materials that are fully representative of the chemical composition of the solar nebula (remember that we called this a *primitive* composition). Recall the data in Figure 2.2. There is clearly a very wide range of abundances of different elements in the Solar System.

- How much less abundant is silver (Ag) than silicon (Si)?
- The abundance of Si is (by convention)  $10^6$ , whereas the abundance of Ag is about  $10^{-1}$  in both the Sun and in carbonaceous chondrites. Thus the abundance of Ag is about seven orders of magnitude less (i.e. seven powers of ten less) than the abundance of Si, which means there are about  $10^7$  atoms of Si for each atom of Ag.

Despite the wide range of abundances, elements that are abundant in carbonaceous chondrites (e.g. Si, Mg, Fe) are also abundant in the Sun, and those that are rare in carbonaceous chondrites (e.g. Ag, Eu, Rh) are also among the rarest in the Sun. This can be seen by the fact that the elemental abundances in Figure 2.2 fall fairly close to the straight line representing equal abundances in the Sun and carbonaceous chondrites. The relative abundances of the elements in the carbonaceous chondrites are often referred to as representing **chondritic composition**.

Thus, so far as we can tell by examining primitive meteorites, they have pretty much the same composition as the Sun (gas-forming elements such as H and He excepted), and so appear to reflect the composition of at least that part of the solar nebula in which they formed.

All but one of the CI chondrites are of type CI1. Only recently has a CI2 chondrite been found. Thus CI chondrites are often referred to as a single group (see Box 9.2).

We have already said that Allende and Murchison are both carbonaceous chondrites. Thus, we would expect them to be very primitive materials, which have not had their chemistry changed by secondary processes. In a general sense this is true, but when we look in detail at carbonaceous chondrites we find that there are various groups that can be distinguished on the basis of slightly different chemical compositions. Allende is a type CV3 carbonaceous chondrite, whereas Murchison is a CM2 (see Box 9.2). The meteorites which most closely resemble the Sun are the CI carbonaceous chondrites. The meteorite Ivuna is a CI1 chondrite and chemically one of the most primitive of all; a progression away from primitiveness is observed in samples of successively higher types (i.e. from CI1 to CM2 to CV3). This can be understood by looking at Figure 9.12; here are plotted the abundances of certain elements found in the silicate and oxide minerals of Murchison and Allende. The elements are arranged from left to right according to volatility. It would be meaningless to plot absolute concentrations in Figure 9.12 since carbonaceous chondrites contain variable amounts of water, as hydrated minerals and organic compounds. Instead, the elemental data are normalized to a non-volatile element – in this case silicon (so, for instance, the Ca/Si mass ratio is used). These are then plotted with respect to the corresponding ratios found in CI meteorites. This may all seem a little complicated until you realize that in Figure 9.12 the chemical composition of a typical CI meteorite would plot as a horizontal line, at a value of 1.0.

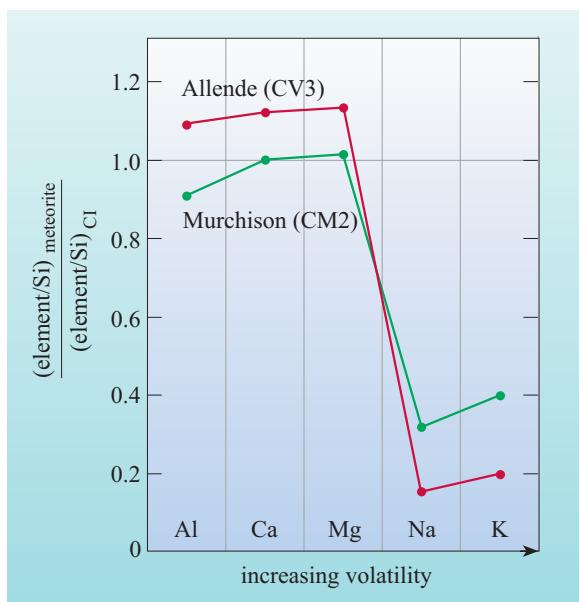


**Figure 9.12** Plot of elemental concentrations of aluminium, calcium, magnesium, sodium and potassium (all normalized to silicon) in Allende (CV3) and Murchison (CM2), relative to data from CI meteorites. The most primitive samples are represented by the CI data, i.e. a horizontal line at a value of 1.0.

## BOX 9.2 TYPES OF CHONDRITES

Chondritic meteorites, those that contain chondrules, comprise the bulk of the meteorite specimens available for study. You do not need to understand the details of how chondrites are classified, that is beyond the scope of this book, however you will come across the abbreviations that are used to refer to different types of chondrites and this box outlines how these are derived.

Chondrites have been classified on the basis of their mineralogical and chemical composition into 3 main types and a series of letter and number abbreviations are used to refer to them:

- 1 The carbonaceous chondrites, which can contain up to 5 wt% carbon, are denoted by the letter C. This important, although relatively rare class of meteorites, has been further sub-divided on the basis of chemical and mineralogical composition into about 7 sub-groups. These sub-groups include the CI chondrites such as the Orgueil meteorite, CM chondrites such as the Murchison meteorite and CV chondrites such as the Allende meteorite. The second letter refers to what is considered to be the characteristic meteorite from each sub-group. For the CI chondrites this is the meteorite Ivuna, for the CM chondrites it is the meteorite Murray and for the CV chondrites it is the meteorite Vigarano.
- 2 The enstatite chondrites that contain the mineral enstatite ( $\text{Mg}_2\text{Si}_2\text{O}_6$ ), a form of pyroxene, are denoted by the letter 'E' and are therefore referred to as the E chondrites.
- 3 The ordinary chondrites, which comprise the majority of observed falls. The initial letter designation for ordinary Chondrites, O, is usually deleted. Instead, this group is subdivided into meteorites that are relative high in iron, the H chondrites, those with a low iron content of 5 to 10% metallic iron, the L chondrites, and those with very low iron contents (less than 2%) the LL chondrites.



When examined in detail, many classified chondrites are given a further number designation to indicate the state of preservation of the chondrules they contain. For example, the Allende meteorite is classified as a CV3. This number is called the petrologic type of the meteorite and a designation of 3 indicates that the meteorite contains essentially unaltered chondrules. Higher numbers indicate progressively greater amounts of thermal metamorphism, for example the Glatton meteorite found by Mr Pettifor (Figure 9.5) is an L5 indicating that its chondrules have been fairly extensively altered by thermal metamorphism. A designation of 6 would indicate that the meteorite's chondrules had been almost entirely obliterated by thermal metamorphism. Numbers of 1 or 2 indicate that the meteorite's chondrules have been altered by aqueous processes with a designation of 1 denoting that the chondrules have been completely altered by water. Thus the Murchison meteorite, a CM2, contains evidence that liquid water existed for periods of time on the asteroid from which it was derived.

You will find in the scientific literature and in this book that the CI chondrites are usually referred to as a single group without an indication of petrologic type, hence we refer to data being normalized to CI chondrite elemental abundances (see Box 2.3). In fact, all but one of the CI chondrites that have been studied in detail are of type CI1, the exception being the Tagish Lake meteorite that fell in Canada in 2000, which is thought to be of type CI2. You should note that data on Tagish Lake are not included in the average CI chondrite chemical compositions used to compare the elemental concentrations between meteorites and other samples.

- Refer back to Table 2.4 and assess the volatilities of aluminium and calcium relative to other elements.
- Corundum ( $\text{Al}_2\text{O}_3$ ) and perovskite ( $\text{CaTiO}_3$ ) are some of the first minerals predicted to condense (at temperatures in excess of 1600 K) from a cooling gas of solar composition. Al and Ca are thus refractory elements (the least volatile). For comparison, the volatile elements Na and K are incorporated into alkali feldspars and appear in the condensation sequence at <1000 K.

You can see from Figure 9.12 that the elements Al, Ca and Mg are somewhat more abundant (relative to silicon) in Allende (CV3) than in the other two types. These elements also lie on roughly horizontal lines (other refractory elements also display this trend, although for simplicity these have been left off the figure), showing that refractory elements occur in approximately the same relative proportions to each other in CI–CV3 carbonaceous chondrites (the Ca/Al ratio is virtually constant, for instance). The volatiles in Murchison and Allende (Na and K) are depleted with respect to the refractory elements. Note that the depletion is greater in the CV3 sample than the CM2. Thus, in going from CI to CV3 meteorites, the chemical compositions become progressively less like that of the Sun, i.e. less primitive.

Although the CI meteorites are the most primitive in a chemical sense, it transpires that they have suffered the complication of **hydrothermal alteration**. CI meteorites were endowed with a large complement of volatiles; they contain about 20% (by mass) of  $\text{H}_2\text{O}$ , for instance. Transient heating events on the parent bodies of these meteorites (during impacts, for instance) have acted to mobilize volatiles such as



water, which in turn have reacted with the more refractory components. The effect of this alteration is so intense that recognizing primary physical features is difficult – the bulk of the meteorites have been converted into complex hydrated minerals somewhat similar to those found in terrestrial clays.

#### QUESTION 9.4

The chemical composition of CI meteorites is considered to be the same now as it was when they were formed, even though the original minerals have been altered. What can you say about the nature of the alteration process that has affected CI meteorites?

A detailed look at carbonaceous chondrites shows that the effects of hydrothermal alteration are most intense in CI samples, less so in CM2s and are virtually absent in CV3s. Thus, although a CV3 meteorite like Allende is not the most chemically primitive of samples, it is representative of the least-altered of carbonaceous chondrites. It is therefore a good place to commence the study of meteorites.

Allende is composed of rounded chondrules and large irregular-shaped white inclusions set in a fine-grained, dark matrix. Some examples of chondrules were shown in Figure 9.11. This collection of materials was assembled from nebular dust, upon the outer layers of a planetesimal. This action can be likened to the deposition of a sediment – for this reason we think of carbonaceous chondrites as **cosmic sediments**. Be sure that you understand that there were no liquids present during the meteorite formation process. The water which was imparted to CI and CM2 meteorites settled out with the refractory dust as solid ice grains.

#### QUESTION 9.5

Consider the refractory elements Ca and Al shown in Figure 9.12. What differences in chemical composition exist between CI, CM2 and CV3 meteorites? How could this be explained?

### 9.2.2 Refractory bits and pieces

The white inclusions in Allende contain refractory elements. Because of their chemical compositions they are frequently referred to as **calcium–aluminium-rich inclusions**, or **CAIs** for short. The mineralogy of these refractory inclusions matches very well with what is predicted to form at high temperatures in the condensation sequence (see Table 2.4). It would appear, therefore, that the inclusions contain some of the first minerals to form in the cooling solar nebula. Equally well, however, they may represent evaporation residues (i.e. aggregations of minerals that lost all traces of volatile materials through heating and evaporation). Yet another way of looking at the nature of CAIs may be to consider that since they are so refractory, then perhaps they represent lumps of unmelted pre-solar material. In principle a material which condenses from the cooling gas cloud associated with the solar nebula could also have formed by condensation processes operating around other astronomical objects. The chemistry and mineralogy of such materials might be identical in both cases.

Is there a way that we can try to distinguish between the competing theories for the origins of refractory inclusions? Two measurements are of relevance here: age-dating and stable isotope compositions (see below). You have already met radiometric age-dating in Section 2.4.3. Earth Scientists use techniques of this sort in order to date the

timing of geological processes. Since the very earliest rocks formed on Earth have all been reprocessed by the action of geology we use meteorites to date the formation of the Earth. A range of different meteorite types give ages that are around 4.5 or 4.6 Ga. For most geologists this is all they need to know. But for meteoriticists they want to understand the detailed chronology of meteorites in order to understand the sequence of events that took place in the solar nebula, and which led to diverse entities such as chondrules, CAIs, primitive melt residues, and so on. And for this purpose a different type of radiometric dating is used, one which uses short-lived radionuclides.

We will not go into the details of the technique here, but in many ways the principles are similar to that of the normal dating techniques. Consider a radioactive isotope like  $^{26}\text{Al}$ , which has a half-life of  $7.2 \times 10^5$  years, and decays to non-radioactive  $^{26}\text{Mg}$  by a process known as positron decay. From various lines of evidence we know that  $^{26}\text{Al}$  was present at the time when the Solar System formed – we say that the  $^{26}\text{Al}$  was ‘live’ at this time. Where the  $^{26}\text{Al}$  came from is another matter and one of continued research – the essential fact is that live  $^{26}\text{Al}$  was brought in from the pre-solar environment and then, once in the nebula, began to decay (i.e.  $^{26}\text{Al}$  was not being produced within the solar nebula). Consider that if the radioactive aluminium was to become incorporated into minerals (one of those present in the CAIs, for instance) then it would be observable today as a small amount of  $^{26}\text{Mg}$ . On the other hand, if the timescales involved in the solar nebula were such that before any Al-bearing minerals could form, all of the  $^{26}\text{Al}$  had decayed, then CAIs measured today would contain no  $^{26}\text{Mg}$ . Measuring the precise abundance of  $^{26}\text{Mg}$  therefore constrains the formation times of minerals *relative* to the time after which the nebula became cut off from its supply of  $^{26}\text{Al}$ . The technique can be used to obtain relative ages equivalent to a few half-lives of the radiometric system concerned (at which point scientific instruments become insensitive to the small amounts of decay products that would have accumulated). In the case of the Al–Mg system this means relative ages of a few million years at most. To look at longer or shorter timescales we use different isotopic systems.

Figure 9.13 shows the chronology of the early Solar System, assessed using a different age-dating technique: the  $^{53}\text{Mn}$ – $^{53}\text{Cr}$  system (half-life of  $^{53}\text{Mn} = 3.7$  Ma). The reason that we have shown the  $^{53}\text{Mn}$ – $^{53}\text{Cr}$  system is that this can be easily applied to two groups of igneous meteorites (known as HEDs and angrites), which can also be dated using normal (long-lived) radiometric methods. It is not possible to use the  $^{26}\text{Al}$ – $^{26}\text{Mg}$  system in this case because the mineralogy of these samples is not appropriate. Using a combination of ages derived by the short-lived  $^{53}\text{Mn}$ – $^{53}\text{Cr}$  system and absolute ages determined in the normal way it is possible to construct a highly detailed chronology of events in the early Solar System. You will learn more about an HED meteorite in Section 9.2.5; the age of 4.563 Ga shown in Figure 9.13 represents the onset of differentiation of the HED meteorite parent body (actual formation ages of HED meteorites span a range from this figure up to about 4.53 Ga, i.e. a range of about 4.53 to 4.56 Ga). Angrites are a very distinctive group of igneous meteorites which all show a similar formation age (of 4.558 Ga).

The exact interpretation of information from radiometric chronometers is the subject of much discussion. Indeed, as you can see from Figure 9.13, there are two possible interpretations when the ages are considered in absolute terms. In contrast, the relative ages are far less ambiguous – as such, we can say with certainty that the time interval represented in Figure 9.13 represents a period of 13 Ma. The processes, as recorded in meteorites, began with the formation of CAIs, which formed by direct condensation

The acronym ‘HED’ stands for Howardite–Eucrite–Diogenite.

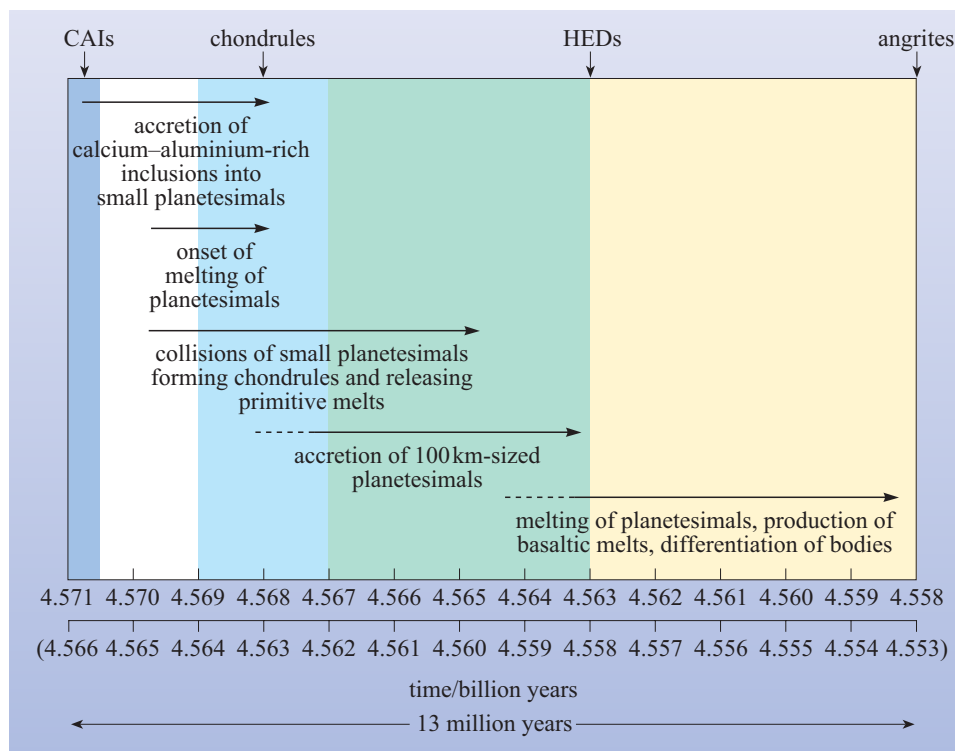


**Figure 9.13** Chronology of the early Solar System – an interpretation based on the short-lived radionuclide  $^{53}\text{Mn}$ , which decays to  $^{53}\text{Cr}$ . The relative ages obtained by the  $^{53}\text{Mn}$ – $^{53}\text{Cr}$  system are converted into absolute ages by measurements of long-lived radionuclides found in two particular meteorite groups (HEDs and angrites) – these are the ages given in the upper scale. The scale enclosed in brackets (which is displaced from the above by 5 Ma) represents yet another attempt to combine data from short- and long-lived radionuclides.

from a nebular gas of solar composition (a process which lasted less than a million years). Once formed these CAIs began to assemble into small planetesimals; as these bodies grew they started to melt because of impact processes and the effects of heat generated from the decay of short-lived radionuclides (of which the decay of  $^{26}\text{Al}$  to  $^{26}\text{Mg}$  was the most important). Some 2 Ma after the first CAIs had formed, collisions of CAI-bearing planetesimals were implicated in the formation of chondrules (and at the same time, examples of primitive melts were injected back into the nebula). The chondrule-forming period lasted for about 2 Ma. As this episode began to wane, planetesimals up to about 100 km in size started to form. And as these grew to larger sizes, melting processes operating on planetesimal scales resulted in the differentiation of bodies – i.e. the formation of iron-rich cores, and basaltic mantle rocks (the first examples of geological processing within the Solar System).

You should note that there are some disagreements in detail regarding the absolute ages recorded from meteoritic components. It is for this reason that we assign the age of the Solar System to be a rather non-committal 4.56 Ga. Within the context of Figure 9.13 this represents a time period in which planetesimals were accreting and melting. For the purists the age of the Solar System is considered to be that time when CAIs started to form – some scientists would say that this was 4.571 Ga ago, while others would have this at 4.566 Ga (and, be advised, there are others who would advocate slightly different dates). For our purposes, 4.56 Ga is an honourable compromise!

Meteorites like Allende contain a vast number of CAIs and we have age-dating measurements for just a few of them. Thus, confidence in our belief that CAIs formed in the solar nebula needs to come from other measurements. In this regard **stable isotope compositions** can be used to provide additional information. Stable isotopes are introduced in Box 9.3 using oxygen as a pertinent example.

BOX 9.3 STABLE ISOTOPE COMPOSITIONS

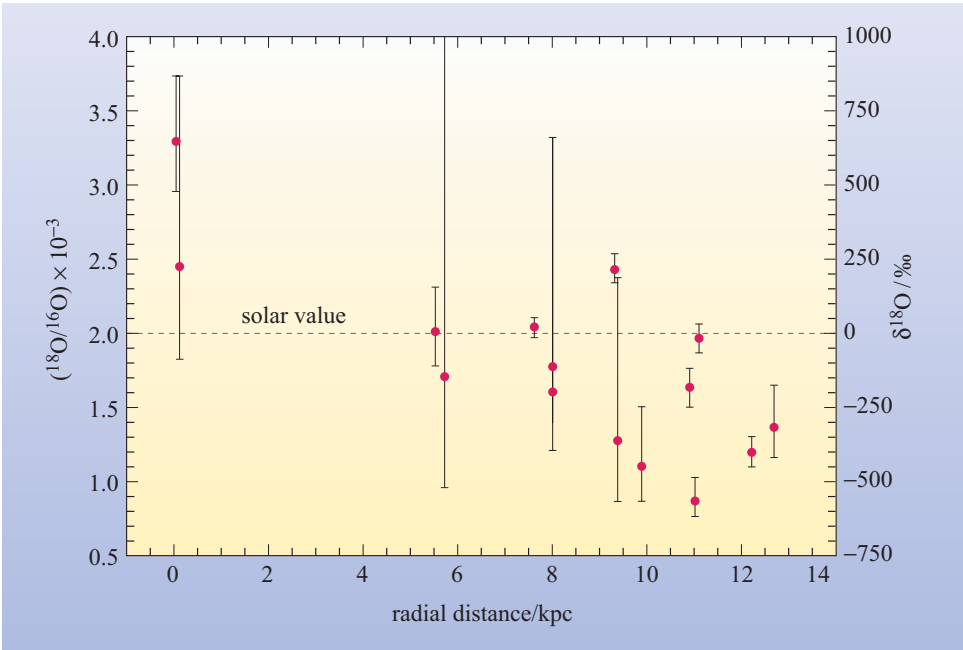
You saw above that certain elements have radioactive isotopes. Aluminium, for instance, has a radioactive isotope,  $^{26}\text{Al}$ , which decays to give  $^{26}\text{Mg}$ . But aluminium also has another isotope,  $^{27}\text{Al}$ , which is not radioactive. Furthermore, the decay product itself,  $^{26}\text{Mg}$ , is also not radioactive.  $^{27}\text{Al}$  and  $^{26}\text{Mg}$  are called **stable isotopes** because they do not decay. Most elements consist of mixtures of stable isotopes (in this regard aluminium is unusual). Oxygen has three stable isotopes:  $^{16}\text{O}$ ,  $^{17}\text{O}$  and  $^{18}\text{O}$ . All the isotopes of oxygen contain 8 protons – this is the atomic number. However, the isotopes differ in their number of neutrons;  $^{16}\text{O}$ ,  $^{17}\text{O}$  and  $^{18}\text{O}$  have 8, 9 and 10 neutrons respectively.

In astronomical entities, such as stars, the variations in oxygen isotope compositions can be quite large and so the differences are described in terms of their  $^{17}\text{O}/^{16}\text{O}$  and  $^{18}\text{O}/^{16}\text{O}$  ratios. An example of the radial variation of  $^{18}\text{O}/^{16}\text{O}$  ratios of stars within our Galaxy is shown in Figure 9.14 (note that, as yet,  $^{17}\text{O}/^{16}\text{O}$  ratios cannot be measured with sufficient precision to provide meaningful results). What we call the ‘solar value’ of  $^{18}\text{O}/^{16}\text{O}$  is shown as the horizontal line in Figure 9.14 (in fact this is the isotopic composition of seawater on Earth, of which more below).

It transpires that those meteorites we describe as cosmic sediments contain, in addition to materials formed within the solar nebula, small isolated grains of unmelted materials which pre-date the Solar System. These  $\mu\text{m}$ -sized pre-solar grains are remnants of dust from the protostellar disc; their extraction from meteorites, and their ultimate explanation, was one of the major triumphs of meteorite research towards the end of the 20th century. Detailed study of individual grains, which is entirely possible with appropriate laboratory equipment, allows us to investigate nucleosynthetic products from a range of astronomical objects.

$1\ \mu\text{m} = 10^{-6}\ \text{m}$ .

**Figure 9.14** Plot of  $^{18}\text{O}/^{16}\text{O} \times 10^{-3}$  versus radial distance (i.e. outwards from the centre) for stars in our Galaxy. Note that the distance scale is given in kpc, or kiloparsec (where  $1\ \text{kpc} = 3.084 \times 10^{19}\ \text{m}$ , or 3260 light-years). On this scale the Solar System would plot at 8.5 kpc. You may be able to detect a trend of gradually decreasing  $^{18}\text{O}/^{16}\text{O}$  with radial distance – this actually represents a Galactic evolutionary phenomenon (which we will not study further here). The figure also includes a scale for oxygen isotope measurements as  $\delta^{18}\text{O}$ , which is described in the text.



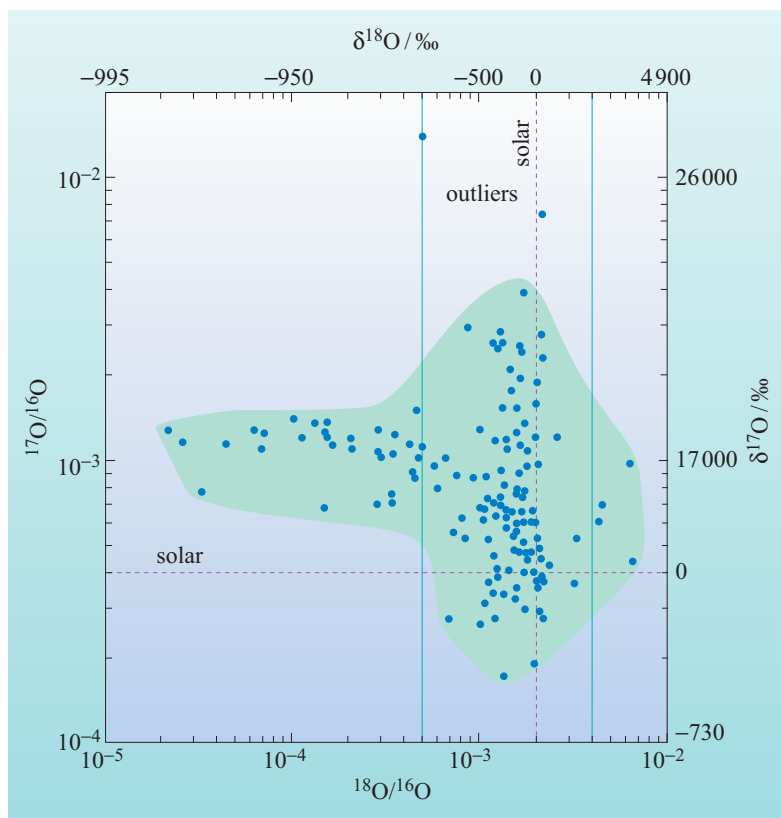


**Figure 9.15** Plot of  $^{17}\text{O}/^{16}\text{O}$  versus  $^{18}\text{O}/^{16}\text{O}$  for pre-solar  $\text{Al}_2\text{O}_3$  grains extracted from meteorites. The figure includes scales for oxygen isotope measurements as  $\delta^{17}\text{O}$  and  $\delta^{18}\text{O}$ , which are described in the text. The majority of the data for the grains plot within the shaded field. The two outliers probably represent some unusual example of stellar processing. The two solid vertical lines constrain the range of  $^{18}\text{O}/^{16}\text{O}$  values shown in Figure 9.14. While most data for the grains are included within these lines there are clearly points outside this range. Again this represents an interesting aspect of the workings of stars, a phenomenon which can now be studied in great detail by making measurements in the laboratory. The vertical dashed line represents the solar value for  $^{18}\text{O}/^{16}\text{O}$ ; similarly the horizontal equivalent is for  $^{17}\text{O}/^{16}\text{O}$ . Their intersection represents where the Solar System would plot.

Figure 9.15 shows the  $^{17}\text{O}/^{16}\text{O}$  and  $^{18}\text{O}/^{16}\text{O}$  ratios measured from individual grains of meteoritic corundum,  $\text{Al}_2\text{O}_3$  (we should stress here that these isolated grains of  $\text{Al}_2\text{O}_3$  are relatively rare and have nothing to do with the bulk of the aluminium and oxygen which is found in CAIs). There are a couple of things to note here. Firstly, the laboratory measurements are much better than those made by observations of stars (Figure 9.14) and, of course, we have measurements of  $^{17}\text{O}$  as well. In order to compare the meteorite data with those from stellar measurements, the two vertical solid lines in Figure 9.15 represent the limits of  $^{18}\text{O}/^{16}\text{O}$  represented by the boundaries of the plot in Figure 9.14. The two points shown as outliers in Figure 9.15 have error bars within the individual points – compare those with the data in Figure 9.14. Secondly, the range of  $^{18}\text{O}/^{16}\text{O}$  values recorded from the pre-solar grains is much larger than those measurements of stars – it is information like this that is allowing astrophysicists to refine their models of nucleosynthesis.

For meteorite samples (or indeed, terrestrial rocks) plotting oxygen isotope ratios as shown in Figures 9.14 and 9.15 is not practical because the variations in oxygen isotope composition are relatively minor – tremendous significance may be placed on deviations of less than 1%. In order to describe these small variations it is convenient to express the *differences* in isotope compositions, rather than the absolute ratios. This is done by relating the sample ratio to a reference point. In the case of oxygen, the water which makes up the Earth's oceans is usually used as a reference since this is essentially homogeneous with respect to isotope composition, having  $^{18}\text{O}/^{16}\text{O}$  of 0.002 0052 (which is approximately equivalent to 1/499, i.e. a  $^{16}\text{O}/^{18}\text{O} = 499$ ) and  $^{17}\text{O}/^{16}\text{O}$  of 0.000 372 (1/2690, i.e.  $^{16}\text{O}/^{17}\text{O} = 2690$ ). On the other hand, the oxygen that makes up the rocks of the Earth's crust has a somewhat variable isotope composition (dependent upon many factors, including formation conditions,

temperature, etc.). A typical basaltic rock may have  $^{16}\text{O}/^{18}\text{O} = 496$  and  $^{16}\text{O}/^{17}\text{O} = 2682$ . Be sure that you take note of whether we are using, for instance,  $^{16}\text{O}/^{18}\text{O}$  or  $^{18}\text{O}/^{16}\text{O}$  ratios. Astronomers tend to quote isotope ratios as high/low abundance (e.g.  $^{16}\text{O}/^{18}\text{O}$ ), whereas stable isotope chemists would use  $^{18}\text{O}/^{16}\text{O}$  (there are good reasons for this but we do not have space to go into them here). The net result is that one has to become accustomed to switching between the systems. Colloquially, at least, most people prefer to talk in terms of ratios like  $^{16}\text{O}/^{18}\text{O}$ , but as you will see below, data manipulation relies on  $^{18}\text{O}/^{16}\text{O}$ . That's life!

The difference between the oxygen isotope composition of ocean water and rocks is relatively small but easily and reproducibly measurable using an instrument known as a mass spectrometer.

It is a convention to relate the stable isotope composition of an unknown sample to that of a reference material. Thus if  $R_s$  is the isotope ratio of the sample and  $R_r$  is the corresponding ratio in the reference, the difference is  $R_s - R_r$ , which when expressed as a fraction of  $R_r$ , becomes

$$\frac{R_s - R_r}{R_r} = \frac{R_s}{R_r} - 1$$

In this formula, we use the ratio of the rare to the abundant isotopes since, in effect, we are interested in variations of the rare isotopes. Because these differences are very small, they are usually quoted in parts per thousand (known as parts per mil), abbreviated to ‰.

Comparing this with parts per hundred, that is per cent (%), you can see that  
1% = 10‰.

The calculated result,  $\delta$  (delta, in ‰), is called the *differential isotope composition*, or more commonly ‘the  $\delta$  value’. Thus

$$\delta(\text{in } \text{‰}) = \left( \frac{R_s}{R_r} - 1 \right) \times 1000 \quad (9.1)$$

Since oxygen has three stable isotopes there are two different delta values,  $\delta^{18}\text{O}$  and  $\delta^{17}\text{O}$ , defined relative to the abundant isotope,  $^{16}\text{O}$ . Thus, for a  $\delta^{18}\text{O}$  value,  $R_s$  and  $R_r$  refer to  $^{18}\text{O}/^{16}\text{O}$  ratios. Similarly, for a  $\delta^{17}\text{O}$  value,  $R_s$  and  $R_r$  refer to  $^{17}\text{O}/^{16}\text{O}$  ratios. For the basaltic rock referred to above, inserting values into Equation 9.1 we get

$$\delta^{18}\text{O} = \left( \frac{1/496}{1/499} - 1 \right) \times 1000 \approx 6\text{‰}$$

Since  $\delta$  values can be either positive or negative numbers, we explicitly give each of them a sign, thus, in the above example,  $\delta^{18}\text{O} = +6\text{‰}$ , rather than just 6‰. It can be shown that for this basaltic rock,  $\delta^{17}\text{O}$  is  $H \approx +3\text{‰}$ , equivalent to about one-half of the value of  $\delta^{18}\text{O}$ . The factor of about 0.5 difference between  $\delta^{17}\text{O}$  and  $\delta^{18}\text{O}$  holds true for almost all oxygen-containing materials on Earth. This relationship, which can be related to the difference in mass between the isotopes, is a consequence of the process known as *isotope fractionation*, which occurs when isotopes become separated from each other, or fractionated. (Isotope fractionation can happen during chemical reactions, or during physical processes such as the movement of a gas or liquid through a porous medium.)



## QUESTION 9.6

What are the  $\delta^{17}\text{O}$  and  $\delta^{18}\text{O}$  of ocean water? What are the  $\delta^{17}\text{O}$  and  $\delta^{18}\text{O}$  of pure  $^{16}\text{O}$ ?

On a plot of  $\delta^{17}\text{O}$  and  $\delta^{18}\text{O}$ , the oxygen isotope composition of samples from the Earth lie on the line called the **terrestrial fractionation line (TFL)** which has a slope of about 0.5 and passes through the point (0, 0) where ocean water would plot.

No matter what oxygen isotope composition an individual body (planetary or otherwise) has initially, *secondary* processes that result in isotope fractionation produce data that fall on lines of slope 0.5. When this is observed it is a good indicator that materials are related in some way. Two lines of slope 0.5 that are *not* coincident, imply different *initial* oxygen isotope compositions.

- What do you think would be the slope of an oxygen isotope fractionation line for Mars (i.e. an MFL)?
- The MFL value would be 0.5. Indeed, this has been measured for different constituents of Martian meteorites. For information note that the MFL is offset from the TFL, showing that the two planets formed from materials that were slightly different in terms of their oxygen isotopic composition (which means that even though a particular rock from Mars might look identical to one from Earth, it can be distinguished on the basis of its oxygen isotopic composition).

A plot of  $\delta^{17}\text{O}$  and  $\delta^{18}\text{O}$  for whole-rock meteorites is shown in Figure 9.16. Compare the scales of this plot with those of Figure 9.15; while astronomical entities display astronomical variations in oxygen isotopic compositions, those of materials formed within the solar nebula are much less variable (although the small differences which can be measured are of immense importance). Note the line of slope 0.5 representing the TFL.

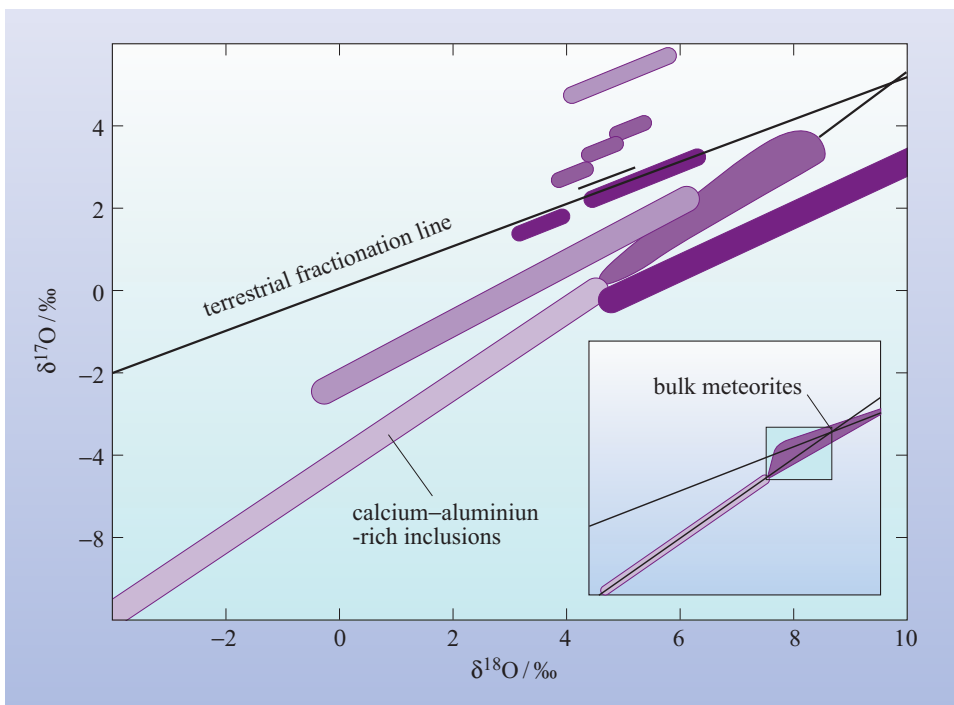
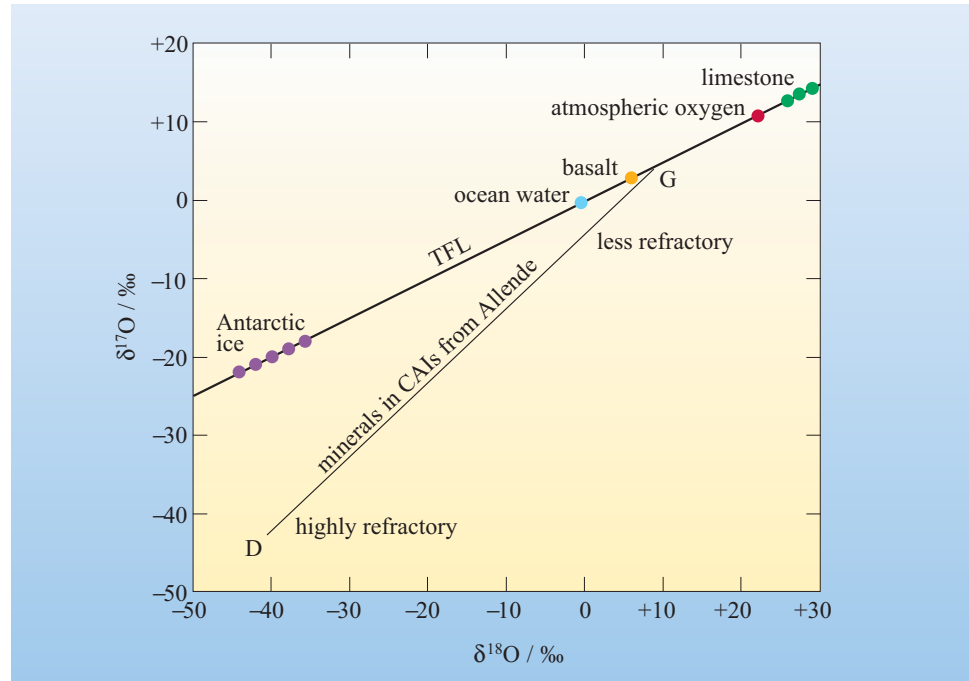


**Figure 9.16** Plot of  $\delta^{17}\text{O}$  and  $\delta^{18}\text{O}$  for whole-rock meteorite samples. Each different coloured field represents a different type of meteorite group (included on the plot are fields for different groups of carbonaceous chondrites, different types of ordinary chondrites, Martian meteorites, HEDs, and so on). The inset shows the range in oxygen isotopic composition of all bulk meteorite samples and covers a range in  $\delta^{18}\text{O}$  values from  $-40$  to  $+20\text{‰}$  and in  $\delta^{17}\text{O}$  values from  $-40$  to  $+30\text{‰}$ . The region of the main graph is shown by the shaded box in the inset.

**Figure 9.17** Plot of oxygen isotope compositions ( $\delta^{17}\text{O}$  versus  $\delta^{18}\text{O}$ ) of different minerals from refractory inclusions in Allende. The Allende data fall on a line (DG) with a slope of about 1. For reference, a line of slope about 0.5 and labelled TFL is also shown. Almost any sample from the Earth will have an oxygen isotope composition that falls somewhere on this TFL line (a few examples are shown).



Returning to the CAIs, if the inclusions represent samples of pre-solar dust, we may expect them to have a variety of different oxygen isotope compositions, like the isolated  $\text{Al}_2\text{O}_3$  grains which we encountered in Figure 9.15. This is because the oxygen isotopes would have been synthesized in various ways, with materials from different stars having different isotopic characteristics. In contrast, if CAIs were formed during condensation in the solar nebula we might expect a fairly straightforward relationship between the oxygen isotope compositions of the different inclusions. This is because a hot, turbulent nebula environment will act to homogenize the isotope compositions of pre-solar gas and dust.

A plot of  $\delta^{17}\text{O}$  versus  $\delta^{18}\text{O}$  for data from the Allende CAIs is shown in Figure 9.17. In contrast to samples from the Earth, the oxygen isotope composition of different minerals from CAIs define a line labelled DG which has a slope of about 1. That the data fall on a line, rather than at random across the plot, tends to suggest that the minerals were all formed in a common event. As it happens, refractory minerals, like spinel (Table 2.4), fall close to the lower end of the line (D), while less refractory minerals plot close to G.

- Remember that refractory minerals condense early in the condensation sequence. How can we explain the oxygen isotope data for the different minerals in CAIs?
- The oxygen isotope composition for spinel must have differed from that of less refractory minerals, in the reservoir from which the minerals condensed.

The data have been explained in terms of a dust reservoir (D) and gas (G). The solar nebula started as a mixture of gas and very fine dust. It is proposed that of the minerals that we find in the CAIs, the first to form, were somehow derived from the dust and reflect its initial oxygen isotope composition. This involved reprocessing of dust material, and so it is appropriate to refer to a dust *reservoir* rather than dust

particles. As mineral formation proceeded, the isotope composition of the dust reservoir became modified by a process known as **isotope exchange** with the gas reservoir. The gas reservoir was much the larger, and so this exchange led to the dust reservoir becoming more like the gas reservoir. In consequence, the less refractory minerals that formed later, and now constitute part of the CAIs, lie closer to point G.

#### QUESTION 9.7

Consider for a moment that the dust and gas reservoirs in the solar nebula *both* had oxygen isotope compositions at G in Figure 9.17. Where would the isotope compositions plot if we mixed small quantities of pure  $^{16}\text{O}$  into the system? (Remember the  $\delta$  values of pure  $^{16}\text{O}$  from Question 9.6 and consider where this would fall on a plot like Figure 9.17.)

There are two important conclusions from the study of Allende CAIs. Firstly, not all of the oxygen in the solar nebula had the same initial isotope composition. This means that the solar nebula was not completely homogenized before condensation began (if this had happened the dust and gas reservoirs would be related to each other along a line of slope 0.5 in Figure 9.17, in the same way that different components from the Earth are related). Thus, meteorites contain some relicts of the pre-solar gas and dust which coalesced to form the solar nebula. Secondly, the oxygen isotope compositions of minerals in CAIs show a relatively simple pattern, i.e. evidence for only two major components with isotope exchange between them. This simple pattern was almost certainly established within the solar nebula, rather than before the solar nebula formed.

If we were to plot oxygen isotope data for the chondrules in Allende in Figure 9.17, we would find that they fall on a different line from that shown by CAIs. Although one end of the line would be coincident with D, the other would be slightly displaced from G. Thus it would seem that in between the formation of CAIs and chondrules, the oxygen isotope composition of the solar nebula had changed.

#### QUESTION 9.8

What are the consequences for planetary bodies in general for a variation with time in the oxygen isotope composition of the solar nebula?

#### QUESTION 9.9

Different sorts of matrix materials from Murchison have oxygen isotope compositions which, on a plot of  $\delta^{17}\text{O}$  versus  $\delta^{18}\text{O}$ , fall on a line with a slope of about 0.5. This line is parallel to, although displaced from, the TFL. How can the results be interpreted?

### 9.2.3 Riding the x-wind

It seems appropriate here to delve back into the details of solar nebular dynamics to show how data from meteorites and other samples are helping to constrain models of Solar System formation (Box 9.4). The idea we describe here, known colloquially as the ‘x-wind model’, is very much a crossover from astrophysics to the planetary sciences. Here a generalized theory of the formation of low-mass stars has been extended to incorporate mechanisms that would allow production of the two main

high-temperature features of chondritic meteorites, namely chondrules and CAIs. The formation model starts off with a relatively dense protostar forming at the core of a molecular cloud following the loss of the supporting magnetic field. Rotation involved with the cloud collapse produces, not only a disc around the central protostar, but also a strong stellar wind operating outwards from the polar regions of the star.

■ What is this phenomenon called?

□ A bipolar outflow (Chapter 8).

Dust and gas accrete onto the central star via the disc, although at the same time the outflow begins to push away the outer envelope of the cloud. Eventually the outflow blows away the surrounding gas and dust entirely and the young stellar object and associated disc becomes visible (and hence observable by telescopes).

■ What name do we give to these kinds of objects?

□ T Tauri stars (Chapter 8).

It is known that protostars emit more x-rays than young Sun-like stars in more advanced stages of their formation. This is taken as evidence for enhanced magnetic activity on the surfaces of protostars. It is the detailed evaluation of the magnetic fields around the protostar, and how these affect the flow of gas and dust, that results in the identification of the so-called x-wind. In Figure 9.18 we show an overall schematic of the magnetic field lines associated with a typical Sun-like protostar. The x-region is effectively the boundary of the inner edge of the accretion disc (a distance of perhaps 0.075 AU or so, i.e. close to the protostar's surface, but

#### BOX 9.4 THE GENESIS MISSION

The origin of the oxygen isotopic variations in solar system materials has been a major puzzle for planetary scientists for nearly 30 years. To help solve it, the Genesis spacecraft was launched in August, 2001. The spacecraft contains a number of instruments to monitor the stream of atoms ejected from the Sun into space, i.e. the solar wind. Several different collectors can also be exposed, allowing collection of samples of the solar wind for return to Earth. The abundance of approximately 70 different elements in the periodic table are scheduled for measurement in this way, with the isotopic composition determined for almost 20 of these elements, including the isotopes of oxygen. By returning the samples to the laboratory, high precision measurements can be made at a level unattainable remotely.

It is hoped that a more accurate determination of the oxygen isotopic composition of the Sun, and hence the solar nebula, will provide a test for different theories for the origin of the oxygen isotopic variations among CAIs, chondrules, asteroids and planets. The samples will be returned via a re-entry capsule, which separates from the main portion of the spacecraft and returns to Earth in September 2004.

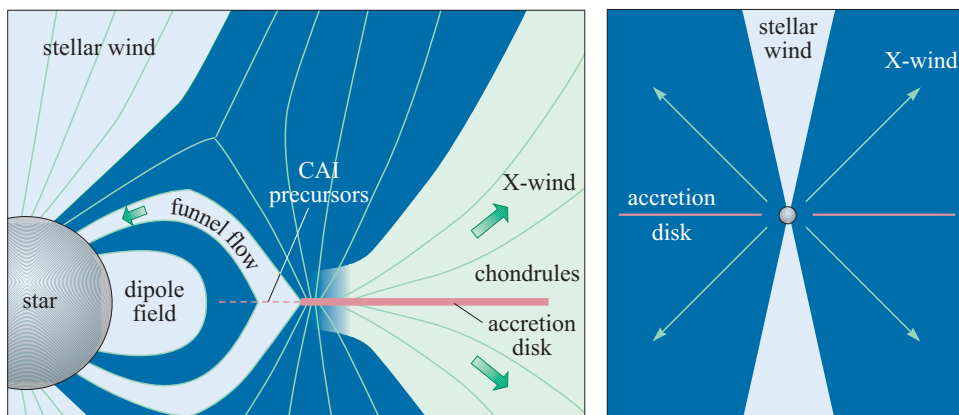


**Figure 9.18** Schematic diagram of the magnetic field lines near to a Sun-like protostar. The accretion disc extends inwards to a point which is close to, but not touching, the surface of the protostar. This inner edge of the accretion disc marks the position of the x-region. Dust spiralling towards the protostar, from within the disc, is either accreted onto it (via funnel flow) or blown upwards and outwards (via the x-wind).

not touching it). Materials heading towards the central regions of the solar nebula, i.e. spiralling inwards within the accretion disc, arrive at the x-region and either get channelled towards the protostar (along a trajectory labelled as the ‘funnel flow’ in Figure 9.18), or blown back out of the system by the x-wind. About two-thirds of the material accretes onto the star, the rest is carried off by the x-wind.

Dust grains arriving near the x-region can become heated and melted by the radiation streaming off the protostar, ultimately forming CAIs and chondrules. These are then either accreted onto the star or sent back out of the system by the x-wind. In this way CAIs and chondrules become dispersed across the entire solar system. It is these materials which ultimately aggregate to form planetesimals and planets.

There are some interesting testable aspects to this hypothesis. Firstly, by direct study of CAIs and chondrules it should be possible to infer some of the characteristics of the x-wind all of which have long since disappeared. Secondly, since CAIs and chondrules are essentially the fundamental building blocks of Solar System objects, they should be present, for instance, in comets. Note also that if the x-wind model is a truly generic process then chondrules and CAIs will be a universal feature of solar systems. In other words, we should not be surprised to see chondrite-like debris if we ever get to visit another solar system. Additionally, we have to keep an open mind when considering the characteristics of interstellar dust. Clearly some of the materials which originally coalesced to form our own solar nebula may have included chondrule-like objects from previous generations of solar systems.

### 9.2.4 Low-temperature materials

In addition to chondrules and CAIs, Allende and Murchison also contain a dark, fine-grained **matrix** – effectively, everything else. The matrix is dark in colour, partly because it is fine-grained, but also because it contains carbonaceous materials. In Allende the matrix is predominantly an assemblage of mineral components such as olivine and sulfides (e.g. troilite, FeS). These minerals formed as a logical progression in the condensation sequence (see Table 2.4). The fine-grained nature of the constituent grains may be due to fragmentation processes occurring in the solar nebula. In contrast to Allende, the matrix of Murchison contains a large proportion of hydrated minerals. You can see from the condensation sequence that in a cooling gas of solar composition, hydrated minerals condense directly in the nebula at temperatures of 330 to 550 K.

- What can you deduce from the presence of hydrated minerals in the matrix of Murchison (and their absence in Allende)?
- The temperature of the nebula was in the region of 330 to 550 K when the matrix of Murchison was formed. That of Allende, on the other hand, must have formed at temperatures in excess of 550 K.

Not all of the features displayed by the matrix of Murchison can be explained by processes which took place during the condensation sequence. For instance, water-soluble substances, such as carbonates and sulfates, are found deposited as veins running through the fabric of the meteorite. It seems that Murchison, like CI meteorites, has been affected by the action of fluids some time after it formed. Unlike the CI meteorites, however, the alteration in Murchison is not that extensive – the primary constituents such as chondrules and CAIs are still recognizable. On the basis of geochemical evidence it can be deduced that the hydrothermal alteration took place at about 300 K.

Amorphous means having no definite shape or form. Thus, amorphous carbon is an occurrence of the element in no obvious crystallographic form – here it implies something that is intermediate between graphite (an obvious crystal form) and a complex of macromolecular organic compounds. Soot and lamp black are good examples of amorphous carbon found on Earth.

Turning now to the carbonaceous materials, the matrix of Allende contains about 0.25% by mass of carbon, mainly in an amorphous form. Murchison, on the other hand, contains about an order of magnitude more carbon (i.e. about ten times more), not in amorphous form but as *organic compounds*, i.e. materials made up from the elements carbon and hydrogen, with the possible involvement of nitrogen, oxygen, sulfur, etc. Most of the organic material in Murchison exists as a complex macromolecular substance, meaning a component comprising many hundreds of atoms which has no clearly defined structure. This is analogous in many ways to the material that on Earth occurs in some sedimentary rocks and is responsible for generating oil. Of the organic compounds that are not part of macromolecular structures, many different constituents are present. Some examples of compounds in meteorites are shown in Figure 9.19. Benzene is a hydrocarbon, notorious because of its carcinogenic properties. Adenine and alanine are, respectively, examples of a purine and an amino acid. On Earth, purines are found in nucleic acids and amino acids are found in proteins. That is not to say that there are nucleic acids or proteins in meteorites! What is present in Murchison are the building blocks of these materials. These same building blocks were presumably brought to the surface of the Earth early in the history of the Solar System, and *may* have triggered the development of life.

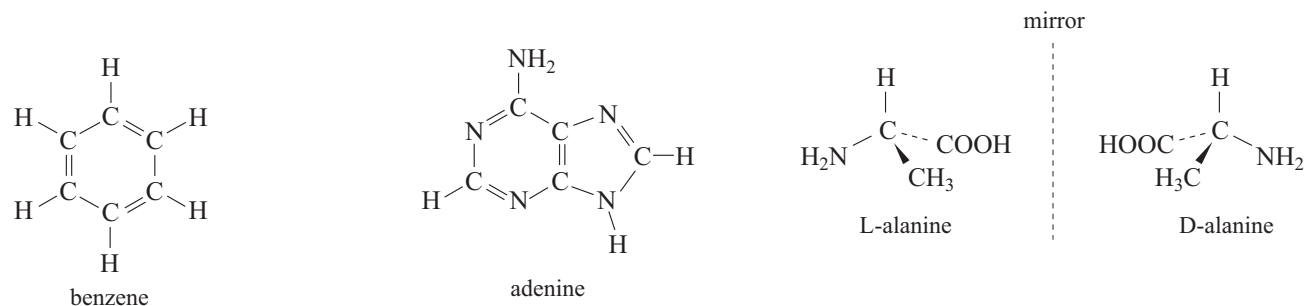


**Figure 9.19** Three examples of organic compounds from Murchison. Benzene is a hydrocarbon (a compound made only of hydrogen and carbon). Adenine is a purine, a more complicated molecule than benzene, which includes nitrogen in its structure. Alanine is an amino acid; it can exist in two different structural forms, L and D, which are mirror images of each other. (The dashed lines denote bonds directed behind the plane of the paper, and the wedges are bonds coming up out of the plane of the paper.)



Given that organic compounds abound in the Solar System beyond the Earth (not only in primitive meteorites but also in comets, and probably within some of the satellites of the giant planets), mechanisms which might lead to the large-scale production of them in the solar nebula are of great interest. It transpires that there are many different ways in which organic materials can be formed. It is not possible to describe all of these here; we will consider just one possibility. If we continue with the notion of a condensation sequence, then at temperatures below 400 K, gases such as CO (carbon monoxide) and H<sub>2</sub> undergo reactions on the surfaces of earlier-formed mineral grains to form organic compounds. This mechanism, along with others proposed, produces organic materials abiotically, i.e. life-forms are *not* involved. Can we be absolutely certain of this? Let us consider the case of amino acids, since these are so closely linked with life. There are many different amino acids; and some of the ones found in Murchison do not form biologically on Earth. At very least, we can be sure that these are not simply terrestrial contaminants introduced to Murchison by micro-organisms.

- Based on your experience with the study of refractory inclusions, how could we discern whether all the organic compounds in Murchison had a common origin?
- One possibility would be to determine the isotope compositions of the constituent elements (carbon, hydrogen and nitrogen) to see if these show any obvious relationships.

The carbon and nitrogen isotope compositions of organic compounds in Murchison are generally fairly uniform, being similar to values found in organic compounds on Earth. This similarity in isotope compositions is taken by some to imply that the majority of organic compounds found in Murchison formed within the solar nebula. However, the hydrogen in some of the organics in Murchison is found to be highly enriched in the isotope deuterium (D, or <sup>2</sup>H). It has been calculated that the magnitude of the observed enrichment cannot be attained in the solar nebula, even under the most extreme conditions imaginable. On the other hand, large deuterium enrichments have been detected in the interstellar medium, using infrared astronomy. The enrichments are found in organic molecules present in dense clouds and are the result of reactions between molecules and ions. It seems, therefore, that some of the organic compounds in Murchison were produced in the interstellar medium. These have survived the processes of heating and mixing in the solar nebula to end up in the organic material found in carbonaceous chondrites.

#### QUESTION 9.10

If the majority of organic compounds in Murchison were formed in the solar nebula, as a consequence of condensation, how can we interpret the survival of interstellar organic molecules in this meteorite?

#### QUESTION 9.11

Allende contains carbon mainly in an amorphous form but also as diamonds. How might we try and assess if these elemental forms of carbon are related?

### 9.2.5 Asteroidal melting processes

Juvinas is an achondrite which, as you should remember, means that it is a stony meteorite containing no chondrules. In detail it is one of the HED meteorites which made an appearance in Figure 9.13. It is thought to have been formed near to the surface of its parent body by an igneous process, i.e. a high-temperature melting event which involved the creation of a magma, of which Juvinas is a fragment. The Cape York meteorite is also the product of melting, although its parent body was different from that of Juvinas. Cape York is an iron meteorite and represents part of an asteroid's core.

Because of melting, Juvinas and Cape York no longer retain their primary chemical and physical characteristics. They are referred to as differentiated meteorites.

#### ■ What is differentiation?

- It is the process by which a hot, possibly molten, planetary body segregates into compositionally distinct layers of different density (Chapter 2).

Consideration of iron will help to explain differentiation. When the parent bodies of meteorites were first formed they probably all had a chondritic composition. We know that in primitive chondrites, iron constitutes 20 to 25% by mass and is present in silicates and sulfides, and as the metal itself. However, in Juvinas, iron is present at about 14% by mass, and is almost entirely in silicate minerals – so clearly there is a deficiency of iron in this meteorite. The depletion can be explained by the effects of partial melting (Chapter 2), whereby the magma that solidified to form Juvinas became separated from its source region, which was left with a relatively higher proportion of iron. The extent of partial melting was fairly limited in this case – thus, although the source region became enriched in iron it probably did not form into a metallic core. In contrast, Cape York is >90% iron metal, which represents almost the end-point of total melting. In this case the silicates have been completely removed, leaving a residue of iron–nickel metal.

The observation of meteorites with a variety of iron content led early workers to propose that all of these materials came from a single disrupted planet which once occupied an orbit between Mars and Jupiter. The irons were thought to represent the core of this planet and the igneous samples were considered to be derived from its crust or mantle. The chondrites were assumed to represent samples of unmelted material which had survived unaltered at the planet's surface. This single-parent model has long since been untenable as detailed chemical and isotope evidence demands many different parent bodies for meteorites, e.g. recall the plot of  $\delta^{17}\text{O}$  versus  $\delta^{18}\text{O}$  for whole-rock meteorites shown in Figure 9.16. It is now considered that the larger asteroids are planetesimals which were large enough to have undergone a variety of geological-type processes, but (as noted in Chapter 8) were *prevented* from accreting into a single planetary body by the gravitational influence of Jupiter.

Juvinas is one of a group of about 60 related meteorites. The parental material of Juvinas and its associates must have been extruded onto the surface of an asteroid as a thin layer of magma which then cooled relatively quickly. By studying the chemistry and mineralogy of Juvinas we can learn about the magma itself and also about the source region from which it was extracted.

Looking at a specimen of Juvinas shows it to be a basalt, i.e. comprised mostly of the silicate minerals pyroxene and feldspar. From the mineralogical evidence it is possible to conclude that the sample crystallized within the temperature range 1300 to 1500 K. Be sure that you understand this is the magmatic temperature, and not a measure of temperature during condensation from the nebula.

As already stated, the heating and melting episode that produced Juvinas has acted to change the original chondritic composition. But how can we be absolutely sure that the parent body of Juvinas had a chondritic composition to start with? All we have to work with is a sample of solidified magma, and we have already seen that the chemical composition of this has been changed by the melting process. Consider two more ways in which the chemistry has been changed. Firstly, you saw in a previous section that carbonaceous chondrites contain carbon – however, Juvinas contains hardly any carbon. This is because any organic materials that were once present in the parent body have been destroyed by heating and lost as  $\text{H}_2\text{O}$  and  $\text{CO}_2$ . Secondly, refractory elements, such as osmium, rhenium and iridium, are depleted relative to chondrites; like iron, these elements were left behind in the source region during partial melting. Fortunately there is a way to assess the original chemical composition of Juvinas. This is by consideration of the **rare earth elements (REE)**, a group of 15 related elements spanning the Periodic Table from atomic number 57 (lanthanum) to 71 (lutetium).

The REE are not present in any meteorite samples at high enough concentrations to form minerals in their own right. Instead they are found as substitutions for other elements in host minerals. The different mechanisms by which REE become incorporated into minerals tend to produce characteristic abundance patterns. The abundances of REE in Juvinas are shown in Figure 9.20, where it can be seen that

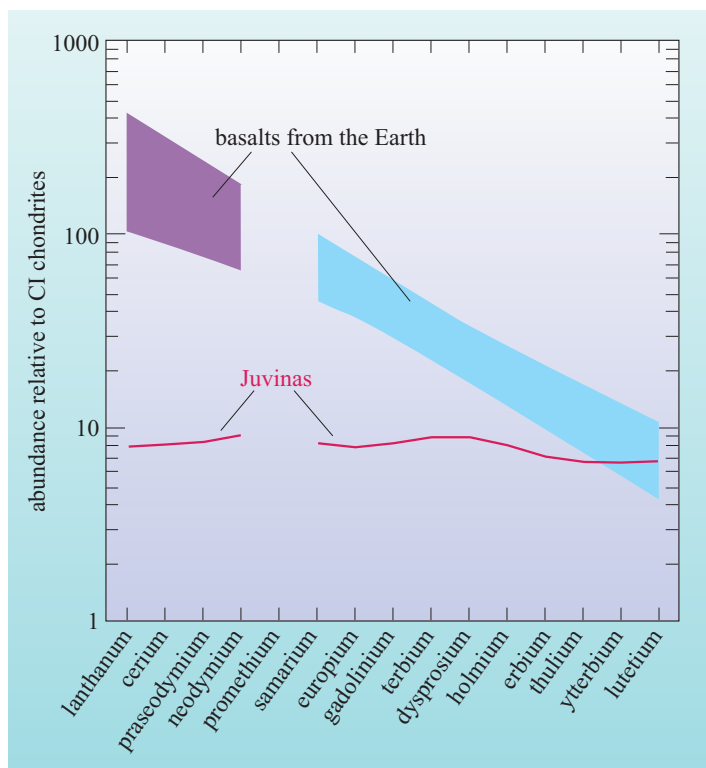


**Figure 9.20** Rare earth element abundances in Juvinas and in basalts from the Earth. The data are related to the abundances present in CI chondrites (which, if plotted, would fall on a horizontal line at a value of 1). Since different rock types show a wide range of REE abundances it is useful to plot the data on a logarithmic scale. Note that there are no data for promethium since this element is entirely radioactive.

when compared to CI chondrites, they are uniformly enriched by a factor of about eight. The reason for the enrichment is that during partial melting the REE have become concentrated in the magma rather than the residual solid. Note that the REE in Juvinas plot on what is roughly a horizontal line. This is known as a chondritic pattern since chondrites also plot on a horizontal line (at a value of 1). In contrast, data from basalts found on Earth plot on a steeply sloping line, which demonstrates that these rocks have formed by a more complex series of processes than the simple melting experienced by meteorites like Juvinas.

Let us now consider how the parent body of Juvinas became heated to temperatures great enough to produce magmas.

■ How might the parent body have been heated?

□ As outlined in Chapter 2, accretion, impacts, core formation, radioactive decay and tidal heating are all possible sources for the thermal energy that causes melting in planetary bodies.

For various reasons, we can discount all but one of these heat-producing mechanisms as causes of melting in asteroids.

- A small body, such as an asteroid, has a large surface-to-volume ratio (compared to a large body) and so thermal energy within the body is rapidly radiated away from its surface. Thus, although kinetic and gravitational energy can be converted to heat during accretion, for small bodies this source is insufficient to cause melting.
- Heating by core formation is discounted since, as you have already seen, a metallic core was probably not formed in the case of the Juvinas parent body.
- Radiogenic heating by long-lived radioactive isotopes, such as  $^{40}\text{K}$ ,  $^{232}\text{Th}$ ,  $^{235}\text{U}$  and  $^{238}\text{U}$ , can produce high temperatures in large planetary bodies, but is again insufficient in small ones.
- Tidal heating may be an important process for the satellites of the giant planets, but not for asteroids.
- Heating through asteroid collisions may be a possibility, but if the process is too violent the bodies will be totally disrupted instead.

So, how *did* asteroids melt? There are two possibilities. The first involves heat production by electromagnetic induction, which you have not met before in this Course. This could arise as the bodies moved through a dense solar wind-like plasma, as might have been produced by the young Sun (during its T Tauri phase). However, there is still some debate about the details of this period of evolution and so it is impossible to assess the significance of this mechanism. A second plausible way of producing heat in asteroids is by short-lived isotopes, such as  $^{26}\text{Al}$ . Since the half-life of  $^{26}\text{Al}$  is only  $7.2 \times 10^5$  years, the heat potential from this source is confined to the very early stages of Solar System development. The  $^{26}\text{Al}/^{27}\text{Al}$  ratio in the interstellar medium is about  $10^{-5}$  (recall that  $^{27}\text{Al}$  is the only stable isotope of aluminium). If aluminium with this isotope composition was present in chondritic materials, the heat energy released by the radioactive decay of  $^{26}\text{Al}$  would be sufficient to melt an asteroid of a few kilometres diameter.

## QUESTION 9.12

(a)  $^{26}\text{Al}$  decays by positron emission to give stable  $^{26}\text{Mg}$ . How could you tell whether a mineral component from a meteorite had once contained  $^{26}\text{Al}$ ? (b) In what sorts of minerals would the occurrence of previous  $^{26}\text{Al}$  radioactivity be most easily recognized?

Unfortunately, as far as Juvinas is concerned, it is impossible to discern absolutely whether  $^{26}\text{Al}$  was responsible for melting. However, we do know that  $^{26}\text{Al}$  was present in the solar nebula since evidence of its decay product  $^{26}\text{Mg}$  has been found in CAIs from meteorites like Allende and Murchison (Section 9.2.2). That the chondritic meteorites did not melt shows that, in those samples at least, the overall concentration of  $^{26}\text{Al}$  was not high enough. Thus, while it is a commonly held belief that  $^{26}\text{Al}$  was a heat source in the early Solar System, the exact influence is still being actively researched.

Notwithstanding the lack of a consensus regarding the heat source for asteroidal melting processes, the timing of this event can be reliably established by using a radiometric dating technique.

■ What are the formation ages of HED meteorites?

□ 4.53 to 4.56 Ga ago.

■ If the ages obtained from the oldest meteorites represent the age of the Solar System, what constraints do radiometric ages of meteorites like HEDs put on formation conditions in the solar nebula?

□ Melting processes on meteoritic parent bodies took place only a short time after the Solar System was formed.

The reflectance spectra properties of meteorites like Juvinas resemble those of the asteroid (4) Vesta, a roughly spherical body of 250 km radius (which makes it one of the largest asteroids). As far as we can tell, the composition of Vesta is uniform across its surface and so, we consider it to be a largely intact body. That is not to say that it necessarily represents an entire, original planetesimal. There is every possibility that Vesta has been subjected to collisional processes that have resulted in fragmentation (we can only speculate about the parent of Vesta itself). However, if Juvinas does come from Vesta then we can constrain the age of any fragmentation events to a period very early in the history of Solar System evolution. And so, it follows that what we see today as Vesta has survived largely intact for at least 4.53 Ga. Of course, in detail, the outer layers will have been eroded to some extent by impacts – one such impact will have removed the fragment which ultimately fell to Earth as the body we now know as Juvinas. But since Vesta is intact, we cannot expect to have samples of its interior. However, we do have several hundred specimens of iron meteorites that are thought to represent the cores of other asteroids. Cape York is one such sample.

Cape York is part of one of the largest meteorite showers from which we have samples. The meteorite fell to Earth over 1000 years ago in Greenland; eight individual specimens have so far been collected, totalling  $5.9 \times 10^4$  kg. In historical times, fragments of the meteorite were used extensively by the Inuit (Eskimos) in the manufacture of tools. When tools were traded between the Inuit and European explorers, it became apparent to the scientific community that there must be an iron meteorite somewhere in Greenland. In 1897 the largest known fragment of the meteorite ( $3.1 \times 10^4$  kg) was found and taken by sea to New York; another large mass ( $2.1 \times 10^4$  kg), which was unknown to the Inuit, was removed in 1965 by a Danish expedition.

Iron meteorites originate from asteroidal bodies – the processes which contributed heat were similar to those that produced meteorites like Juvinas. However, iron meteorites are not the result of partial melting. They represent the end-product of differentiation and segregation of metal. In other words, the parental magmas of iron meteorites were, at some point in their history, completely molten. During this process, high-density metallic elements percolated down towards the centre of their parent bodies while low-density silicates floated outwards. As such, most iron meteorites represent samples of the cores of asteroids. We can be certain that a number of different parent bodies are represented among all the iron meteorites, since the concentrations of trace elements, such as iridium, gallium and germanium, vary in ways which could not be produced in a single body.

#### QUESTION 9.13

List the mechanisms that are likely to have contributed heat to asteroids.

Iron meteorites are alloys of iron and a relatively small proportion of nickel. Cape York, for instance, contains about 7.5% nickel. When a meteorite like Cape York is sawn open, polished and then etched with a mild acid, a characteristic pattern can be observed. This is known as the **Widmanstätten pattern** and while it can be reproduced to a very limited extent in the laboratory it is not a normal feature of terrestrially produced iron. An example of an iron meteorite displaying the Widmanstätten pattern can be seen in Figure 9.10a. The pattern is caused by the segregation, during extremely slow cooling, of nickel-rich and nickel-poor alloys. Cooling rates, calculated from the different scales of pattern that have been found in iron meteorites, vary from 0.5 to 500 K Ma<sup>-1</sup>, and these differences reflect parent bodies of different sizes – larger bodies cooled more slowly. Some iron meteorites, which have related chemical compositions but different cooling rates, are considered to have formed at varying depths within an individual body, i.e. samples closer to the centre cooled more slowly. If this is true, the parent asteroids cannot have had single cores of iron, which has a high thermal conductivity, but must have been composed of individual pods of metal surrounded by silicates. Such parent bodies are said to have a *raisin-bread* structure.

Most iron meteorites are not composed of pure iron–nickel metal. They contain various quantities of phosphorous-containing minerals, sulfide nodules and graphite. Other irons contain inclusions of silicates, which have chemical compositions similar to chondrites.



- Does the presence of silicate inclusions pose any constraint on the formation conditions of iron meteorites?
- The presence of silicate inclusions shows that these samples were never completely molten.

Thus not all iron meteorites were formed by processes that produced total melting. Those with silicate inclusions are considered to be the result of impact melting and mechanical mixing of iron-containing materials with silicate-rich bodies. This happened early in the history of the Solar System when newly-formed bodies were colliding with each other. Thus, not all iron meteorites can be thought of as being the cores of asteroids.

#### QUESTION 9.14

Some of the observable asteroids, classified as M-type, have a metallic composition. What does this tell us about processes within the asteroid belt?

#### QUESTION 9.15

Kodaikanal is an unusual iron meteorite which has a radiometric formation age of 3.8 Ga. This is within the range recorded in the majority of impact-produced rocks from the Moon (3.8 to 4.0 Ga). What can we infer here?

## 9.3 Summary of Chapter 9

- Meteorites may come from asteroids, the Moon or Mars, and small micrometeorites (dust particles) can come from comets.
- Meteorites can be broadly classified into stones, irons and stony–irons. The stones are by far the most common variety.
- Juvinas and Cape York are examples of meteorites which have been subjected to melting processes on asteroidal bodies. We refer to these meteorites and their parent bodies as differentiated.
- Meteorites like Juvinas are comprised of materials which are the result of primary igneous activity, i.e. magmas produced via the partial melting of a chondritic source. They may all come from a single asteroid (Vesta).
- Most iron meteorites are the result of the total melting which produced layering within asteroids. In the case of Cape York, the iron–nickel body formed the core of an asteroid. However, iron meteorites could also arise from asteroids which have a raisin-bread structure, in which there are discrete pods of iron–nickel metal.
- Some iron meteorites were not formed by processes that produced total melting but were instead produced by impact melting and mixing at the surfaces of asteroidal bodies.
- The short-lived radioactive isotope  $^{26}\text{Al}$  may have been responsible for heating and melting asteroids.
- The formation ages of meteorites can be assessed by radiometric dating.
- Allende and Murchison are representatives of a chemically primitive group of meteorites known as carbonaceous chondrites. By chemically primitive we mean having a composition which approximates that of the Sun.
- The carbonaceous chondrites are referred to as cosmic sediments because they represent a collection of materials, formed in different thermal regimes, which settled out from the solar nebula onto the surfaces of parent bodies.
- Refractory inclusions, composed of minerals containing elements such as calcium and aluminium, are present in Allende and Murchison. These materials formed early in the solar nebula.
- The oxygen isotope compositions of refractory inclusions show that the solar nebula was never completely homogenized. In other words, these entities retain a signature of the pre-existing materials which became incorporated into the solar nebula.
- Carbonaceous chondrites also contain materials formed at low temperatures, such as carbonates, sulfates and hydrated minerals. The carbonates and sulfates were formed during secondary aqueous activity on the parent bodies.
- Murchison contains 2.5% by mass of carbon in the form of organic compounds. The exact formation mechanism of these materials is unclear. A small fraction of the organic compounds is demonstrably pre-solar in origin and clearly shows that such material was able to survive the conditions prevailing in the solar nebula. For the rest of the material, which is isotopically similar to organic materials on Earth, there are plausible mechanisms which suggest formation in the solar nebula.

## ANSWERS AND COMMENTS

### QUESTION 6.1

For Enceladus,  $a = 238\,000\text{ km}$  and  $P = 1.370 \times 24 \times 3600\text{ s}$ . Using the equation given

$$M_{\text{Sat}} = 4\pi^2 \frac{a^3}{GP^2}, \text{ we have}$$

$$\begin{aligned} M_{\text{Sat}} &= \frac{4\pi^2 (238\,000 \times 10^3\text{ m})^3}{(6.67 \times 10^{-11}\text{ N m}^2\text{ kg}^{-2})(1.370 \times 24 \times 3600\text{ s})^2} \\ &= \frac{4\pi^2 (1.348 \times 10^{25}\text{ m}^3)}{(6.67 \times 10^{-11}\text{ N m}^2\text{ kg}^{-2})(1.401 \times 10^{10}\text{ s}^2)} \\ &= 5.69 \times 10^{26}\text{ m}^3\text{ N}^{-1}\text{ m}^{-2}\text{ kg}^2\text{ s}^{-2} \end{aligned}$$

Now  $1\text{ N} = 1\text{ kg m s}^{-2}$  (as given in Appendix B, Table B1), so  $1\text{ N}^{-1} = 1\text{ kg}^{-1}\text{ m}^{-1}\text{ s}^2$ .

Therefore

$$\begin{aligned} 1\text{ m}^3\text{ N}^{-1}\text{ m}^{-2}\text{ kg}^2\text{ s}^{-2} &= 1\text{ m}^3 (1\text{ kg}^{-1}\text{ m}^{-1}\text{ s}^2)\text{ m}^{-2}\text{ kg}^2\text{ s}^{-2} \\ &= 1\text{ kg} \end{aligned}$$

So the units of  $M_{\text{Sat}}$  are kg as expected and

$$M_{\text{Sat}} = 5.69 \times 10^{26}\text{ kg}$$

Density is mass per unit volume. The approximate volume was calculated as  $9.0 \times 10^{23}\text{ m}^3$ . Hence the density of Saturn is approximately

$$\frac{5.69 \times 10^{26}\text{ kg}}{9.0 \times 10^{23}\text{ m}^3} = 0.69 \times 10^3\text{ kg m}^{-3}.$$

(This is a very low density. It is lower than the density of water at the surface of the Earth, which is  $1000\text{ kg m}^{-3}$ .)

### QUESTION 6.2

Liquid mercury, Hg, has a very high density, and a substantial layer of Hg (which would be needed to produce the magnetic field) would make the average densities far higher than those observed.

Hg is not a very abundant element and so a substantial layer of it would be ruled out if we assume roughly solar abundances.

(The form of Hg at the temperatures and pressures in the interior of Saturn is not given, but at such high pressures it is likely that Hg will still be a conducting fluid.)

## QUESTION 6.3

(a) For Earth the mean density is  $5.51 \times 10^3 \text{ kg m}^{-3}$  and its mean radius is 6371 km. The formula given yields for the pressure at the centre of the Earth

$$\begin{aligned}
 P_c &\approx \frac{2\pi G}{3} \rho_m^2 R^2 \\
 &= \frac{2\pi \times 6.67 \times 10^{-11} \text{ N m}^2 \text{ kg}^{-2} \times (5.51 \times 10^3 \text{ kg m}^{-3})^2 \times (6.371 \times 10^6 \text{ m})^2}{3} \\
 &= 1.72 \times 10^{11} \text{ Pa} \\
 &= 1.72 \text{ Mbar}
 \end{aligned}$$

The accepted value is 3.3 Mbar.

(b) For Saturn the mean density is  $690 \text{ kg m}^{-3}$  and the mean radius is 58 230 km. The pressure at the centre is calculated as

$$\begin{aligned}
 P_c &\approx \frac{2\pi G}{3} \rho_m^2 R^2 \\
 &= \frac{2\pi \times 6.67 \times 10^{-11} \text{ N m}^2 \text{ kg}^{-2} \times (690 \text{ kg m}^{-3})^2 \times (5.8230 \times 10^7 \text{ m})^2}{3} \\
 &= 2.3 \times 10^{11} \text{ Pa} \\
 &= 2.3 \text{ Mbar}
 \end{aligned}$$

(c) For Jupiter the mean density is  $1330 \text{ kg m}^{-3}$  and the mean radius is 69 910 km. The pressure at the centre is calculated as

$$\begin{aligned}
 P_c &\approx \frac{2\pi G}{3} \rho_m^2 R^2 \\
 &= \frac{2\pi \times 6.67 \times 10^{-11} \text{ N m}^2 \text{ kg}^{-2} \times (1330 \text{ kg m}^{-3})^2 \times (6.9910 \times 10^7 \text{ m})^2}{3} \\
 &= 1.21 \times 10^{12} \text{ Pa} \\
 &= 12.1 \text{ Mbar}
 \end{aligned}$$

(Because we have only considered self-compression and mean density, the values obtained are much lower than the accepted values. However they do show that the pressure at the centre of Jupiter is considerably larger than at the centre of Saturn.)

## QUESTION 6.4

The heat produced by radiogenic decay on Earth is  $4.8 \times 10^{-12} \text{ W kg}^{-1}$ . Four Earth masses is  $5.97 \times 10^{24} \times 4 \text{ kg}$ , so a core of four Earth masses on Jupiter would produce

$$\begin{aligned}
 &(4.8 \times 10^{-12} \text{ W kg}^{-1}) \times (5.97 \times 10^{24} \times 4 \text{ kg}) \\
 &= 1.1 \times 10^{14} \text{ W}.
 \end{aligned}$$

To obtain the flux per unit surface area, we have to divide this by the surface area of Jupiter. As an approximation we take the emitting layer as the 1 bar layer and the planet as spherical.

(In fact, different wavelengths of radiation are emitted from different depths in the atmosphere, but IR radiation all comes from layers close to 1 bar and the distance of these layers from the 1 bar level will be negligible compared with the radius of Jupiter.)

The approximate surface area is  $4\pi R_J^2 = 4\pi \times (6.9910 \times 10^7 \text{ m})^2 = 6.1 \times 10^{16} \text{ m}^2$ .  
The flux is thus

$$\frac{1.1 \times 10^{14} \text{ W}}{6.1 \times 10^{16} \text{ m}^2} = 1.8 \times 10^{-3} \text{ W m}^{-2}$$

This is far too small to account for the observed flux ( $7 \text{ W m}^{-2}$ ).

#### QUESTION 6.5

This could be evidence *against* the theory of the origin of Saturn's heat excess that we have just described, because helium lost from the metallic hydrogen layer by differentiation would have to be replaced by helium from the molecular layer. Helium lost from the molecular layer would in turn be replaced by helium from the atmosphere.

#### QUESTION 6.6

Neon like helium is a noble gas and does not form molecules, so in particular,  $\text{Ne}_2$  does not exist. It cannot therefore be detected through vibrational spectroscopy. Its atomic spectrum would have to be used.

(The atomic spectrum is in a more accessible region than that of helium.)

The solar abundance of neon is much less than that of helium and so we would only expect a small amount to be present in the atmosphere. This would make Ne harder to detect by its atomic spectrum and rules out the indirect methods used for helium. The Galileo probe detected neon using mass spectrometry.

#### QUESTION 6.7

When considering how we could estimate the temperature using an ideal-gas model (Section 6.3.2), we rearranged Equation 6.1 to give

$$T = \frac{Pm}{(1.38 \times 10^{-23})\rho}$$

In this question you were given the number density,  $n = \rho/m$ .

The temperature is thus given by

$$\begin{aligned} T &= \frac{P}{(1.38 \times 10^{-23})n} \\ &= \frac{0.42 \times 10^5}{(1.38 \times 10^{-23}) \times (2.4 \times 10^{25})} \\ &= 127 \text{ K} \end{aligned}$$

**QUESTION 6.8**

For methane to condense out, its partial pressure must exceed that of the saturation vapour pressure curve at the temperature of Jupiter's atmosphere. Although relatively abundant, methane does not have a sufficiently high partial pressure to condense out at the temperatures in the atmospheres of Jupiter and Saturn.

**QUESTION 6.9**

A windless atmosphere would be rotating with the same rotational speed as the core of the planet. At the equator, a piece of atmosphere at the 1 bar level travels the circumference of the equator in 0.412 days. The circumference is given by  $2\pi R$  where  $R$  is the equatorial radius. Hence the windless atmosphere travels  $2 \times \pi \times 71\,490$  km in 0.412 days, which gives a speed of

$$\frac{2 \times \pi \times 71\,490 \text{ km}}{(0.412 \times 24 \times 60 \times 60) \text{ s}} = 12.6 \text{ km s}^{-1}$$

$$= 12\,600 \text{ m s}^{-1}$$

**QUESTION 6.10**

A negative velocity corresponds to a piece of atmosphere rotating more slowly than the centre of the planet. A piece of atmosphere moving in the same direction as material at the centre but at a lower speed will have negative velocity.

(A similar effect occurs if you are sitting in an express train and look at a slower train which you are passing. The slower train appears to be going backwards.)

**QUESTION 6.11**

Jupiter's bow shock will be produced when the field strength of Jupiter's magnetic field is sufficient to resist the interplanetary magnetic field. This is the same mechanism as for the Earth.

**QUESTION 6.12**

Rocky cores are not essential to produce the average density: as long as it can be shown that the proposed interior is sufficiently dense to reproduce the average density of the planet, then there is no conflict with the observed density.

Gravitational field measurements indicate a dense core but this does not have to be rocky. Again there is no conflict with observation.

The magnetic field originates in a liquid layer outside the core. A solid icy core is compatible with this.

The interior heat is not well understood but the evidence on this does not rule out the model described.

**QUESTION 6.13**

The oxygen-containing molecule most likely to be found in the atmosphere of Uranus is water,  $\text{H}_2\text{O}$ , as there is a high abundance of hydrogen present. At the atmospheric temperatures in the accessible region of Uranus, water at the abundance expected would be condensed out as ice. The icy layers, presumably, contain a considerable quantity of liquid water which is prevented from reaching the atmosphere.



**QUESTION 6.14**

Uranus has a substantial atmosphere which would be ionized in the upper reaches to form an ionosphere. Thus in the absence of a magnetic field, the magnetosphere would resemble that of Venus with the ionosphere rather than the magnetic field lines interacting with the IMF. The magnetosphere would be smaller, roughly the size of the planet on the sunward side rather than 18 times the size of the planet, as observed.

**QUESTION 6.15**

The far greater mass of Jupiter means that self-compression is greater, and were Jupiter and Rhea made of the *same* materials, the density of Jupiter would be far greater. Having the same average density is thus evidence *against* the two bodies being made of similar material and *for* them being different.

**QUESTION 6.16**

Nitrogen is a homonuclear diatomic molecule and so could not be observed through its vibrational spectrum. (Furthermore, its electronic spectrum lies in the UV and much UV radiation is absorbed by the Earth's atmosphere, making it difficult to observe the electronic spectrum using ground-based instruments.)

**QUESTION 6.17**

Your list might include the following:

- Jupiter has an internal heat source and also receives energy from the Sun.
- The rate of loss of heat to space is low owing to the low temperatures of the radiating levels in the atmosphere.
- The rate of decline of temperature in the troposphere is close to the adiabatic lapse rate.

**QUESTION 6.18**

The solar wind is deflected around the planet but there are energetic particles within the magnetosphere stemming from Io and other sources. Thus you would be at danger from high-energy particles even if not from the solar wind.

**QUESTION 6.19**

Both Uranus and Neptune are observed to have magnetic fields, and so the prediction that Neptune has a solid core and no magnetic field does not agree with observation. The electrically conducting liquid layer is found to lie not in the core but further out. The observed magnetic field data thus do not rule out the model but do not support it as an explanation of the magnetic fields in these planets.

Neptune's internal heat shows that its core is hot but not necessarily molten rock. There is no observational evidence for a hot molten interior in Uranus, although, from our observations on other planets, it would be almost inconceivable that the temperature did not increase towards the centre.

**QUESTION 6.20**

As on Jupiter and Saturn, the most abundant species is the hydrogen molecule so emissions from H and H<sub>2</sub> would be expected.

**QUESTION 7.1**

The perihelion distance is given by  $q = a(1 - e)$  and so,

$$q = (39.48 \text{ AU}) \times (1 - 0.249) = 29.65 \text{ AU}$$

The aphelion distance is given by  $Q = a(1 + e)$  and so,

$$Q = (39.48 \text{ AU}) \times (1 + 0.249) = 49.31 \text{ AU}$$

**QUESTION 7.2**

As with Question 7.1, for Neptune we obtain

$$q = (30.07 \text{ AU}) \times (1 - 0.009) = 29.80 \text{ AU}$$

The aphelion distance is given by  $Q = a(1 + e)$  and so,

$$Q = (30.07 \text{ AU}) \times (1 + 0.009) = 30.34 \text{ AU}$$

**QUESTION 7.3**

As Pluto's perihelion distance is less than both Neptune's perihelion and aphelion distances, then Pluto must sometimes be closer to the Sun than Neptune. So Pluto is not always the outermost planet – an inconvenience for compilers of general knowledge quizzes!

**QUESTION 7.4**

Rearranging Equation 7.3 gives  $P = \sqrt{ka^3}$  and as  $k = 1 \text{ yr}^2 \text{ AU}^{-3}$ , then we calculate  $\sqrt{0.39^3}$  (which can also be written  $0.39^{3/2} = \sqrt{0.0593} = 0.24$ ). So the orbital period is 0.24 years (about 88 days).

**QUESTION 7.5**

- (a) This satellite will undergo some tidal heating, as the satellite is rotating (like the Earth is rotating while it orbits the Sun), so producing frictional heating due to the movement of the tidal bulge.
- (b) This satellite will not undergo tidal heating, as the circular orbit and the synchronous rotation mean that the tidal bulge does not move (and thus no frictional heating is produced).
- (c) This satellite will undergo some tidal heating. While there is no contribution solely from the rotation of the satellite, as it has synchronous rotation, the eccentric orbit means that the tidal bulge will move slightly back and forth with respect to the direction of the gravitational force (i.e. libration), producing frictional heating.

**QUESTION 7.6**

Jupiter has a semimajor axis of 5.20 AU (from Appendix A, Table A1). Using  $P^2 = ka^3$  (and remembering that  $k = 1 \text{ yr}^2 \text{ AU}^{-3}$  from Section 7.2), Jupiter's orbital period is given by  $5.2^{3/2} = 11.86$  years. An object in the 3 : 1 resonance has an orbital period one-third of this, i.e. 3.95 years. Using  $P^2 = ka^3$  again, we calculate that the value of semimajor axis associated with this period is  $3.95^{2/3}$ , i.e. a semimajor axis of 2.50 AU. An alternative way to calculate this is to note that Kepler's third law equation can be rearranged such that  $k = P^2/a^3$ . This is true for any object orbiting

the Sun, and the value of  $k$  remains constant such that  $P^2/a^3$  for object 1 equals  $P^2/a^3$  for object 2. Thus equating these expressions, we can write

$$\frac{P_1^2}{a_1^3} = \frac{P_2^2}{a_2^3}$$

thus 
$$\left(\frac{P_1}{P_2}\right)^2 = \left(\frac{a_1}{a_2}\right)^3$$

where the subscripts, refer to object 1 (e.g. our asteroid) and object 2 (e.g. Jupiter). For our object in the 3 : 1 resonance, the ratio of periods ( $P_1/P_2$ ) is simply 1/3, and noting that Jupiter's semimajor axis is 5.20 AU we have  $(1/3)^2 = (a_1/5.20)^3$  which by solving gives us a semimajor axis of our asteroid  $a_1 = 2.50$  AU.

#### QUESTION 7.7

For an asteroid that has an eccentricity value that is *not* zero (i.e. basically *all* asteroids!), then its aphelion will lie beyond the distance associated with the given Kirkwood Gap, and its perihelion will lie within the distance associated with that Kirkwood Gap. Thus, twice per orbit, the asteroid will be at a distance from the Sun associated with the Kirkwood Gap. Therefore the gaps are not actually regions of space vacant of asteroids. They are just gaps in a diagram of asteroid semimajor axis.

#### QUESTION 7.8

The craters on Ida are simple bowl shapes, rather than complex craters with central peaks. They are mostly circular with many of the craters (particularly the ones seen at the right-hand side of the image) appearing to have very well defined, and relatively deep bowls, i.e. there is little sign of significant gravitational collapse of the crater walls (as you might expect for a low gravity environment).

#### QUESTION 7.9

An S-type asteroid would have a higher density (perhaps  $2500 \text{ kg m}^{-3}$ ) than a C-type (perhaps  $1300 \text{ kg m}^{-3}$ ) and so, if the 1 km diameter asteroid were an S-type, it would be considerably more massive than if it were a C-type. Thus the S-type would have a greater impact energy, and hence give rise to a somewhat larger impact crater.

#### QUESTION 7.10

To impact, or have close approaches with, a giant planet, a Kuiper Belt object must have a perihelion distance generally smaller than the semimajor axis of the giant planet. Thus some of the Scattered Disc objects may impact a giant planet (particularly Uranus and Neptune), as Scattered Disc objects can have large eccentricities and relatively small perihelion distances.

#### QUESTION 7.11

Most comets are thought to actively eject material from only a fairly small area of their surface at any one time (the rest being covered with insulating dust). If however a nucleus were to split apart, then presumably this would expose faces of new 'active' ices, which would then sublimate, producing an outburst of cometary activity.

**QUESTION 7.12**

The presence of Jupiter, which has the largest gravitational influence of all the planets, can essentially provide some ‘shielding’ from comets coming from the outer Solar System. Many comets that might otherwise have been destined for the inner Solar System, can suffer impacts with Jupiter or be scattered back to the outer Solar System due to a close approach with Jupiter. (Indeed all the giant planets offer some shielding, but Jupiter’s effect is greatest.)

**QUESTION 7.13**

The effect of seeing more meteors after local midnight is a bit like the reason you get more rain drops hitting the front windscreen of a moving car. The Earth gets more meteoroid impacts on its leading side. As the Earth is spinning, a local observer rotates into the leading side after local midnight (and remains on this leading side for 12 hours). Most sporadic meteors are in fact usually seen just before dawn.

**QUESTION 7.14**

The impact energy is equal to the kinetic energy, which is  $\frac{1}{2}mv^2$ .

For the car,  $m = 1000$  kg, and  $v = 20$  m s<sup>-1</sup>. So

$$\text{kinetic energy} = 0.5 \times (1000 \text{ kg}) \times (20 \text{ m s}^{-1})^2 = 2 \times 10^5 \text{ J.}$$

For the meteoroid,  $m = 1$  g =  $10^{-3}$  kg, and  $v = 20$  km s<sup>-1</sup> =  $2 \times 10^4$  m s<sup>-1</sup>. So

$$\text{kinetic energy} = 0.5 \times (10^{-3} \text{ kg}) \times (2 \times 10^4 \text{ m s}^{-1})^2 = 2 \times 10^5 \text{ J.}$$

So the impact energy of the 1 g meteoroid (which would be about 1 cm in diameter) is the same as that of the car travelling at 50 mph!

**QUESTION 8.1**

From the Solar System data given in Appendix A you can see that the orbits of Uranus and Neptune lie at 19.2 AU and 30.1 AU respectively. Since the inner edge of the  $\beta$  Pictoris disc is at about 20 AU, any planetary formation in this system could result in bodies that are an equivalent distance from the central star as some of those in our own Solar System. The outer limit of the  $\beta$  Pictoris disc (at a radius of 750 AU) lies at a much greater distance than that of Pluto (39.5 AU), or the anticipated spread of orbits of Kuiper Belt objects (20 to 50 AU), but far less than that of the Oort cloud ( $10^4$  AU and more) where most of the Solar System cometary bodies reside.

**QUESTION 8.2**

- (a) As described by Kepler’s third law (Equation 7.3), a particle in an inner orbit would have a shorter orbital period than one in an outer orbit.
- (b) The slow outer part of the disc would tend to slow down the faster inner part, at the same time as the fast inner part would tend to speed up the slower outer part.

**QUESTION 8.3**

The disc shape is the result of conservation of angular momentum, which inhibits collapse in the equatorial plane, but has no effect on matter collapsing from above the poles. In the hot, dense inner part of the disc, collapse is also inhibited by gas pressure. (Collapse may also be inhibited by magnetic forces, which we do not consider in this book.)

**QUESTION 8.4**

Viscous drag within the solar nebula while the protoSun was forming will have led to outward transfer of angular momentum and inward transfer of mass. The material falling into the protoSun would tend to be that whose speed of rotation had been slowed down by viscous drag. The T Tauri solar wind which occurred later (we will consider how much later, in Section 8.2.8) could also have carried away angular momentum.

**QUESTION 8.5**

According to Table 2.4, FeS could not have condensed from the solar nebula unless the temperature had dropped below about 700 K, so this value provides an upper limit on the possible temperature at which the chondrules originated.

**QUESTION 8.6**

The lines on Figure 8.14 are parallel, implying no change in relative composition throughout the solar nebula. The most convenient place for us to read off the proportions of the three components is at the point where the column mass of dust steps up from just rock, to rock plus ice, i.e. at the radius corresponding to Jupiter.

(a) Immediately to the right of the step-up in column mass of dust, the column mass of rock plus ice is about  $60 \text{ kg m}^{-2}$ , whereas the column mass of gas at this point is about  $2.8 \times 10^3 \text{ kg m}^{-2}$ . To two significant figures, this value is also the same as the total column mass of the nebula. The amount of rock plus ice expressed as a fraction of this is given by:

$$\frac{60 \text{ kg m}^{-2}}{2.8 \times 10^3 \text{ kg m}^{-2}} = 0.021$$

(Your reading of Figure 8.14 is likely to differ slightly from ours, because of difficulties in precisely reading values off the scale, but you should have got a reasonably similar result to ours.)

(b) Immediately to the left of the step-up in column mass of dust, the column mass of rock is about  $15 \text{ kg m}^{-2}$ . The column mass of rock plus ice dust at the same distance (immediately to the right of the step-up) is  $60 \text{ kg m}^{-2}$ , so the ratio of rock to ice is given by

$$\begin{aligned} \frac{\text{rock}}{(\text{rock plus ice}) - \text{rock}} &= \frac{15 \text{ kg m}^{-2}}{60 \text{ kg m}^{-2} - 15 \text{ kg m}^{-2}} \\ &= \frac{15}{45} \\ &= \frac{1}{3} \end{aligned}$$

(Your reading of the graph may have been different from ours, but you should have ended up with a fraction with a value of approximately 0.3. Note that this is actually an upper limit because Figure 8.14 shows only the contribution of  $\text{H}_2\text{O}$  to the ice, and does not include other volatiles such as ammonia that add to the amount of ice condensing at greater distances from the Sun. However,  $\text{H}_2\text{O}$  is considerably more abundant than any other ice-forming substance.)

**QUESTION 8.7**

The volume of a spherical planetesimal that has a diameter of 10 km, and thus a radius of 5 km, is:

$$\frac{4}{3} \times \pi \times (5 \times 10^3 \text{ m})^3 = 5.2 \times 10^{11} \text{ m}^3$$

The mass of an object is given by volume  $\times$  density, so the mass of a planetesimal with the specified density is

$$(5.2 \times 10^{11} \text{ m}^3) \times (3 \times 10^3 \text{ kg m}^{-3}) = 1.6 \times 10^{15} \text{ kg}$$

The number of such planetesimals necessary to make up the Earth is given by

$$\begin{aligned} \frac{\text{mass of Earth}}{\text{mass of planetesimal}} &= \frac{6.0 \times 10^{24} \text{ kg}}{1.6 \times 10^{15} \text{ kg}} \\ &= 3.8 \times 10^9 \\ &\approx 4 \times 10^9 \end{aligned}$$

**QUESTION 8.8**

These are cumulative curves. As we follow a curve from right to left it climbs, which shows that the total (i.e. cumulative) number of bodies greater than the mass indicated on the horizontal axis, is increasing. At times later than  $t = 0$ , the slope to the left of about  $10^{16}$  kg shows that bodies of less mass than this have been produced. This can be explained by fragmentation during collision, even though collisions have also resulted in an increase in the maximum size of planetesimals (see bottom right of curves). (In the discussion of asteroid formation in Section 8.2.10 you will see that under certain conditions the rate of fragmentation can stop runaway growth.)

**QUESTION 8.9**

The terrestrial planets formed within 3 AU of the Sun, where the temperature was too hot for water (the least volatile hydrogen-rich compound in the condensation sequence) to condense (as ice) from the solar nebula; most of their water probably arrived in the form of hydrated minerals. The terrestrial planets are too small to have collected much nebula gas directly by gravitation, and what they (or their planetary embryo precursors) did collect would have been lost during the Sun's T Tauri phase. The giant planets formed beyond 5 AU, so water was able to condense at Jupiter, and other hydrogen-rich substances such as methane and ammonia could condense at greater distances. Thus planetesimals colliding to form the kernels of the giant planets would be rich in these materials as well as the more refractory elements. Furthermore, the kernels of the giant planets were sufficiently massive that each was able to capture and retain a large mass of gas (which would be mainly hydrogen and helium) directly from the nebula. This capture was interrupted by the onset of the T Tauri phase, which explains the decreasing volatile-to-rock ratio outwards from Jupiter (which began to form earliest) to Neptune (which began to form last).

**QUESTION 8.10**

(a) Density decreases outwards from Jupiter, running from  $3.53 \times 10^3 \text{ kg m}^{-3}$  for the innermost large Galilean satellite, Io, to  $1.85 \times 10^3 \text{ kg m}^{-3}$  for the outermost large Galilean satellite, Callisto.



(b) The densities in Appendix A, Table A2 are mean densities for each satellite as a whole. The mean densities of Ganymede and Callisto are most simply explained if they are mixtures of rock and ice, with roughly equal proportions of each. Europa can be explained by being composed almost entirely of rock, but it would appear that we need to call on a denser component within Io (probably iron or iron and sulfur in its core). (Strictly speaking we should take self-compression into account, but in bodies this small its effects are too slight to affect our argument.)

#### QUESTION 8.11

The gravitational field of the planet would cause gravitational focusing, whereby the trajectories of incoming projectiles would be deviated towards the planet. As a result, the closer a satellite is to a planet, the more likely it is to be hit. A subsidiary factor is that the planet's gravity would accelerate incoming projectiles, so that those hitting an inner satellite would, on average, be travelling faster than those striking an outer satellite. The smaller the satellite, the less the energy required to break it up, so an incoming projectile carrying a given kinetic energy would be more able to fragment a small satellite.

#### QUESTION 8.12

The large prograde satellites of Jupiter, Saturn and Uranus probably grew within protosatellite discs around each planet. Neptune's large retrograde satellite, Triton, may be a captured planetary embryo. *Small* satellites in prograde orbits can be formed by collisions involving *larger* ones, but those in retrograde orbits are more likely to be captured asteroids or comet nuclei.

#### QUESTION 8.13

As Question 8.1 and the associated text discussed, the observable part of the  $\beta$  Pictoris dust cloud extends inwards to about 20 AU (where the orbit of Uranus would be). The dust suggests that the  $\beta$  Pictoris 'solar nebula' has probably completed its condensation phase, and grain growth by coagulation could be well advanced. There is no observational evidence bearing on whether planetesimal formation and subsequent growth of planetary embryos has begun. However, the apparent absence of dust within about 20 AU of  $\beta$  Pictoris could mean planets have already formed in this region. Now,  $\beta$  Pictoris should have already undergone its T Tauri phase, but if this is the case, the survival of dust is perplexing. Probably the best bet is that this is how our own Solar System would have looked while Uranus was growing but before the Neptune kernel had had a chance to form. Section 8.2.8 suggests that there would be an interval of 20 Ma between these events. (This is not to say that we should expect  $\beta$  Pictoris to form planets with the same masses and orbits as those in our own Solar System, because planetary formation must be influenced by the original mass and angular momentum of the nebula, and by subsequent random events; especially during and after runaway growth.)

#### QUESTION 9.1

The total mass of material added = (yearly flux)  $\times$  (length of time over which material has been added).

Thus, total mass =  $10^8 \text{ kg yr}^{-1} \times 10^9 \text{ yr} = 10^{17} \text{ kg}$ .

$$\text{The volume of material added} = \frac{\text{mass}}{\text{density}} = \frac{10^{17} \text{ kg}}{1.5 \times 10^3 \text{ kg m}^{-3}} = 6.67 \times 10^{13} \text{ m}^3.$$

$$\text{The surface area of a sphere} = 4\pi R^2.$$

Thus, the volume of the layer =  $4\pi R^2 \times h$ , where  $R$  = radius of the Earth and  $h$  = the depth of the layer. Therefore

$$6.67 \times 10^{13} \text{ m}^3 = 4\pi(6.378 \times 10^6 \text{ m})^2 \times h$$

$$h = \frac{6.67 \times 10^{13} \text{ m}^3}{5.099 \times 10^{14} \text{ m}^2} \\ = 0.13 \text{ m}$$

Therefore the depth of the layer  $h$  is 0.13 m.

#### QUESTION 9.2

It is an impact-produced sample of some description. It is probable that the chondritic, achondritic and metal-rich parts of the meteorite were all formed separately by normal processes. These were then assembled in a regolith during an impact event – for instance, an iron meteorite may have hit the surface of a silicate-rich parent body. (The meteorite described is not a hypothetical example but one member of a well documented, albeit rather rare, class of unusual samples.)

#### QUESTION 9.3

$$\text{The surface area of a sphere} = 4\pi R^2.$$

$$\text{The surface area of the Earth} = 4\pi \times (6371 \text{ km})^2 = 5.101 \times 10^8 \text{ km}^2.$$

If we assume (reasonably) that meteorites fall evenly over all parts of the Earth, then in one year a single meteorite falls in an area of  $\frac{5.101 \times 10^8}{20\,000} \text{ km}^2 = 25\,505 \text{ km}^2$ .

$$\text{The area of the town} = \pi r^2 = \pi \times 5^2 \text{ km}^2 = 78.5 \text{ km}^2.$$

$$\text{In an area of } 25\,505 \text{ km}^2 \text{ there could be } \frac{25\,505}{78.5} = 325 \text{ towns of radius 5 km.}$$

On average, a meteorite of >0.1 kg size would fall in a town of radius 5 km, every 325 years.

#### QUESTION 9.4

The alteration has taken place in a closed system. Although fluids have been formed and these have reacted with the original minerals to form new phases, there has been no net change in chemical composition. (Presumably, there was not a great deal of fluid flow through the parent body, otherwise the fluids would have taken up certain elements into solution, or suspension, and removed them, thereby changing the chemical composition.)

#### QUESTION 9.5

Compared to CI and CM2 meteorites, CV3 samples are enriched in Ca and Al. This can be explained by a relatively higher proportion of Ca- and Al-rich minerals in CV3 meteorites.

**QUESTION 9.6**

The  $\delta^{18}\text{O}$  of ocean water is  $\left(\frac{1/499}{1/499} - 1\right) \times 1000$  which is 0‰. Similarly  $\delta^{17}\text{O}$  can be shown to be 0‰. In other words, the reference point always has a  $\delta$  value of 0‰. Relative enrichments of the isotopes  $^{17}\text{O}$  and  $^{18}\text{O}$  result in  $\delta$  values which have a positive sign. Pure  $^{16}\text{O}$  would have

$$\delta^{18}\text{O} = \left(\frac{1/\infty}{1/499} - 1\right) \times 1000 = \left(\frac{0}{1/499} - 1\right) \times 1000 = -1000\text{‰}$$

**QUESTION 9.7**

Remember that pure  $^{16}\text{O}$  has both  $\delta^{17}\text{O} = -1000\text{‰}$  and  $\delta^{18}\text{O} = -1000\text{‰}$ . Starting at G and adding  $^{16}\text{O}$  to the system would produce a line which has a slope of about 1 on Figure 9.17. If you have trouble with understanding this, draw an expanded graph with axes that go from  $-1000$  to  $0$  for each  $\delta$  value. Pure  $^{16}\text{O}$  plots at  $(-1000, -1000)$ , while pure G is approximately at  $(0, 0)$ . A line drawn between these points will have a slope of 1, and any mixture of pure  $^{16}\text{O}$  with pure G will plot somewhere along this line. (When the oxygen isotope data from CAIs in Allende were first obtained, the addition of pure  $^{16}\text{O}$  to materials with an isotope composition somewhere in the vicinity of G was considered a reasonable explanation of the data (the  $^{16}\text{O}$  was assumed to have been injected into the solar nebula at a late stage from a supernova). However, for this theory to have gained acceptance it was considered that further oxygen isotope measurements would have eventually uncovered more extreme values than point D, and ideally all the way down to  $(-1000, -1000)$ . Thus far, innumerable measurements have failed to exceed the limit set by D which seems to suggest that this was the isotope composition of a large reservoir of dust.)

**QUESTION 9.8**

The simple answer is that planets and asteroids formed at different times will have different oxygen isotope compositions. (The variation in oxygen isotope compositions displayed by meteorites provides a very valuable classification scheme. Note that some of the differences may be related to formation locale, rather than the timing of formation.)

**QUESTION 9.9**

That the data from the matrix materials plot on a line of slope 0.5 suggests that the oxygen isotopes in these minerals have been subjected to processes of isotope fractionation, which have resulted in  $\delta^{18}\text{O}$  being twice that of  $\delta^{17}\text{O}$ . This is evidence that matrix materials were formed on a parent body, rather than in the solar nebula. Since the line of slope 0.5 is not coincident with the TFL it shows that the reservoir from which the carbonaceous chondrites were extracted was not exactly the same as that which formed the Earth.

**QUESTION 9.10**

The survival of interstellar organic molecules shows us that there must have been places within the solar nebula that were never heated significantly above 400 K.

(Although at the centre of the nebula, in the region of the Sun, temperatures were high, the outer parts, where comets formed, remained relatively cold. Carbonaceous chondrites sample materials from both extremes, demonstrating considerable turbulent mixing in the nebula.)

#### QUESTION 9.11

A very simple way would be to measure the stable isotope composition of carbon in each form. If there is no difference in  $^{12}\text{C}/^{13}\text{C}$  ratios then the two forms might be related. (In reality there is a distinct difference in carbon isotope composition between the diamond and the amorphous carbon. While it is entirely possible that diamond can be formed from amorphous carbon by shock processes (which result in high pressures) the isotope evidence is at variance with such an origin. Several other lines of evidence also militate against shock.)

#### QUESTION 9.12

- (a) By measuring the content of  $^{26}\text{Mg}$ . (This is carried out by measuring the  $^{26}\text{Mg}/^{24}\text{Mg}$  ratio and looking for anomalously high values.)
- (b) Because some minerals contain Al and Mg it is difficult in these instances to measure any excess  $^{26}\text{Mg}$ . It is desirable to search for the effects of  $^{26}\text{Al}$  decay in minerals which contain very little, or no, magnesium.

#### QUESTION 9.13

Electromagnetic induction and heating through impact events are possibilities. However, the decay of short-lived radionuclides, such as  $^{26}\text{Al}$ , is the most likely process to have contributed heat.

#### QUESTION 9.14

If we assume that all meteorite parent bodies started off with a chondritic composition then in order to obtain a metal-rich body there has to be extensive melting and differentiation. Upon total melting, silicate materials migrate to the outermost parts of an asteroid while metal sinks to the centre of the body. If the metallic asteroids we can observe today are original cores then the silicate crusts and mantles of these bodies must have been removed (most probably by collisional processes in the asteroid belt). Unlike the asteroid Vesta, which is still largely intact, a metallic asteroid represents the remnants of an original parent body.

#### QUESTION 9.15

With just the knowledge that Kodaikanal has a radiometric formation age of 3.8 Ga we may be inclined to think that this was the age of the meteorite's formation. However, as stated in the text, most meteorite ages fall in the range 4.5 to 4.6 Ga. Perhaps, therefore, we should consider that Kodaikanal formed at this earlier time and that the age of 3.8 Ga represents something that happened subsequently to the meteorite's parent body. Now, the impact-produced rocks from the Moon document a period of Solar System history when planetary bodies were undergoing intense bombardment by meteoroids. Thus, we can infer that the age of Kodaikanal might also document this same period, but in this case the impact event that affected the Kodaikanal parent body occurred in the asteroid belt, rather than on the Moon.

## APPENDIX A USEFUL PLANETARY DATA

**Table A1** Basic data on the planets (including the Moon).

	Mercury	Venus	Earth	Moon	Mars	Jupiter	Saturn	Uranus	Neptune	Pluto
Mass										
/10 <sup>24</sup> kg	0.330	4.87	5.97	0.074	0.642	1900	569	86.8	102	0.013
/Earth masses	0.055	0.815	1.00	0.012	0.107	318	95.2	14.4	17.1	0.002
Orbital semimajor axis <sup>a</sup>										
/10 <sup>6</sup> km	57.91	108.2	149.6	149.6	227.9	778.4	1427	2871	4498	5906
/AU	0.39	0.72	1.00	1.00	1.52	5.20	9.54	19.19	30.07	39.48
Orbital eccentricity	0.206	0.007	0.017	0.055	0.093	0.048	0.054	0.047	0.009	0.249
Orbital inclination /degrees	7.0	3.4	0.0	5.2	1.9	1.3	2.5	0.8	1.8	17.1
Orbital period <sup>b</sup>	88.0	224.7	365.0	27.3	686.5	11.86	29.42	83.75	163.7	248.0
days	days	days	days	days	days	yr	yr	yr	yr	yr
Axial rotation period <sup>b</sup> /days	58.6	243	0.997	27.3	1.03	0.412	0.444	0.718	0.671	6.39
Axial inclination /degrees	0.1	177.3	23.5	6.7	25.2	3.1	26.7	97.9	29.6	119.6
Polar radius/km	2440	6052	6357	1738	3375	66 850	54 360	24 970	24 340	1137
Equatorial radius/km	2440	6052	6378	1738	3397	71 490	60 270	25 560	24 770	1137
Mean radius <sup>c</sup> /km	2440	6052	6371	1738	3390	69 910	58 230	25 360	24 620	1137
Density/10 <sup>3</sup> kg m <sup>-3</sup>	5.43	5.20	5.51	3.34	3.93	1.33	0.69	1.32	1.64	2.1
Surface gravity/m s <sup>-2</sup>	3.7	8.9	9.8	1.6	3.7	23.1	9.0	8.7	11.1	0.7
Mean surface temperature/K	443	733	288	250	223					≥40
Effective cloud-top temperature/K						120	89	53	54	
Temperature at 1 bar pressure/K						165	135	75	70	
Rings	0	0	0	0	0	few	many	several	few	0
Satellites	0	0	1		2	≥39	≥30	≥21	≥8	1
Atmospheric surface pressure/bar <sup>d</sup>	≈10 <sup>-15</sup>	92.1	1.01	≈10 <sup>-14</sup>	6.3 × 10 <sup>-3</sup>					≈10 <sup>-5</sup>
Atmospheric surface density/kg m <sup>-3</sup>	≈10 <sup>-13</sup>	67	1.293	≈10 <sup>-13</sup>	0.018					≈10 <sup>-4</sup>
Atmospheric column mass <sup>e</sup> /kg m <sup>-2</sup>	≈10 <sup>-11</sup>	1.03 × 10 <sup>6</sup>	1.03 × 10 <sup>4</sup>	≈10 <sup>-11</sup>	1.69 × 10 <sup>2</sup>					≈1
Atmospheric main components	O	CO <sub>2</sub>	N <sub>2</sub>	Ar	CO <sub>2</sub>	H <sub>2</sub>	H <sub>2</sub>	H <sub>2</sub>	H <sub>2</sub>	N <sub>2</sub>
(relatively minor components in parentheses)	Na H <sub>2</sub> (He)	(N <sub>2</sub> )	O <sub>2</sub> (H <sub>2</sub> O) (Ar)	H <sub>2</sub> He Na	(N <sub>2</sub> ) (Ar) (O <sub>2</sub> )	He (CH <sub>4</sub> )	He (CH <sub>4</sub> )	He (CH <sub>4</sub> )	He (CH <sub>4</sub> )	(CH <sub>4</sub> ) (CO <sub>2</sub> )

<sup>a</sup> Semimajor axis also represents the *mean* distance from the Sun.

<sup>b</sup> These are sidereal periods (i.e. referenced to the stars rather than to the Sun) quoted in Earth days or years.

<sup>c</sup> The mean radius is defined as the *volumetric* radius (i.e. the radius the body would have if it were a sphere of the same mass), and is calculated by  $(R_e^2 R_p)^{1/3}$ . The values quoted here for the gas giants are for the atmospheric layer where the pressure is equal to 1 bar (this also applies to the values for surface gravity).

<sup>d</sup> Although the SI unit for pressure is the pascal, we use bar here for simplicity and easy comparison, as the Earth's surface atmospheric pressure ≈ 1 bar. Note 1 bar = 10<sup>5</sup> Pa.

<sup>e</sup> Column mass is the mass of atmosphere situated above each unit area (1 m<sup>2</sup>) of the planet's surface.

Table A2 Planetary satellites.

Planet	Satellite	Mean distance from planet/10 <sup>3</sup> km	Orbital period/days	Mean radius <sup>a</sup> /km	Mass/10 <sup>20</sup> kg	Density/ 10 <sup>3</sup> kgm <sup>-3</sup>
Earth	Moon	384	27.3	1738	735	3.34
Mars	Phobos	9.4	0.32	11.1	0.00011	1.90
	Deimos	23.5	1.26	6.2	0.000018	1.76
Jupiter	Io	422	1.77	1821	893	3.53
	Europa	671	3.55	1565	480	2.99
	Ganymede	1070	7.15	2634	1482	1.94
	Callisto	1883	16.7	2403	1076	1.85
	≥35 others					
Saturn	Mimas	186	0.94	199	0.38	1.14
	Enceladus	238	1.37	249	0.73	1.21
	Tethys	295	1.89	530	6.2	1.00
	Dione	377	2.74	560	10.5	1.44
	Rhea	527	4.52	764	23.1	1.24
	Titan	1222	15.95	2575	1346	1.88
	Iapetus	3561	79.3	718	15.9	1.02
	≥23 others					
Uranus	Miranda	130	1.42	236	0.66	1.20
	Ariel	191	2.52	579	13.5	1.7
	Umbriel	266	4.14	585	11.7	1.4
	Titania	436	8.71	789	35.3	1.71
	Oberon	583	13.46	761	30.1	1.63
	≥16 others					
Neptune	Proteus	118	1.12	209	≈0.5?	≈1.2?
	Triton	355	5.88	1353	215	2.05
	Nereid	5513	360	170	≈0.3?	≈1.2?
	≥5 others					
Pluto	Charon	19.4	6.39	586	19.0	2.2

<sup>a</sup> The mean radius is defined as the *volumetric* radius (i.e. the radius the body would have if it were a sphere of the same mass).

Table A3 Asteroids that have been targets of spacecraft fly-bys or encounters.

Asteroid <sup>a</sup>	Spacecraft	Encounter date	Asteroid size/km	Mean radius <sup>b</sup> /km	Density/kg m <sup>-3</sup>	Semimajor axis/AU
(951) Gaspra	Galileo	29 Oct 1991	19 × 12	6.1	2500 ±1000?	2.21
(243) Ida	Galileo	28 Aug 1993	58 × 23	15.8	2600 ±500	2.86
(253) Mathilde	NEAR	27 Jun 1997	59 × 47	26.4	1300 ±200	2.65
(9969) Braille	Deep Space 1	29 Jul 1999	2 × 1	0.7	not known	2.34
(433) Eros	NEAR	14 Feb 2000 <sup>c</sup>	33 × 13	9.69	2670 ±30	1.46
(5535) Annefrank	Stardust	2 Nov 2002	8 × 4	2.5	not known	2.21

<sup>a</sup> Asteroids are initially numbered, and are then usually named also. We refer to them by (*number*) *name*.

<sup>b</sup> The mean radius is defined as the *volumetric* radius (i.e. the radius the body would have if it were a sphere of the same mass).

<sup>c</sup> NEAR went into orbit around Eros on this date. It remained there for a year and then landed on the surface of Eros on 12 Feb 2001.



**Table A4** The largest known minor bodies in the Solar System.

Object	Semimajor axis/AU	Orbital period/yr	Orbital inclination	Orbital eccentricity	Mean radius <sup>a</sup> /km
Largest bodies in the asteroid belt:					
(1) Ceres	2.77	4.61	10.6°	0.079	457
(2) Pallas	2.77	4.61	34.8°	0.230	261
(4) Vesta	2.36	3.63	7.1°	0.090	250
(10) Hygiea	3.14	5.59	3.8°	0.121	215
(511) Davida	3.17	5.65	15.9°	0.180	163
Largest <i>known</i> (as of mid-2002) bodies in the Kuiper Belt (excluding Pluto):					
2002 LM <sub>60</sub> ('Quaoar')	43.2	284	8.0°	0.036	650
2002 AW <sub>197</sub>	47.5	327	24.3°	0.128	400–650?
(28978) Ixion	39.3	246	19.7°	0.245	400–650?
2002 TX <sub>300</sub>	43.3	284	25.9°	0.121	350–600?
(20000) Varuna	43.3	285	17.1°	0.054	450

<sup>a</sup> The mean radius is defined as the *volumetric* radius (i.e. the radius the body would have if it were a sphere of the same mass).

**Table A5** Some selected comets.

Comet <sup>a</sup>	Perihelion distance/AU	Semimajor axis/AU	Orbital period/yr	Eccentricity	Inclination	Velocity at perihelion/km s <sup>-1</sup>
2P/Enke	0.338	2.22	3.30	0.847	11.8°	69.6
46P/Wirtanen	1.059	3.09	5.44	0.658	11.7°	37.3
81P/Wild 2	1.590	3.44	6.40	0.539	3.2°	29.3
26P/Grigg–Skjellerup	1.118	3.04	5.31	0.663	22.3°	36.0
55P/Tempel–Tuttle	0.977	10.3	33.2	0.906	162.5°	41.6
1P/Halley	0.587	17.9	76.0	0.967	162.2°	54.5
109P/Swift–Tuttle	0.958	26.3	135	0.964	113.4°	42.6
153P/Ikeya–Zhang	0.507	51.0	367	0.990	28.1°	59.0
Hale–Bopp	0.925	184	≈2500	0.995	89.4°	43.8
Hyakutake	0.230	1490	≈58000	0.9998	124.9°	87.8

<sup>a</sup> Well observed periodic comets (i.e. short-period comets) are numbered, somewhat like asteroids, and this is indicated by the designation *number P*/, for example 2P/Enke.

**Table A6** Major annual meteor showers.

Date of maximum rate	Name of shower	Hourly meteor rate	Parent comet
3 Jan	Quadrantids	130	unknown
12 Aug	Perseids	80	Swift–Tuttle
21 Oct	Orionids	25	Halley
17 Nov	Leonids	25 <sup>a</sup>	Tempel–Tuttle
13 Dec	Geminids	90	(3200) Phaethon <sup>b</sup>

<sup>a</sup> This rate is usually what is observed, but every 33 years or so, this shower can display much higher rates.

<sup>b</sup> When discovered, Phaethon was assumed to be an asteroid as no cometary coma was observed. However it is likely that some activity has been present in the past.

**Table A7** Some notable Solar System exploration missions.

Mission	Launch	Description
Sputnik 1 (USSR)	4 Oct 1957	First Earth-orbiting satellite. Remained in orbit for 92 days.
Pioneer 4 (USA)	3 Mar 1959	4 Mar 1959: first lunar fly-by (within 60 000 km of Moon’s surface).
Luna 2 (USSR)	12 Sep 1959	14 Sep 1959: first spacecraft to land (impact) on the Moon.
Venera 1 (USSR)	12 Feb 1961	19 May 1961: first Venus fly-by. (Contact lost before fly-by.)
Mars 1 (USSR)	1 Nov 1962	19 Jun 1963: first Mars fly-by. (Contact lost before fly-by.)
Venera 3 (USSR)	16 Nov 1965	1 Mar 1966: first spacecraft to land on Venus. (Contact lost before landing.)
Luna 9 (USSR)	31 Jan 1966	3 Feb 1966: First soft landing on the Moon. TV pictures returned to Earth.
Zond 5 (USSR)	14 Sep 1968	First spacecraft to orbit the Moon (18 Sep 1968) and return a payload safely to Earth (21 Sep 1968). Payload included turtles, flies, worms and plants.
Apollo 8 (USA)	21 Dec 1968	First manned mission to orbit the Moon (24 Dec 1968). Returned 27 Dec 1968.
Apollo 11 (USA)	16 July 1969	First manned landing on the Moon (20 July 1969). Crew: Neil Armstrong, Edwin ‘Buzz’ Aldrin, Michael Collins (orbiter). Returned 24 July 1969.
Apollo 12 (USA)	14 Nov 1969	Second manned landing on the Moon (19 Nov 1969). Crew: Charles Conrad, Alan Bean, Richard Gordon (orbiter). Returned 24 Nov 1969.
Apollo 13 (USA)	11 Apr 1970	Moon mission aborted after onboard explosion on 14 Apr 1970. Crew: James Lovell, Fred Haise, John Swigert (orbiter). Returned 17 Apr 1970.
Luna 16 (USSR)	12 Sep 1970	First robotic sample-return from the Moon. Returned approximately 100 g of lunar material.
Apollo 14 (USA)	31 Jan 1971	Third manned landing on the Moon (5 Feb 1971). Crew: Alan Shepard, Edgar Mitchell, Stuart Roosa (orbiter). Returned 9 Feb 1971.
Mars 3 (USSR)	28 May 1971	2 Dec 1971: first spacecraft to land on Mars. Soft landing. Images returned.
Apollo 15 (USA)	26 Jul 1971	Fourth manned landing on the Moon (30 Jul 1971). Crew: David Scott, James Irwin, Alfred Worden (orbiter). Returned 7 Aug 1971. First lunar rover used.
Pioneer 10 (USA)	3 Mar 1972	First outer Solar System mission. 3 Dec 1973: fly-by of Jupiter. Currently ≈80 AU from the Sun. Will reach the star Aldebaran in 2 million years!
Apollo 16 (USA)	16 Apr 1972	Fifth manned landing on the Moon (21 Apr 1972). Crew: John Young, Charles Duke, Thomas Mattingly (orbiter). Returned 27 Apr 1972.
Apollo 17 (USA)	7 Dec 1972	Sixth (and final) manned landing on the Moon (11 Dec 1972). Crew: Eugene Cernan, Harrison Schmitt, Ronald Evans (orbiter). Returned 19 Dec 1972.
Pioneer 11 (USA)	6 Apr 1973	4 Dec 1974: Jupiter fly-by. 1 Sep 1979: Saturn fly-by.
Skylab (USA)	14 May 1973	First manned orbiting ‘space station’. Manned until 8 Feb 1974. Final usage of the Apollo Saturn V rocket.
Mariner 10 (USA)	3 Nov 1973	First (and only) spacecraft to go to Mercury. 5 Feb 1974: Venus fly-by. Mercury fly-bys on 29 Mar 1974, 21 Sep 1974 and 16 Mar 1975.
Viking 1 (USA)	20 Aug 1975	Mars orbiter and lander. 19 June 1976: reached Mars. 20 Jul 1976: lander touched down.

**Table A7** continued.

Mission	Launch	Description
Viking 2 (USA)	4 Sept 1975	Mars orbiter and lander. 7 Aug 1976: reached Mars. 3 Sep 1976: lander touched down.
Voyager 2 (USA)	20 Aug 1977	First (only) spacecraft to undertake a tour of all the giant planets. 9 Jul 1979: Jupiter fly-by. 26 Aug 1981: Saturn fly-by. 24 Jan 1986: Uranus fly-by. 25 Aug 1989: Neptune fly-by.
Voyager 1 (USA)	5 Sep 1977	5 Mar 1979: Jupiter fly-by. 12 Nov 1980: Saturn fly-by.
ISEE-3/ICE (USA)	12 Aug 1978	11 Sep 1985: first spacecraft to ‘distant fly-by’ a comet (Giacobini–Zinner).
Venera 13 (USSR)	30 Oct 1981	1 Mar 1982: Venus landing. Returned colour images from the surface.
Giotto (ESA)	2 Jul 1985	13 Mar 1986: first close (600 km) fly-by of a cometary nucleus (comet Halley).
Magellan (USA)	4 May 1989	Venus orbit insertion 10 Aug 1990. Mapped Venus surface with radar (1990–1994).
Galileo (USA)	18 Oct 1989	First spacecraft to orbit one of the giant planets. 29 Oct 1991: fly-by of asteroid (951) Gaspra. 28 Aug 1993: fly-by of asteroid (243) Ida. 7 Dec 1995: Galileo reaches Jupiter and deployed probe enters the atmosphere of Jupiter. 21 Sept 2003: Galileo impacts Jupiter.
Ulysses (ESA)	6 Oct 1990	First spacecraft to leave the ecliptic plane and orbit around the Sun, passing over the north and south poles. 8 Feb 1992: Jupiter fly-by.
Near Earth Asteroid Rendezvous (NEAR) Mission (USA)	17 Feb 1996	First spacecraft to orbit and land on an asteroid. 27 Jun 1997: fly-by of asteroid (253) Mathilde. 14 Feb 2000: started orbiting near Earth asteroid, (433) Eros. 12 Feb 2001: spacecraft landed on Eros.
Mars Global Surveyor (USA)	7 Nov 1996	Highly successful Mars remote sensing mission. 12 Sep 1997: reached Mars. Mar 1999: began mapping planet.
Mars Pathfinder (USA)	4 Dec 1996	4 Jul 1997: landed on Mars. 6 Jul 1997: deployed the Sojourner rover.
Cassini–Huygens (USA + Europe)	15 Oct 1997	Mission to Saturn and Titan. 30 Dec 2000: Jupiter fly-by. 1 Jul 2004: Saturn orbit insertion. 14 Jan 2005: Huygens probe lands on Titan.
Deep Space 1 (USA)	24 Oct 1998	22 Sep 2001: close fly-by of comet Borrelly’s nucleus. Images returned. 29 Jul 1999: fly-by of (9969) Braille.
Stardust (USA)	7 Feb 1999	Fly-by and cometary dust sample return mission to comet Wild 2. 2 Nov 2002: fly-by of asteroid (5535) Annefrank. 2 Jan 2004: fly-by of comet Wild 2. 15 Jan 2006: capsule carrying cometary dust lands on Earth for analysis.
2001 Mars Odyssey (USA)	7 Apr 2001	11 Jan 2002: entered Mars orbit. Acts as relay for 2003 rover missions.
Genesis (USA)	8 Aug 2001	Solar wind particle sample return mission. 3 Dec 2001: capture experiment deployed. Sep 2004: samples returned to Earth.
Rosetta (ESA)	2003	Comet orbiter and lander. Nominal mission plan: 10 Jul 2006: fly-by of asteroid (4979) Otawara. 24 Jul 2008: fly-by of asteroid (140) Siwa. 29 Nov 2011: orbit entry around comet Wirtanen. Sep 2012: lander deployed. (Note: exact mission plan may change.)
Mars Express (ESA) + Beagle 2	≈1 Jun 2003	Mars orbiter and lander. 26 Dec 2003: Mars Express enters Mars orbit, and the Beagle 2 spacecraft lands on the surface to look for isotope ratios indicative of life.

## APPENDIX B SELECTED PHYSICAL CONSTANTS AND UNIT CONVERSIONS

**Table B1** SI fundamental and derived units.

Quantity	Unit	Abbreviation	Equivalent units
mass	kilogram	kg	
length	metre	m	
time	second	s	
temperature	kelvin	K	
angle	radian	rad	
area	square metre	m <sup>2</sup>	
volume	cubic metre	m <sup>3</sup>	
speed, velocity	metre per second	m s <sup>-1</sup>	
acceleration	metre per second squared	m s <sup>-2</sup>	
density	kilogram per cubic metre	kg m <sup>-3</sup>	
frequency	hertz	Hz	(cycles) s <sup>-1</sup>
force	newton	N	kg m s <sup>-2</sup>
pressure	pascal	Pa	N m <sup>-2</sup> , kg m <sup>-1</sup> s <sup>-2</sup>
energy	joule	J	kg m <sup>2</sup> s <sup>-2</sup>
power	watt	W	J s <sup>-1</sup> , kg m <sup>2</sup> s <sup>-3</sup>
specific heat capacity	joule per kilogram kelvin	J kg <sup>-1</sup> K <sup>-1</sup>	m <sup>2</sup> s <sup>-2</sup> K <sup>-1</sup>
thermal conductivity	watt per metre kelvin	W m <sup>-1</sup> K <sup>-1</sup>	m kg s <sup>-3</sup> K <sup>-1</sup>

**Table B2** Selected physical constants and preferred values.

Quantity	Symbol	Value
speed of light in a vacuum	$c$	$3.00 \times 10^8 \text{ m s}^{-1}$
Planck constant	$h$	$6.63 \times 10^{-34} \text{ J s}$
Boltzmann constant	$k$	$1.38 \times 10^{-23} \text{ J K}^{-1}$
gravitational constant	$G$	$6.67 \times 10^{-11} \text{ N m}^2 \text{ kg}^{-2}$
Stefan–Boltzmann constant	$\sigma$	$5.67 \times 10^{-8} \text{ W m}^2 \text{ K}^{-4}$
Avogadro constant	$N_A$	$6.02 \times 10^{23} \text{ mol}^{-1}$
molar gas constant	$R$	$8.31 \text{ J K}^{-1} \text{ mol}^{-1}$
charge of electron	$e$	$1.60 \times 10^{-19} \text{ C}$ (negative charge)
mass of proton	$m_p$	$1.67 \times 10^{-27} \text{ kg}$
mass of electron	$m_e$	$9.11 \times 10^{-31} \text{ kg}$
Astronomical quantities:		
mass of the Sun	$M_\odot$	$1.99 \times 10^{30} \text{ kg}$
radius of the Sun	$R_\odot$	$6.96 \times 10^8 \text{ m}$
photospheric temperature of the Sun	$T_\odot$	$5770 \text{ K}$
luminosity of the Sun	$L_\odot$	$3.84 \times 10^{26} \text{ W}$
astronomical unit	AU	$1.50 \times 10^{11} \text{ m}$

**Table B3** Some useful conversions from alternative unit systems to SI units.

Quantity	Unit	SI equivalent
angle	1 degree	$(\pi/180)\text{rad}$
pressure	1 bar	$10^5\text{Pa}$
temperature	1°C	1 K
energy	1 erg	$10^{-7}\text{J}$
	1 electron volt	$1.60 \times 10^{-19}\text{J}$
	1 ton of TNT	$4.18 \times 10^9\text{J}$
length	1 foot	0.305m
	1 mile	$1.61 \times 10^3\text{m}$
area	1 square inch	$6.45 \times 10^{-4}\text{m}^2$
	1 square mile	$2.59 \times 10^6\text{m}^2$
mass	1 pound	0.454kg
speed, velocity	1 mile per hour	$0.447\text{ms}^{-1}$

**Table B4** The Greek alphabet.

Name	Lower case	Upper case
Alpha	$\alpha$	A
Beta (bee-ta)	$\beta$	B
Gamma	$\gamma$	$\Gamma$
Delta	$\delta$	$\Delta$
Epsilon	$\epsilon$	E
Zeta (zee-ta)	$\zeta$	Z
Eta (ee-ta)	$\eta$	H
Theta (thee-ta – ‘th’ as in theatre)	$\theta$	$\Theta$
Iota (eye-owe-ta)	$\iota$	I
Kappa	$\kappa$	K
Lambda (lam-da)	$\lambda$	$\Lambda$
Mu (mew)	$\mu$	M
Nu (new)	$\nu$	N
Xi (cs-eye)	$\xi$	$\Xi$
Omicron	$\omicron$	O
Pi (pie)	$\pi$	$\Pi$
Rho (roe)	$\rho$	P
Sigma	$\sigma$	$\Sigma$
Tau	$\tau$	T
Upsilon	$\upsilon$	Y
Phi (fie)	$\phi$	$\Phi$
Chi (kie)	$\chi$	X
Psi (ps-eye)	$\psi$	$\Psi$
Omega (owe-me-ga)	$\omega$	$\Omega$

APPENDIX C THE ELEMENTS

Table C1 The elements and their abundances.

The relative atomic mass,  $A_r$ , is the average mass of the atoms of the element as it occurs on Earth. It is thus an average over all the isotopes of the element. The scale is fixed by giving the carbon isotope  $^{12}_6\text{C}$  a relative atomic mass of 12.0. By convention, the Solar System abundance is normalized to  $10^{12}$  atoms of hydrogen, whereas the CI chondrite abundance is normalized to  $10^6$  atoms of silicon. To directly compare chondrite abundance to Solar System abundance (by number), you would multiply chondrite abundance by 35.8.

Atomic number, $Z$	Name	Chemical symbol	Relative atomic mass, $A_r$	Solar System abundance		CI chondrite abundance by number
				by number	by mass	
1	hydrogen	H	1.01	$1.0 \times 10^{12}$	$1.0 \times 10^{12}$	$2.79 \times 10^{10}$
2	helium	He	4.00	$9.8 \times 10^{10}$	$3.9 \times 10^{11}$	$2.72 \times 10^9$
3	lithium	Li	6.94	$2.0 \times 10^3$	$1.4 \times 10^4$	57.1
4	beryllium	Be	9.01	26	$2.4 \times 10^2$	0.73
5	boron	B	10.81	$6.3 \times 10^2$	$6.8 \times 10^3$	21.2
6	carbon	C	12.01	$3.6 \times 10^8$	$4.4 \times 10^9$	$1.01 \times 10^7$
7	nitrogen	N	14.01	$1.1 \times 10^8$	$1.6 \times 10^9$	$3.13 \times 10^6$
8	oxygen	O	16.00	$8.5 \times 10^8$	$1.4 \times 10^{10}$	$2.38 \times 10^7$
9	fluorine	F	19.00	$3.0 \times 10^4$	$5.7 \times 10^5$	843
10	neon	Ne	20.18	$1.2 \times 10^8$	$2.5 \times 10^9$	$3.44 \times 10^6$
11	sodium	Na	22.99	$2.0 \times 10^6$	$4.7 \times 10^7$	$5.74 \times 10^4$
12	magnesium	Mg	24.31	$3.8 \times 10^7$	$9.2 \times 10^8$	$1.074 \times 10^6$
13	aluminium	Al	26.98	$3.0 \times 10^6$	$8.1 \times 10^7$	$8.49 \times 10^4$
14	silicon	Si	28.09	$3.5 \times 10^7$	$1.0 \times 10^9$	$1.00 \times 10^6$
15	phosphorus	P	30.97	$3.7 \times 10^5$	$1.2 \times 10^7$	$1.04 \times 10^4$
16	sulfur	S	32.07	$1.9 \times 10^7$	$6.0 \times 10^8$	$5.15 \times 10^5$
17	chlorine	Cl	35.45	$1.9 \times 10^5$	$6.6 \times 10^6$	5240
18	argon	Ar	39.95	$3.6 \times 10^6$	$1.5 \times 10^8$	$1.01 \times 10^5$
19	potassium	K	39.10	$1.3 \times 10^5$	$5.2 \times 10^6$	3770
20	calcium	Ca	40.08	$2.2 \times 10^6$	$8.8 \times 10^7$	$6.11 \times 10^4$
21	scandium	Sc	44.96	$1.2 \times 10^3$	$5.5 \times 10^4$	34.2
22	titanium	Ti	47.88	$8.5 \times 10^4$	$4.1 \times 10^6$	2400
23	vanadium	V	50.94	$1.0 \times 10^4$	$5.3 \times 10^5$	293
24	chromium	Cr	52.00	$4.8 \times 10^5$	$2.5 \times 10^7$	$1.35 \times 10^4$
25	manganese	Mn	54.94	$3.4 \times 10^5$	$1.9 \times 10^7$	9550
26	iron	Fe	55.85	$3.2 \times 10^7$	$1.8 \times 10^9$	$9.00 \times 10^5$
27	cobalt	Co	58.93	$8.1 \times 10^4$	$4.8 \times 10^6$	2250
28	nickel	Ni	58.69	$1.8 \times 10^6$	$1.0 \times 10^8$	$4.93 \times 10^4$
29	copper	Cu	63.55	$1.9 \times 10^4$	$1.2 \times 10^6$	522
30	zinc	Zn	65.39	$4.5 \times 10^4$	$2.9 \times 10^6$	1260
31	gallium	Ga	69.72	$1.3 \times 10^3$	$9.4 \times 10^4$	37.8
32	germanium	Ge	72.61	$4.3 \times 10^3$	$3.1 \times 10^5$	119



Atomic number, $Z$	Name	Chemical symbol	Relative atomic mass, $A_r$	Solar System abundance		CI chondrite abundance by number
				by number	by mass	
33	arsenic	As	74.92	$2.3 \times 10^2$	$1.8 \times 10^4$	6.56
34	selenium	Se	78.96	$2.2 \times 10^3$	$1.8 \times 10^5$	62.1
35	bromine	Br	79.90	$4.3 \times 10^2$	$3.4 \times 10^4$	11.8
36	krypton	Kr	83.80	$1.7 \times 10^3$	$1.4 \times 10^5$	45
37	rubidium	Rb	85.47	$2.5 \times 10^2$	$2.1 \times 10^4$	7.09
38	strontium	Sr	87.62	$8.5 \times 10^2$	$7.5 \times 10^4$	23.5
39	yttrium	Y	88.91	$1.7 \times 10^2$	$1.5 \times 10^4$	4.64
40	zirconium	Zr	91.22	$4.1 \times 10^2$	$3.7 \times 10^4$	11.4
41	niobium	Nb	92.91	25	$2.3 \times 10^3$	0.698
42	molybdenum	Mo	95.94	91	$8.7 \times 10^3$	2.55
43	technetium	Tc <sup>a</sup>	98.91	— <sup>b</sup>	— <sup>b</sup>	— <sup>b</sup>
44	ruthenium	Ru	101.07	66	$6.8 \times 10^3$	1.86
45	rhodium	Rh	102.91	12	$1.3 \times 10^3$	0.344
46	palladium	Pd	106.42	50	$5.3 \times 10^3$	1.39
47	silver	Ag	107.87	17	$1.9 \times 10^3$	0.486
48	cadmium	Cd	112.41	58	$6.5 \times 10^3$	1.61
49	indium	In	114.82	6.6	$7.6 \times 10^2$	0.184
50	tin	Sn	118.71	140	$1.6 \times 10^4$	3.82
51	antimony	Sb	121.76	11	$1.3 \times 10^3$	0.309
52	tellurium	Te	127.60	170	$2.2 \times 10^4$	4.81
53	iodine	I	126.90	32	$4.1 \times 10^3$	0.90
54	xenon	Xe	131.29	170	$2.2 \times 10^4$	4.7
55	caesium	Cs	132.91	13	$1.8 \times 10^3$	0.372
56	barium	Ba	137.33	160	$2.2 \times 10^4$	4.49
57	lanthanum	La	138.91	16	$2.2 \times 10^3$	0.4460
58	cerium	Ce	140.12	41	$5.7 \times 10^3$	1.136
59	praseodymium	Pr	140.91	6.0	$8.5 \times 10^2$	0.1669
60	neodymium	Nd	144.24	30	$4.3 \times 10^3$	0.8279
61	promethium	Pm <sup>a</sup>	146.92	— <sup>c</sup>	— <sup>c</sup>	— <sup>c</sup>
62	samarium	Sm	150.36	9.3	$1.4 \times 10^3$	0.2582
63	europium	Eu	151.96	3.5	$5.3 \times 10^2$	0.0973
64	gadolinium	Gd	157.25	12	$1.8 \times 10^3$	0.3300
65	terbium	Tb	158.93	2.1	$3.4 \times 10^2$	0.0603
66	dysprosium	Dy	162.50	14	$2.3 \times 10^3$	0.3942
67	holmium	Ho	164.93	3.2	$5.2 \times 10^2$	0.0889
68	erbium	Er	167.26	8.9	$1.5 \times 10^3$	0.2508
69	thulium	Tm	168.93	1.3	$2.3 \times 10^2$	0.0378
70	ytterbium	Yb	170.04	8.9	$1.5 \times 10^3$	0.2479
71	lutetium	Lu	174.97	1.3	$2.3 \times 10^2$	0.0367

Atomic number, $Z$	Name	Chemical symbol	Relative atomic mass, $A_r$	Solar System abundance		CI chondrite abundance by number
				by number	by mass	
72	hafnium	Hf	178.49	5.3	$9.6 \times 10^2$	0.154
73	tantalum	Ta	180.95	1.3	$2.4 \times 10^2$	0.0207
74	tungsten	W	183.85	4.8	$8.8 \times 10^2$	0.133
75	rhenium	Re	186.21	1.9	$3.5 \times 10^2$	0.0517
76	osmium	Os	190.2	24	$4.6 \times 10^3$	0.675
77	iridium	Ir	192.22	23	$4.5 \times 10^3$	0.661
78	platinum	Pt	195.08	48	$9.3 \times 10^3$	1.34
79	gold	Au	196.97	6.8	$1.3 \times 10^3$	0.187
80	mercury	Hg	200.59	12	$2.5 \times 10^3$	0.34
81	thallium	Tl	204.38	6.6	$1.4 \times 10^3$	0.184
82	lead	Pb	207.2	110	$2.3 \times 10^4$	3.15
83	bismuth	Bi	208.98	5.1	$1.1 \times 10^3$	0.144
84	polonium	Po <sup>a</sup>	209.98	— <sup>c</sup>	— <sup>c</sup>	— <sup>c</sup>
85	astatine	At <sup>a</sup>	209.99	— <sup>c</sup>	— <sup>c</sup>	— <sup>c</sup>
86	radon	Rn <sup>a</sup>	222.02	— <sup>c</sup>	— <sup>c</sup>	— <sup>c</sup>
87	francium	Fr <sup>a</sup>	223.02	— <sup>c</sup>	— <sup>c</sup>	— <sup>c</sup>
88	radium	Ra <sup>a</sup>	226.03	— <sup>c</sup>	— <sup>c</sup>	— <sup>c</sup>
89	actinium	Ac <sup>a</sup>	227.03	— <sup>c</sup>	— <sup>c</sup>	— <sup>c</sup>
90	thorium	Th <sup>a</sup>	232.04	1.2	$2.8 \times 10^2$	0.0335
91	protoactinium	Pa <sup>a</sup>	231.04	— <sup>c</sup>	— <sup>c</sup>	— <sup>c</sup>
92	uranium	U <sup>a</sup>	238.03	0.32	$7.7 \times 10^1$	0.0090
93	neptunium	Np <sup>a</sup>	237.05	— <sup>c</sup>	— <sup>c</sup>	— <sup>c</sup>
94	plutonium	Pu <sup>a</sup>	239.05	— <sup>c</sup>	— <sup>c</sup>	— <sup>c</sup>
95	americium	Am <sup>a</sup>	241.06	— <sup>c</sup>	— <sup>c</sup>	— <sup>c</sup>
96	curium	Cm <sup>a</sup>	244.06	— <sup>c</sup>	— <sup>c</sup>	— <sup>c</sup>
97	berkelium	Bk <sup>a</sup>	249.08	— <sup>c</sup>	— <sup>c</sup>	— <sup>c</sup>
98	californium	Cf <sup>a</sup>	252.08	— <sup>c</sup>	— <sup>c</sup>	— <sup>c</sup>
99	einsteinium	Es <sup>a</sup>	252.08	— <sup>c</sup>	— <sup>c</sup>	— <sup>c</sup>
100	fermium	Fm <sup>a</sup>	257.10	— <sup>c</sup>	— <sup>c</sup>	— <sup>c</sup>
101	mendelevium	Md <sup>a</sup>	258.10	— <sup>c</sup>	— <sup>c</sup>	— <sup>c</sup>
102	nobelium	No <sup>a</sup>	259.10	— <sup>c</sup>	— <sup>c</sup>	— <sup>c</sup>
103	lawrencium	Lr <sup>a</sup>	262.11	— <sup>c</sup>	— <sup>c</sup>	— <sup>c</sup>

<sup>a</sup>No stable isotopes.  
<sup>b</sup>Detected in spectra of some rare evolved stars.  
<sup>c</sup>Too scarce to have been detected beyond the Earth (i.e. abundance value not well known).

## ACKNOWLEDGEMENTS

Grateful acknowledgement is made to the following sources for permission to reproduce material in this book.

*Cover photos:* NASA.

*Figures 6.1, 6.11, 6.15, 6.18, 6.20, 6.21, 6.22, 6.25, 6.27, 6.28, 6.29, 6.33, 6.34, 6.36 and 6.37* NASA;

*Figure 6.13* Reprinted ‘Voyager 2 Radio Observations of Uranus with permission from Warwick, J W. Science, Volume 233. Copyright 1986 American Association of the Advancement of Science;

*Figure 6.19* Painting by Duragel, Courtesy of the Observatoire de Paris;

*Figure 6.23 and 6.24* European Southern Observatory, Germany;

*Figure 6.29* J.T. Trauger (Jet Propulsion Laboratory) and NASA;

*Figure 6.32* Reprinted from Science, Vol. 153. Hammel, H. B. et al, ‘New measurements of the winds of Uranus’, pp. 229 - 235, 2001 with permission from Elsevier Science;

*Figures 7.13, 7.14, 7.15, 7.16, 7.17, 7.18, 7.20, 7.22, 7.23, 7.31a, 7.32, 7.38* NASA;

*Figure 7.19* Reprinted ‘Toutatis - Asteroid, 4179 with permission from Calvin J. Hamilton. Copyright 1995 American Association of the Advancement of Science;

*Figure 7.25* Credit: D Jewitt and J Luu, (University of Hawaii);

*Figure 7.29* Copyright Johns Hopkins University;

*Figures 7.30a and b* David Malin Images;

*Figure 7.31b* Copyright © 2000 European Space Agency. All rights reserved;

*Figure 7.33* Copyright Don Davis;

*Figures 7.37a and b* NASA/Armagh Planetarium;

*Figure 7.40* Juraj Toth (Comenius U. Bratislava), Modra Observatory;

*Figure 7.43* J.C. Casado;

*Figures 8.2, 8.3, 8.4, 8.15, 8.16, 8.17, 8.18* Space Telescope Science Institute;

*Figure 8.5* Copyright © 2001 Axel Mellinger;

*Figure 8.6* Akira Fujii, Tokyo;

*Figures 8.7, 8.19, 8.20, 8.21, 8.22 and 8.25* NASA;

*Figures 8.8 and 8.10* Anglo Australian Telescope Board. Photograph by David Malin;

*Figure 8.11* Ronald Snell;

*Figure 8.23* US Geological Survey;

*Figure 8.24* Dr Michael H. Carr, National Space Science Data Center.

*Figure 9.1* Copyright S. Eichmiller, Altoona, Pennsylvania;

*Figure 9.2* Photograph by [www.nyrockman.com](http://www.nyrockman.com) © 2002;

*Figure 9.4* ‘Hoba Meteorite, Namibia, Copyright [www.suedafrica.net](http://www.suedafrica.net) Online Travel Guide;

*Figures 9.5, 9.10 and 9.11* Copyright © Natural History Museum, London;

*Figure 9.7a* University of Leiden, The Netherlands;

*Figure 9.7b* Dr I. A. Franchi/The Open University;

*Figure 9.8* Wasson, J. T., (1985) *Meteorites*. Copyright © 1985 by W. H. Freeman and Company. Used with permission;

*Figure 9.9* D. Brownlee, University of Washington;

*Figure 9.16* Franchi, I. A., et al (2001). *Philosophical Transactions: Mathematical, Physical and Engineering Sciences*. Reprinted with permission by The Royal Society;

*Figure 9.18* Reprinted with permission from, Shu, S. H. et al (1997), ‘X-rays and fluctuating X-winds from protostars’. *Science*, Vol. 227. Copyright © 1997 American Association for the Advancement of Science;

Every effort has been made to trace all the copyright owners, but if any has been inadvertently overlooked, the publishers will be pleased to make the necessary arrangements at the first opportunity.

# INDEX

Glossary terms are in bold. Italics indicate items mainly, or wholly, in a figure or table.

## A

**ablation**, 318  
**absorption spectrum**, 164, 180  
**accretion**, 23, 50, 51, 55, 302  
     planetary embryos, 304  
     Solar System, 299–300  
**accretional heating**, 61–2  
**achondrites**, 321  
**adiabatic lapse rate**, 175–6, 218  
 advection, 69  
**aerodynamic drag**, 108  
**albedo**, 178, 256, 259  
 Allende, meteorite, 323  
 altitude, effect on temperature, 173–6  
 ammonia, 214, 217, 219  
 angrites, 328, 329  
**angular momentum**, 189–90  
     mass relationship, 282, 283  
     solar, 296–7  
**angular speed**, 189–90  
**aphelion**, 246  
**aphelion distance**, 246  
 Ariel satellite, 124  
**asteroid belt**, 11, 251, 254  
     interplanetary dust, 275  
 asteroidal meteorites, 315, 316, 318, 320–3  
**asteroids**, 4, 11, 251–4  
     data from spacecraft, 257–61  
     images, 261, 263  
     impactors, 145–6  
     melting processes, 340–5  
     origins of, 308  
     size, 254–5  
     types, 256–7, 322  
**asthenosphere**, 68, 69, 72  
**astronomical unit (AU)**, 24  
 atmospheres,  
     circulation, 189–94  
     composition of, 170–4

Jupiter and Saturn, 214–23  
 Mars, 160  
 Mercury, 160  
     origins of, 159–60  
     Uranus and Neptune, 235–40  
 atmospheric pressure,  
     effect of altitude, 174–5  
     Venus, 117  
**atmospheric structure**, 173–5  
 atoms,  
     chemical bonds, 48–9  
     electronic energy levels, 164, 166  
 aurora borealis, 158, 197  
 Auroral oval, 232, 233  
 axial rotation, Sun, 282

## B

**basalt**, 46  
     chemical composition, 341, 342  
     chemistry, 90–3  
     oxygen isotope ratios, 332, 333, 334  
**basalt lavas**, 74, 97, 98, 100–2  
**belts**, 224, 225, 226  
 binary planetary system, 21–2  
 bipolar outflow, 292–3  
 black-body radiation, 177, 179–80  
 bombardment *see* giant impacts  
**bow shock**, 195–6  
**breccia lens**, 138

## C

**CAIs**, 327, 328, 329  
     formation, 337  
     refractory inclusions, 334  
**calcium–aluminium-rich inclusions**, 327 *see* CAIs  
**calderas**, 104  
 carbon dioxide,  
     Earth's atmosphere, 181, 188  
     terrestrial planets, 171

carbon monoxide, electronic energy levels, 166, 168  
**carbonaceous chondrites**, 320, 321, 323–4  
     elemental abundances, 324–5  
     rare earth elements, 341, 342  
     *see also* CI carbonaceous chondrites  
**carbonatites**, 112  
 Cassini spacecraft, 202  
**Centaurs**, 262, 263, 272  
     reflectance spectra, 266–7  
**Chapman scheme**, 183, 184  
 chemical bonds, atoms, 48–9  
 chemical composition,  
     meteorites, 35–7, 38–41  
     solar atmosphere, 37  
     solar nebula, 47, 49  
     terrestrial layers, 32–41  
**chemical equilibrium**, 218–20  
**chondrites**, 301, 320–1  
     types of, 325–6  
     *see also* carbonaceous chondrites  
**chondritic composition**, 324  
**chondrules**, 37, 301, 320–1, 337  
 chronology, *see* timescale  
**CI carbonaceous chondrites**, 35, 37  
     chemical composition, 39  
     *see also* meteorites  
**circumstellar disc**, 285, 286  
     formation, 294, 295, 296  
 clouds, 185–8, 192  
**coagulation**, 298, 299–301  
 Coal Sack, 288  
**column mass**, 172, 173, 299–300  
**coma**, 268  
**cometary nucleus**, 268–9, 270  
**comets**, 4, 22, 268–72  
     impactors, 145–6  
     orbits, 272–4  
     origin of, 308

**compatible elements**, 91–2

**condensation**, 187–8  
solar nebula, 297–8, 300

**condensation flow**, 192, 193

**condensation sequence**, 47, 55, 298  
formation of matrix, 337–8  
refractory elements, 327, 334

**conduction**, 67, 71, 174

Cone Nebula, 284

conservation of angular momentum, 294, 296

continental crust,  
basalt lava, 100–2  
chemical composition, 35, 39  
decompression melting, 87

**continental flood basalt provinces (CFBP)**, 99, 100–2, 114

**continuous spectra**, 163, 164

**convection**, 68, 69, 174–6  
giant planets, 213, 226

convection cells, 224, 225, 226

**convection currents**, 174

**convective ascent region**, 106, 107, 111

cooling rates, iron meteorites, 344

core,  
Earth, 45  
formation, 57, 62  
terrestrial planets, 46, 60

**Coriolis effect**, 190–2, 226

cosmic sediments, 323–7, 330

**cosmic spherules**, 318–19

craters,  
asteroidal, 255  
chronology, 130–4, 148–51  
formation, 136, 137–8  
morphology, 139–43  
multi-ring basins, 142–3  
rock analysis, 143–5  
statistics, 148–51  
types, 146–8  
*see also* lunar craters

**crust**,  
Earth, 31, 46  
Mars, 79–80  
*see also* continental crust; mantle; oceanic crust

**cryovolcanism**, 13, 84, 113–14, 124

cumulative size distribution *see* size-frequency distributions

## D

**dark halo craters**, 116

**decompression melting**, 86–7  
mantle plumes, 102

**dense clouds**, 288–91  
fragmentation, 292

**density**, 4, 5  
asteroids, 257, 260  
Galilean satellites, 309–10  
giant planets, 206–7, 209, 210, 306  
radius relationship, 26, 27, 28  
terrestrial planets and Moon, 74  
terrestrial rocks, 32–4

diameter, asteroids, 254–5

**diatomic molecules**, 161, 168

differential isotope composition, 332–3

**differentiation**, 56, 57  
asteroids, 260  
meteorites, 340  
planetary embryos, 51

**distal ejecta**, 143

distances, *see* solar distances

dust,  
coagulation, 298–301, 302  
column mass, 300  
comets, 268, 269, 275–6  
protostellar disc, 330–1  
solar nebula, 334–5  
stellar formation, 284, 285–6

## E

Earth, 7–9  
atmosphere, 171–2, 180, 181, 188  
chronology, 63, 75  
comet impact, 274  
density, 32–4  
element abundances, 58, 59, 60  
giant impacts, 128–9  
magnetic field, 44–5  
mantle, 69  
meteorite finds, 315–16, 317  
orbit, 248, 253, 276  
plate tectonics, 70, 71, 72–5  
radiogenic heating, 63–6  
rotation, 63, 189–91  
volcanism, 94–109, 114–15

**eccentricity**, 246, 247  
asteroid orbits, 257  
Kuiper Belt, 264, 265, 266

**ecliptic plane**, 25, 248, 249  
asteroid belt, 251

**effusive volcanism**, 94, 95, 96–102

**ejecta**, volcanic, 108

**electric dipole**, 168

**electromagnetic radiation**, 167

**electromagnetic spectrum**, 167

electronic energy levels, 164, 166

**element partitioning**, 58

**ellipse**, 245–7

elliptical orbits, 245–7, 250

**emission spectrum**, 164, 165

**energy-level diagram**, 164, 165, 166

**equilibrium constant**, 218, 220, 221

**eruption columns**, 102–3, 105, 106–9  
extraterrestrial, 111, 113, 122

**escape velocity**, 128  
effect on atmospheric gases, 159, 160

Europa, 81, 124, 309

**explosive volcanism**, 94–5, 102–9  
extraterrestrial, 111

extraterrestrial planets,  
volcanic eruptions, 109–14  
volcanism, 117–25

## F

**fire fountains**, 102

**fluidized ejecta**, 146

**free-fall velocity**, 134

**fusion crust**, 318

## G

Galaxy, Milky Way, 287–8

**Galilean satellites**, 309–10

Galileo spacecraft, 203, 214, 221, 257

**gamma-rays**, 167

**gas chromatography**, 161–2

**gas giants**, 12

**gas thrust region**, 106, 107

gases,  
analysis, 161–2



cometary, 268, 269  
 giant planets, 204, 214–16  
 solar nebula, 297, 300, 334–5  
 stellar formation, 284, 285  
 terrestrial planets, 159, 160, 170–2

Gaspra asteroid, 11

Genesis spacecraft, 336

giant impacts,  
   Earth, 128–9  
   heat from, 61–2  
   lunar, 127  
   planet formation, 51, 55–6  
   planetary embryos, 51, 55–6, 57

**giant planets, 3, 201**  
   cross-sections, 205  
   formation, 304–6  
   icy surfaces, 146–7  
   magma generation, 94  
   orbital radius, 306–7  
   satellites, 308–12  
   structure,  
     evidence for, 206–9  
     models of, 202, 204–5  
   winds, 223–4

**glass, 133, 145**

global warming, 181–2

**granite, 46**

**gravitational focusing, 302**

gravitational force,  
   effect on asteroids, 251–2, 254  
   effect on atmosphere, 159  
   effect on orbits, 249–50, 253  
   in dense clouds, 290–2

Great Dark Spot, 19, 20

**Great Red Spot, 12, 227–9**

**Great White Spot, 230**

**greenhouse effect, 158, 179–82**

## H

**Hadley cell, 189, 190–2**

half-life, isotopes, 64

Halley's Comet, 268, 269

Hawaii, volcanoes, 74, 75, 85, 95

**heat excess, 207, 212, 213**

heat loss,  
   plate tectonics, 69–71  
   terrestrial planets, 66, 73

heat transfer, terrestrial planets, 67–9, 73

heating,  
   greenhouse effect, 179–82  
   ozone layer, 182–3  
   solar radiation, 189  
   thermosphere, 184

HED meteorites, 328, 329, 343

helium,  
   abundance, 217, 218, 220  
   Saturn and Jupiter, 213, 215–16  
   spectra, 165

**heteronuclear diatomic molecules, 168**

**homonuclear diatomic molecules, 168, 169**

**hot spots, 70, 87**

Hubble Space Telescope (HST) images, 284, 285, 286

**hydration-induced melting, 86, 89**

hydrocarbons, 217, 220, 236

**hydrocode analysis, 134**

hydrogen,  
   abundance, 217, 218, 220  
   dense clouds, 288–9  
   Jupiter and Saturn, 213, 215–16  
   spectra, 165

**hydrothermal alteration, 326–7**

**hypervelocity impacts, 128, 133, 135**

## I

**ices, 84**  
   cometary, 269, 270, 272  
   cryovolcanism, 113–14, 124  
   magma formation, 94

**igneous rocks, 46**

**impact cratering, 127, 132, 134–8**

**impact craters, 4, 5**

**impact ejecta, 132, 133, 138**

**impact flux, 148–9**

impact speeds  
   comets, 274  
   meteorites, 322

impactors, 148–9  
   types of, 145–6

impacts,  
   Kuiper Belt, 267  
   meteoroids, 277  
   numerical models, 134  
   shock effects, 143–5  
   Solar System, 127

  source of dust, 275  
   terrestrial, 128–9

**inclination, 248, 249**  
   comets, 273

inclusions, 301

**incompatible elements, 91–2**

**infrared radiation, 167, 169**  
   dense clouds, 290  
   giant planets, 214  
   Venus, 185

**interplanetary dust, 275–9**

**interplanetary dust cloud, 275**

**interplanetary magnetic field (IMF), 195–6**

interstellar medium, 288–91

Io, 309  
   aurora, 232  
   plasma torus, 231  
   structure, 80–1  
   tidal heating, 249  
   volcanism, 83, 121–3

ionic bonding, 48–9

**ionopause, 196**

**ionosphere, 184–5, 194–8**

**iron meteorites, 320, 340, 344–5**

**isotope exchange, 335**

isotope fractionation, 332–3

isotopes, radioactive decay, 63–6

**isotopic signatures, 58**

## J

**Jeans mass, 290–1**

Jupiter, 12–14  
   atmospheres, 214–23  
   comet impact, 274  
   effect on asteroids, 251–2  
   effect on planetesimals, 308  
   formation, 305  
   interior, 209–13  
   magnetospheres, 230–2  
   winds, 224–9

Juvinas, meteorite, 340–3

## K

Kelvin, Lord William, 63–4

**Kepler's first law, 245–6**

**Kepler's second law, 247, 250**

**Kepler's third law**, 247–8, 252  
**Keplerian orbit**, 248  
**kernel**, 305–6  
**Kirkwood Gaps**, 252–3  
**komatiites lavas**, 92–3  
**Kuiper Belt**, 22, 262–7, 271, 272  
     comets from, 273

## L

Laplace, Pierre-Simon, 282  
**lava**, 4  
**lava flow**, 96–102  
     lunar, 76, 116  
     Venus, 112, 118  
**lava inflation**, 99, 100, 101  
**lava tubes**, 99, 100  
**libration**, 250  
**lightcurve**, 259–60  
     Kuiper Belt, 267  
line spectra,  
     *see* absorption spectrum;  
     emission spectrum  
**lithosphere**, 68, 69, 72  
     Mercury, 77  
log-linear graphs 26, 27  
Long Duration Exposure Facility  
 (LDEF), 139  
**long-period comets**, 272  
**low velocity zone**, 68  
low-mass stars,  
     *see* protostars; T Tauri stars  
lunar craters, 116, 130, 139  
     Copernicus, 140, 141  
     Messier, 141  
     Plaskett, 127, 140  
     size-frequency distributions, 150  
lunar meteorites, 323

## M

**magma**, 56  
     basaltic, 97, 98  
     explosive eruptions, 103–4, 106,  
     108  
     from volcanism, 85–9  
     gravity effect, 110  
     heat transfer, 69  
     in meteorites, 342

    in silicates, 90–4  
     *see also* lava  
**magnetic dipole**, 44, 45  
magnetic fields,  
     giant planets, 207, 208, 212, 234  
     protostars, 336, 337  
**magnetopause**, 196  
**magnetosphere**, 44, 194–8  
     giant planets, 230–2, 240, 241  
major elements, rocks, 34, 36  
**mantle**, 31  
     chemical composition, 39, 45–6, 60  
     melting, 86–9  
     *see also* peridotite  
**mantle plumes**, 70, 87  
     decompression melting, 102  
**maria**, lunar surface, 76  
Mariner 10 spacecraft, 10, 128  
Mars, 9–11  
     atmospheric gases, 160  
     clouds, 186  
     craters, 140, 141, 146, 147  
         statistics, 151  
     crust, 120  
     dust storms, 194  
     fluvial processes, 152  
     meteorites, 323  
     Planitia impact basin, 83  
     spacecraft missions, 120, 169  
     structure, 79–80  
     volcanism, 119–21  
     wind patterns, 192, 194  
Mars Orbiting Camera (MOC), images,  
 152, 153, 154, 155  
mass,  
     angular momentum relationship,  
     282, 283  
     asteroids, 255, 260  
     giant planets, 204, 206, 209, 210  
     meteorites, 321  
     planetary bodies, 285  
     terrestrial planets and Moon, 74

mass eruption rate, 107–8  
**mass extinctions**, 128, 129  
mass loss,  
     comets, 268  
     solar nebula, 295–7  
**mass spectrometry**, 162  
**massive solar nebula model**, 295–7

**matrix**, meteorites, 337–8  
melting,  
     asteroidal, 340–5  
     mantle, 86–9  
Mercury, 4, 5  
     atmospheric gases, 160  
     core, 60  
     Mariner 10 spacecraft, 128  
     structure, 77  
     volcanism, 117  
**mesosphere**, 174, 184  
**metallic bonding**, 211–12  
**metallic hydrogen**, 211–12  
**metamorphic rocks**, 46  
**meteor**, 36, 276–7  
**Meteor Crater**, 132, 133  
**meteor shower**, 276–7, 278  
**meteorite fall**, 315  
meteorite finds, 315  
**meteorites**, 36, 315–19  
     asteroid connection, 320–3  
     chemical composition, 35–7, 38–41  
     cosmic sediments, 323–7  
     formation, 340–2  
     low-temperature materials, 337–9  
     rare earth elements, 341, 342  
     refractory elements, 327–35  
**meteoroid stream**, 276–7  
**meteoroids**, 36, 275, 277, 316  
meteors, 319  
     asteroidal, 315, 316, 318, 320–3  
     in Earth's atmosphere, 276, 277  
methane, 217, 220, 234  
Mexico, Chicxulub impact site, 61  
microcraters, 139  
**micrometeorites**, 318, 321  
**micrometeoroids**, 318–19  
**microwaves**, 167  
**mid-ocean ridge** systems, 69  
Milky Way, 287–8  
**minerals**, 31  
     effect of pressure, 33–4  
     properties, 35  
**minimum solar nebula model**, 295–7  
**minor bodies**, 25  
Moho discontinuity, 42, 43

molecules,  
     chemical bonds, 49  
     electronic energy levels, 164, 166  
     vibrational spectra, 214–15

Moon, 8–9

    chronology, 75  
     cross-section, 72  
     element abundances, 58, 59, 60  
     formation, 54, 58–60  
     giant impacts, 127  
     orbital radius, 307  
     physical properties, 74  
     structure, 76  
     volcanism, 116

moons, 3,

*see also* satellites

Mount St Helens, 85, 95, 97, 106

## N

**Near Earth Asteroids (NEAs), 253–4**

**Near Earth Objects, 134**

NEAR spacecraft, 257, 258, 260–1

**nebula hypothesis, 282–3, 295**

Neptune, 19–21

    atmosphere, 235–40  
     composition and interior, 233–5  
     magnetosphere, 240, 241

nickel–iron minerals,

    Earth core, 62  
     planet formation, 56–7, 58

nitrogen, terrestrial planets, 171

**noble gases, 161**

**non-thermal sources of radiation, 163**

nuclear fusion, protostars, 293

**nuée ardente, 106**

## O

oceanic crust,

    basaltic, 90, 92, 93  
     chemical composition, 35, 39  
     melting, 87

Olympus Mons, Mars, 119

**Oort cloud, 26, 272**

**orbit, 3**

orbital eccentricity, *see* eccentricity

**orbital evolution, 253, 254**

    Centaur, 262  
     comets, 270, 273

orbital inclination, *see* inclination

**orbital period, 8, 247–8**

    comets, 272, 273  
     satellites, 250

orbital radius,

    giant planets, 306–7  
     Moon, 307

**orbital resonance, 252–3**

    Kuiper Belt, 264, 265

orbits, 245–51

    Centaur, 263  
     comets, 272–4  
     dust particles, 276, 278  
     Kuiper Belt, 263, 264–5  
     meteorites, 318

**ordinary chondrites, 321, 325**

organic compounds, Solar System,  
 338–9

Orion Nebula, 289, 290

**oxidation, 171, 172**

**oxidized atmospheres, 171**

**oxidizing atmosphere, 172**

oxygen,

    Earth's atmosphere, 171–2  
     isotope ratios, 330–5

**ozone, 170**

ozone layer, 158, 182–3, 184

## P

**partial melting, 56–7, 58, 89–90**

    icy magma, 94  
     meteorite formation, 340–2  
     volcanism, 91–2

**partial pressure, 186–8**

**peridotites, 34, 35**

    chemical composition, 93  
     magma generation, 91–2

**perihelion, 246, 268–9**

**perihelion distance, 246, 247**

photons, dust particle collisions, 278–9

**planar deformation features, 143, 144**

**planetary bodies, 3**

    physical properties, 26–9

**planetary embryos, 23, 51, 55–6, 57,  
 302–4, 305**

planetary migration, 306–7

planetary systems, stellar, 286–7

**planetesimals, 23, 301, 302**

    comets, 270  
     evolution, 303–4  
     formation, 50–1, 55  
     formation of Jupiter, 305  
     Kuiper Belt, 262

**planets, 3**

    relative sizes, 11, 25  
     *see also* oceanic planets;  
     terrestrial planets

**plate recycling, 69, 88–9**

**plate tectonics, 32, 69–71, 72–5**

Pluto, 21–2, 262, 265

**plutonic rocks, 32**

**polyatomic molecules, 168**

porosity, asteroids, 257, 260

**Potentially Hazardous Asteroids  
 (PHAs), 253, 254**

**Poynting–Robertson effect, 279**

pressure,

    effect on minerals, 33–4  
     giant planets, 12, 204, 209, 210

**primitive meteorites, 37**

primordial heat, 61–2

**prograde motion, 248, 249, 273**

    Solar System, 294

**protoplanetary disc, 23,**

    condensation, 55  
     *see also* solar nebula

**protosatellite disc, 308, 310**

**protostars, 292**

    formation, 287–93  
     magnetic field lines, 336, 337

protostellar disc, 330–1

**protoSun, 282, 283, 294, 295**

**pseudotachylite rocks, 144**

**pumice, from lava, 103, 105**

**P-waves, 41–2, 44**

**pyroclastic flow, 105, 104–6**

**pyroclastic materials, 94, 96, 103**  
     Martian, 121

## R

**radiation pressure, 278**

radiation, sources of, 163, 164, 169

**radio waves, 167, 184, 215–16**  
     asteroids, 259

radioactive decay, 63–7  
 radiogenic heating, 63–7, 178–9  
**radiometric dating, 63**  
   meteorites, 328–9  
 radionuclides, short-lived 316, 328, 329, 342  
 radius, density relationship, 26, 27, 28  
**rampart craters, 146**  
**rare earth elements (REE), 341, 341, 342**  
**reball, 319**  
**reducing atmospheres, 171**  
**reduction, 171, 172**  
**reflectance spectrum, 256, 266–7**  
   meteorites, 343  
**refractory minerals, 55, 58, 59, 298**  
   meteorites, 327–35  
**regolith, 10**  
**relative molecular mass (RMM), 162**  
 resurfacing,  
   Earth, 72–5, 128  
   Io, 123  
   Venus, 78  
**retrograde motion, 248, 249**  
**rhyolite magmas, 97**  
**rifting, continental crust, 102**  
 rocks,  
   composition, 32–41  
   impact effects, 143–5  
   partial melting, 90  
   *see also* igneous rocks;  
   sedimentary rocks  
**rotation period, 8**  
   Earth, 63, 189–91  
   giant planets, 223, 224  
**rubble pile, 260–1, 270**  
**runaway growth, 302–3, 305**

## S

**satellites, 3,**  
   giant planets, 308–12  
   Jupiter, 12–13, 14, 124  
   Mars, 10–11  
   Neptune, 20–21  
   Pluto, 21–2  
   Saturn, 15–17  
   synchronous rotation, 250–1  
   Uranus, 18–19, 124, 125

**saturated surface, 149**  
**saturation vapour pressure diagram, 186–8**  
 Saturn, 14–17  
   atmosphere, 214–23  
   interior, 209–13  
   magnetosphere, 232  
   rings, 311  
   winds, 229–30  
**seasons, 193**  
**secondary craters, 150**  
**sedimentary rocks, 46, 153**  
**seismic waves, 41–4, 46**  
 Self, Steve, 98  
**self-compression, 33–4, 306**  
**semimajor axis, 245–8**  
   asteroids, 252, 257  
   comets, 272, 273  
   Kuiper Belt, 264, 265  
**semiminor axis, 245–6**  
**shatter cones, 144**  
**shock metamorphism, 143, 144**  
**shock pressure, 133, 135**  
**short-period comets, 273**  
 siderophile elements, *see* nickel–iron minerals  
**silicate minerals, 34**  
   magma generation, 90–4  
   meteorites, 37  
   planet formation, 56–8  
**size-frequency distribution, 149, 150–1**  
   asteroids, 254–5  
 Sojourner rover, Mars Pathfinder mission, 120  
 solar atmosphere, element abundances, 37  
 solar distances, 24, 25, 26  
   asteroids, 257  
   comets, 271  
**solar nebula, 23, 293–7,**  
   chemical compounds, 47, 49  
   comet formation, 272  
   composition, 36–7  
   condensation, 50, 55  
   formation, 287, 298–301  
   origins, 334–5  
   *see also* protoplanetary disc

solar radiation, 178–9, 180, 189  
   ionosphere, 194  
   ozone formation, 182–3

**Solar System, 3**

  accretion, 299–300  
   beyond Neptune, 262  
   chronology, 328–9  
   comet entry, 269, 270  
   comet numbers, 271  
   diagram, 25  
   elemental abundances, 324, 336  
   formation, 23–4, 281–7, 294–5  
   impacts, 127  
   layout, 24–6  
   orbital evolution, 253–4  
   organic compounds, 338–9  
   protostar formation, 287–93

**solar wind, 195–6, 197**

**solid-state convection, 68**

space probe,  
   Galileo, 203, 214, 221  
   Voyager I, 80

spacecraft,  
   Galileo, 203, 214, 221, 257  
   Mariner 10, 128  
   Voyager, 80, 203

spacecraft missions, 169, 257, 259, 267

**spatter, 104****spectroscopy, 162, 163–5**

**spectrum, 163**  
   black-body, 177, 179–80

**spidergram, 38, 40****stable isotope compositions, 329–30****stable isotopes, 330, 332****star, 3**

  star clusters, 292

  Stardust mission, 257, 259

  stellar formation, 283–6, 290

  stellar material, cycling of, 281

  stellar planetary systems, 286–7

  stellar winds, 292–3, 301, 336–7

**stony–iron meteorites, 320****stony meteorites, 320**

  storms, giant planets, 227–9, 230, 238

**stratigraphic record, 128****stratosphere, 174, 182–3, 184****subduction zones, 69**

**suevite rocks, 144**

sulfur,

giant planets, 217, 220, 222, 231  
Io, 122–3

Sun, 3, 4

angular momentum, 296–7  
axial rotation, 282  
elemental abundances, 324–5  
*see also* solar

**super-rotation, 192**

surface area to volume ratio, 66

**surface heat flow, 121**

**S-waves, 41–2, 44**

**synchronous rotation, 8, 250–1**

## T

**T Tauri stars, 293, 301, 306**

formation models, 335–7

**taxonomic classes, 256–7**

**tectonic processes, 63**

*see also* plate tectonics

**tektites, 61**

temperature,

effect of altitude, 173–6  
effect on atmospheres, 159, 160  
effect on volcanism, 111–13  
giant planets, 204, 205, 207–8  
solar nebula, 297  
solar, 3  
terrestrial planets, 176, 178–9  
Venus, 181, 182

**terminal fall velocity, 108–9, 111**

terrestrial depth, 34, 42

**terrestrial fractionation line (TFL), 333**

terrestrial layers, 31, 56–8

chemical composition, 45–9  
seismic evidence, 41–4

**terrestrial planets, 3**

atmospheres, 170–4  
core size, 46  
cross-sections, 72  
formation, 50–3  
heat transfer, 67–9, 73  
magma generation, 93  
physical properties, 74  
plate tectonics, 73  
temperature, 176, 178–9  
temperature profile, 173–6  
*see also* extraterrestrial planets

**terrestrial-like bodies, 3**

**thermal sources of radiation, 163, 164, 169**

**thermal tide, 192**

**thermosphere, 174, 184, 218, 219**

**tidal heating, 13, 62–3, 123, 249–51**

Io, 80–1

timescales,

craters, 130–4, 148–51  
Earth and Moon, 75  
giant planet formation, 305  
Moon, 76  
Solar System, 281, 328–9  
terrestrial planets, 304

trace elements, 34, 36, 59

**transient cavity, 137, 138**

Trapezium, 289

Triton, 311, 312

volcanism, 84

**troposphere, 174, 218, 219**

**tuff, 104**

**turbulence, 296**

## U

**ultraviolet (UV) radiation, 166, 167**

**umbrella region, 107**

uranium, 64–5, 66

Uranus, 17–19

atmosphere, 235–40  
composition and interior, 233–5  
magnetosphere, 240, 241  
radio-frequency emission, 224

## V

Valhalla impact site, 142

Van Allen radiation belts, 197

Venus 6–7

cloud layer, 185  
craters, 147  
images, 157, 185  
radiogenic heating, 67  
spacecraft missions, 169  
structure, 78  
temperature, 181, 182  
volcanism, 112, 117–18  
winds, 192

Vesta, asteroid, 343

**vibrational spectrum, 168–9**

molecules, 214–15

**vibrational transition, 168**

viscosity,

effect on eruptions, 103–4  
magmas, 97, 98

**viscous drag, 296**

**viscous relaxation, 143, 147**

**visible light, 167**

reflectance value, 256

**volatile inventory, 171**

**volatile minerals, 55, 59, 60, 298**

carbonaceous chondrites, 326

**volcanic arcs, 88**

**volcanic bombs, 104**

volcanic eruptions,

causes of, 103–4, 106, 108  
Etna, 95  
extraterrestrial, 109–14  
Hawaii, 85, 95  
Mount Pelée, 106  
Mount St Helens, 85, 95, 97, 106  
sizes of, 96  
Toba, 104  
Vesuvius, 109  
*see also* volcanoes

volcanic explosive activity (VEI), 96

**volcanism, 4, 83–6**

basaltic, 90–3  
Earth, 72, 74, 94–109, 114–15  
extraterrestrial, 117–25  
magma generation, 86–9  
Mars, 119–21  
Moon, 116  
Venus, 112, 117–18

**volcanoes, 74, 75**

Hawaii, 74, 75  
Io, 83, 121, 122, 123  
Laki, Iceland, 83  
Lesser Antilles, Caribbean, 88  
Mars, 79, 80, 83, 119, 121  
Solar System, 84, 89  
Triton, 84  
*see also* volcanic eruptions

Voyager spacecraft, 80, 203

W

water, terrestrial planets, 171  
**Widmanstätten pattern**, 344  
wind patterns, 190–1, 192, 194  
**wind speed**, 223, 224  
**wind velocity**, 223–4, 225  
winds, giant planets, 223–30, 237–9

X

**X-rays**, 167  
x-wind, 335–7  
**xenoliths**, 32  
    chemical composition, 35  
    *see also* mantle

Y

**yield strength**, 97

Z

**zodiacal light**, 279  
**zones**, 224, 225, 226